Sclérochronologie à Saint-Pierre et Miquelon : de l'échelle sub-horaire aux reconstructions multi-décennales

Pierre Poitevin

UNIVERSITE SCIENCES BRETAGNE DE LA MER LOIRE ET DU LITTORAL

UBO Université de Bretagne Occidentale

THESE DE DOCTORAT DE

L'UNIVERSITE
DE BRETAGNE OCCIDENTALE
COMUE UNIVERSITE BRETAGNE LOIRE

ECOLE DOCTORALE N° 598
Sciences de la Mer et du littoral
Spécialité : Écologie Marine

Par

Pierre POITEVIN

« Sclérochronologie à Saint-Pierre et Miquelon : De l'échelle sub-horaire aux reconstructions multi-décennales »

Thèse présentée et soutenue à Plouzané, le 17/12/2018

Unité de recherche : Laboratoire des sciences de l'environnement marin (UMR 6539)

Rapporteurs avant soutenance :

Philippe ARCHAMBAULT Professeur, Université Laval

Matthieu CARRÉ Chargé de recherches, CNRS

Composition du Jury :

Anne LORRAIN (Examinatrice) Chargée de recherches, IRD

Claire LAZARETH (Examinatrice) Chargée de recherches, IRD

Stéphanie THIÉBAULT (Présidente) Directrice de recherches, CNRS

Philippe ARCHAMBAULT (Rapporteur) Professeur, Université Laval

Directeurs de thèse :

Laurent CHAUVAUD Directeur de recherches, CNRS

Pascal LAZURE Chercheur, Ifremer

LEMAR laboratoire des sciences de l'environnement marin UBO | CNRS | IRD | Ifremer

LOPS

BeBEST

« Va prendre tes leçons dans la nature, c'est là qu'est notre futur. »

Léonard de Vinci

Remerciements

Il est temps d'entamer cet exercice difficile mais néanmoins agréable, qu'est celui des remerciements. Difficile, car celui-ci se doit d'être le plus exhaustif possible, même si cela me semble impossible. Agréable, car il marque la fin d'une belle aventure et je l'espère le commencement de beaucoup d'autres.

En premier lieu, je tiens à remercier Philippe Archambault et Matthieu Carré pour avoir accepté d'être rapporteurs de ce manuscrit. Un grand merci également à Claire Lazareth, Anne Lorrain et Stéphanie Thiébault de m'avoir fait l'honneur d'évaluer ce travail en tant qu'examinatrices. Je suis extrêmement honoré par cette marque de reconnaissance à l'égard de mon travail.

J'en arrive maintenant à mes collègues, mes amis et ma famille qui ont participé à cette aventure. Pour tenter de n'oublier personne et donner une certaine cohérence à cette partie, qui peut vite devenir décousue. Je vais rester dans le thème de la sclérochronologie et procéder à ces remerciements, au moins au début, de manière chronologique.

Difficile de savoir où tout a commencé... Peut-être, lorsque Jacques Clavier alors co-responsable du Master Sciences Biologiques Marines à Brest m'a envoyé une offre d'emploi d'ingénieur d'étude à Saint-Pierre et Miquelon. Jacques, je te remercie pour ce coup de pouce, ainsi que pour la qualité de tes enseignements que j'ai eu le privilège de suivre pendant mes deux années de Master.

C'est alors que j'ai rencontré Philippe Goulletquer qui m'a offert l'opportunité d'aller pour la première fois dans cet archipel magnifique qu'est Saint-Pierre et Miquelon. Je n'ai pas de mots suffisamment forts pour l'en remercier. J'ai ainsi eu la chance de collaborer quotidiennement avec Herlé Goraguer (Ifremer) et Alain Orsiny (ARDA) qui ont été d'un soutien sans faille tant professionnellement que personnellement pendant ces trois années passées à Miquelon. Il y aurait certainement un livre à écrire pour remercier toutes les personnes rencontrées sur ces îles, mais le temps et l'espace me sont comptés alors que j'écris ces quelques lignes. Je me contenterai donc de les citer : Juantxo, Sébastien, Christian, Paul-André, Yannick, Jean-Jacques, Philippe, Yann, Marie-Josée, Gwenaël, Laura, Vicky, Jason, Aurélie, Jonathan, Aymeric, Solenne, Marine, Garry, Aldric, Gérard, Brigitte, Thierry, Laure, Yoann, Aurélie,

Chichi, Sandra, Mariano… et j'en oublie certainement. Ces trois années à Saint-Pierre et Miquelon m'auront également permis de rencontrer de manière plus ou moins régulière un grand nombre de techniciens, d'ingénieurs, et de chercheurs français et canadiens : Stéphane, Olivier, Philippe, Jean-Michel, James, Xavier, Michel, David, Michelle, Réjean, Leslie Anne, Kevin et bien entendu Pascal Lazure qui mérite une place plus qu'importante dans ces remerciements.

Pascal, merci d'avoir fait du lobbying auprès de Laurent en lui présentant les particularités hydrologiques de ces îles et en lui transmettant des coquilles géantes et des palourdes centenaires. Je te suis infiniment reconnaissant d'avoir accepté de codiriger cette thèse, d'avoir pris du temps pour mettre en place ce sujet, même si celui-ci sort un peu de tes thématiques de recherches habituelles. Tout au long de cette thèse, tu as su me faire profiter avec une grande simplicité et humanité de ta rigueur et de ta culture scientifique, en étant à chaque fois disponible pour toutes ces discussions à essayer de marier physique, biologie et écologie. J'en arrive à Laurent Chauvaud, qui a accepté de se lancer dans cette aventure en codirigeant cette thèse. Pendant ces trois années, j'ai découvert une personne exceptionnelle, tant par ses qualités humaines que scientifiques. Ces quelques lignes sont donc bien courtes pour résumer tous ces moments passés ensembles au bureau, au labo, en mission et en plongée. Une chose est certaine, c'est qu'à chaque fois ceux-ci étaient empreint d'une certaine touche humoristique, parfois potache, mais toujours assumée. Bref, les mots me manquent pour vous exprimer à tous les deux l'amitié, la reconnaissance et le respect que je vous porte.

Pas sur le papier mais pleinement investi dans l'encadrement de ces travaux, je tiens également à remercier Julien Thébault. Merci de m'avoir aussi bien guidé dans les méandres de la sclérochronologie pendant toutes ces années. Tu as toujours été là pour discuter de mes résultats et m'aider à les mettre en forme avec la rigueur et l'honnêteté scientifique qui te caractérisent. Sur le terrain également, tu n'as pas hésité à venir tremper tes palmes avec moi à Saint-Pierre et Miquelon pour y faire des plongées plus ou moins agréables… Ça a été un véritable plaisir de partager ces moments avec toi.

Pour rester dans le thème de la plongée, un grand merci à Erwan Amice qui nous a accompagnés à Saint-Pierre et Miquelon en 2016 et 2017 pour participer à la partie terrain de ces travaux de thèse. Un grand merci également pour ces milliers de photos sous-marines

illustrant nos « chantiers subaquatiques » qui n'auraient jamais pu voir le jour sans l'implication des plongeurs locaux. Pour la location du bateau et la disponibilité des pilotes, je tenais à remercier l'ensemble du Club Nautique Saint-Pierrais, notamment son président Stéphane Salvat. Pour leur connaissance du terrain, leur flexibilité et leurs participations aux plongées je voulais également remercier les plongeurs d'état de la DTAM : Yoann Busnot, Luc Thillais et Jean-Marc Derouet, sans qui ce travail n'aurait pas eu la même ampleur.

Pour continuer dans le contexte des missions et du terrain, un grand merci à l'ensemble de l'équipage du navire océanographique ANTEA qui a délaissé les tropiques pour venir passer plus d'un mois à Saint-Pierre et Miquelon en 2017. Pour leur bonne humeur et les agréables moments passés ensembles un grand merci aux équipes scientifiques du LEG 2 et 3 : Marion M., Vincent, Gabin, Jacques, François, Frédéric, Cécile, Louis, Marion B., Olivier. Pour son regard extérieur et décalé sur nos activités de recherche et la qualité de ses clichés, merci à Benjamin Deroche artiste photographe qui nous a accompagnés pendant cette mission. Pour son prêt d'instruments de mesures et son assistance dans leurs programmations, je tenais également à remercier Shawn Hinz de la société Gravity Marine.

Revenons maintenant à Plouzané, plus exactement à l'IUEM et au LEMAR, structures qui m'ont accueillie à mon retour de Saint-Pierre et Miquelon en 2015. Merci à l'ensemble du LEMAR et plus particulièrement aux deux directeurs qui ont dirigés successivement ce laboratoire pendant ces trois années, Olivier Ragueneau et Luis Tito de Morais. Merci également aux responsables de « l'Équipe Discovery » anciennement « Équipe 3 » : François Le Loc'h, Geraldine Sarthou et Olivier Gauthier. Merci à mes supers « colocataires de bureau » qui ont su m'intégrer, d'abord au sein de celui-ci, puis du laboratoire : Ika, Fabi, Marie, Gaspard et Luc. Pour les parties de ping-pong méridiennes, digestives mais néanmoins endiablées, un grand merci à l'équipe des pongistes du LEMAR qui se reconnaitra. À mes amis thésards : Gaël, Bruno, Émilien, Marc, Valentin, Justine, Margaux, Aurélien, Élodie, Pauline, Guillaume, William et les autres… Pour leurs regards extérieurs au cours de ces trois années je voulais également remercier les membres de mon comité de thèse interne au laboratoire, Fabrice Pernet et Olivier Gauthier. Je renouvelle également mes remerciements aux deux membres externes de mon comité de suivi individuel, Philippe Gouletquer et Frédéric Olivier, pour leurs conseils avisés et le temps qu'ils m'ont consacrés. De nombreux chercheurs de ce laboratoire ont également mis leurs compétences au service de ce travail. Je tiens à remercier

en particulier Jean-Marc et Jennifer Guarini pour m'avoir constamment poussé à sortir du confort de mes certitudes. Pour le temps qu'ils m'ont consacré lors de mes réflexions sur la circulation océanique de l'Atlantique Nord, je voulais remercier Herlé Mercier, Pascal Rivière, Damien Desbruyére, et Pascale Lherminier. Je remercie également, Aurélie Jolivet, Marion Bezaud, Jean-Alix Barrat, Yves Marie Paulet, Gregory Charrier, William Handal, Gauthier Schaal, Sebastien Artigaud, Fabienne Legrand, Vianney Pichereau, Eric Dabas et Ewan Harney pour leurs influx et les nombreux échanges que nous avons eu dans le cadre de collaborations diverses. Pour leur aide précieuse lors des phases, de préparation et de retour de mission, d'achat de matériel et leur bonne humeur quotidienne. Je voulais remercier l'équipe administrative du LEMAR, du Labex et de l'IUEM: Anne-Sophie, Geneviève, Yves, Céline, Patricia, Lionel, Corinne. Un grand merci également à l'administration de l'EDSM pour son efficacité redoutable : Elisabeth et Élodie.

Au cours de cette thèse, j'ai eu la chance de gouter, pendant deux ans, aux joies de l'enseignement universitaire. Je voulais donc remercier les enseignants du département de biologie de l'UBO qui ont pris du temps pour me former à ce nouvel exercice et qui ont su me transmettre leur passion pour l'enseignement : Jean Laroche, Frédéric Jean, Philippe Pondaven, Michaël Théron et bon nombre d'enseignants chercheurs et ATER déjà cités précédemment. Toujours dans le cadre de la formation et de la transmission de connaissances, j'ai eu la chance pendant ma thèse d'encadrer deux stagiaires : Valentin Siebert et Lucie Goraguer, merci à tous les deux de m'avoir supporté. De mon côté, ça a été un véritable plaisir de travailler avec vous pendant ces quelques mois. Pour leur bonne humeur et les agréables moments partagés au PNBI, merci également aux autres stagiaires côtoyés pendant ces trois ans : Guillaume, Arthur, Pierre et Johann.

Par ailleurs, j'ai eu la chance au cours de ma thèse d'intégrer différentes structures d'accueil et de nouer des contacts avec de nombreuses personnes extérieures au « Technopôle Brest Iroise ». Pour les deux séjours passés à la Plateforme PAMAL de Pau, à mettre au point une stratégie d'analyse, la plus fine possible, des coquilles de *Placopecten magellanicus*, je veux remercier Christophe Pécheyran et Gaëlle Barbotin. Merci également à l'ensemble de l'équipe de l'IPREM pour les agréables moments passés en leur compagnie et leur incroyable gentillesse, je pense particulièrement à Manu et son estive de brebis tout simplement divine. Merci également à Messieurs Bernd R. Schöne, Eric Otto Walliser et Michael Maus de m'avoir

accueilli, au sein du département de Géosciences de l'Université de Mayence, pour partager votre expertise en matière d'analyses isotopiques. Je tenais aussi à remercier Gerard Sinquin et Philippe Eliès de la plate-forme d'imagerie et de mesures en microscopie (PIMM) de l'UBO pour leur patience, leur écoute et leur motivation lors des essais réalisés sur le microscope confocal et le MEB.

Trois ans de thèse, ce sont aussi des rencontres et des amis à l'extérieur du labo ou à la frontière entre les deux. Un grand merci à mes amis avec qui je partage ma passion pour la chasse sous-marine : Christophe, Gildas, Florian, les Jérôme(s) pour les sorties « poissons » du bord et surtout en bateau. Sans vous, je n'aurais jamais eu le plaisir de goûter aux joies de la chasse aux gros lieus à Ouessant et à la sortie des Abers. Pour toutes les heures passées ensembles sur et sous l'eau, de jour ou de nuit, je voulais remercier Youenn Jézéquel. Pendant ces quelques années, tu m'as transmis ta passion pour la recherche des crustacés bleus qui occupent une bonne partie de ta vie. J'espère que tu réussiras à mieux les comprendre pendant ta thèse... Pour les sorties de chasse sous-marine passées à traquer le « poisson roi » qu'est le mulet, les cueillettes de champignons dans les Monts-d'Arrés mais surtout pour sa gentillesse, je voulais remercier Nicolas Henry. Pour m'avoir changé les idées tout en s'intéressant à mes recherches, je voulais aussi remercier mes amis : Richard, Julie, Samuel, Paola, Adrien, les Marion(s), Morgan, Nolwenn, Camille, Damien, Vivien, Amélie, Gaël, Émilie, Victo, Élo, Tiffany, Simon, Alice, David, Manon, Benoît, Habiba, Gildas, Aurélie, Yoann, Bruno, Angela, Lionel, Laetitia, Daniel, Mélanie, Alex, Julie D., François et les autres.

Je remercie également du fond du cœur ma famille qui m'a toujours soutenu et tout particulièrement mes parents qui ont toujours été là pour moi, au risque de me voir partir pendant plusieurs années à quelques milliers de kilomètres. C'est vous qui avez su éveiller ma passion pour la mer et les mots me manquent pour vous dire ce que je ressens aujourd'hui.

Dans ces remerciements deux personnes méritent une place particulière. Tout d'abord, merci à Marion pour tes conseils, ton réconfort, ta patience, tous les sacrifices que tu as consentis et surtout, pour t'être lancé avec moi dans une magnifique aventure en donnant la vie à Malo il y a maintenant quelques mois. Ce travail de thèse est aussi un peu le vôtre et c'est pourquoi je vous le dédie.

Sclérochronologie à Saint-Pierre et Miquelon: De l'échelle sub-horaire aux reconstructions environnementales multi-décennales

Résumé

Les écosystèmes côtiers sont exposés aux changements climatiques globaux entraînant des modifications de leur structure et de leur fonctionnement. Cependant, nous disposons de peu d'information sur la variabilité de leurs propriétés physiques avant 1950, principalement à cause de l'absence de mesures *in situ* à long terme. Les parties dures des organismes marins longévifs ont le potentiel d'étendre les observations instrumentales, à différentes échelles spatiales et temporelles, afin d'améliorer notre compréhension des processus environnementaux passés.

Cette thèse de doctorat a pour cadre Saint-Pierre & Miquelon (SPM), un petit archipel situé à la confluence de grands courants océaniques marquant la frontière entre les gyres subtropicaux et subpolaires de l'Atlantique Nord. Outre sa position clé à l'échelle mondiale comme indicateur de l'évolution du climat, des spécificités locales induisent une dynamique très particulière. Le changement bathymétrique se produisant au nord-ouest de l'île de Miquelon génère la propagation anticyclonique d'une onde interne côtière piégée autour de cet archipel. Ce phénomène local conduit, au cours de la période stratifiée, à la génération des plus importantes oscillations thermiques (d'une amplitude pouvant atteindre 11,5°C) quotidiennes (25,8 h) jamais observées, quelle qu'en soit la fréquence, sur un plateau continental stratifié d'une latitude moyenne.

Ce travail est basé sur l'analyse des structures calcifiées d'organismes marins locaux, afin de mieux comprendre la variabilité environnementale passée à ces deux échelles. Tout d'abord, il convenait de s'approprier différentes méthodes sclérochronologiques. Cette étape a été réalisée à travers l'étude de *Spisula solidissima* (Chapitre 1). Puis, les variations océanographiques à grandes échelles des dernières décennies ont été étudiées en utilisant le bivalve et l'algue calcaire présentant les plus longues périodes de croissance connues à ce jour, *Arctica islandica* (Chapitre 2) et *Clathromorphum compactum (*Chapitre 3), respectivement. Les relations observées entre les enregistrements sclérochronologiques issus de ces deux modèles biologiques et plusieurs types de données environnementales acquises à différentes échelles géographiques, nous ont permis de mieux décrire la variabilité océanographique à grande échelle ainsi que ses impacts sur la dynamique des écosystèmes infralittoraux de SPM. Enfin, les effets des oscillations locales de température à haute fréquence (25,8 h) ont été suivis à l'aide des informations sclérochimiques contenues dans la coquille de *Placopecten magellanicus* (Chapitre 4), une espèce de bivalve présentant une croissance coquillère extrêmement rapide (500 µm / jour).

Cette étude a, *in fine*, mis en avant la position privilégiée de SPM pour étudier la variabilité océanographique, les réponses biologiques de différentes espèces benthiques et la dynamique des écosystèmes côtiers, à différentes échelles de temps (de celle de la marée aux 165 dernières années) et d'espace (de celle de l'archipel à celle de l'Atlantique Nord).

Mots clefs : Sclérochronologie, Changement climatique, Atlantique Nord, proxies environnementaux, Océanographie, Saint-Pierre et Miquelon

Sclerochronological approaches in Saint-Pierre & Miquelon: from sub-hourly to multidecadal environmental reconstructions

Abstract

Coastal ecosystems are exposed to global climate change leading to modifications of their structure and functioning. However, little is known about the variability of their physical properties before 1950, mainly because of the lack of long-term instrumental measurements. The hard parts of long-lived marine *biota* hold the potential to extend instrumentally derived observations, at different temporal and spatial resolutions, in order to enhance our understanding of past environmental processes.

This PhD dissertation takes place on Saint-Pierre & Miquelon (SPM), a small archipelago at the confluence of major oceanic currents marking the boundary between the North Atlantic Ocean subtropical and subpolar gyres. In addition to its global key position, the abrupt bathymetric change occurring in the North West of Miquelon Island generates the anti-cyclonic propagation of a tidal coastal trapped wave around this archipelago. This local phenomenon, leads during the stratified period to the largest (up to 11.5°C amplitude) daily (25.8 h) temperature oscillations ever observed-at any frequency-on a stratified mid latitude continental shelf.

This work is based on the analyses of local marine biota hard parts to gain insights about past environmental variability at these two scales. First, I have learned different sclerochronological methods through *Spisula solidissima* study (Chapter 1). Global and multi-decadal time scales were reached using the longest lived bivalve known to date *Arctica islandica* (Chapter 2), and *Clathromorphum compactum* a newly discovered long-lived coralline alga (Chapter 3). The relationships observed at SPM between *A. islandica* and *C. compactum* sclerochronological records and different geographical scales environmental datasets yield details about past large-scale oceanographic variability and ecosystem dynamics. Local, high-frequency (25.8 h) temperature oscillations were tracked using sclerochronological information contained in *Placopecten magellanicus* (Chapter 4) a fast growing (ca. 500 µm / day) bivalve species.

This study points out the relevant position of this archipelago for studying multiple scale oceanographic variability, biological responses and ecosystem dynamics facing global changes.

Keywords: Sclerochronology, Climate change, North Atlantic, environmental proxies, Labrador Current, Saint-Pierre and Miquelon, Coastal Trapped Wave.

Table des matières :

Introduction : 1

Les changements climatiques globaux et l'océan 2

Circulation océanique de l'Atlantique Nord 3

Les oscillations thermiques à l'interface eau/sédiment 7

Saint-Pierre et Miquelon à l'interface de ces deux échelles 8

L'apport de la sclérochronologie 10

Les différentes espèces étudiées 14

Objectifs et structure de la thèse 19

Références 22

Chapitre 1 : Ligament, hinge, and shell cross-sections of the Atlantic surfclam (*Spisula solidissima*): Promising marine environmental archives in NE North America 34

Contexte et résumé de l'étude 34

Abstract 37

Introduction 38

Materials & Methods 40

Results 46

Discussion 54

Conclusions 58

Acknowledgements 58

References 59

Chapitre 2 : Growth response of *Arctica islandica* to North Atlantic oceanographic conditions since 1850 67

Contexte et résumé de l'étude 67

Abstract 70

Introduction 71

Materials & Methods 72

Results 78

Discussion 83

Acknowledgements 88
References 89

Chapitre 3 : Do *Clathromorphum compactum* growth patterns and geochemical composition archive Saint-Pierre & Miquelon environmental variabilities? 97
Contexte et résumé de l'étude 97
Abstract 100
Introduction 101
Materials & Methods 104
Results 112
Discussion 121
Acknowledgements 126
References 128

Chapitre 4 : A new ultra-high resolution method developed to track trace elements variations in *Placopecten magellanicus* associated to large diurnal bottom temperature oscillations 135
Contexte et résumé de l'étude 135
Abstract 138
Introduction 139
Materials & Methods 141
Results 144
Discussion 150
Conclusion 154
Acknowledgements 155
References 156

Discussion générale : 163
Suivi des variations environnementales à grande échelle 163
Suivi des variations environnementales à l'échelle sub-horaire 170
Références 178

Introduction

Introduction

Ce manuscrit rassemble la majorité des travaux de recherche effectués durant mon doctorat. Tous sont centrés sur les réponses d'invertébrés benthiques aux variations environnementales et leur aptitude à les enregistrer. Le choix du site d'étude et des modèles biologiques a été conditionné par notre volonté de considérer simultanément différentes échelles spatiales et temporelles. Cela a été fait pour plusieurs raisons essentielles, définies en amont de notre discipline initiale qu'est l'écologie marine.

Les changements climatiques globaux et l'océan

Connaître le climat pour en comprendre les effets est un défi auquel les sociétés humaines se sont attelées depuis longtemps. Étant donné son influence, sur la température de l'air, les principaux cycles biogéochimiques dont celui de l'eau, la végétation et une multitude d'autres variables qui déterminent la qualité de notre environnement, il est aisé d'en identifier l'importance pour la survie de nos sociétés. Or, depuis le début de l'ère industrielle, les activités humaines modifient drastiquement le climat, notamment à travers les émissions de gaz à effet de serre et d'aérosols dans l'atmosphère (Hartmann *et al.*, 2013). Les manifestations de ces changements globaux sont visibles autour du monde et affectent de nombreuses composantes de nos sociétés. Celles-ci peuvent-être environnementales mais aussi socio-économiques et même géopolitiques (Jeandel & Mosseri, 2011).

Le système climatique comprend cinq grandes enveloppes (compartiments) : l'atmosphère, l'hydrosphère, la cryosphère, la lithosphère et la biosphère, qui interagissent entre elles via plusieurs types d'échanges. Depuis quelques dizaines d'années d'importants progrès ont été réalisés en météorologie de concert avec l'océanographie. Ces travaux ont permis une compréhension plus fine des composantes physiques du système climatique. L'étude de l'atmosphère se base sur les observations du réseau mondial des stations météorologiques mis en place à la fin du 19ème siècle par l'Organisation Mondiale de la Météorologie. En revanche, les observations et études océanographiques sont plus contemporaines. En effet, jusqu'au début des années 1960, l'océan était considéré comme un milieu passif répondant au forçage de l'atmosphère. Aujourd'hui, on sait au contraire que l'océan est une composante essentielle du système climatique, qu'il module à différentes échelles, de par sa nature et ses interactions avec l'atmosphère. Ces interactions peuvent être quantifiées et leurs évolutions

prédites à travers le développement de modèles numériques basés sur les équations de la dynamique des fluides.

Actuellement, les principaux modèles couplés océan/atmosphère destinés à prévoir les changements environnementaux futurs ont des résolutions spatiales relativement faibles de l'ordre de la centaine de kilomètres (Flato *et al.,* 2013). Ce type de modélisation peut alors affecter la représentation de phénomènes régionaux ayant une influence majeure sur les projections climatiques futures (Stock *et al.*, 2011). C'est notamment le cas dans l'Atlantique Nord-Ouest, en particulier sur le plateau continental Nord-Américain où les modèles climatiques globaux possèdent un biais chaud en matière de représentation des températures de surface de l'océan (Wang *et al.*, 2014). Connu sous le nom de « Gulf Stream separation problem » (Dengg *et al.*, 1996) ce biais continu à exister dans de nombreux modèles climatiques globaux ayant une trop faible résolution spatiale de la composante océanique (Bryan *et al.*, 2007). On comprend alors l'intérêt d'étudier le passé hydrologique de cette région pour en comprendre la dynamique et ainsi réussir à en affiner la modélisation. Il convient donc de revenir à la distribution des masses d'eau et à la nature des courants de l'Atlantique nord.

Circulation océanique de l'Atlantique Nord

L'Océan Atlantique Nord contribue à la régulation du climat mondial à travers son rôle majeur dans la circulation thermohaline globale (Fig. 1) (Broeker, 1991). Les eaux de surface chaudes et salées venant des tropiques sont transportées vers le nord, elles se refroidissent alors peu à peu par le transfert de chaleur vers l'atmosphère. Cette perte de chaleur va alors entrainer une augmentation de la densité de ces eaux tropicales qui vont couler par convection. Les eaux profondes arctiques résultant de ce mélange vont ensuite alimenter un courant froid et profond se dirigeant vers le sud. Bien qu'induite principalement par ces changements de température des eaux de surface, la salinité joue également un rôle dans ce phénomène de convection. En effet, les eaux tropicales plus salées sont également plus denses que les eaux polaires dont les salinités sont moins élevées.

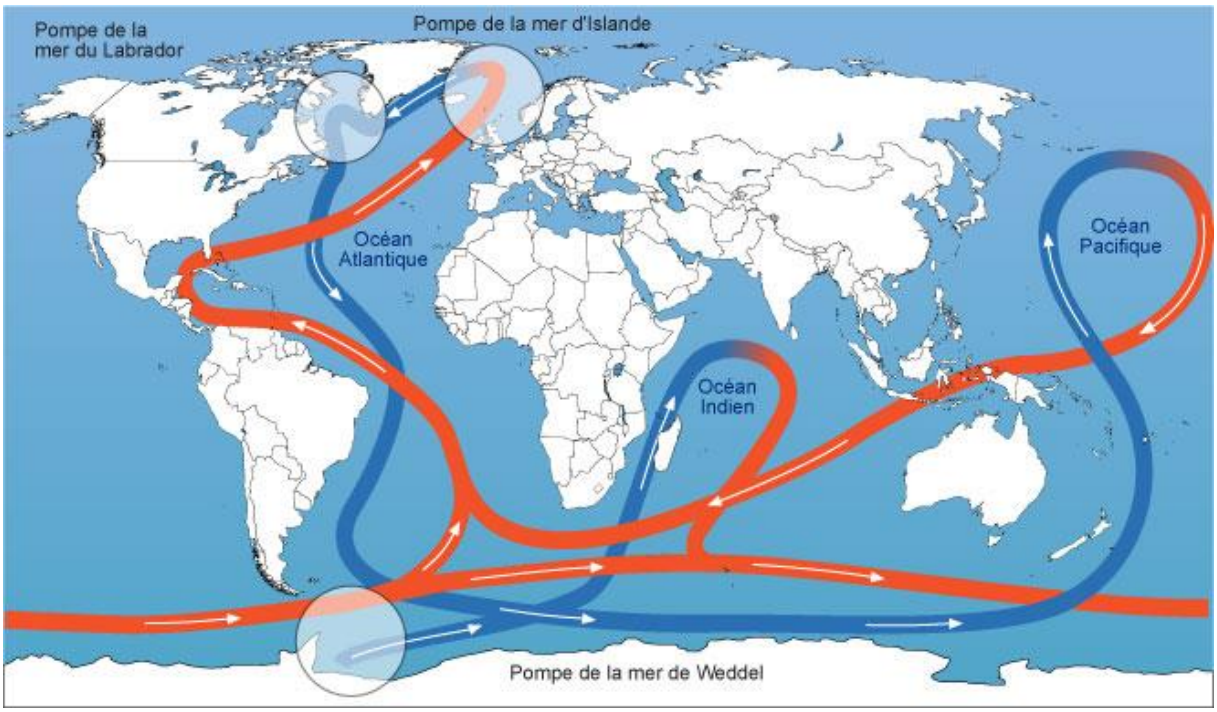

Figure 1 : Schéma de la circulation océanique thermohaline globale. Les courants chauds de surface sont représentés en rouge et ceux de fond plus froids en bleu. Les principaux sites de convection sont indiqués par des cercles plus clairs (Source : IPCC).

La circulation des eaux de surface dans l'Atlantique Nord est principalement contrôlée par les vents qui entrainent mécaniquement l'eau dans leurs mouvements. Ces forçages atmosphériques interviennent dans les 500 premiers mètres de la colonne d'eau et donnent naissance à de grands systèmes océaniques que sont les gyres subtropical et subpolaire. Le gyre subtropical est un vaste tourbillon qui entraine les eaux de surface dans le sens anticyclonique (sens des aiguilles d'une montre) aux basses latitudes. Tandis que le gyre subpolaire circule dans le sens cyclonique aux hautes latitudes (Fig. 2).

Plus précisément, la circulation océanique de l'Atlantique Nord commence à l'ouest par le courant Nord Atlantique (NAC). Le NAC est l'extension vers le Nord-Est du Gulf Stream. La branche principale du NAC traverse la ride médio Atlantique vers 53°N (Schott *et al.*, 2004). Une partie du NAC descend vers le Sud-Est pour alimenter le gyre subtropical, tandis que l'autre partie alimente le gyre subpolaire et les mers nordiques en bifurquant respectivement vers le Nord-Ouest et le Nord-Est. La branche alimentant le gyre subpolaire rejoint le courant d'Irminger sur le flanc Ouest de la dorsale de Reykjanes (Bower *et al.*, 2002). Le courant d'Irminger rejoint la Mer du Labrador en longeant les côtes Groenlandaises. Ces eaux sont

entrainées par le courant Ouest Groenlandais qui circule de manière cyclonique en suivant la bathymétrie de la Mer du Labrador (Cury *et al.*, 2002). Le long des côtes de Terre-Neuve et Labrador, depuis le détroit d'Hudson jusqu'au Sud des Grands Bancs de Terre-Neuve, circule le courant du Labrador. Il transporte les eaux froides et peu salées de la baie de Baffin ainsi qu'une partie des eaux plus salées du courant Ouest Groenlandais du Nord vers le Sud (Lazier & Wright, 1993 ; Han *et al.*, 2008). Sa structure spatiale et son évolution sont très complexes. Il est composé de deux branches principales. La plus importante est la branche offshore qui s'écoule, vers le sud, sur la bordure Est du talus continental des côtes du Labrador et de l'Est de Terre Neuve pour rejoindre le NAC complétant ainsi la boucle du gyre subpolaire. La branche inshore, dont le volume transporté est dix fois plus faible que celui de la branche offshore, s'écoule sur le plateau continental des côtes de Terre-Neuve et Labrador (Lazier & Wright, 1993).

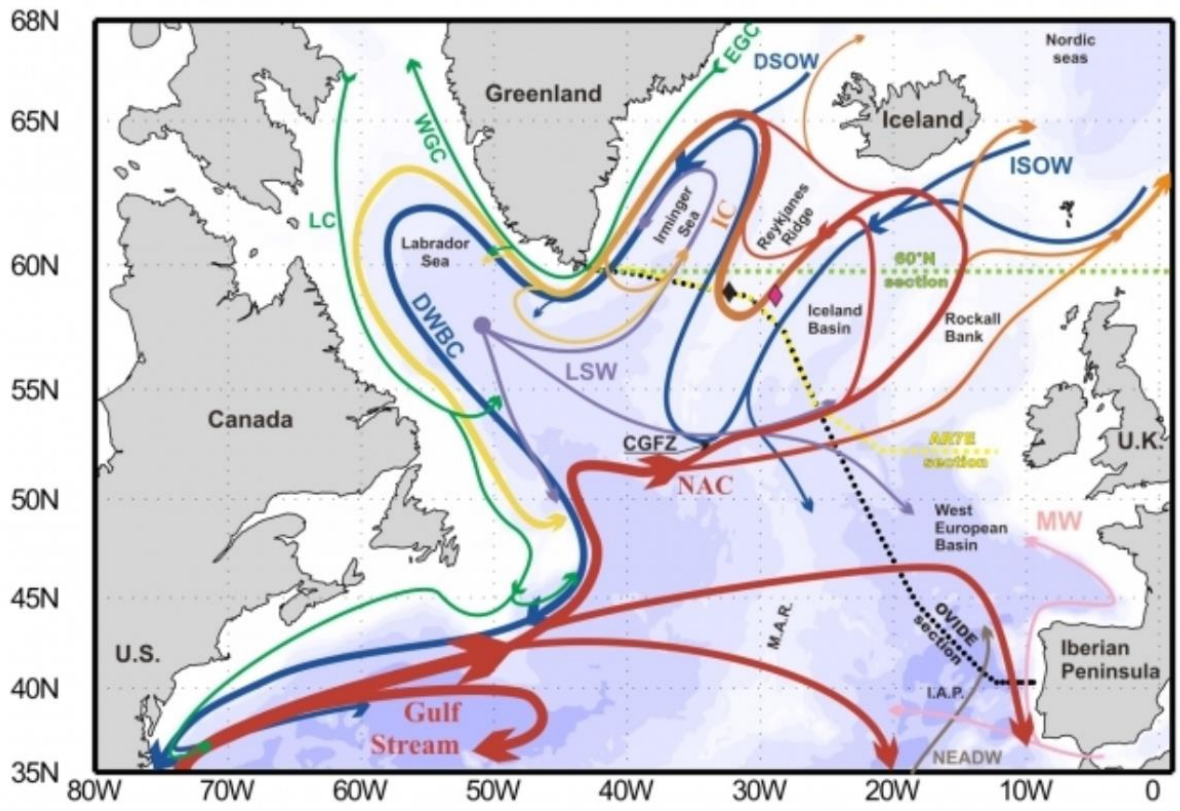

Figure 2 : Schéma de la circulation océanique dans l'Atlantique Nord. Les principaux acronymes utilisés sont les suivants : courant Nord Atlantique (NAC), courant d'Irminger (IC), Courants Est et Ouest du Groenland (respectivement EGC et WGC) et courant du Labrador (LC). (Source : Figure 1 de Daniault *et al.*, 2016)

Ce système n'est bien entendu pas statique et varie de manière saisonnière et interannuelle dans son intensité. À une échelle interannuelle, la circulation océanique de l'Atlantique Nord varie en fonction de deux composantes majeures (Penduff *et al.*, 2011) : une première composante intrinsèque due au caractère turbulent de l'océan et une seconde forcée, induite par la variabilité atmosphérique.

Dans l'Atlantique Nord le mode de variabilité atmosphérique dominant est l'Oscillation Nord Atlantique (NAO) (Hurrell, 1995). La NAO est un indice représentant des oscillations de pressions entre l'anticyclone des Açores et la dépression d'Islande (Hurrell, 1995). Un affaiblissement de ces deux systèmes est associé à un indice NAO négatif (Fig. 3). Au contraire, un creusement de la dépression d'Islande associé à un gonflement de l'anticyclone des Açores correspond à une phase positive de la NAO. Celle-ci s'accompagne d'une augmentation de l'intensité des vents d'Ouest entre 40°N et 60°N et d'un renforcement des alizés dans les subtropiques (Fig. 3). Cette oscillation est en général plus forte pendant les mois d'hiver durant lesquels la dynamique atmosphérique est exacerbée.

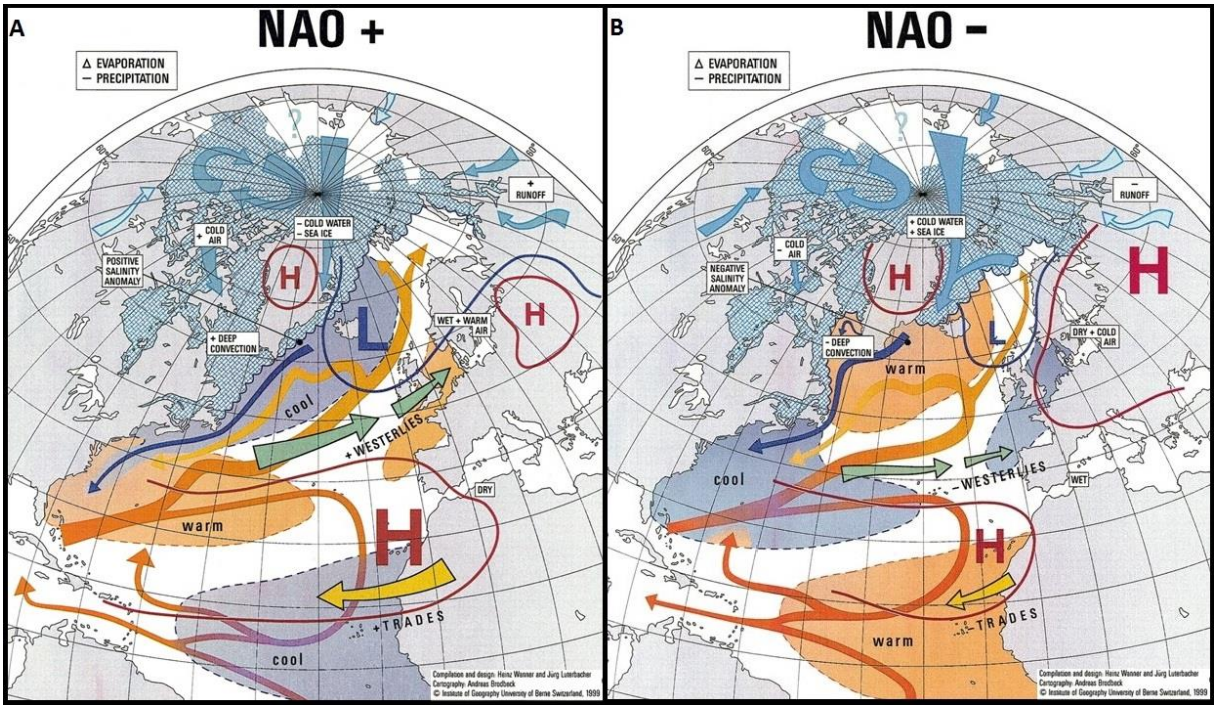

Figure 3 : Représentations graphiques des phases positive (A) et négative (B) de la NAO (Source : Figure 9 de Wanner *et al.*, 2001).

À la différence de la NAO qui est un forçage atmosphérique, l'oscillation pluri décennale Atlantique (AMO) est un indice représentant des variations de la température des eaux de

surface de l'Atlantique Nord entre l'équateur et 70°N. L'AMO varie en fonction de plusieurs composantes, une première endogène liée aux fluctuations de la circulation thermohaline globale relatives aux transports de glace de mer et d'eau douce en provenance de l'Arctique (Dima & Lohmann, 2007). L'AMO inclut également une seconde composante due aux forçages exogènes anthropiques tels que les émissions de gaz à effet de serre et d'aérosols (Booth *et al.*, 2012). Quelles que soient l'origine des différentes composantes de l'AMO, ses fluctuations sont associées à de nombreux phénomènes climatiques (Knight *et al.*, 2006).

De plus en plus d'études s'intéressent donc aux interactions Océan/Atmosphère en confrontant l'évolution de ces deux indices (AMO/NAO). La majorité de celles-ci suggèrent que l'AMO et la NAO hivernale sont corrélés négativement (e.g. Gastineau *et al.*, 2013 ; Msadek *et al.*, 2011) et que les phases positives de l'AMO diminuent la circulation atmosphérique dans l'Atlantique Nord et donc la NAO (Hakkinen *et al.*, 2011).

Il convient ici de noter que si cette variabilité à grande échelle est susceptible d'impacter des écosystèmes hauturiers, elle affecte également l'environnement côtier.

Les oscillations thermiques à l'interface eau/sédiment

Des oscillations thermiques à l'interface eau/sédiment ont déjà été observées dans de nombreuses zones côtières. Celles-ci ont majoritairement lieu dans des environnements stratifiés et possèdent un large spectre harmonique haute-fréquence qui va de quelques heures à plusieurs jours (Leichter *et al.*, 2012 ; Mihanovic *et al.*, 2009 ; Mihanovic *et al.*, 2014 ; Wall *et al.*, 2012 ; Wang *et al.*, 2007). Dans les régions côtières de la plupart des plateaux continentaux, les oscillations thermiques à l'interface eau/sédiment sont généralement faibles, de l'ordre de quelques degrés. Les plus fortes ont été observées au niveau du front de marée du Banc Georges où elles peuvent atteindre 7°C à 60m avec une fréquence semi-diurne (Guida *et al.*, 2013) et (ii) sur les côtes Californiennes où des oscillations de 6°C ont lieu de manière diurne et semi-diurne à 15 m de profondeur (Pineda, 1994).

Plusieurs facteurs, tels que les marées et les vents ont été proposés pour expliquer ces observations, en fonction de la stratification, de la fréquence de ces oscillations et de la latitude (force de Coriolis). La majorité des oscillations périodiques a été attribuée à la marée, majoritairement semi diurne sur le plateaux continentaux bien qu'en certaines régions (côte de l'Oregon, NW Ecosse,...), les ondes diurnes puissent dominer et se confondre avec les effets

des brises marines quotidiennes (Cudaback & McPhee-Shaw, 2009 ; Mihanovic *et al.*, 2006 ; Orlic *et al.*, 2013). Aux latitudes moyennes, les oscillations diurnes sont sous-inertielles (la période diurne ~24h est supérieure à la période d'inertie ~17h par 47°N). Différentes théories montrent que ces oscillations ne peuvent se propager librement. Elles sont piégées par la topographie, peuvent générer de forts courants diurnes et ne peuvent se propager qu'en laissant la côte sur leur droite dans l'hémisphère nord. Il s'agit alors d'ondes côtières piégées (CTW) qui apparaissent généralement dans les zones où la topographie est accidentée. De plus, lorsque la zone d'intérêt présente des contours topographiques fermés, comme c'est le cas pour un mont sous-marin ou une île, cela peut entrainer une amplification des CTW (Huthnance, 1974 ; Mihanovic *et al.*, 2009 ; Mihanovic *et al.*, 2014).

Saint-Pierre et Miquelon à l'interface de ces deux échelles

Dans ce contexte, Saint-Pierre et Miquelon (SPM) (Fig. 4) se situe sur le plateau continental Nord-Américain et à l'intersection des courants du Gulf Stream et du Labrador qui jouent un rôle clef dans la circulation Nord Atlantique décrite précédemment. Cependant, à notre connaissance, cet archipel n'a jamais fait l'objet d'étude océanographique spécifique. Ce n'est que très récemment que des suivis environnementaux locaux, dédiés à l'aquaculture, ont permis de mettre en évidence la présence d'oscillations thermiques quotidiennes supérieures à 10°C à proximité du fond pendant l'été.

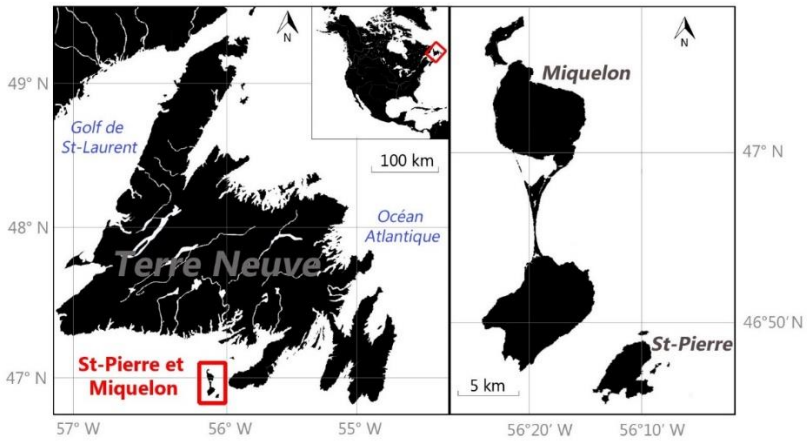

Figure 4 : Situation géographique de l'archipel de Saint-Pierre et Miquelon (Source : Poitevin et al., 2018).

À SPM la colonne d'eau est stratifiée uniquement en été. Les températures de surface sont aux alentours de 2°C au milieu du printemps puis vont se réchauffer jusqu'à atteindre leur maximum autour de 15°C à la fin de l'été pour ensuite redescendre vers 8°C à la mi-novembre. Les températures de fond présentent quant à elles des variations hautes fréquences dont l'amplitude augmente en même temps que les températures de surface. Pendant les deux premières semaines de septembre, l'amplitude de ces oscillations est la plus forte avec un maximum de 11.5°C à 60m et 9.5°C à 30m le 7 septembre 2011 (Fig. 5).

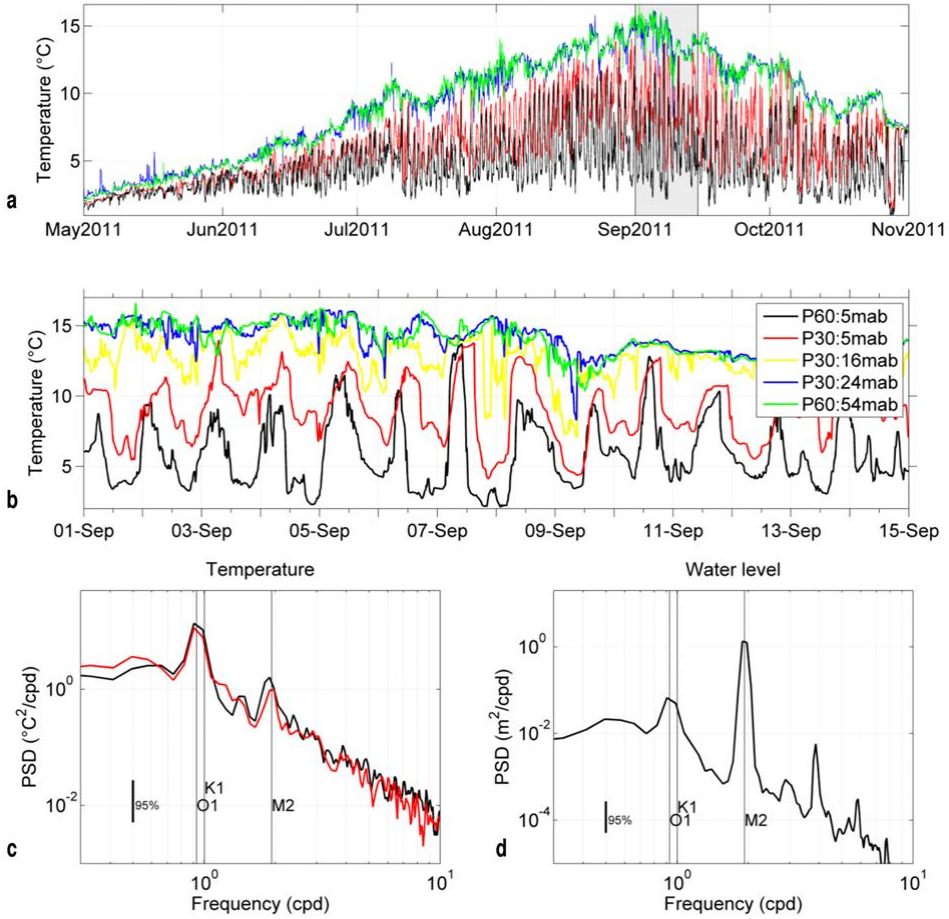

Figure 5 : (a)-Séries de mesures de 2011 présentant les températures à 6m sous la surface (courbes bleu et verte) et à 5m au-dessus du fond (courbes rouge et noire) aux stations 30m et 60m, respectivement, situées à la sortie de la rade de Miquelon. (b)-Zoom sur les deux premières semaines de septembre 2011 (grisées en (a)) avec en plus un enregistrement des températures 16m au-dessus du fond (mab) à la station 30m (courbe jaune). (c)-Analyse spectrale des températures de fond du 1er au 15 août 2011à 30m (courbe rouge) et 60m (courbe noire). (d)-Analyse spectrale du niveau de la mer pendant la même période. (Source : Lazure *et al.*, 2018)

Une analyse spectrale a permis d'identifier les fréquences dominantes de ces oscillations thermiques (Fig. 5). Celle qui influence principalement ces variations est de 0.93 cycle par jour (cpd) soit 25.82 h ce qui correspond à la fréquence de l'onde de marée O1. La seconde est de 1 cpd et correspond à l'onde K1 tandis que l'onde M2 (1.93 cpd) qui influence principalement les niveaux a beaucoup moins d'importance sur la régulation des oscillations thermiques. La marée semble donc être à l'origine de ces variations périodiques de température dans la colonne d'eau à SPM, le vent jouant un rôle certainement très secondaire. La génération de ce phénomène à SPM peut s'expliquer par la présence, sur la pente continentale du plateau de Terre Neuve, d'une onde côtière de plateau de mode 1 (Han, 2000 ; Wright & Xu, 2004 ; Xu & Loder, 2004). Le changement bathymétrique brutal qui se produit au Nord-Ouest de l'île de Miquelon affecte probablement la propagation de cette onde. Ce changement pourrait alors aboutir à la propagation dans le sens horaire d'une onde côtière piégée autour de l'archipel. SPM pourrait ainsi être résonnant à la période O1, avec un mode azimutal 2 (ce qui correspond à deux longueurs d'onde le long du périmètre de SPM) et un mode cross-shore 1 (Lazure *et al.*, 2018). Ces observations sont assez similaires à celles déjà rapportées sur le Banc de Rockall (Huthnance, 1974) et autour de l'île de Latsovo en mer Adriatique (Mihanovic *et al.*, 2014) à la différence près qu'autour de l'archipel de SPM, l'amplitude des oscillations de température près du fond est largement supérieure. Néanmoins d'autres mécanismes sont susceptibles d'affecter la propagation de ces ondes, tels que : des changements de stratification, des forçages atmosphériques, ou encore des spécificités bathymétriques.

L'apport de la sclérochronologie

C'est dans ce contexte hydroclimatique complexe, où la variabilité des circulations atmosphériques et océanographiques se superposent à des oscillations locales diurnes que nous plaçons ce travail sclérochronologique. En effet, les reconstructions hydroclimatiques à SPM aux deux échelles spatiales (de la dizaine de centimètres au bassin Nord Atlantique) et temporelles (de l'heure au siècle) considérées précédemment, nous permettraient de calibrer de nouveaux outils sclérochronologique et de mieux comprendre le fonctionnement passé de cet écosystème afin d'en anticiper l'évolution future en fonction des différents scenarios de l'évolution du climat envisagés par le GIEC.

Reposant sur l'étude des profils de croissance et des propriétés physico-chimiques des structures calcifiées bio-construites des organismes, la sclérochronologie (du Grec skleros : dur ; khronos : temps ; logos : parole) offre des informations, sur l'autoécologie des organismes étudiés, sur l'environnement passé dans lequel ils ont vécu et dans certains cas sur l'usage fait de ces organismes par les sociétés humaines passées. Les principales caractéristiques qui rendent les mollusques bivalves particulièrement intéressants pour ce type d'études sont, en plus du caractère pérenne de leurs exosquelette et de leur apparition au cambrien il y a 500 millions d'années : (a) leurs larges répartitions géographiques ; (b) la diversité de leurs modes de vie ; (c) le caractère périodique de leur croissance et le synchronisme de celle-ci entre les individus d'une même population ; (d) l'extraordinaire longévité de certaines espèces et (e) le caractère emblématiques de leurs coquilles pour les sociétés humaines passées.

Au cours de leur vie, les mollusques bivalves croissent par incréments successifs en précipitant du carbonate de calcium ($CaCO_3$) le long de la marge ventrale de leurs coquilles. Cette croissance coquillière n'est pas linéaire et ralentie ou cesse à intervalles réguliers. C'est lors de ces périodes que de la matière organique s'accumule au niveau de la zone d'accrétion coquillière, formant des lignes appelées lignes de croissance (Fig. 6) (Clark, 1974 ; Checa, 2000). Ces lignes de croissance se forment à des échelles temporelles sub-journalières à annuelles (Schöne & Surge, 2012) et sont le résultat d'une combinaison de facteurs physiologiques et environnementaux (e.g. Lutz & Rhoads, 1980 ; Steinhardt *et al.,* 2016). On appelle « incrément de croissance » la portion de coquille contenue entre deux de ces lignes (Fig. 6) et leurs largeurs reflètent différents taux de croissance qui sont calculés en utilisant des outils mathématiques issus d'études dendrochronologiques.

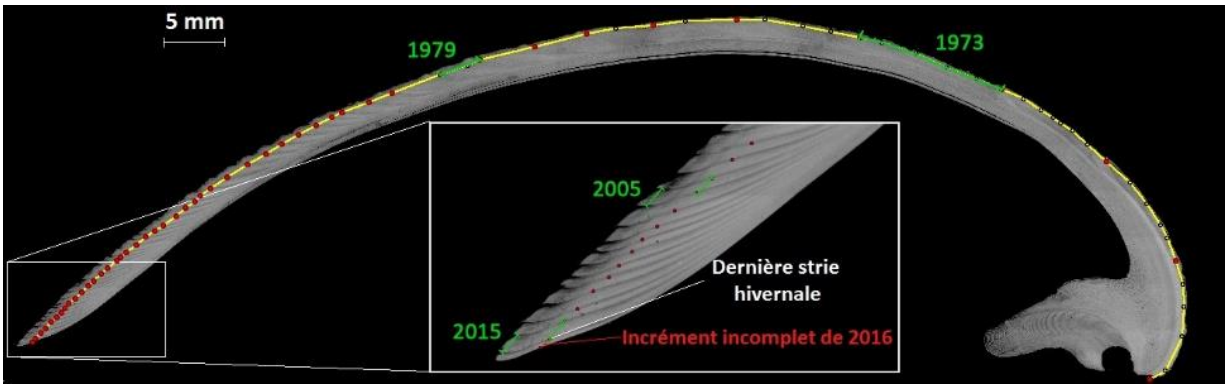

Figure 6 : Coupe suivant l'axe de croissance maximale d'un spécimen d'*Arctica islandica* collecté à SPM en 2016 (ce travail). La ligne jaune indique la trajectoire sur laquelle les lignes de croissance ont été placées (points rouges). Les segments verts correspondent à quelques exemples d'incréments de croissance mesurés associés à une année.

Il est admis que pendant les périodes de l'année où les conditions environnementales sont en adéquation avec les besoins physiologiques de l'espèce étudiée, le taux de croissance de celle-ci est plus important qu'en période de stress métabolique (Schöne, 2008). Ainsi dès lors que les exigences physiologiques d'une espèce sont connues et que l'on peut associer une date précise à un incrément de croissance (date de récolte d'un individu vivant). Ces variations de croissance peuvent nous renseigner sur les conditions environnementales passées. Cependant, la croissance des bivalves ne dépend pas seulement des conditions environnementales mais aussi de l'ontogénie (Schöne, 2008). En effet, leur taux de croissance diminue de manière exponentielle tout au long de leur vie en suivant une trajectoire propre à chaque espèce (e.g., Peharda *et al.*, 2012) et à chaque individu (e.g., Witbaard *et al.*, 1997). Cette décroissance peut être soustraite aux autres informations en comparant les mesures brutes d'incréments à des valeurs théoriques issues de différents modèles mathématiques. Ces modèles peuvent avoir des fondements biologiques comme les équations de von Bertalanffy (von Bertalanffy, 1938) ou être purement théoriques comme des splines cubiques (Schöne *et al*., 2003). Une fois cette tendance retirée, les taux de croissance ainsi obtenus sont à même de fournir des informations sur des phénomènes environnementaux passés qui ont eu lieu ces dernières décennies (Ramsay *et al.,* 2000; Strom *et al.*, 2005; Brocas *et al.*, 2013), siècles (Wanamaker *et al.*, 2008 ; Reynolds *et al.*, 2013 ; Bonitz *et al.*, 2018) ou millénaires lorsque des chronologies de croissances d'individus fossiles chevauchent celles de coquilles contemporaines (Butler *et al.,* 2013; Holland *et al.*, 2014).

Les lectures de croissance peuvent également servir de cadres temporels lors de la réalisation d'analyses géochimiques de la coquille. En effet, après une phase de calibration, la composition isotopique et élémentaire des coquilles va pouvoir nous renseigner sur différents paramètres environnementaux passés tels que : la température et la salinité (e.g. Carré *et al.*, 2005 ; Wanamaker *et al.*, 2008 ; Jolivet *et al*., 2015,Reynolds *et al*., 2017), la production primaire (e.g. Thébault *et al.*, 2009 ; Barats *et al.*, 2009 ; Thébault & Chauvaud, 2013) et différents types de pollutions (e.g. Carriker *et al*., 1980, Vander Putten *et al*., 2000 ; Gillikin *et al.*, 2005 ; Dunca *et al.*, 2009 ; Holland *et al.*, 2014). Concernant la température, plusieurs études ont essayé d'utiliser la composition en éléments traces des coquilles (Sr/Ca, Mg/Ca) pour reconstruire des variations passées de ce paramètre (e.g. Hart & Blusztajn, 1998; Gillikin *et al.*, 2005; Schöne, 2008). Or, les variations des ratios Sr/Ca et Mg/Ca dans la coquille dépendent aussi de l'espèce étudiée (Freitas *et al.*, 2008), de l'organisation cristallographique de la coquille (Surge & Walker, 2006; Schöne *et al.*, 2013) et donc du taux de croissance (Lorrain *et al*., 2005) et de l'ontogénie (Freitas *et al*., 2005). La température peut également être reconstruite grâce à la composition en $\delta^{18}O$ de la coquille (e.g Dorman & Gill, 1959; Arthur *et al*., 1983; Steuber, 1996) qui est relativement proche de celle du milieu dans lequel celle-ci a été minéralisée (Mook & Vogel, 1968; Grossman & Ku, 1986; Lécuyer *et al.*, 2012). Ainsi, contrairement aux ratios élément/calcium, la composition en isotopes de l'oxygène de la coquille n'est pratiquement pas influencée par la physiologie de l'animal (e.g., Goodwin *et al*., 2001; Surge *et al.*, 2001; Schöne *et al*., 2004). Cependant, estimer des paléotempératures à partir de valeurs isotopiques de l'oxygène d'une coquille peut également être complexe car celles-ci nous renseignent simultanément sur, la signature isotopique de la masse d'eau, la température et la salinité. Par conséquent, il est possible d'estimer correctement les températures passées que si le $\delta^{18}O$ du milieu est connu et la salinité constante ou elle aussi connue, ce qui est rarement le cas.

Dans le cadre de cette thèse, nous avons cherché à croiser des informations sclérochronologiques issues d'une algue calcaire encroûtante et de plusieurs espèces de bivalves toutes présentes à SPM et ayant différentes spécificités écologiques. Le choix des espèces, outre l'homogénéité de lieu, était conditionné par la double contrainte d'une reconstruction paléoenvironnmentale sur des fréquences variables et d'une nécessité de validation croisée des résultats obtenus.

Les différentes espèces étudiées

Arctica islandica

Le quahog nordique (*Arctica islandica*) dont la hauteur coquillière peut être supérieure à 10 cm est l'un des plus grands bivalves de l'Atlantique Nord (Fig. 7). C'est également l'espèce animale non coloniale présentant la plus longue période de croissance connue à ce jour, avec un individu islandais dont l'âge a été estimé à 507 ans (Butler *et al.*, 2013). On retrouve ces animaux fouisseurs dans des sédiments meubles plus ou moins grossiers (Lutz *et al.*, 1981) de la zone intertidale (Lutz *et al.*, 1981) jusqu'à des profondeurs supérieures à 500m (Nicol, 1951). C'est une espèce poïkilotherme dont le spectre de tolérance thermique est compris entre 1 et 16°C. Cependant, des individus matures sexuellement peuvent tolérer des températures supérieures à 20°C (Loosanoff, 1953) ce qui n'est pas le cas des larves dont le développement est optimal entre 13 et 15°C (Lutz *et al.*, 1982). Dans ces conditions le développement larvaire ne dure que 32 jours tandis qu'entre 8.5 et 10°C celui-ci dure 55 jours (Lutz *et al.*, 1981). *A. islandica* est également une espèce euryhaline et supporte des salinités comprises entre 22 et 35 PSU (Winter, 1969). Toutes ces spécificités expliquent la large distribution biogéographique d'*A. islandica* sur les bords Est et Ouest de l'Atlantique Nord. On trouve donc cette espèce sur la façade Est des côtes américaines de la Caroline du Nord (USA) aux côtes Sud de Terre-Neuve (Canada), ainsi que sur les côtes Européennes de la Norvège jusqu'au Golfe de Gascogne en incluant, les îles Britanniques, Féroé, Shetland, l'Islande et le Svalbard (Dahlgren *et al.*, 2000).

Figure 7 : Photo *in situ* d'*A. islandica* à Saint-Pierre et Miquelon (Source : E. Amice/CNRS).

Clathromorphum compactum

L'algue rouge encroûtante (*Clathromorphum compactum*) a une structure filamenteuse classique commune à la plupart des rhodophycées. Ses filaments cellulaires, comme ceux des différentes espèces du genre *Clathromorphum*, fusionnent entre eux au sein d'une matrice de calcite magnésienne (Adey *et al*., 2013). Ces algues calcaires se développent sur les fonds rocheux arctiques et subarctiques (Fig. 8), de l'Atlantique et du Pacifique, entre 0 et 40 m de profondeur (Adey *et al.,* 2013). La répartition géographique de cette espèce s'étend alors du Nord-Est de l'île d'Hokkaido (Japon) jusqu'au milieu du Golf du Maine (USA) (Adey *et al*., 2008). La croissance annuelle de cette algue est constante au cours du temps, relativement lente et majoritairement dépendante de la température et de la lumière (Adey *et al.,* 2013). Celle-ci est comprise entre 300 et 400 µm d'épaisseur par an autour des îles Aléoutiennes mais peut être inférieure à 100 µm en Arctique (Adey *et al.,* 2013). Pour se reproduire cette algue forme des structures reproductrices non calcifiées qui sont appelées conceptacles. Celles-ci peuvent être dispersées ou réparties de manière dense sur la surface du tissu périthallial. Ces structures reproductrices commencent leur développement au début de l'automne indépendamment de la latitude où elles se trouvent (Adey *et al.,* 2013). Elles se développent

vers le haut et restent enfoui dans ce tissu contenant du carbonate jusqu'à leurs maturités (Adey, 1965). Ces végétaux se reproduisent tout au long de leur vie et peuvent atteindre une longévité supérieure à 600 ans (Halfar, *et al*., 2013).

Figure 8 : Photo illustrant le prélèvement d'un spécimen de *C. compactum* à Saint-Pierre et Miquelon (Source : E. Amice/CNRS).

Spisula solidissima

La mactre de l'Atlantique (*Spisula solidissima*) est le plus grand bivalve de l'Atlantique Nord-Ouest (Fig. 9). Celui-ci peut atteindre la taille maximale de 226 mm et vivre jusqu'à 37 ans (Ropes & Jearld, 1987). Son aire de distribution s'étend de la baie de Gaspé dans le golfe du Saint-Laurent (Canada) au Cap Hatteras en Caroline du Nord (USA) (Bousfield, 1964). Ce bivalve fouisseur affectionne particulièrement les substrats meubles composés de sable moyen homogène (Dames & Moore, 1993) mais peut aussi se développer dans des sédiments fins (MacKenzie *et al*., 1985) ou limoneux (Meyer *et al.*, 1981). L'habitat de la mactre s'étend de la limite supérieure de l'infralittoral jusqu'à 128 m (Jones *et al.*, 1983). Cependant, les plus fortes concentrations sont observées dans des zones présentant un fort hydrodynamisme entre 8 et 66 m de profondeur (Fay *et al.*, 1983). Le spectre de tolérance thermique de cette espèce s'étend de 0 à 28°C (Spruck *et al.*, 1995) à des salinités toujours supérieures à 28 PSU

(Cargnelli *et al.*, 1999). La croissance de *S. solidissima* est plus rapide au printemps et au début d'été pendant la phase d'augmentation des températures puis diminue de la fin de l'été à l'automne (Jones *et al.*, 1983). La mactre de l'Atlantique est également relativement sensible à l'hypoxie. Dans le New Jersey des épisodes hypoxiques sévères (< 3 ppm) ont déjà conduit à des mortalités massives (Weinberg & Helser, 1996). L'âge de maturité sexuelle de cette espèce varie fortement en fonction de la zone géographique. Dans le New-Jersey (USA) certains auteurs affirment que *S. solidissima* est mature à partir de 3 mois, soit une taille de 5mm (Chintala & Grassle, 1995). En revanche, autours de l'île du Prince Édouard (Canada) la reproduction intervient seulement à partir de 4 ans et à une taille comprise entre 80 et 95 mm (Sephton & Bryan, 1990).

Figure 9 : Photo de *S. solidissima* à Martinique Beach (Source : M. Kira, P. Olivia, V. Ryan)

Placopecten magellanicus

Le pétoncle géant (*Placopecten magellanicus*) (Fig. 10) est un mollusque bivalve dont la taille maximale peut atteindre 211 mm et dont la longévité peut être supérieure à 20 ans (Packer

et al., 1999). Son aire de distribution s'étend de la côte Nord du golfe du Saint-Laurent (Canada) au Cap Hatteras en Caroline du Nord (USA) (Packer *et al.*, 1999). Ce bivalve épigé est capable de se développer sur différents types de substrats meubles ou durs, même si les fonds composés de graviers et de galets semblent les plus adaptés (Thouzeau *et al.,* 1991). On trouve le pétoncle géant à des profondeurs comprises entre 2 et 384 m (Naidu & Anderson, 1984 ; Merrill, 1959), même si la majorité des populations exploitées se trouvent à des profondeurs comprises entre 18 et 110m (Packer *et al.*, 1999). Les pétoncles peuvent être confrontés à des températures comprises entre -2 et 20°C, la croissance de cette espèce est possible entre 8 et 18°C avec un optimum autour de 13.5°C (MPO, 2011). La gamme de salinité supportée par cette espèce varie de 16.5 à 35 PSU (Packer *et al.*, 1999). Le cycle de vie de *P. magellanicus* est relativement complexe et comporte d'importantes spécificités associées à chacun de ces stades. Ces animaux sont gonochoriques et matures sexuellement à partir de l'âge de 3 ans (> 60 mm). La reproduction intervient alors à la fin de l'été entre la fin du mois d'août et le début du mois de septembre. Les deux stades larvaires (trochophore et véligère) du pétoncle géant sont pélagiques et durent un peu plus d'un mois (Posgay, 1982). Cette durée n'est qu'indicative et varie en fonction de la température du milieu dans lequel les larves se développent. Les larves deviennent ensuite benthiques au stade pédivéligère et sécrètent un byssus pour se fixer à un substrat dur (Culliney, 1974). À partir de leur deuxième année de croissance (5-12 mm), les juvéniles se détachent et deviennent relativement mobiles jusqu'à atteindre une taille de 80 mm (Caddy, 1968). Durant cette période les juvéniles peuvent nager activement et se déplacer de 10 à 100 m par jour (Kenchington *et al.,* 1991) et même couvrir des distances de 0,5 km (Parsons *et al*., 1992) à près de 10 km par année (Melvin *et al.,* 1985).

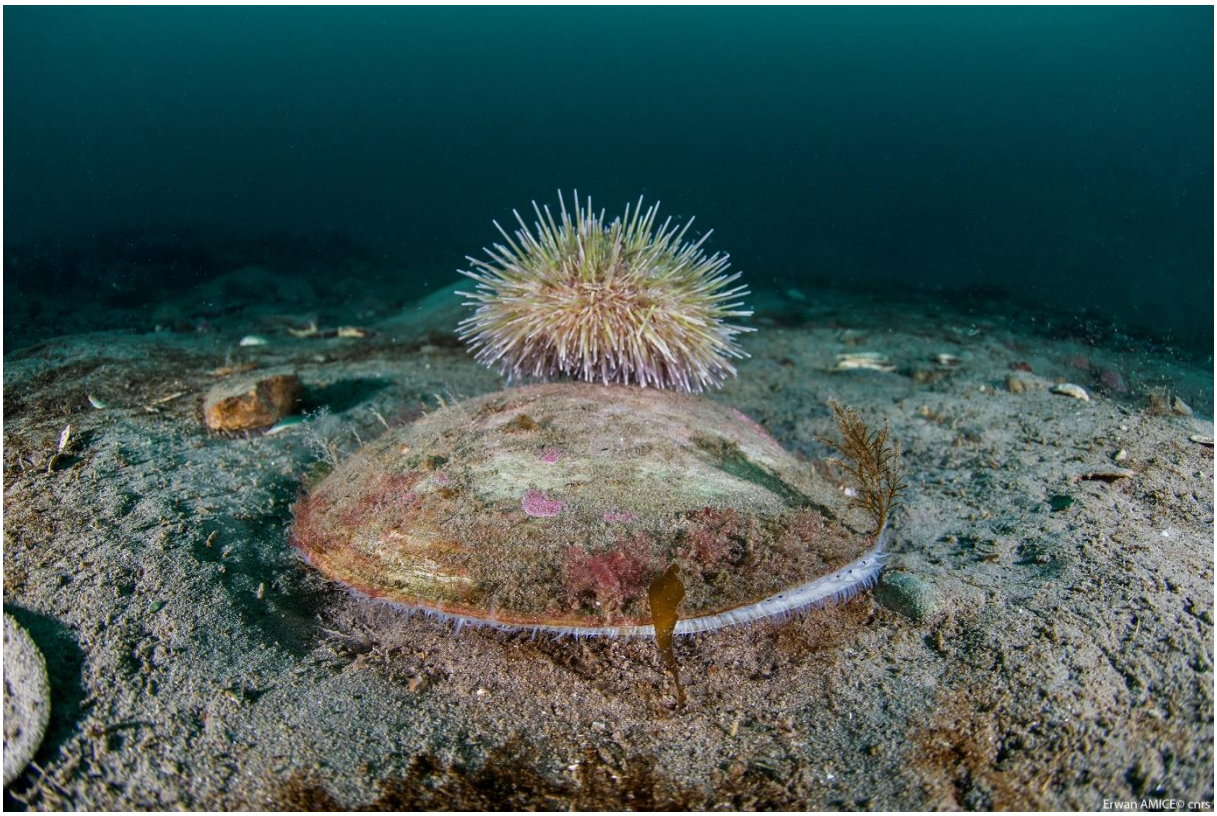

Figure 10 : Photo *in situ* de *P. magellanicus* à Saint-Pierre et Miquelon (Source : E. Amice/CNRS).

Objectifs et structure de la thèse

En résumé, notre étude se déroule dans un écosystème où les connaissances scientifiques sont contrastées voir paradoxales.

D'un point de vue global, nous savons que SPM se situe à la croisée des principales masses d'eaux intervenant dans la circulation des eaux de surface de l'Atlantique Nord. En revanche, comme le soulignent Wu et ses collaborateurs (2012), la circulation océanique autour de SPM et du chenal Laurentien est mal connue, en raison de sa situation en bordure des principaux modèles de circulation océanique de la région (Grands Bancs de Terre-Neuve, Plateau néo-écossais et Golfe du Saint-Laurent). De plus, les mesures environnementales y sont relativement contemporaines et ne remontent que très rarement avant 1950. Même si, Petrie & Anderson (1983) supposent que les eaux de SPM sont probablement issues d'un mélange d'eaux des courants du Labrador, du Gulf Stream et du Golfe du Saint-Laurent. L'identification de celles-ci et la quantification de leurs influences sur l'hydrodynamisme de SPM restent donc des questions ouvertes. Cette méconnaissance de l'hydrodynamisme local induit également

des incertitudes concernant les variabilités passé et futur du climat à l'échelle mondiale. Cela s'illustre particulièrement lorsque l'on compare les résultats de différents modèles couplés océan/atmosphère (e.g. Danabasoglu *et al.*, 2013). En effet, les difficultés associées à la représentation des courants marins de l'Atlantique Nord-Ouest sont à l'origine de biais récurrents dans les projections climatiques futures (Wang *et al.*, 2014).

Localement, les températures de surface (0-20 m) montrent un cycle saisonnier d'une amplitude d'une quinzaine de degrés caractéristique des latitudes moyennes (Miquelon se situe à la latitude de Nantes). En revanche, les températures de fond (20 m - 80 m) sont affectées par de très fortes oscillations qui s'amplifient à mesure que les températures de surface augmentent. Ces oscillations peuvent atteindre une dizaine de degrés et présentent une période dominante diurne, qui correspond à celle de l'onde de marée O1 (25,8 h), tandis que les variations de hauteur d'eau sont semi-diurnes, en bonne conformité avec les constantes harmoniques de marée calculées par le SHOM.

Dans ce contexte, la mise en évidence de la variabilité environnementale passée à ces deux échelles temporelles prend alors tout son sens. Pour cela, nous utiliserons des outils sclérochronologiques en les appliquant à différentes espèces animale et végétale. Les choix de celles-ci seront dictés par la résolution des informations environnementales passées que nous désirons et les spécificités biologiques de celles-ci. Pour étudier des variations environnementales sur de longues périodes temporelles nous utiliserons des coquilles du plus vieil animal non colonial connu à ce jour : *Arctica islandica.* Les structures calcifiées bio-construites d'une algue coloniale encroûtante *Clathromorphum compactum* pouvant se développer pendant plusieurs siècles seront également étudiées. Puis, pour accéder à des informations environnementales passées à l'échelle sub-journalière, nous étudierons des animaux présentant une très forte croissance coquillière : *Spisula solidissima* et *Placopecten magellanicus.*

Les résultats de ce travail seront alors présentés au sein de différents chapitres :

Le premier sera majoritairement méthodologique et concernera *S. solidissima*. Ainsi, après avoir identifié la périodicité de formation des stries de croissance de cette espèce grâce à des mesures de $\delta^{18}O$ dans la couche externe de sa coquille, les taux de croissance annuels de différentes parties de ce bivalve (chondrophore, couche externe et ligament) seront calculés

afin d'en comparer la dynamique de croissance. Pour finir, ces résultats seront mis en perspective avec ceux d'autres populations de *S. solidissima* au sein de son aire de répartition géographique afin de placer celle de SPM dans un contexte spatio-temporel.

Le second s'intéressera à l'application de ces techniques sclérochronologiques à une espèce longévive, *A. islandica,* présente à SPM. Dans ce chapitre nous allons décrire les liens pouvant exister entre la variabilité de croissance annuelle d'*A. islandica* à SPM depuis 1850 et plusieurs variables environnementales mesurées à différentes échelles : globales, régionales et locales. Ces résultats nous permettront alors de mieux comprendre l'hydrodynamisme passé de cet archipel et d'évaluer la pertinence de ce site pour étudier des variations hydroclimatiques et écosystémiques sur de longues périodes et à l'échelle globale.

Le troisième chapitre visera à étudier le potentiel sclérochronologique d'une algue calcaire encroûtante à Saint-Pierre et Miquelon. Ce travail comportera plusieurs volets. Le premier sera méthodologique et visera à développer une méthode permettant d'effectuer des lectures directes de croissance sur cet organisme. Pour valider cette méthode et engager une réflexion sur la variabilité intra-individuelle de la répartition des éléments traces au sein de ce végétal, un travail microchimique sera également réalisé. Ces résultats sclérochronologique obtenus sur des organismes longévifs d'un autre niveau trophique qu'*A. islandica* seront enfin mis en perspectives avec les variations environnementales passées.

Le dernier chapitre aura pour but d'utiliser la variabilité haute fréquence des températures de fond autour de SPM pour identifier l'aptitude de *P. magellanicus* à enregistrer des informations environnementales sub-journalières dans sa coquille. Pour cela nous avons développé une technique d'ablation laser femto seconde couplée à un spectromètre de masse à plasma induit (LA-ICPMS) pour analyser les éléments traces contenus dans la matrice coquillière de *P. magellanicus* tous les 10 µm.

Ce manuscrit s'achèvera sur une dernière partie ayant pour but de synthétiser les principaux résultats de ce travail et d'engager une réflexion autour des perspectives ouvertes par celui—ci.

Références

Adey WH (1965) The genus *Clathromorphum* (Corallinaceae) in the Gulf of Maine. *Hydrobiologia*, **26**, 539–573.

Adey WH, Lindstrom S, Hommersand M, Muller K (2008) The Biogeographic Origin of Arctic Endemic Seaweeds: A Thermogeographic View. *Journal of Phycology*, **44**, 1384–1394.

Adey WH, Halfar J, Williams B (2013). The coralline genus *Clathromorphum*: biological, physiological, and ecological factors controlling carbonate production in an arctic-subarctic climate archive. *Smithsonian contributions to the marine sciences,* number **40**.

Arthur MA, Williams DF, Jones DS (1983) Seasonal temperature-salinity changes and thermocline development in the mid-Atlantic Bight as recorded by the isotopic composition of bivalves. *Geology*, **11**, 655-659.

Barats A, Amouroux D, Chauvaud L, Pecheyran C, Lorrain A, Thebault J, Church TM, Donard OFX (2009) High frequency Barium profiles in shells of the Great Scallop *Pecten maximus*: a methodical long-term and multi-site survey in Western Europe. *Biogeosciences*, **6**, 157-170.

Bonitz F, Andersson C; Trofimova T; Hátún H (2018) Links between phytoplankton dynamics and shell growth of Arctica islandica on the Faroe Shelf. *Journal of Marine Systems*, **179**, 72-87.

Booth BBB, Dunstone NJ, Halloran PR, Andrews T, Bellouin N (2012) Aerosols implicated as a prime driver of twentieth-century North Atlantic climate variability. *Nature*, **484**, 228–232.

Bousfield EL (1964) Coquillages des côtes canadiennes de l'Atlantique. Musée national du Canada, Ottawa, 89 p.

Bower AS, Le Cann B, Rossby T, Zenk W, Gould J, Speer K, Richardson PL, Prater MD, Zhang HM (2002) Directly measured mid-depth circulation in the northeastern North Atlantic Ocean, *Nature*, **419**, 603–607.

Brocas, WM, Reynolds DJ, Butler PG, Richardson CA, Scourse JD, Ridgway ID, Ramsay K (2013) The dog cockle, *Glycymeris glycymeris* (L.), a new annually-resolved sclerochronological archive for the Irish Sea. *Palaeogeography, Palaeoclimatology, Palaeoecology*, **373**, 133-140.

Broeker WS (1991) The great ocean conveyor. *Oceanography*, **4**, 79-89.

Bryan FO, Hecht MW, Smith RD (2007) Resolution convergence and sensitivity studies with North Atlantic circulation models. Part I: The western boundary current system. *Ocean Modelling*, **16**, 141-159.

Butler PG, Wanamaker AD Jr., Scourse JD, Richardson CA, Reynolds DJ (2013) Variability of marine climate on the North Icelandic Shelf in a 1357-year proxy archive based on growth increments in the bivalve *Arctica islandica*. *Palaeogeography, Palaeoclimatology, Palaeoecology,* **373**, 141-151.

Caddy JF (1968) Underwater observations on scallop (*Placopecten magellanicus*) behaviour and drag efficiency. *Journal of the Fisheries Research Board of Canada*, **25**, 2123-2141.

Cargnelli LM, Griesbach SJ, Packer DB Weissberger E (1999) Essential fish habitat source document: Atlantic surfclam, *Spisula solidissima*, life history and habitat characteristics. NOAA Technical Memorandum NMFS-NE-142. 13 p.

Carre M, Bentaleb I, Blamart D, Ogle N, Cardenas F, Zevallos S, Kalin R, Ortlieb L, Fontugne M (2005) Stable isotopes and sclerochronology of the bivalve *Mesodesma donacium*: Potential application to Peruvian paleoceanographic reconstructions. *Palaeogeography, Palaeoclimatology, Palaeoecology*, **228**, 4-25.

Carriker MR, Palmer RE, Sick LV, Johnson CC (1980) Interaction of Mineral Elements in Sea-Water and Shell of Oysters (*Crassostrea-Virginica* (Gmelin)) Cultured in Controlled and Natural Systems. *Journal of Experimental Marine Biology and Ecology*, **46**, 279-296.

Checa A (2000) A new model for periostracum and shell formation in Unionidae (Bivalvia, Mollusca). *Tissue & Cell*, **32**, 405-416.

Chintala MM, Grassle JP (1995) Early gametogenesis and spawning in "juvenile" Atlantic surfclams, *Spisula solidissima* (Dillwyn, 1819). *Journal of Shellfish Research*, **14**, 301-306.

Clark GR (1974) Growth lines in invertebrate skeletons. *Annual Review of Earth and Planetary Sciences*, **2**, 77-99.

Cudaback CN, McPhee-Shaw E (2009) Diurnal-period internal waves near point conception, California. *Estuarine Coastal and Shelf Science*, **83**, 349–359.

Culliney JL (1974) Larval development of the giant scallop *Placopecten magellanicus* (Gmelin). *The Biological bulletin (Woods Hole)*, **147**, 321-332.

Cuny J, Rhines PB, Niiler PP, Bacon S (2002) Labrador Sea Boundary Currents and the Fate of the Irminger Sea Water. *Journal of Physical Oceanography*, **32**, 627-647.

Dahlgren TG, Weinberg JR, Halanych KM (2000) Phylogeography of the ocean quahog (*Arctica islandica*): influences of paleoclimate on genetic diversity and species range. *Marine Biology*, **137**, 487-495.

Dames & Moore (1993) Benthic animal-sediment assessment of potential beachfill borrow source for the Rehoboth/Dewey Beach, Delaware interim feasibility study. Report to U.S. Army Corps of Engineers, Philadelphia District. Contract No.DACW61-93-D-0001.

Daniault N, Mercier H, Lherminier P, Sarafanov A, Falina A, Zunino P, Pérez FF, Ríos AF, Ferron B, Huck T, Thierry V, Gladyshev S (2016) The northern North Atlantic Ocean mean circulation in the early 21st Century, *Progress in Oceanography*, **146**, 142-158.

Dengg J, Beckmann A, Gerdes R (1996) The gulf stream separation problem. In: Krauss W (ed.) The Warm water sphere of the North Atlantic Ocean, pp. 253–290, Gebruder-Borntraeger, Stuttgart, Germany.

Dima M, Lohmann G (2007) A Hemispheric Mechanism for the Atlantic Multidecadal Oscillation. Journal of Climate, **20**, 2706–2719.

Dorman FH, Gill ED (1959) Oxygen isotope paleotemperature determinations of Australian Cainozoic fossils. Science, **130**, 1576-1576.

Dunca E, Mutvei H, Goransson P, Morth C, Schöne BR, Whitehouse MJ, Elfman M, Baden SP (2009) Using ocean quahog (*Arctica islandica*) shells to reconstruct palaeoenvironment in A-resund, Kattegat and Skagerrak, Sweden. *International Journal of Earth Sciences*, **98**, 3-17.

Fay CW, Neves RJ, Pardue GB (1983) Species profiles: life histories and environmental requirements of coastal fishes and invertebrates (Mid-Atlantic): surf clam. U.S. Fish Wildl. Serv., Div. Biol. Serv., FWS/OBS-82/11.13.23 p.

Flato G, *et al.* (2013) Evaluation of climate models, in Climate Change 2013: The Physical Science Basis. Contribution of Working Group I to the Fifth Assessment Report of the

Intergovernmental Panel on Climate Change, edited by T. F. Stocker et al., pp. 741–866, Cambridge Univ. Press, Cambridge, U.K.

Freitas PS, Clarke LJ, Kennedy HA, Richardson CA, Abrantes F (2005) Mg/Ca, Sr/Ca, and stable-isotope ($\delta^{18}O$ and $\delta^{13}C$) ratio profiles from the fan mussel *Pinna nobilis*: seasonal records and temperature relationships. *Geochemistry, Geophysics, Geosystems*, **6**, Q04D14.

Freitas PS, Clarke LJ, Kennedy HA, Richardson CA (2008) Inter- and intra-specimen variability masks reliable temperature control on shell Mg/Ca ratios in laboratory- and field-cultured *Mytilus edulis* and *Pecten maximus* (bivalvia). *Biogeosciences*, **5**, 1245-1258.

Gastineau G, D'Andrea F, Frankignoul C (2013) Atmospheric response to the North Atlantic Ocean variability on seasonal to decadal time scales. *Climate Dynamics*. **40**, 2311–2330.

Gillikin D, Dehairs F, Baeyens W, Navez J, Lorrain A, Andre L (2005) Inter- and intra-annual variations of Pb/Ca ratios in clam shells (*Mercenaria mercenaria*): A record of anthropogenic lead pollution? *Marine Pollution Bulletin*, **50**, 1530-1540.

Goodwin D, Flessa K, Schöne BR, Dettman D (2001) Cross-calibration of daily growth increments, stable isotope variation, and temperature in the Gulf of California bivalve mollusk *Chione cortezi*: Implications for paleoenvironmental analysis. *Palaios*, **16**, 387-398.

Grossman EL, Ku TL (1986) Oxygen and Carbon Isotope Fractionation in Biogenic Aragonite - Temperature Effects. *Chemical Geology*, **59**, 59-74.

Guida VG, Valentine PC, Gallea LB (2013) Semidiurnal Temperature Changes Caused by Tidal Front Movements in the Warm Season in Seabed Habitats on the Georges Bank Northern Margin and Their Ecological Implications. *Plos One*, **8**, e55273.

Häkkinen S, Rhines PB, Worthen DL (2011) Atmospheric blocking and Atlantic multidecadal ocean variability. *Science*, **334**, 655–659.

Halfar J, Steneck RS, Joachimski M, Kronz A, Wanamaker AD Jr. (2008) Coralline Red Algae as High-Resolution Climate Recorders. *Geology*, **36**, 463–466.

Han G (2000) Three-dimensional modeling of tidal currents and mixing quantities over the Newfoundland Shelf. *Journal of Geophysical Research-Oceans*, 105, 11407–11422.

Han G, Lu Z, Wang Z, Helbig J, Chen N, Young B de (2008) Seasonal variability of the Labrador Current and shelf circulation off Newfoundland. *Journal of Geophysical Research Oceans*, **113**, C10013.

Hart SR, Blusztajn J (1998) Clams as recorders of ocean ridge volcanism and hydrothermal vent field activity. *Science*, **280**, 883-886.

Hartmann, D.L. *et al.*, (2013) Observations: Atmosphere and Surface, in Climate Change 2013: The Physical Science Basis. Contribution of Working Group I to the Fifth Assessment Report of the Intergovernmental Panel on Climate Change, Cambridge University Press.

Holland HA, Schöne BR, Lipowsky C, Esper J, (2014) Decadal climate variability of the North Sea during the last millennium reconstructed from bivalve shells (*Arctica islandica*). *Holocene*, **24**, 771-786.

Hurrell JW (1995) Decadal trends in the North-Atlantic Oscillation - regional temperatures and precipitation. *Science*, **269**, 676–679.

Huthnance J (1974) On the diurnal tidal currents over Rockall Bank. *Deep-Sea Research*, **21**, 23-35.

Jeandel C, Mosseri R (2011) Le climat à découvert. *CNRS Éditions*. Disponible sur Internet : <http://books.openedition.org/editionscnrs/11316>; ISBN : 9782271119162. DOI : 10.4000/books.editionscnrs.11316.

Jolivet A, Asplin L, Strand O, Thebault J, Chauvaud L (2015) Coastal upwelling in Norway recorded in Great Scallop shells. *Limnology and Oceanography*, **60**, 1265-1275.

Jones DS, Williams DF, Arthur MA (1983) Growth history and ecology of the Atlantic surf clam, *Spisula solidissima* (Dillwyn), as revealed by stable isotopes and annual shell increments. *Journal of Experimental Marine Biology and Ecology*, **73**, 225-242.

Kenchington E, Têtu C, Mohn R (1991) Preliminary investigations of juvenile scallops (Placopecten magellanicus) in Nova Scotia inshore habitats. Can. Man. Rep. Fish. Aquat. Sc. Rep. n° 2123.

Knight JR, Folland CK, Scaife AA (2006) Climate impacts of the Atlantic Mulitdecadal Oscillation. *Geophysical Research Letters*, **33**, L17706.

Lazier JRN, Wright DG (1993) Annual velocity variations in the Labrador Current. *Journal of Physical Oceanography*, **23**, 659–678.

Lécuyer C, Hutzler A, Amiot R, Daux V, Grosheny D, Otero O, Martineau F, Fourel F, Balter V, Reynard B (2012) Carbon and oxygen isotope fractionations between aragonite and calcite of shells from modern molluscs. *Chemical Geology*, **332-333**, 92-101.

Leichter JJ, Stokes MD, Hench JL, Witting J, Washburn L (2012) The island-scale internal wave climate of Moorea, French Polynesia. *Journal of Geophysical Research-Oceans*, **117**, C06008.

Loosanoff VL (1953) Reproductive cycle in *Cyprina islandica*. *Biological Bulletin. Marine Biological Laboratory, Woods Hole, Mass*., **104**, 146–155.

Lorrain A, Gillikin DP, Paulet YM, Chauvaud L, Le Mercier A, Navez J, André L (2005) Strong kinetic effects on Sr/Ca ratios in the calcitic bivalve *Pecten maximus*. *Geology*, **33**, 965–968.

Lutz RA, Rhoads DC (1980) Growth patterns within the molluscan shell: an overview. In: Rhoads DC, Lutz RA (eds) Skeletal growth of aquatic organisms. Plenum Press, New York, pp 203–248.

Lutz RA, Goodsell JG, Mann R, Castagna M (1981) Experimental culture of the ocean quahog, *Arctica islandica*. *Journal of the World Aquaculture Society*, **12**, 196-205.

Lutz RA, Mann R, Goodsell J, Castagna M (1982) Larval and early post-larval development of *Arctica islandica*. *Journal of the Marine Biological Association of the United Kingdom*, **62**, 745-769.

Mackenzie CL Jr., Radosh DJ, Reid RN (1985) Densities, growth, and mortalities of juveniles of the surf clam (*Spisula solidissima*) (Dillwyn) in the New York Bight. *Journal of Shellfish Research*, **5**, 81-84.

Melvin GD, Dadswell MJ, Chandler RA (1985) Movements of scallops *Placopecten magellanicus* (Gmelin, 1791) (Mollusca: Pectinidae) on Georges Bank. Can. Atl. Fish. Sci. Adv. Comm. Res. Doc. 85/30.

Merrill AS (1959) A comparison of *Cyclopecten nanus* (Verrill and Bush) and *Placopecten magellanicus* (Gmelin). *Harvard University Museum of Comparative Zoology. Occasional paper on Molluscs*, **2**, 209-228.

Meyer, TL, RA Cooper, Pecci KJ (1981) The performance and environmental effects of a hydraulic clam dredge. *Marine Fisheries Review*, **43**, 14-22.

Mihanovic H, Orlic M, Pasaric Z (2006) Diurnal internal tides detected in the Adriatic. *Annales Geophysicae*, **24**, 2773–2780.

Mihanovic H, Orlic M, Pasaric, Z (2009) Diurnal thermocline oscillations driven by tidal flow around an island in the Middle Adriatic. *Journal of Marine Systems*, **78**, 157–168.

Mihanovic H, Paklar GB, Orlic M (2014) Resonant excitation of island-trapped waves in a shallow, seasonally stratified sea. *Continental Shelf Research*, **77**, 24–37.

Mook WG, Vogel JC (1968) Isotopic equilibrium between shells and their environment. *Science*, **159**, 874-875.

MPO (2011) Évaluation de la pêche du pétoncle (*Placopecten magellanicus*) du sud du golfe du Saint-Laurent. Secr. can. de consult. sci. du MPO, Avis sci. 2011/039.

Msadek R, Frankignoul C, Li LZX (2011) Mechanisms of the atmospheric response to North Atlantic multidecadal variability: A model study. *Climate Dynamics*, **36**, 1255-1276.

Naidu KS, Anderson JT (1984) Aspects of scallop recruitment on St. Pierre Bank in relation to oceanography and implications for resource management. Can. Atl. Fish. Sci. Adv. Comm. Res. Doc. 84/29. 9 p.

Nicol D (1951) Recent species of the veneroid pelecypod *Arctica*. *Journal of the Washington Academy of Sciences*, **41**,102–106.

Orlic M, Beg Paklar G, Dadic V, Leder N, Mihanovic H, Pasaric M, Pasaric Z (2011) Diurnal upwelling resonantly driven by sea breezes around an Adriatic island. *Journal of Geophysical Research-Oceans*, **116**, C006955.

Packer DB, Cargnelli LM, Griesbach SJ, Shumway SE (1999) Essential fish habitat source document: Sea scallop, *Placopecten magellanicus*, life history and habitat characteristics. NOAA Technical Memorandum NMFS-NE-134. 21 p.

Parsons GJ, Waren-Perry CR, Dadswell MJ (1992) Movements of juvenile sea scallop *Placopecten magellanicus* (Gmelin, 1791) in Passamaquoddy Bay, New Brunswick. *Journal of Shellfish Research*, **11**, 295-297.

Peharda M, Crncević M, Buselic I, Richardson CA, Ezgeta-Balic D (2012) Growth and longevity of *Glycymeris nummaria* (Linnaeus, 1758) from the Eastern Adriatic, Croatia. *Journal of Shellfish Research*, **31**, 947-950.

Penduff T, Juza M, Barnier B, Zika J, Dewar WK, Treguier AM, Molines JM, Audiffren N (2011) Sea level expression of intrinsic and forced ocean variabilities at interannual time scales. *Journal of Climate*, **24**, 5652-5670.

Petrie B, Anderson C (1983) Circulation on the Newfoundland Continental Shelf. *Atmosphere-Ocean*, **21**, 207–226.

Pineda J (1994) Internal tidal bores in the nearshore - warm-water fronts, seaward gravity currents and the onshore transport of neustonic larvae. *Journal of Marine Research*, **52**, 427-458.

Poitevin P, Thébault J, Schöne BR, Jolivet A, Lazure P, Chauvaud L (2018) Ligament, hinge, and shell cross-sections of the Atlantic surfclam (*Spisula solidissima*): Promising marine environmental archives in NE North America. *Plos One*, **13(6)**, e0199212.

Posgay JA (1982) Sea scallop Placopecten magellanicus.In Grosslein MD, Azarovitz TR (eds.) Fish distribution. p. 130-133. MESA New York Bight Atlas Monograph 15. N.Y. Sea Grant Institute, Albany, NY.

Ramsay K, Kaiser M, Richardson C, Veale L, Brand A (2000) Can shell scars on dog cockles (*Glycymeris glycymeris* L.) be used as an indicator of fishing disturbance? *Journal of Sea Research*, **43**, 167-176.

Reynolds DJ, Butler PG, Williams SM, Scourse JD, Richardson CA, Wanamaker AD Jr., Austin WEN, Cage AG, Sayer MDJ (2013). A multiproxy reconstruction of Hebridean (NW Scotland) spring sea surface temperatures between AD 1805 and 2010. *Palaeogeography, Palaeoclimatology, Palaeoecology*, **386**, 275-285.

Reynolds DJ, Richardson CA, Scourse JD, Butler PG, Hollyman P, Román-González A, Hall IR (2017) Reconstructing North Atlantic marine climate variability using an absolutely-dated sclerochronological network. *Palaeogeography , Palaeoclimatology , Palaeoecology*, **465**, 333-346.

Ropes JW, Jearld A Jr. (1987) Age determination of ocean bivalves. In: Summerfelt RC, Hall GE (eds.) Age and growth of fish. Iowa State University Press, Iowa, pp 517-526.

Schöne BR (2008) The curse of physiology - challenges and opportunities in the interpretation of geochemical data from mollusk shells. *Geo-Marine Letters*, **28**, 269-285.

Schöne BR, Tanabe K, Dettman DL, Sato S (2003) Environmental controls on shell growth rates and $\delta^{18}O$ of the shallow-marine bivalve mollusk *Phacosoma japonicum* in Japan. *Marine Biology*, **142**, 473-485.

Schöne BR, Freyre Castro AD, Fiebig J, Houk SD, Oschmann W, Kröncke I (2004) Sea surface water temperatures over the period 1884-1983 reconstructed from oxygen isotope ratios of a bivalve mollusk shell (*Arctica islandica*, southern North Sea). *Palaeogeography, Palaeoclimatology, Palaeoecology*, **212**, 215-232.

Schöne B, Surge D (2012) Bivalve Sclerochronology and Geochemistry. In Seldon P, Hardesty J (eds.) Part N, Bivalvia, Revised, Treatise Online, vol. 1, chap. 14, pp.46:1-24.

Schöne BR, Radermacher P, Zhang Z, Jacob DE (2013) Crystal fabrics and element impurities (Sr/Ca, Mg/Ca, and Ba/Ca) in shells of *Arctica islandica*-Implications for paleoclimate reconstructions. *Palaeogeography, Palaeoclimatology, Palaeoecology*, **373**, 50-59.

Schott FA, Zantopp R, Stramma L, Dengler M, Fischer J, Wibaux M (2004) Circulation and Deep-Water Export at the Western Exit of the Subpolar North Atlantic. *Journal of Physical Oceanography*, **34**, 817–843.

Sephton TW, Bryan CF (1990) Age and growth rate determinations for the Atlantic surf clam, Spisula solidissima (Dillwyn, 1817) in Prince Edward Island, Canada. *Journal of Shellfish Research*, **9**, 177-185.

Spruck CR, Walker RL, Sweeney ML, Hurley DH (1995) Gametogenic cycle in the non-native Atlantic surf clam, *Spisula solidissima* (Dillwyn, 1817), cultured in the coastal waters of Georgia. Gulf. *Research and Reports*, **9**, 131-137.

Steinhardt J, Butler PG, Carroll ML, Hartley J (2016) The application of long-lived bivalve sclerochronology in environmental baseline monitoring. *Frontiers in Marine Science*, **3**, 176.

Stock CA, Alexander MA, Bond NA, Brander KM, Cheung WWL, Curchitser EN, Delworth TL, Dunne JP, Griffies SM, Haltuch A (2011) On the use of IPCC-class models to assess the impact of climate on Living Marine Resources. *Progress in Oceanography*, **88**, 1-27.

Strom A, Francis RC, Mantua NJ, Miles EL, Peterson DL (2005) Preserving low-frequency climate signals in growth records of geoduck clams (*Panopea abrupta*). *Palaeogeography, Palaeoclimatology, Palaeoecology*, **228**, 167-178.

Steuber T (1996) Stable isotope sclerochronology of rudist bivalves: growth rates and Late Cretaceous seasonality. *Geology*, **24**, 315.

Surge D, Lohmann KC, Dettman DL (2001) Controls on isotopic chemistry of the American oyster, *Crassostrea virginica*: implications for growth patterns. *Palaeogeography, Palaeoclimatology, Palaeoecology*, **172**, 283-296.

Surge D, Walker KJ (2006) Geochemical variation in microstructural shell layers of the southern quahog (Mercenaria campechiensis): implications for reconstructing seasonality. *Palaeogeography, Palaeoclimatology, Palaeoecology*, **237**, 182-190.

Thebault J, Chauvaud L (2013) Li/Ca enrichments in great scallop shells (*Pecten maximus*) and their relationship with phytoplankton blooms. *Palaeogeography, Palaeoclimatology, Palaeoecology*, **373**, 108-122.

Thebault J, Chauvaud L, L'Helguen S, Clavier J, Barats A, Jacquet S, Pecheyran C, Amouroux D (2009) Barium and Molybdenum records in bivalve shells: Geochemical proxies for phytoplankton dynamics in coastal environments? *Limnology and Oceanography*, **54**, 1002-1014.

Thouzeau G, Robert G, Ugarte R (1991) Faunal assemblage of benthic mega invertebrates inhabiting sea scallop grounds from eastern Georges Bank, in relation to environmental factors. *Marine Ecology Progress Series*, **74**, 61-82.

Vander Putten E, Dehairs F, Keppens E, Baeyens W (2000) High resolution distribution of trace elements in the calcite shell layer of modern *Mytilus edulis*: Environmental and biological controls. *Geochimica et Cosmochimica Acta*, **64**, 997-1011.

von Bertalanffy L (1938) A quantitative theory of organic growth. *Human Biology*, **10**, 181-213.

Wall M, Schmidt GM, Janjang P, Khokiattiwong S, Richter C (2012) Differential Impact of Monsoon and Large Amplitude Internal Waves on Coral Reef Development in the Andaman Sea. *PloS ONE*, **7**, e50207.

Wanamaker AD Jr, Kreutz KJ, Schöne BR, Pettigrew N, Borns HW, Introne DS, Belknap D, Maasch KA, Feindel S (2008) Coupled North Atlantic slope water forcing on Gulf of Maine temperatures over the past millennium. *Climate Dynamics*, **31**, 183-194.

Wanner H, Brönnimann S, Casty C et al. (2001) North Atlantic Oscillation – concepts and studies. *Surveys in Geophysics*, **22**, 321–382.

Wang YH, Dai CF, Chen YY (2007) Physical and ecological processes of internal waves on an isolated reef ecosystem in the South China Sea. *Geophysical Research Letters*, **34**, L18609.

Wang C, Zhang L, Lee SK, Wu L, Mechoso CR (2014) A global perspective on CMIP5 climate model biases. *Nature Climate Change*, **4**, 201-205.

Weinberg JR, Helser TE (1996) Growth of the Atlantic surfclam, *Spisula solidissima*, from Georges Banks to the Delmarva Peninsula, USA. *Marine Biology*, **126**, 663–674.

Winter JE (1969) Über den Einfluß der Nahrungskonzentration und anderer Faktoren auf Filirierleistung und Nahrungsausnutzung der Muscheln *Arctica islandica* und *Modiolus modiolus*. *Marine Biology*, **4**, 87-135.

Witbaard R, Franken R, Visser B (1997) Growth of juvenile *Arctica islandica* under experimental conditions. *Helgoländer Meeresuntersuchungen*, **51**, 417-431.

Wright D, Xu Z (2004) Double Kelvin waves over the Newfoundland Shelf-break. *Atmosphere-Ocean*, **42**, 101–111.

Wu Y, Tang C, Hannah C (2012) The circulation of eastern Canadian seas. *Progress in Oceanography*, **106**, 28–48.

Xu Z, Loder J (2004) Data assimilation and horizontal structure of the barotropic diurnal tides on the Newfoundland and southern Labrador Shelves. *Atmosphere-Ocean*, **42**, 43–60.

Chapitre 1

Ligament, hinge, and shell cross-sections of the Atlantic surfclam (*Spisula solidissima*): Promising marine environmental archives in NE North America

Contexte et résumé de l'étude

Ce premier chapitre présente une étude sclérochronologique portant sur *Spisula solidissima*. Ce travail a été pour moi l'occasion de m'approprier et de mettre en place des méthodes sclérochronologiques qui constitueront la base des chapitres suivants. Cette partie est donc majoritairement méthodologique et constitue une étape essentielle au sein de mon projet doctoral.

Cette première étude concerne la Mactre de l'Atlantique (*S. solidissima*), une espèce d'intérêt commercial des eaux nord-américaines particulièrement sensible aux changements climatiques. En effet, de récentes études ont déjà démontré des modifications de son aire de répartition (plusieurs centaines de kilomètres) et de sa dynamique de croissance, en réponse à l'augmentation des températures de fond, de l'eutrophisation des zones côtières et de l'activité de pêche. Un des moyens de reconstruire la dynamique de ces changements passés, au sein des individus de cette espèce, passe par la réalisation d'études sclérochronologiques de leurs coquilles. Ces études peuvent concerner leurs compositions élémentaire et isotopique mais nécessitent au préalable d'en étudier la croissance. La croissance des organismes représente une variable qui intègre de multiples facteurs physico-chimiques et biologiques. Elle constitue donc une variable intégrative idéale pour suivre l'impact des changements environnementaux, des dernières décennies, sur différentes populations de *S. solidissama* le long d'un gradient géographique. Il convient de noter que l'analyse de la croissance de cette espèce est complexe car, (i) la présence de marques surnuméraires, (ii) l'érosion de la couche externe vers la charnière et (iii) les contraintes techniques liées à la préparation des coquilles, en perturbent la détermination. La présente étude propose une méthode alternative pour décrire la croissance annuelle de *S. solidissima.*

Pour ce faire, nous avons analysé 27 coquilles de *S. solidissima* prélevées à Saint-Pierre et Miquelon (SPM). Pour valider la périodicité annuelle des stries de croissance de cette espèce à SPM, nous avons analysé la composition isotopique ($\delta^{18}O_{shell}$) de la couche externe de deux

coquilles. Les valeurs maximales de $\delta^{18}O_{shell}$ étant concomitantes aux stries de croissances observées dans chacun des spécimens analysés, nous pouvons alors affirmer la périodicité annuelle de ces stries et leur occurrence pendant l'hiver à SPM. La taille des incréments de croissance visibles dans la couche externe des valves, ceux du chondrophore et enfin ceux du resilium, de tous les individus, ont ensuite été mesurés et leurs indices de croissance standardisés (SGI) ont été comparés. De fortes corrélations positives et significatives ont alors été trouvées entre ces trois chronologies de SGI ($p < 0,001$; $0,55 < \tau < 0,68$). Cela confirme que les lignes de croissance observées dans le ligament fournissent une nouvelle méthode pour déterminer l'âge et le taux de croissance de *S. solidissima*. Les croissances mesurées lors de cette étude ont également été comparés à celles d'autres populations, dans le cadre d'une approche biogéographique replaçant les performances de croissance de *S. solidissima* à Saint-Pierre et Miquelon, d'abord dans un contexte régional puis dans un contexte de changement global.

Ligament, hinge, and shell cross-sections of the Atlantic surfclam (*Spisula solidissima*): Promising marine environmental archives in NE North America

Pierre Poitevin[1], Julien Thébault[1], Bernd R. Schöne[2], Aurélie Jolivet[3], Pascal Lazure[4], Laurent Chauvaud[1]

[1] *Université de Bretagne Occidentale, Laboratoire des Sciences de l'Environnement Marin (UMR6539 UBO/CNRS/IRD/Ifremer), 29280 Plouzané, France*

[2] *Institute of Geosciences, University of Mainz, Johann-Joachim-Becher-Weg 21, 55128 Mainz, Germany*

[3] *TBM environnement/Somme, 115 rue Claude Chappe, Technopole Brest-Iroise, 29280 Plouzané, France*

[4] *Ifremer, Laboratoire d'Océanographie Physique et Spatiale (UMR6523 CNRS/Ifremer/IRD/UBO), 29280 Plouzané, France*

Email addresses:

Pierre Poitevin: pierre.poitevin@univ-brest.fr

Julien Thébault: julien.thebault@univ-brest.fr

Bernd R. Schöne: schoeneb@uni-mainz.de

Aurélie Jolivet: a.jolivet@tbm-environnement.com

Pascal Lazure: pascal.lazure@ifremer.fr

Laurent Chauvaud: laurent.chauvaud@univ-brest.fr

Corresponding author:

Pierre Poitevin

Université de Bretagne Occidentale

Institut Universitaire Européen de la Mer

Laboratoire des Sciences de l'Environnement Marin (UMR6539 UBO/CNRS/IRD/Ifremer)

F-29280 Plouzané

Tel: +33 2 90 91 55 78

Fax: +33 2 98 49 86 45

Abstract

The Atlantic surfclam (*Spisula solidissima*) is a commercially important species in North American waters, undergoing biological and ecological shifts. These are attributed, in part, to environmental modifications in its habitat and driven by climate change. Investigation of shell growth patterns, trace elements, and isotopic compositions require an examination of growth lines and increments preserved in biogenic carbonates. However, growth pattern analysis of *S. solidissima* is challenging due to multiple disturbance lines caused by environmental stress, erosion in umbonal shell regions, and constraints related to sample size and preparation techniques. The present study proposes an alternative method for describing chronology. First, we analyzed growth patterns using growth lines within the shell and hinge. To validate the assumption of annual periodicity of growth line formation, we analyzed the oxygen isotope composition of the outer shell layer of two specimens (46°54'20"N; 56°18'58"W). Maximum $\delta^{18}O_{shell}$ values occurred at the exact same location as internal growth lines in both specimens, confirming that they are formed annually and that growth ceases during winter. Next, we used growth increment width data to build a standardized growth index (SGI) time-series (25-year chronology) for each of the three parts of the shell. Highly significant correlations were found between the three SGI chronologies ($p < 0.001$; $0.55 < \tau < 0.68$) of all specimens. Thus, ligament growth lines provide a new method of determining ontogenetic age and growth rate in *S. solidissima*. In a biogeographic approach, the shell growth performance of *S. solidissima* in Saint-Pierre and Miquelon was compared to those in other populations along its distribution range in order to place this population in a temporal and regional context.

Keywords:

Spisula solidissima, mollusk ligament, growth comparisons, sclerochronology, Saint-Pierre and Miquelon.

Poitevin P, Thébault J, Schöne BR, Jolivet A, Lazure P, Chauvaud L (2018) Ligament, hinge, and shell cross-sections of the Atlantic surfclam (*Spisula solidissima*): Promising marine environmental archives in NE North America. *Plos One*, **13(6)**, e0199212.

Introduction

The Atlantic surfclam (*Spisula solidissima*) is the largest bivalve in the western North Atlantic, reaching a maximum length of 226 mm (commercial minimum size: 120 mm in USA and 90 mm in Canada) and longevity of 37 years in the Middle Atlantic Bight population [1]. *S. solidissima* is a commercially important species in Canada and the US Exclusive Economic Zone (EEZ). The US fishery represents nearly 75% of Atlantic surfclam global landings between 1965 and 2011. In 2011, approximately 20 000 tons of Atlantic surfclam meats were landed, 93% of which came from the US EEZ, corresponding to nominal revenues of $29 million, making this fishery one of the most valuable single species fisheries in the US [2].

S. solidissima is a good example of a commercially important species undergoing biological and ecological changes that have been attributed to increased bottom water temperature, fishery activity, or a combination of both [3-4-5-6-7-8]. These changes are measured within the accretionary hard parts of the clam [9-10-11]. Shell growth, a variable that integrates multiple physical and biological factors, represents an integrative approach to monitor the impact of environmental changes in *S. solidissima* populations along a geographic gradient during the last few decades [7-12-13-14].

Previous studies have reported that *S. solidissima* is an aragonitic bivalve [15] that forms one growth line per year during fall [9]. Based on this observation, different methods have been used to measure growth rates in Atlantic surfclam shells, including the size distribution of single cohorts [16], analysis of growth increments following mark-and-recapture experiments using different labeling techniques [17], external shell growth line measurements [18], internal growth line analysis in shell cross-sections [1], and elemental and stable oxygen isotope analyses [19-20-21]. However, disturbance rings caused by storms, thermal stress, predators, diseases, spawning, gonad development, and dredging are often indistinguishable from (periodic) annual growth lines, leading to unreliable results [9-22]. Further limitations occur in older specimens, in which it is sometimes a bit more difficult to resolve the most recently formed growth lines and the umbonal region may be eroded. In addition, the cutting, polishing, and examination procedures are considered to be time-consuming [19]. In order to resolve some of these problems, [19] proposed another method for determining the age and growth rate using internal growth lines preserved in the chondrophore, a structure that is

particularly well developed in members of the Mactridae family. This method, which was improved by Ropes [23-24], is still used every 2-3 years on surfclams sampled in the framework of the NEFSC clam surveys [2]. Although this method has solved the problems related to outer shell layer degradation and time required, the problems related to disturbance lines persist [24].

The present study analyzed growth lines present in the outer layer of the shell and the chondrophore and compared them to those readily observed in the internal ligament (resilium) of Atlantic surfclam shells. A strong relationship has been identified between growth patterns in the shell and ligament in several bivalve species, including *Placopecten magellanicus*, *Pedum spondyloideum*, *Radiolites angeoides*, and *Crassostrea gigas* [25-26-27-28-29]. *S. solidissima* has two physically separated ligaments: a small external uncalcified ligament (tensilium) and a larger internal partially calcified ligament (resilium) attached to the chondrophore [30]. In the rest of this article the hinge ligament refers to the elastic part composed of oriented aragonite crystals in a protein matrix that connects the shell valves dorsally (resilium). Our study focused on *S. solidissima* from Saint-Pierre and Miquelon (SPM), one of the northernmost populations along the eastern coast of North America. Despite the relevance of investigating the growth dynamics of a given species close to the limits of its ecological distribution, to the best of our knowledge, no investigation has yet been conducted on *S. solidissima* in SPM. Moreover, the SPM archipelago is free of any commercial and recreational surfclam exploitation. Thus, the objectives of this study were to gain insights into the seasonal dynamics of *S. solidissima* shell growth cessation in SPM using oxygen isotope thermometry in the outer shell layer, compare the growth lines present in the outer layer of the shell, the chondrophore, and the resilium (Fig 1), and give SPM population growth results a temporal and regional perspective.

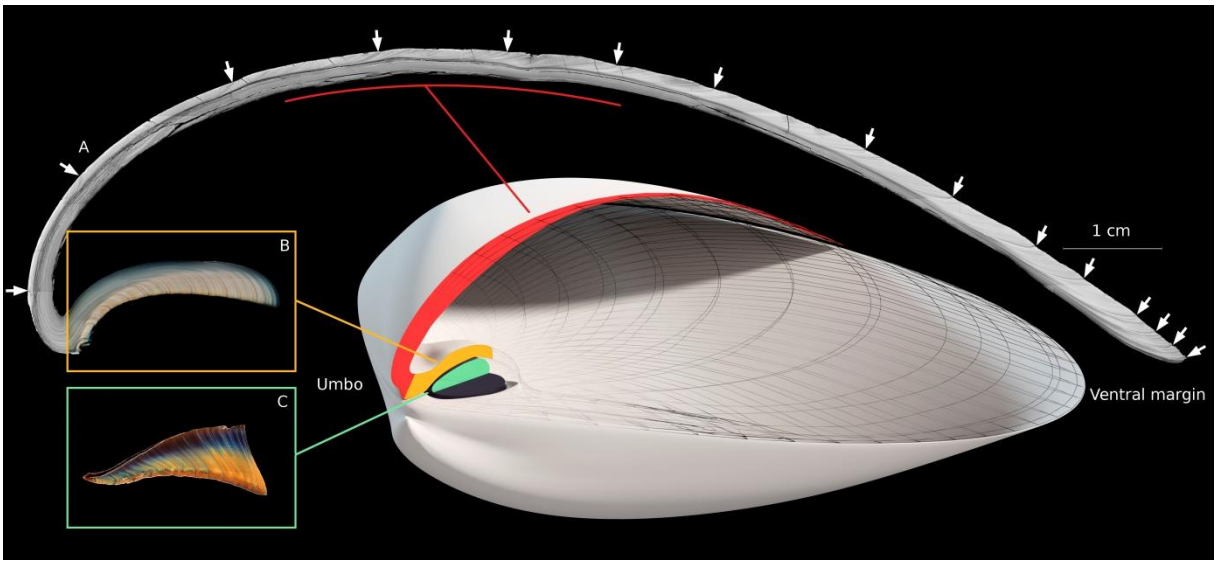

Figure 1: 3D representation of the general structure of the shell and hinge ligament of *S. solidissima*. The outer shell layer (A - red) and chondrophore (B - yellow) of the right valve, as well as the right half of the hinge ligament (C - green), are sectioned along the axis of maximal growth (from the umbo to the ventral margin). White arrows are placed at the locations of annual lines in the outer shell layer. These three structures are associated with the corresponding photomosaic, all of which were obtained from the same individual.

Materials & Methods

Sampling

Twenty-seven *S. solidissima* specimens (shell length ranging from 130 to 171 mm) were analyzed in the present study. They were collected alive at a depth of 0 - 5 m by scuba diving along the southeastern shore of Miquelon-Langlade sandy isthmus (46°54'20"N; 56°18'58"W) in November 2015 (site A on Fig 2). The habitat at the sampling station consisted of compacted and stable fine sand. Soft tissues, except the hinge ligament, were removed from the live-collected shells immediately after collection. All specimens were carefully cleaned with freshwater to remove adherent sediment and biological tissues.

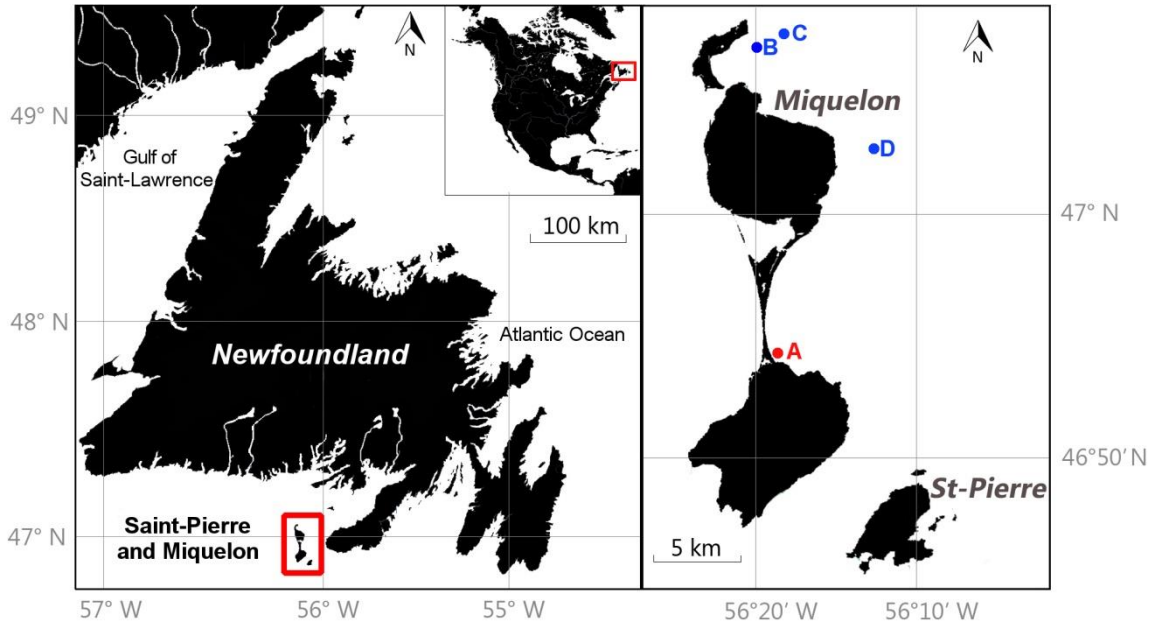

Figure 2: Map of Saint-Pierre and Miquelon and neighboring countries. (A) Location of the *S. solidissima* sampling site. (B and C) The two temperature and pressure monitoring sites. (D) The vertical salinity profile site.

Environmental monitoring

Two multi-parameter probes measuring temperature and pressure every 15 minutes were deployed at a depth of 5 m on two ropes moored at a water depth of 30 m and 60 m, respectively, at Miquelon Bay outlet (sites B and C on Fig 2, respectively). A daily average temperature was calculated for the periods 12/07/2010 (day/month/year)-29/11/2010 and 15/06/2011-03/11/2011. Vertical profiles of salinity from a CTD cast run at site D (Fig 2) were performed at water depth of 0-40 m on 04/08/2010, 15/09/2010, 04/10/2010, and 16/11/2010. Measurements were taken at 10 s intervals. We assessed the mean salinity at this time of the year between 0 and 5 m.

Sample preparation and image analysis

After removal of the ligament, the right valves were embedded in a thin layer of metal epoxy resin (Araldite Metal, Huntsman Advanced Materials) along the axis of maximal growth, from the umbo to the ventral margin. These reinforced parts of the shells were cut using a robust tile saw. Thick cross-sections were then embedded in a polyester mounting resin (SODY 33,

ESCIL) to prevent cracking during sectioning. A thin cross-section (2 mm thickness) was cut along the axis of maximum growth using a low-speed precision saw (Struers, Secotom 10; rotation speed 500 rpm; feed rate 200 µm s^{-1}) equipped with a 600-µm-thick diamond-coated blade continuously cooled by deionized water. Thin sections were carefully ground on a rotating polishing table (Struers, TegraPol-35) with a sequence of 800, 1200, 2500, and 4000 grit wet-table carborundum paper, followed by polishing with 3-µm diamond liquid (Struers) to remove any saw marks. Cross-sections were ultrasonically cleaned with deionized water between each grinding or polishing step to remove residual abrasive material.

To study the ligament growth lines, the right half of dry hinge ligaments were embedded in a polyester mounting resin (SODY 33, ESCIL). A 2-mm cross-section was cut along the axis of maximum growth using a low-speed precision saw (Struers-Isotom 50; rotation speed 500 rpm; feed rate 100 µm s^{-1}) equipped with a 400-µm-thick diamond-coated blade continuously cooled by deionized water. No additional treatment was performed on these sections.

Shell and ligament sections were imaged under reflected light (Zeiss, KL 2500 LCD) using an AxioCam MRc5 installed on a Zeiss Lumar.V12 stereomicroscope equipped with a motorized stage (Fig 1). The outer shell layer sections were photographed under 10x magnification, chondrophores and ligaments under 25x magnification. Photomosaics were constructed using AxioVision 4.9.1 software (Zeiss). The width of each growth increment was measured digitally using the image processing and analysis software Image J (NIH Image).

Isotopic validation of annual banding

Seawater oxygen isotope composition is controlled by the balance between evaporation and precipitation. Due to their offshore island status, SPM is not subjected to major riverine inputs and associated variations in salinity. Moreover, the calcium carbonate phase of most bivalve mollusks is in oxygen isotope equilibrium with the ambient seawater and not affected by the physiology of the animal [31]. Given that annual variations in salinity are very limited and seawater temperature has a broad annual range at SPM, $\delta^{18}O$ variations in *S. solidissima* shells are expected to reflect the annual seawater temperature cycle. Thus, shell oxygen isotope-derived water temperature estimates were used to reconstruct the growth dynamics of *S. solidissima*.

Two *S. solidissima* specimens, S-SPM4-06112015-2 and S-SPM4-06112015-16 (hereafter referred to as shell #2 and #16, respectively), with a maximum shell length of 130 mm and 140 mm, respectively, were analyzed between their third and fourth year of growth in calendar years 2010 and 2011. These two specimens were selected because they were the youngest in our shell collection, with the exact same age. Shell aragonite samples were collected from thick cross-sections using an automated high-resolution micro-sampling device (MicroMill, New Wave Research) equipped with a 300-µm conical drill bit (model H71.104.003, Gebr. Brasseler GmbH & Co. KG). Between 32 and 47 samples were drilled from each annual growth increment with an average distance between successive samples of 500 µm. A total of 165 discrete aragonite samples weighing 59-100 µg were collected. All samples were analyzed on a Thermo Finnigan MAT 253 continuous flow—isotope ratio mass spectrometer coupled to a GasBench II at the Institute of Geosciences of the University of Mainz (Germany). Stable oxygen isotope ratios were reported relative to the Vienna Pee-Dee Belemnite (VPDB) standard based on a NBS-19 calibrated IVA Carrara marble ($\delta^{18}O$ = –1.91‰). The internal precision, based on eight injections per sample, was 0.04‰. The long-term accuracy (external precision) of the mass spectrometer based on 421 NBS-19 measurements over 1.5 years was better than 0.04‰. For reasons described by Füllenbach et al. [32], the shell $\delta^{18}O$ values were not corrected for the different acid fractionation factors of the samples (aragonite) and standards (calcite).

In order to relate $\delta^{18}O$ to past temperatures, we used a fractionation equation written by Grossman and Ku [33] and calibrated for biogenic aragonite, to which we applied the small modification required for $\delta^{18}O_{seawater}$ described by Sharp [34]:

$$T(°C) = 20.6 - 4.34 \times \left(\delta^{18}\mathrm{O}_{\mathrm{aragonite}} - (\delta^{18}\mathrm{O}_{\mathrm{seawater}} - 0.27)\right)$$

The temperature range covered by this equation (2.6-22.0°C) is consistent with the seawater temperature measured at SPM during the main growing season for *S. solidissima*. This paleo-temperature equation was also used by Ivany et al. [21] in the last study addressing *S. solidissima* $\delta^{18}O_{shell}$ composition. As $\delta^{18}O_{seawater}$ has not yet been measured at the sampling site, we used an average and constant $\delta^{18}O_{seawater}$ value of -1.66‰ VSMOW calculated using

an equation determined by LeGrande and Schmidt [35] for the North Atlantic and an annual average salinity of 31.49 ± 0.03 measured at a water depth of 0-5 m during the growing season.

We calculated error propagation in our estimation of seawater temperature (reconstructed from $\delta^{18}O_{shell}$ variations), considering (1) uncertainty (1σ) of the mass spec measurements, (2) 1σ of the slope of the $\delta^{18}O_{seawater}$/S equation, (3) 1σ of the intercept of the $\delta^{18}O_{seawater}$ /S equation, and (4) 1σ of the salinity variations in the area (cf. fig 4). The resulting uncertainty is ± 0.75 °C.

Sclerochronological analysis

The main objective of the sclerochronological analysis was to compare the growth rates of the three anatomical parts. Similar to other bivalves, the growth rate of *S. solidissima* varies from year to year and exponentially decreases throughout ontogeny. This ontogenetic trend can be mathematically estimated by a growth equation. In the present study, the generalized von Bertalanffy growth function (gVBGF) was chosen because of its biological meaning [36]. The growth model was fitted to size-at-age data for each anatomical part of the 27 individuals using the following equation:

$$L(p)_t = L(p)_\infty * \left(1 - e^{-K(t-t_0)}\right)^D$$

Where $L(p)_t$ is the predicted shell length (in mm) at time *t* (in years), $L(p)_\infty$ is the length reached after an infinite time of growth (in mm), *K* is the Brody growth constant defining the "speed" of growth (per year), t_0 is the theoretical age at which the size would be zero (in years), and *D* determines the shape of the curve (more or less sigmoid). In order to remove this ontogenetic trend, growth indices (GIs) were calculated for each year and each anatomical part of each individual by dividing the measured increment width by the predicted increment width [31] as follows:

$$GI_t = \frac{L_{t+1} - L_t}{L(p)_{t+1} - L(p)_t}$$

Where GI_t is the growth index at t (in years), $L_{t+1} - L_t$ is the measured shell increment at t, and $L(p)_{t+1} - L(p)_t$ is the predicted shell increment length at the same time t. Individual time-series of GI were then standardized as follows [31]:

$$SGI_t = \frac{GI_t - \mu}{\sigma}$$

Where μ is the average of all GI values and σ the standard deviation. The standardized growth index (SGI) is a dimensionless measure of how growth deviates from the predicted trend. Positive values represent greater than expected growth, whereas negative values represent less than expected growth. Finally, the mean SGI and standard error were calculated for each year and each anatomical part to create three SGI chronologies.

Statistical analysis

The robustness of the three SGI chronologies was tested. A frequently used assessment of the robustness of composite chronologies is the expressed population signal (EPS) [37], which is expressed as:

$$EPS = \frac{n * R_{bar}}{\left(n * R_{bar} + (1 - R_{bar})\right)}$$

Where R_{bar} is the average of all correlations between pairs of SGI chronologies and n is the number of specimens used to construct the stacked chronology. EPS > 0.85 indicates that the variance of a single SGI chronology sufficiently expresses the common variance of all SGI series.

To measure the ordinal association between two anatomical parts (chondrophore – external layer; external layer – ligament; ligament – chondrophore), the Kendal rank coefficient correlations of the SGI chronologies were calculated. All statistical analyses were performed using R statistical analysis software [38].

Regional growth comparison

A specialized von Bertalanffy growth function (sVBGF) for *S. solidissima* at SPM was applied to 532 size-at-age data pairs of the external layer using the following equation:

$$L(p)_t = L(p)_\infty * \left(1 - e^{-K(t-t_0)}\right)$$

As age *versus* size relationships are always given in the literature in terms of age at a given shell length using sVBGF, we converted our curvilinear shell height data to shell length data before applying the same growth model. This conversion was achieved using the average curvilinear height:length ratio (0.92) of all 27 surfclams used in this study [19].

A direct comparison of growth patterns calculated in previous studies using the two parameters $L(p)_\infty$ and K may be mathematically feasible, but is not biologically consistent, as K negatively correlates with $L(p)_\infty$. Pauly [39] was the first to develop the concept of overall growth performance (OGP) to make individual growth comparable. Pauly and Munro [40] later introduced a closely related index of OGP (Φ') that is derived from the sVBGF as follows:

$$\phi' = \log K + 2\log(0.1 * L(p)_\infty)$$

Where $L(p)_\infty$ is in mm and K given per year.

Finally, we compared the growth parameters and OGP index of the SPM population to those of other populations along a latitudinal gradient from the Gulf of St. Lawrence in Canada (Prince Edward Island [41] - Northumberland Straight [42] - Magdalen Islands [43-44] to the Northeast coast of the USA (Southern New England, New Jersey, Delmarva [45-46]).

Results

Environmental monitoring

Seawater temperatures recorded in 2010 and 2011 revealed a strong seasonal pattern, ranging from 0.95°C (28/03/2011) to 17.85°C (29/08/2010). We clearly saw two different thermal profiles in 2010 and 2011 (Fig 3). Higher temperatures were observed in 2010, especially during the temperature increase phase. Between mid-July (15/07) and early September (04/09), we observed an average daily difference of 1.7°C between the two years. This difference was less obvious during the second part of the year (05/09 until 04/11), with the average daily temperature of 2010 being only 0.4°C warmer than during 2011.

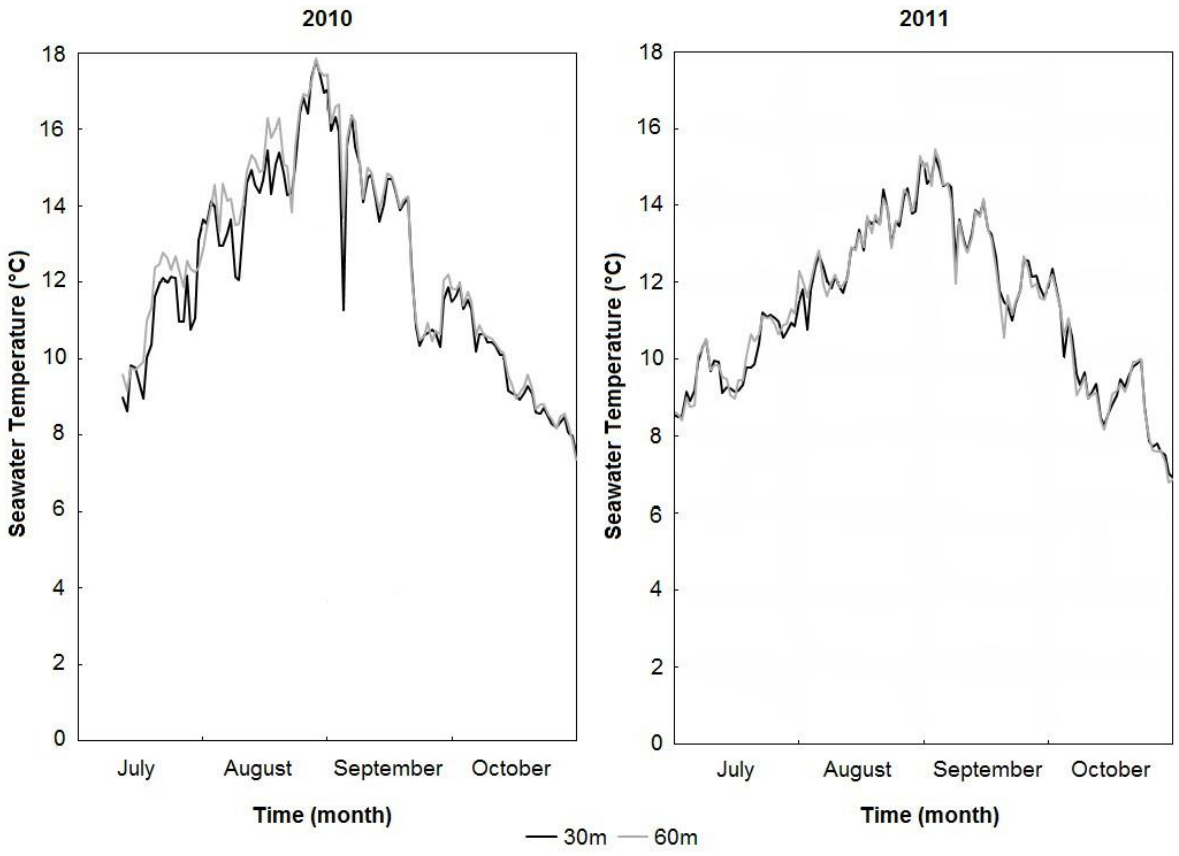

Figure 3: Seawater temperature variation at Miquelon Bay outlet. Measurements were made at a depth of 5 m on ropes moored at 30 m (grey curves) and 60 m (black curves). Values are presented as daily means during two periods from 10/07/2010 to 31/10/2010 and from 01/07/2011 to 31/10/2011.

Mean salinity at a depth of 0-5 m was calculated from 85 measurements recorded between the beginning of August 2010 and the middle of November 2010 near the *S. solidissima* collection site and found to be 31.49 ± 0.03 (Fig 4).

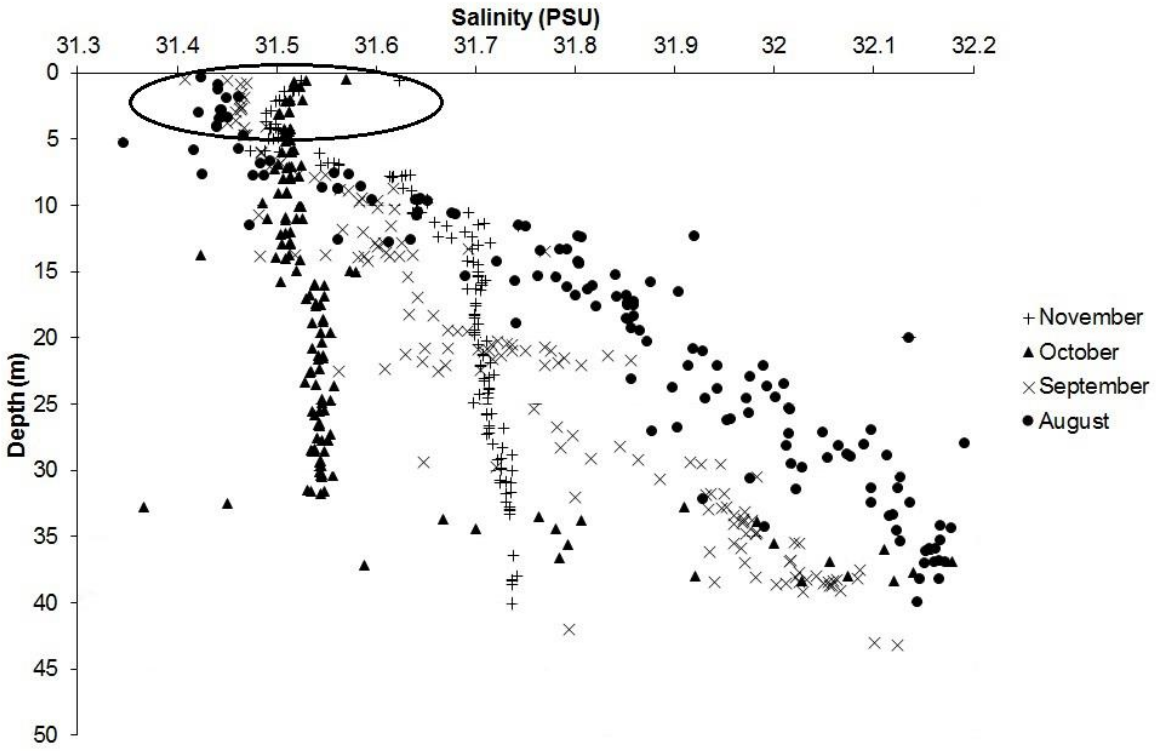

Figure 4: Salinity measured along a vertical profile at a water depth of 0-40 m on 04/08/2010, 15/09/2010, 04/10/2010, and 16/11/2010. The circled points are those between 0 and 5m which were used to calculate the mean salinity used to reconstruct the $\delta^{18}O_{seawater}$.

Oxygen isotope composition of shells

The oxygen isotope profiles obtained from the third and fourth year of growth (2010 and 2011) of shells #2 and #16 were characterized by distinct seasonal variations in $\delta^{18}O_{shell}$. Maximum $\delta^{18}O_{shell}$ values occurred at the exact same position in both specimens, i.e., at major growth lines (Fig 5), confirming that they are formed annually and that shell growth ceases during the winter. The $\delta^{18}O_{shell}$ values fluctuated around a mean of ≈ 0‰. The largest $\delta^{18}O_{shell}$ amplitudes of 3.35‰ and 3.18‰ were observed in 2010. This amplitude decreased considerably in 2011 to a low of 2.40‰ and 2.30‰ (Fig 5).

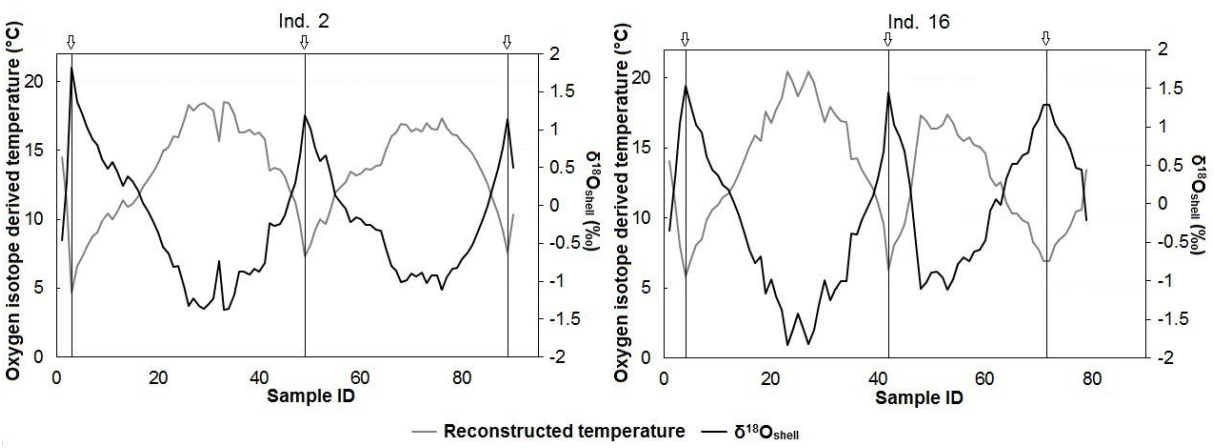

Figure 5: Comparison of $\delta^{18}O_{shell}$ (black) and the reconstructed temperature (grey) for two *S. solidissima* shells. Shells #2 and #16 were sampled from the end of the second year of life toward the beginning of the fifth year. Vertical lines placed under the arrows indicate the position of shell growth lines.

Seawater temperatures calculated from the $\delta^{18}O_{shell}$ values were between 4.7°C and 20.5°C. These temperatures agree with instrumentally recorded temperatures. Moreover, the observed cyclicality is consistent with the position of the annual growth lines (Fig 5). In all studied years for both specimens, annual growth lines were formed when the temperature was very close to the seasonal minimum. However, there were some differences between the two specimens. Despite similar shapes of the reconstructed temperature curves, in 2010, shell #16 recorded higher temperatures (20.5°C) than shell #2 (18.5°C). This offset falls within the uncertainty of temperature reconstruction and is therefore likely not significant. As sampling spots for isotope analysis were evenly spaced, the number of $\delta^{18}O_{shell}$ measurements during the phases of temperature increase and decrease provides a semi-quantitative estimate of the seasonal shell growth rate. In three of four cycles, the growth rate was higher during the summer than during the fall (Fig 5), with the only exception occurring in 2011 (shell #16).

Sclerochronological analysis

All subsequent results were calculated under the assumption of annual growth line formation, as confirmed by $\delta^{18}O$ analysis. Growth analyses were performed on 27 individuals with ontogenetic ages of 8 to 27 based on annual increment counts in the three anatomical parts: the outer shell layer, the resilium, and the chondrophore.

The mean annual SGI values and standard errors are shown in Fig 6. Before 1998, the EPS values of all anatomical parts remained below the critical threshold of 0.85. Therefore, the

stacked SGI chronologies were robust only during the period 1998-2014 (sample depth > 16 shells).

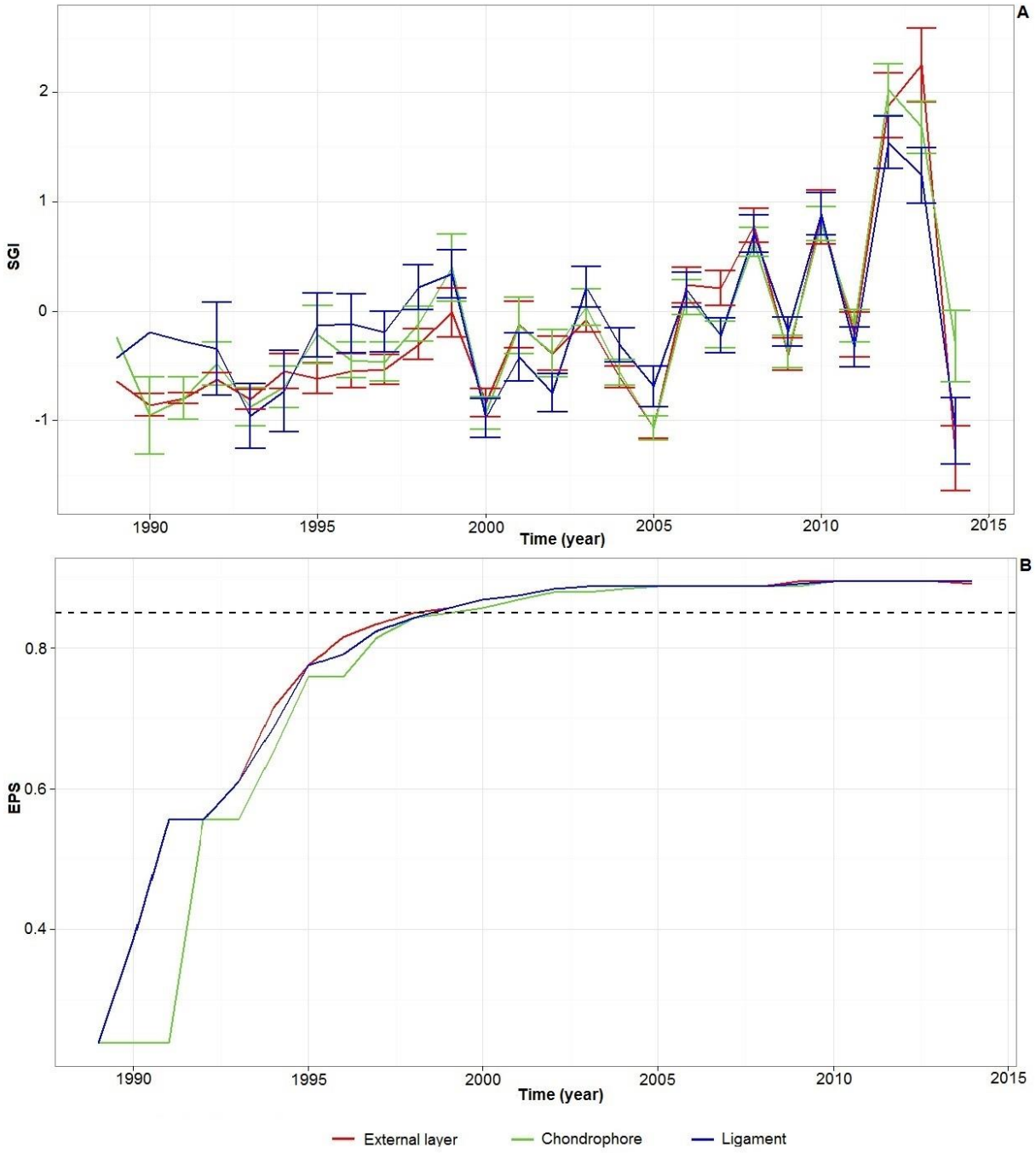

Figure 6: SGIs and EPS values. A) Mean annual SGI and associated standard errors calculated from 27 live-collected *S. solidissima* during the period 1989-2014. **B**) Expressed population signal (EPS) values associated with each anatomical part SGI series.

Pairwise correlations calculated on SGI time-series were significant ($p < 0.001$) between the external layer and chondrophore ($\tau = 0.68$), between the ligament and chondrophore ($\tau = 0.65$), and between the external layer and ligament ($\tau = 0.55$).The three SGI curves follow the same zigzag pattern, with an alternation of high and low values approximately every second year, which is very clear after the calendar year 2000 (Fig 6). The mean annual SGI varied considerably over the 25-year period, ranging from a minimum of -1.37 in 2014 to a maximum of 2.36 in 2013. The highest mean annual SGI variations were observed for the external shell layer. Notably, inter-annual SGI variations increased after 2005 and were at a maximum between 2013 and 2014 (Fig 6).

Regional growth comparisons

According to the specialized von Bertalanffy growth function applied to growth data from the SPM population, $L_{(p)\infty}$ was 163.5 mm, K 0.18, and t_0 0.77 (Table 1). Even if this growth function fits this size-at-age dataset almost perfectly ($R^2 = 0.96$), important variations in growth rates were observed between individuals. The growth dynamics of the SPM *S. solidissima* population are particularly close to those of Northumberland Straight [42], making it closer to Canadian populations. A distinct difference exists between US and Canadian surfclam populations in terms of growth dynamics (Fig 7).

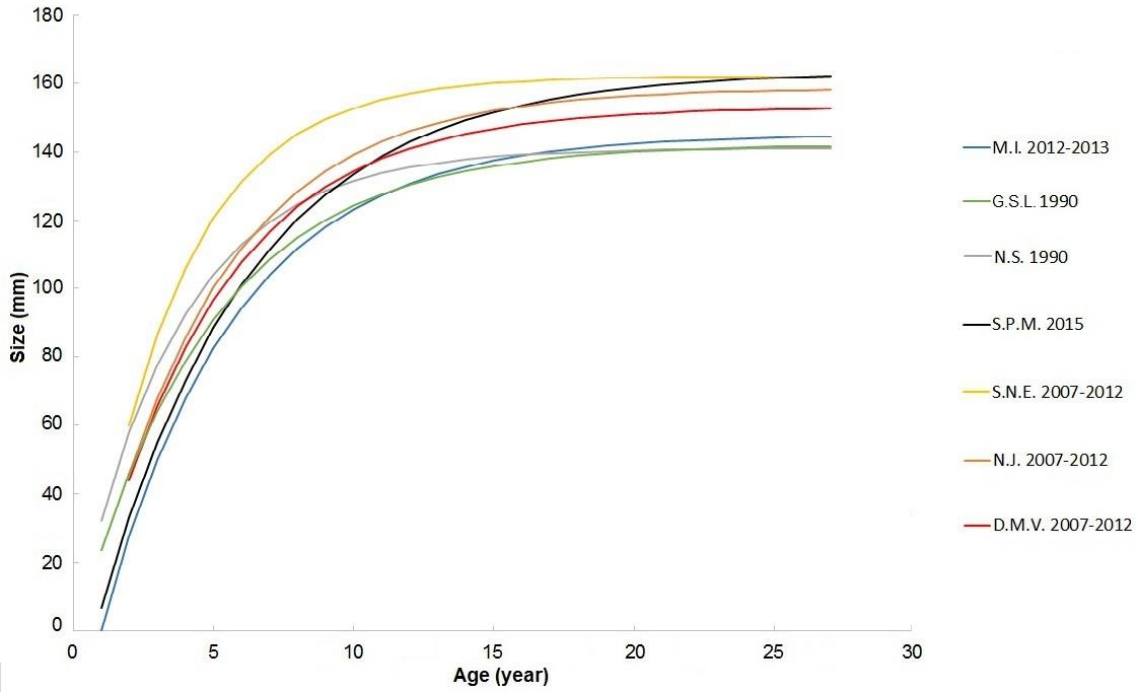

Figure 7: sVBGF curves in the last study from each geographic zone (details in Table 1).

The growth constant *K* is higher in the US than in Canada or at SPM except for GSL 1990 (Fig 8). Thus, American surfclams reach the asymptotic phase of shell growth faster than the Canadian or SPM populations. Regarding the L_∞, the only population that differs from the others is from Magdalen Islands, with a L_∞ value 2 or 3 cm lower than the others (Table 1).

The OGP index (ϕ') was lower for the three Canadian populations (~1.65), slightly increased at SPM, and reached a maximum value of 1.9 on the coast of southern New England. ϕ' decreased to approximately 1.7 close to the southern limit of the distribution area of *S. solidissima* (Fig 8).

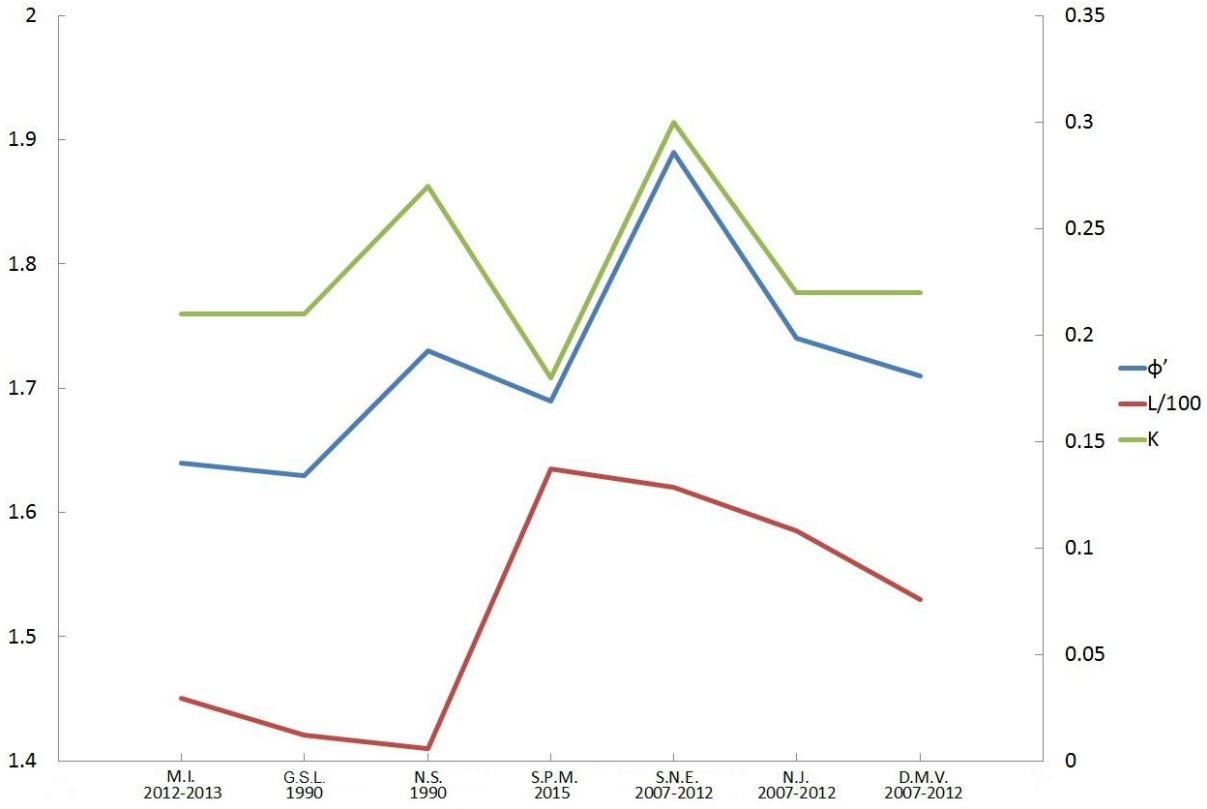

Figure 8: L_∞/100, *K* and Overall growth performance (ϕ') calculated using the sVBGF parameters of the last study from each geographic zone (details in Table 1).

Table 1: Specialized von Bertalanffy growth parameters (L_∞, K) and overall growth performance index (ϕ') from various studies on *S. solidissima* shell growth along the northeastern American coast, from the Gulf of St. Lawrence (GSL, Canada) to Delmarva (USA).

Site	Year	L_∞	K	ϕ'	Method	Reference
GSL (Magdalen Islands)	1986	133	0.2	1.55		Gendron 1988 [43]
GSL (Magdalen Islands)	2012-2013	145	0.21	1.64	Chondrophore and/or outer shell layer	Brulotte 2016 [44]
GSL (N-Prince Edward Island)	1984	142.1	0.21	1.63	Chondrophore	Sephton and Bryan 1990 [41]
GSL (Northumberland Straight)	1981	172.2	0.15	1.65	Shell growth ring measurement following Kerswill 1944 [18]	Roberts 1981 [42]
GSL (Northumberland Straight)	1984	141	0.27	1.73	Chondrophore	Sephton and Bryan 1990 [41]
Saint-Pierre and Miquelon	2015	163.5	0.18	1.69	Outer shell layer	Present study
Southern New England	1980	166.5	0.3	1.93	Chondrophore	Weinberg and Helser 1996 [45]
Southern New England	1989-1992	165.4	0.31	1.90	Chondrophore	Weinberg and Helser 1996 [45]
Southern New England	2007-2012	162	0.3	1.89	Chondrophore	Chute et al. 2016 [46]
New Jersey	1980	170.8	0.25	1.87	Chondrophore	Weinberg and Helser 1996 [45]
New Jersey	1989-1992	163.7	0.22	1.76	Chondrophore	Weinberg and Helser 1996 [45]
New Jersey	2007-2012	158.5	0.22	1.74	Chondrophore	Chute et al. 2016 [46]
Delmarva	1980	171	0.26	1.87	Chondrophore	Weinberg and Helser 1996 [45]
Delmarva	1989-1992	164	0.18	1.68	Chondrophore	Weinberg and Helser 1996 [45]
Delmarva	2007-2012	153	0.22	1.71	Chondrophore	Chute et al. 2016 [46]

Discussion

Isotopic validation of annual banding

The two isotopic profiles obtained from the third and fourth years of growth (2010-2011) of two *S. solidissima* shells from SPM agreed well with each other. The correspondence between the dark growth lines and $\delta^{18}O_{shell}$ maxima confirms the findings in previous studies [9-19] reporting that *S. solidissima* forms annual shell growth increments during the warmest months. Sea surface temperature measurements (top 5 m of the water column) showed that 2010 was a bit warmer than 2011, which was reflected by higher $\delta^{18}O_{shell}$ amplitude in the shells of both specimens. In the absence of $\delta^{18}O_{seawater}$ data from the sampling site, we used a constant $\delta^{18}O_{seawater}$ value of -1.66‰. This value was calculated using the equation from LeGrande and Schmidt [35] for the North Atlantic basin and an average salinity of 31.49, which was measured at SPM in the upper 5 m of the water column between August and November 2010. Reconstructed seawater temperatures were 4.7°C to 20.5°C. According to these results, there is an offset of a few degrees between measured and reconstructed temperature maxima. This offset can be explained by a difference in the thermal profiles between the localities at which the measurements were made, or by a difference in the $\delta^{18}O_{seawater}$ value. Combined with the instrumental measurements of seawater temperature, these results allow us to determine the growing season of *S. solidissima* during its third and fourth years of growth at SPM. Because the reconstructed temperature minimum occurred only once in the chronologies (in shell #2: 4.7°C during winter 2009/2010) and >90% of shell growth occurred when the seawater temperature was >8°C, we can assume that the main growing season during the third and fourth year of life occurred between the end of June and the end of October. For comparison, Ivany et al. [21] showed that, during the third year of growth, *S. solidissima* from New Jersey grew for 72.3% of the year, i.e., the growing season was almost twice as long as at SPM (for a comparable annual growth of slightly over 20 mm in both cases).

Similar observations have been made for pectinid bivalves of various species living in contrasting environments. For example, Heilmayer et al. [47] accumulated strong empirical evidence that a lower metabolic rate, a measure of the energy consumed by vital functions, including the maintenance and production of gametes, in colder environments reduces the energy cost of maintenance. Thus, a larger fraction of metabolic energy can be allocated to

growth-enhancing levels of growth performance and efficiency at lower temperatures. Moreover, except for shell #16 in 2011, oxygen isotope analyses revealed that shell growth at SPM occurs most rapidly during the first half of the year, between the beginning of July and the end of August. This finding is consistent with those of Jones et al. [9] and Ivany et al. [21], who also used stable oxygen isotopes and noted that growth of *S. solidissima* in New Jersey occurs most rapidly in spring and early summer, slowly in late summer, and extremely slowly or is non-existent in winter. The slowly decreasing $\delta^{18}O_{shell}$ values for the earliest part of each increment could reflect the spring phytoplankton bloom when the increase in temperature is still small. The slowing of shell growth observed during fall could be associated with a metabolic strategy of *S. solidissima*; the energy assimilated by an organism during fall could be preferentially allocated to energy reserves for winter rather than shell production. To confirm this hypothesis, field studies are needed on phytoplankton dynamics and the physiology of *S. solidissima*. The growth anomaly observed during the phase of temperature increase in 2011 for shell #16 could be explained by an individual event, such as predation or disease. This is consistent with the presence of a disturbance line within this annual increment. Moreover, at the collection site we clearly observed the presence of many *S. solidissima* predators [13], such as naticid snails (*Euspira heros*), sea stars (*Asterias* spp.), and crabs (*Cancer irroratus*).

Sclerochronological analysis

Analysis of the oxygen isotope composition of the outer shell layer of *S. solidissima* was useful to obtain insights into the seasonal timing of the growth line and increment formation. We also noted the occasional presence of disturbance lines in the outer shell layer (e.g., in shell #16 during summer 2011). The growth increment analysis in thin sections was also challenging due to erosion of the umbonal shell regions and constraints related to sample size and preparation techniques. This led us to investigate whether dark lines observed on the chondrophore and ligament cross-sections can provide an alternative record of the life-history traits of *S. solidissima*. Growth lines were used to calculate mean annual SGI values for each anatomical part studied. All pairwise correlations performed on these three SGI series were significant, suggesting that growth lines form annually in the external layer, chondrophore, and ligament of *S. solidissima*. Although the interest of using thin chondrophore sections for age and growth rate studies was highlighted previously for this species [46], we noted here

that this hard part also exhibits disturbance lines. Growth lines in the resilium seem to be less ambiguous to read because of higher contrast (Fig 1). Moreover, identifying and counting growth lines in the ligament is straightforward and allowed us to save time, as no additional grinding or polishing was required. Another advantage of using ligament cross-sections is the composition of this archive, i.e., aragonitic crystals embedded in an organic matrix, making it less prone to breakage than other shell parts composed mainly of calcium carbonate. Although micrometer-scale chemical studies of the hinge ligament have not yet been conducted, we can assume that the composition of this archive could lead to the development of new proxies.

SGI time-series of all specimens and anatomical parts of *S. solidissima* with overlapping lifespans exhibited a high degree of running similarity, i.e., relative changes in annual shell growth were similar among different specimens and anatomical parts. The standardized growth record of *S. solidissima* at SPM shows that growth was greater than expected during the years 2008, 2010, 2012, and 2013, whereas growth was less than expected in 2000, 2005, and 2014.

In the present study, we found that 2010 was warmer than 2011. This is especially true during the first half of the growing season, which seems to be the most important period of growth for *S. solidissima* at SPM and other localities [9-21]. This observation suggests that higher temperatures during summer are favorable for the growth of *S. solidissima* at SPM, which is expected for a species at the northern limit of its distribution area. However, during 2014, which was not reported to have an unusually cold summer, the shell grew slower than expected, suggesting that the annual shell growth of *S. solidissima* is governed by a combination of different external drivers and not only by seawater temperature. Additional environmental factors governing shell growth may include food quality and quantity [45-7], temperature [49], salinity [49], and dissolved oxygen [45]. More detailed instrumental records of such environmental factors would be useful for better understanding the drivers of changed in shell growth at SPM.

Regional growth comparisons

Growth is not uniform in the different settings in which *S. solidissima* is distributed. Such differences were observed previously along the east coast of the US [46]. Our study compared the shell growth of SPM populations with that of populations from the US and Canadian coasts to identify potential differences. The SPM population has some similarities with Canadian populations with regard to the parameters *K* and *ϕ'*. Slower growth (*K*) observed in two from three Canadian and SPM populations may be controlled, at least in part, by the environment. The environmental conditions are actually less favorable for growth in the northern and southern limits of the geographic range of *S. solidissima,* and previous studies have reported slower shell growth in southern populations [46]. Other possible sources of regional growth variation are genetic differences, as the only regional population with a distinctive genetic makeup comes from the Gulf of St. Lawrence [50]. All Canadian populations, differs from the others by low L_∞ values. In terms of environmental conditions, SPM and the Canadian populations do not differ much. A major difference between these two sites is the historic surfclam fishery which occur in Canada, whereas the SPM archipelago is free of any *S. solidissima* exploitation. The low L_∞ values observed for the Canadian surfclams may be at least partially induced by fishery activities because the largest specimens were preferentially removed from the population [51].

Other interesting features are the ontogenetic age and maximum shell length of inshore SPM surfclams used here. According to previous studies, *S. solidissima* tends to be smaller in size and to have a shorter lifespan in inshore populations. These trends have been attributed to high population density, differences in annual mean temperature, and more extreme temperature and salinity regimes [19-52-49]. However, based on the ages and sizes observed in this study, this does not seem to be the case at SPM, most likely due to its geographic position at the northern limit of the geographical distribution area of this species. This localization probably limits stresses related to high temperatures during summer. Moreover, the offshore position of SPM and the absence of major freshwater influx limit stress related to variations in salinity.

Conclusions

This study demonstrates that surfclams from SPM have annual shell growth increments. In addition, *S. solidissima* shell growth at that site mostly occurs over a 4-month period between the end of June and the end of October. The three different methods used to investigate shell growth suggest that growth lines appear to form on a periodic annual basis in the outer shell layer, chondrophore, and ligament of *S. solidissima*. This suggests that ligament cross-sections can provide an accurate estimate of age and growth, which is less ambiguous to read and requires less preparation time than the chondrophore and outer shell layer. The SGI chronologies vary greatly between years, and these variations have been more important since 2005. However, these results are challenging to interpret because suitable data on the environment and physiology of this species are lacking. Finally, from a regional perspective, this population is interesting because of its geographic setting at the Gulf of Saint Lawrence outlet and due to the absence of commercial and recreational fisheries.

Acknowledgements

We thank Cédric Épaule for providing *S. solidissima* shell samples from Saint-Pierre and Miquelon. We also thank Eric Dabas for his technical assistance during sclerochronological sample preparation and Sébastien Hervé for conceiving Fig 1. This work was supported by the EC2CO program MATISSE of the CNRS INSU, the Cluster of Excellence LabexMER, and the LIA BeBEST CNRS INEE. This research was carried out as part of the Ph.D. thesis of Pierre Poitevin for the University of Western Brittany with a French Ministry of Higher Education and Research grant. This manuscript greatly benefited from very useful comments made by two anonymous referees.

References

1 Ropes, J.W., and Jearld, A.Jr. 1987. Age determination of ocean bivalves. *In* Age and growth of fish. *Edited by* Summerfelt R.C. and Hall. G.E. Iowa State University Press, Ames, IA. pp. 517–526.

2 Northeast Fisheries Science Center (NEFSC). 2013. *In* 56th Northeast Regional Stock Assessment Workshop (56th SAW) Assessment Report. Northeast Fisheries Science Center Reference Document 13-10. U.S. Department of Commerce, NOAA Fisheries, Northeast Fisheries Science Center. 868 pp.

3 Weinberg, J. R., Dahlgren T. G., and Halanych, K.M. 2002. Influence of rising sea temperature on commercial bivalve species of the US Atlantic coast. Am. Fish. Soc. Symp. : 131-140.

4 Weinberg, J. R. 2005. Bathymetric shift in the distribution of Atlantic surfclams: response to warmer ocean temperature. ICES J. Mar. Sci. 62: 1444–1453. doi: 10.1016/j.icesjms.2005.04.020

5 Jacobson, L., and Weinberg, J.R. 2006. Atlantic surfclam (*Spisula solidissima*). Status of fishery resources of the northeastern. NOAA/NEFSC — Resource Evaluation and Assessment Division. Available from: http://www.nefsc.noaa.gov/sos/spsyn/iv/surfclam/index.html [Accessed August 2017]

6 Marzec, R. J., Kim, Y., and Powell E. N. 2010. Geographical trends in weight and condition index of surfclams (*Spisula solidissima*) in the Mid-Atlantic Bight. J. Shellfish Res. 29: 117-128. doi: https://doi.org/10.2983/035.029.0104

7 Munroe, D.M., Powell, E.N., Mann R., Klinck, J.M., and Hofmann, E.E. 2013. Underestimation of primary productivity on continental shelves: evidence from maximum size of extant surfclam (*Spisula solidissima*) populations. Fish. Oceanogr. 22: 220–233. doi: 10.1111/fog.12016

8 Narvaez, D. A., Munroe, D. M., Hofmann, E. E., Klinck, J. M., Powell, E. N., Mann, R., and Curchitser, E. 2015. Long-term dynamics in Atlantic surfclam (*Spisula solidissima*) populations: the role of bottom water temperature. J. Mar. Syst. 141: 136–148.

9 Jones, D.S, Williams, D.F., and Arthur, M.A.. 1983. Growth history and ecology of the Atlantic surf clam, *Spisula solidissima* (Dillwyn), as revealed by stable isotopes and annual shell increments. J. Exp. Mar. Biol. 73: 225-242.

10 Goodwin, D.H., Schöne, B.R., and Dettman, D.L., 2003. Resolution and fidelity of oxygen isotopes as paleotemperature proxies in bivalve mollusk shells: models and observations. Palaios 18: 110–125.

11 Steinhardt, J., Butler, P.G., Carroll, M.L., and Hartley, J. 2016. The application of long-lived bivalve sclerochronology in environmental baseline monitoring. Front. Mar. Sci. 3: 176. doi: https://doi-org.scd-proxy.univ-brest.fr/10.3389/fmars.2016.00176

12 Fay, C.W., Neves, R.J., Pardue, G.B., 1983. Species profiles: life histories and environmental requirements of coastal fishes and invertebrates (Mid-Atlantic) . . . surfclam. US Fish. Wildlife Serv. Div. Biological Services, FWS / OBS-82 / 11.13. US Army Corps of Engineers, TR EL-82-4, 23 p.

13 Cargnelli, L.M., Griesbach, S.J., Packer, D.B. and Weissberger, E. 1999. Essential fish habitat source document: Atlantic surfclam, *Spisula solidissima*, life history and habitat characteristics. NOAA Tech. Memo. NMFS NE 1999; 142: 13 p. Available from: http://www.nefsc.noaa.gov/nefsc/publications/tm/tm142 [Accessed August 2017]

14 Woodin, S.A., Hilbish, T.J., Helmuth, B., Jones, S.J., and Wethey, D.S. 2013. Climate change, species distribution models, and physiological performance metrics: predicting when biogeographic models are likely to fail. Ecol. Evol. 3 (10): 3334-3346. doi: http://dx.doi.org/10.1002/ece3.680

15 Taylor, J.D., Kennedy, W.J., and Hall, A. 1969. The shell structure and mineralogy of the Bivalvia. Introduction. Nuculacea-Trigonacea. Bull. Br. Mus. Nat. Hist. (Suppl.) 3: 1-125.

16 Belding, D.L. 1910. The growth and habits of the sea clam (*Mactra solidissima*). Rep. Comm. Fish. Game Mass. 1909 Publ. Doc. 25: 26-41.

17 Ropes, J.W., and Merrill, A.S. 1970. Marking surf clams. Proc. Nat. Shellfish. Assoc. 60: 99-106.

18 Kerswill, C.J. 1944. The growth rate of bar clams. Fish. Res. Board Can. Prog. Rep. Atl. Coast Stn 35: 18-20.

19 Jones, D.S., Thompsom, I., and Ambrose, W. 1978. Age and growth rate determinations for the Atlantic surf clam *Spisula solidissima* (Bivalvia: Mactracea), based on internal growth lines in shell cross-sections. Mar. Biol. 47: 63–70.

20 Stecher, H.A., Krantz, D.E., Lord, C.J., Luther, G.W., and Bock, K.W. 1996. Profiles of strontium and barium in *Mercenaria mercenaria* and *Spisula solidissima* shells. Geochim. Cosmochim. Acta 60 (18): 3445–3456.

21 Ivany, L.C., Wilkinson, B.H., and Jones, D.S. 2003. Using stable isotope data to resolve rate and duration of growth throughout ontogeny: an example from the surf clam *Spisula solidissima*. Palaios 18: 126–137

22 Gaspar, M. B., Castro, M., and Monteiro, C. C. 1995. Age and growth rate of the clam *Spisula solida* L., from a site off Vilamoura, south Portugal, determined from acetate replicas of shell sections. Sci. Mar. 59 (Suppl. 1): 87–93.

23 Ropes, J.W., and O'Brien, L. 1979. A unique method of aging surf clams. Bull. of the Am. Mal. U. for 1979: 58-61.

24 Ropes, J.W., and Shepherd, G.R. 1988. Surf clam *Spisula solidissima*. *In*: Age Determination Methods for Northwest Atlantic Species. *Edited by* Penttila, J., and Dery, L.M. NOAA Tech. Rep. NMFS 72: pp. 125-132.

25 Owen, G., Trueman, E.R., and Yonge, C.M. 1953. The ligament in the Lamellibrancia. Nature 171: 73-75.

26 Merrill, A.S., Posgay, J.A., and Nighy, F.E. 1961. Annual marks on the shell and ligament of sea scallop (*Placopecten magellanicus*). Fish. Bull. 65: 299-311.

27 Yonge, C.M. 1967. Form, habit, and evolution in the Chamidae (Bivalvia) with reference to the conditions in the rudists (Hippuritacea). Phil. Trans. R. Soc. Lond. B 252: 49-105.

28 Skelton, P.W. 1979. Preserved ligament in a radiolitid rudist bivalve and its implication of mantle marginal feeding in the group: Paleobiology 5: 90-106.

29 Fan, C., Koeniger, P., Wang, H. and Frechen, M. 2011. Ligamental increments of the mid-Holocene Pacific oyster *Crassostrea gigas* are reliable independent proxies for seasonality in the western Bohai Sea, China. Palaeogeogr. Palaeoclimatol. Palaeo-ecol. 299: 437–448. doi: 10.1016/j.palaeo.2010.11.022

30 Marsh, M., Hopkins, G., Fisher, F., and Sass, R.L. 1976. Structure of the molluscan bivalve hinge ligament, a unique calcified elastic tissue. J. Ultrastruct. Res. 54: 445–450.

31 Schöne, B. R. 2013. *Arctica islandica* (Bivalvia): a unique paleoenvironmental archive of the northern North Atlantic Ocean. Glob. Planet. Change 111: 199-225. doi: 10.1016/j.gloplacha.2013.09.013

32 Füllenbach, C. S., Schöne, B. R., and Mertz-Kraus, R. 2015. Strontium/lithium ratio in aragonitic shells of *Cerastoderma edule* (Bivalvia) — A new potential temperature proxy for brackish environments. Chem. Geol. 417: 341–355. doi: 10.1016/j.chemgeo.2015.10.030

33 Grossman, E.L., and Ku, T.L. 1986. Oxygen and carbon isotope fractionation in biogenic aragonite: temperature effects. Chem. Geol. 59: 59-74.

34 Sharp, Z. 2006. Biogenic carbonates: Oxygen. in: Prentice-Hall (Ed.), Principles of Stable Isotopes Geochemistry. Upper Saddle River, N.J., New Jersey, pp. 120-149.

35 LeGrande, A.N., and Schmidt, G.A. 2006. Global gridded data set of the oxygen isotopic composition in seawater. Geo. Res. Lett. 33: *LI2604.* doi: 10.1029/2006GL026011.

36 Brey, T. 2001. Population dynamics in benthic invertebrates. A virtual handbook. Alfred Wegener Institute for Polar and Marine Research, Bremerhaven, Germany. Available from: http://www.awibremerhaven.de/Benthic/Ecosystem/FoodWeb/Handbook/main.html.

37 Wigley, T.M.L., Briffa, K.R., and Jones, P.D. 1984. On the average value of correlated time-series, with applications in dendroclimatology and hydrometeorology. J. of Clim. and App. Meteo. 23 (2): 201–213.

38 R Core Team (2016). R: A Language and Environment for Statistical Computing. R Foundation for Statistical Computing, Vienna, Austria. URL https://www.R-project.org/

39 Pauly D., 1979. Gill size and temperature as governing factors in fish growth: a generalization of von Bertalanffy's growth formula. Ber. Inst. Meereskd. Christian-Albrechts-Univ. Kiel 63, 1–156.

40 Pauly D., and Munro J.L. 1984. Once more on the comparison of growth in fish and invertebrates. Fishbyte 2, 21.

41 Sephton T.W., and Bryan C.F. 1990. Age and growth rate determinations for the Atlantic surf clam Spisula solidissima (Dillwyn, 1817) in Prince Edward Island, Canada. J. Shellfish Res. 9: 177-185.

42 Roberts, G. 1981. Dynamics of an exploited population of bar clam, *Spisula solidissima*. Can. Manuscr. Rep. Fish. Aquat. Sci. 1607: iv + 13 p.

43 Gendron, L. 1988. Exploitation et état du stock de mactres (*Spisula solidissima*) des Îles-de-la-Madeleine en 1986. Rap. manus. can. sci. halieut. aquat. 1993: v + 17 p.

44 Brulotte, S. 2016. Évaluation des stocks de mactre de l'Atlantique, *Spisula solidissima*, des Îles-de-la-Madeleine, Québec en 2015 – méthodologie et résultats. Secr. Can. de Consult. Sci. du MPO. Doc. de Rech. 2016/074. x + 51 p.

45 Weinberg, J.R., and Hesler, T.E. 1996. Growth of the Atlantic surfclam, *Spisula solidissima*, from Georges Banks to the Delmarva Peninsula, USA. Mar. Biol. 126: 663 – 674

46 Chute, A.S., McBride, R. S., Emery, S.J., and Robillard, E. 2016. Annulus formation and growth of Atlantic surfclam (*Spisula solidissima*) along a latitudinal gradient in the western North Atlantic Ocean. J. Shellfish Res. 35: 729-737. doi: 10.2983/035.035.0402

47 Heilmayer, O., Honnen, C., Jacob U., Chiantore, C., Cattaneo-Vietti, R., and Brey, T. 2005. Temperature effects on summer growth rates in the Antarctic scallop, *Adamussium colbecki*. Polar Biol. 28: 523–527.

48 Ropes, J.W., Merrill, A.S., Murawski, S.A., Chang, S., MacKenzie, C.L. Jr. 1979. Impact on clams and scallops. Part I. Field survey assessments. *In* Oxygen Depletion and Associated Benthic Mortalities in New York Bight, 1976. *Edited by* Swanson, R.L., and Sindermann, C.J. NOAA Professional Paper 11, pp. 263–275.

49 Cerrato, R.M., and Keith, D.L. 1992. Age structure, growth, and morphometric variations in the Atlantic surf clam, *Spisula solidissima*, from estuarine and inshore waters. Mar. Biol. 114: 581-593. doi: 10.1007/BF00357255

50 Hare, M.P., and Weinberg, J.R. (2005) Phylogeography of surfclams, *Spisula solidissima*, in the western North Atlantic based on mitochondrial and nuclear DNA sequences. Mar. Biol. 146: 707–716. doi: 10.1007/s00227-004-1471-y

51 Munroe, D. M., Narvaez, D. A., Hennen, D., Jacobson, L., Mann, R., Hofmann, E. E., Powell, E. N., and Klinck, J.M. 2016. Fishing and bottom water temperature as drivers of change in maximum shell length in Atlantic surfclams (*Spisula solidissima*). Estuar. Coast. Shelf Sci. 170: 112–122. doi: 10.1016/j.ecss.2016.01.009

52 Ambrose, W.G., Jr., Jones, D. S., and Thompson, I. 1980. Distance from shore and the growth rate of the suspension feeding bivalve, *Spisula solidissima*. Proc. Natl. Shellfish. Assoc. 70: 207–215.

Chapitre 2

Growth response of *Arctica islandica* to North Atlantic oceanographic conditions since 1850

Contexte et résumé de l'étude

Ce deuxième chapitre utilise une partie des techniques sclérochronologiques mises en place lors du chapitre précédent, en les appliquant au bivalve présentant la plus longue période de croissance connu à ce jour. Nous nous intéresserons au sein de ce chapitre aux liens pouvant exister entre la variabilité de la croissance d'*A. islandica* à Saint-Pierre et Miquelon (SPM) depuis 1850 et plusieurs variables environnementales mesurées à différentes échelles : globales, régionales et locales afin de mieux comprendre l'hydrodynamisme passé de cet archipel.

Pour ce faire, nous avons utilisé les coquilles de trente-deux individus d'*A. islandica* prélevés vivants à SPM. La taille des incréments a été mesurée dans la couche externe des valves de chacun des individus, puis la tendance ontogénique associée a été retirée grâce à un modèle de croissance dynamique, que nous avons développé, basé sur l'équation générale de von Bertalanffy. La fiabilité statistique de cette chronologie de croissance, a ensuite été vérifiée à l'aide des différents indicateurs présentés dans le chapitre précédent. Ce signal de croissance populationnel a ensuite été comparé à des indices climatiques globaux tels que l'AMO, la NAO et l'indice SPG. Des corrélations significatives entre les variations de ces mesures de croissances et celles de ces indices ont alors été identifiées. D'un point de vue spatial, de fortes corrélations positives entre les variations de croissance d'*A. islandica* et les températures de surface (0-100m) au sein du Gyre Sub-Polaire (SPG) ont également été mises en lumière. Nous avons alors cherché des explications, locales et régionales, pouvant lier les réponses biologiques de ces organismes à SPM avec ces indices très généraux. Des corrélations ont alors été mises en évidence entre les informations enregistrées au sein des coquilles d'*A. islandica* et : (i) la température et la salinité (Station 27) de la branche côtière du courant du Labrador, (ii) la couverture de glace de mer le long des côtes Terre-Neuviennes, (iii) le transport vers l'Ouest du courant du Labrador offshore au sud des Grands Bancs, (iv) la dynamique du Shelf Slope Front au sud de l'archipel ainsi qu'avec (v) les mesures satellitaires de chlorophylle *a* à SPM. Ces principaux résultats nous ont finalement permis d'identifier clairement des masses d'eau qui influencent l'hydrodynamisme de SPM. D'un point de vue écosystémique, nous

disposons maintenant d'une description plus fine des conditions hydroclimatiques passées associées aux variations de croissance d'*A. islandica* à SPM. Ce travail a également pointé du doigt des difficultés liées à l'absence totale d'observations récurrentes de plusieurs paramètres physiques et biologiques dans les eaux côtières de SPM.

Growth response of *Arctica islandica* to

North Atlantic oceanographic conditions since 1850

Pierre Poitevin[1*], Julien Thébault[1], Valentin Siebert[1], Sébastien Donnet[2], Justine Doré[1], Laurent Chauvaud[1], Pascal Lazure[3]

[1] *Université de Bretagne Occidentale, Laboratoire des Sciences de l'Environnement Marin (UMR6539 UBO/CNRS/IRD/Ifremer), 29280 Plouzané, France*

[2] *Fisheries and Oceans Canada, Northwest Atlantic Fisheries Centre (NAFC), 80 East White Hills Road, St. John's, NL, Canada, A1C 5X1*

[3] *Ifremer, Laboratoire d'Océanographie Physique et Spatiale (UMR6523 CNRS/Ifremer/IRD/UBO), 29280 Plouzané, France*

Email addresses:

Pierre Poitevin: pierre.poitevin@univ-brest.fr

Julien Thébault: julien.thebault@univ-brest.fr

Valentin Siebert: siebert.valentin@gmail.com

Sébastien Donnet: sebastien.donnet@dfo-mpo.gc.ca

Justine Doré: justine.dore@univ-brest.fr

Laurent Chauvaud: laurent.chauvaud@univ-brest.fr

Pascal Lazure: pascal.lazure@ifremer.fr

Corresponding author:

Pierre Poitevin

Université de Bretagne Occidentale

Institut Universitaire Européen de la Mer

Laboratoire des Sciences de l'Environnement Marin (UMR6539 UBO/CNRS/IRD/Ifremer)

F-29280 Plouzané

Tel: +33 2 90 91 55 78

Fax: +33 2 98 49 86 45

Abstract

The Northwest Atlantic is a key region with an essential role in global climate regulation, redistributing heat and influencing the carbon cycle. However, little is known about its variability before 1950, mainly because of the lack of long-term instrumental measurements. The hard parts of long-lived marine biota hold the potential to extend instrumentally derived observation by several decades or centuries and enhance our understanding of global climate processes. Here we investigate the effects of local, regional, and large-scale climate variability on the marine bivalve, *Arctica islandica* (Linnaeus 1767) from Saint-Pierre & Miquelon (SPM). This archipelago lies at the boundary zone between the cold Labrador Current in the north and the warm Gulf Stream waters to the south. This study presents the northernmost statistically robust *A. islandica* growth chronology (1850–2015) from the Western North Atlantic and its potential as an environmental proxy record for past climatic and hydrographic variabilities at different time and geographical scales. The chronology correlates significantly and positively with the Atlantic Multidecadal Oscillation (AMO; N=142, r=0.34, p<0.05) and negatively with the North Atlantic Oscillation (NAO; N=66, r=-0.36, p<0.05), two global climatic indices. The North Atlantic spatial pattern of correlation shows significant (p<0.05) and positive correlations of 0–100-m temperatures from 1950 with *A. islandica* growth in SPM encompassing the Sub-Polar Gyre area. These global-scale relationships are refined and the mechanisms leading to them explained by comparing *A. islandica* growth chronology to regional environmental datasets such as the Shelf Slope Front position, Tail of Grand Bank Transport, and Station 27 temperature and salinity. These relationships between the *A. islandica* shell growth record at SPM and environmental datasets covering different geographical scales yield details about SPM hydrodynamics. Moreover, these findings confirm the key role of this archipelago for studying large-scale hydrographic variability and ecosystem dynamics facing global changes.

Keywords:

Arctica islandica, Paleoecology, North Atlantic, Sub Polar Gyre, Labrador Current, Growth Chronology, Bivalve, Coastal.

Introduction

Over the past few decades, the earth's climate system has undergone deep and rapid changes. The oceans and their interaction with the atmosphere have become a focal point of climate studies because of the ocean's role in ongoing global warming. The subpolar North Atlantic is one of the most climate-relevant regions of the ocean for observing these interactions (Rhein et al., 2011) because it is the starting point of the Atlantic Meridional Overtuning Circulation. Southern Newfoundland's coast and the Saint-Pierre & Miquelon (SPM) region lie at the confluence of the main oceanographic currents ruling the North Atlantic Basin hydrodynamics (the Gulf Stream and Labrador Current [LC]). However, despite its importance, the physical flow dynamics of this region is poorly understood (e.g., Wu et al., 2012). This gap exists mainly because of the lack of long-term environmental records in this area, where they are sparse and spatiotemporally incomplete before the mid-20th century (Halfar et al., 2011).

Proxy data allow us to generate such records retrospectively. In boreal and temperate regions, most paleoenvironmental reconstructions are based on terrestrial proxies. However, such data do not necessarily reflect marine environmental conditions. In the oceanic realm, analysis of the carbonate hard structures of long-lived marine species could potentially extend instrument-derived observations by several decades or centuries. As recent studies have demonstrated (e.g., Butler et al., 2013; Bonitz et al., 2018; Schöne et al., 2005a, Wanamaker et al., 2012; Witbaard et al., 1997), shells of the bivalve mollusc *Arctica islandica* (Linnaeus, 1767) hold this potential. The main assets of this species are (i) its wide geographic repartition across the North Atlantic in the upper 500 m (Nicol, 1951), and (ii) its extraordinary longevity, with a maximum recorded age of 507 years (Butler et al., 2013).

Like other molluscs, this species contains distinct annual growth increments in its shell (Jones, 1980; Schöne, 2013). The width of the growth increments is defined by annual growth lines formed during certain periods of the year associated with reduced growth rates (Dunca et al., 2009). With this periodic banding, each increment can be placed in a temporal context. Moreover, if the date of a specific growth increment is known (the date of death, for instance), it becomes possible to assign precise calendar dates to an entire shell record. Annual increment size generally results from interactions between the environment and organism physiology (Lutz & Rhoads, 1980, for a review). Although genetic factors can influence

ontogenetic growth trends and other fitness-related traits (David et al., 1995), year-to-year variability is mainly caused by external factors (Marchitto et al., 2000). These external factors have often been related to environmental variables such as food availability (e.g., Ballesta-Artero et al., 2017; Witbaard et al., 1997) or water temperature (e.g., Butler et al., 2010; Marali & Schöne, 2015). However, assigning growth patterns to any single environmental variable or to a combination is challenging because of their interactions, which may also vary in time and space (Butler et al., 2013). Based on synchronous changes in shell growth and a common response to environmental fluctuations, increment width time series of specimens with overlapping lifespans can be combined to build composite or master chronologies (e.g., Bonitz et al., 2018; Schöne et al., 2005a, Wanamaker et al., 2012; Witbaard et al., 1997). These annually resolved and exactly dated paleorecords can cover centuries and provide information about the common environmental variables that influenced the growth of this species in different locations.

This study focuses on SPM to present the northernmost *A. islandica* growth chronology (1850–2015) from the Western North Atlantic and its potential as an environmental proxy record for past climatic and hydrographic variabilities. The objectives of this study were to (i) determine if synchronous changes in shell growth among specimens from surface waters (<15 m) allow construction of a statistically robust composite chronology, and (ii) test whether *A. islandica* shell growth variability can serve as a tool for estimating past environmental variability in SPM and in a broader spatial context.

Materials & Methods

Sample collection

Thirty-two *A. islandica* specimens were analysed. All of them were live collected at 14–15 m depth by scuba diving along the southeastern shore of the Miquelon-Langlade sandy isthmus (46°54'08"N; 56°16'86"W) in September 2016 (Fig. 1).

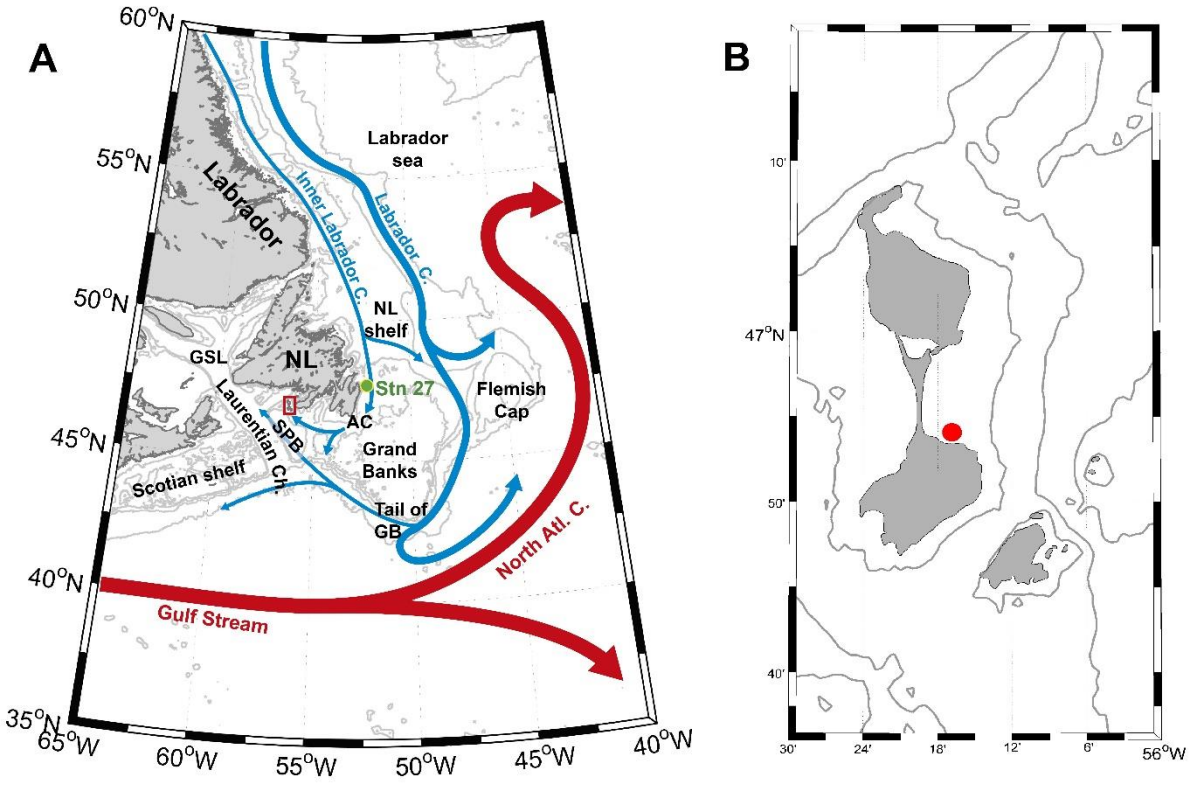

Figure 1: (A) Major features of the regional surface circulation (inspired by Fig.1 in Fratantoni & McCartney, 2009) and main location names. The cold inner and outer LCs are in blue; Gulf Stream and North Atlantic currents are in red. In green is historical hydrographic Station 27 (Stn 27). The main acronyms corresponding to location names are as follows: NL – Newfoundland; SPB – Saint-Pierre Bank; GSL – Gulf of Saint-Lawrence; AC – Avalon Channel; and GB – Grand Banks. (B) Sampling location of *A. islandica* (red dot).

The habitat at the sampling station was homogeneous and consisted of compacted and stable fine sand. Soft tissues were removed from the live-collected shells immediately after collection. All specimens were carefully cleaned with freshwater to remove adherent sediment and biological tissues before sample preparation.

Sample preparation

For each shell, a section roughly 2–3-cm in width was cut using a robust tile saw from the hinge through to the ventral margin encapsulating the apex of the umbo and the axis of maximum growth. The cut section was embedded in a polyester mounting resin (SODY 33, ESCIL) to prevent cracking during sectioning. A thin cross-section (2 mm thick) was cut along the axis of maximum growth using a low-speed precision saw (Struers, Secotom 10; rotation speed 500 rpm; feed rate 200 µm s−1) equipped with a 600-µm-thick diamond-coated blade

continuously cooled by deionized water. Thin sections were carefully ground on a rotating polishing table (Struers, TegraPol-35) with a sequence of 800, 1200, 2500, and 4000 grit wet-table carborundum paper, followed by polishing with 3-µm diamond liquid (Struers) to remove any saw marks. Cross-sections were ultrasonically cleaned with deionized water between each grinding or polishing step to remove residual abrasive material.

The polished shell sections were then etched in a Mutvei's solution (Schöne et al., 2005b) for 45 minutes at room temperature, soaked in a deionized water bath, and left to air dry before imaging. Treatment with Mutvei's solution results in a three-dimensional display of growth patterns and reveals clear annual growth lines.

Shell sections were photographed under reflected light (Carl Zeiss, KL 2500 LCD) using an AxioCam MRC 5 installed on a Carl Zeiss SteREO Lumar.V12 stereomicroscope equipped with a motorized stage, under 25× magnification. Photomosaics were constructed using AxioVision 4.9.1 software (Carl Zeiss). Annual growth increment widths were measured digitally in the outer shell layer (Schone et al., 2005a) to the nearest 1 µm (Fig. 2) using the image processing and analysis software Image J (NIH Image). Each growth increment was assigned to a particular year starting from the ventral margin of the shell, yielding a time series of increment width for each individual.

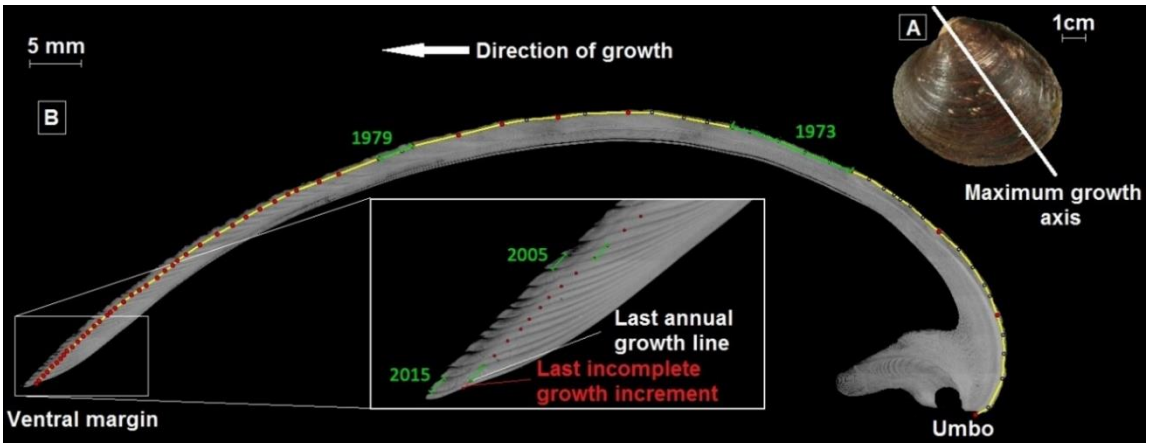

Figure 2: *A. islandica* growth patterns. (A) Outer shell surface of an *A. islandica* left valve and its axis of maximum growth along which thin cross sections were cut. (B) Photomosaic of a cross-section stained by Mutvei's solution. The yellow line corresponds to the trajectory on which annual growth lines (red dots) were placed and growth increments measured (green lines).

Chronology construction

To isolate environmental signals from time series of increment width, ontogenetic age trends were individually removed. This ontogenetic trend can be estimated mathematically by a growth equation. In the present study, a dynamic optimized model deriving the generalized von Bertalanffy growth function (von Bertalanffy, 1938) was fitted to each measured increment width time series. This code was written with Scilab 6.0.0, free and open source software (distributed under CeCILL license - GPL compatible) developed by Scilab Enterprises (2012) and is available upon request.

Growth indices (GIs) were then calculated for each year and each individual by dividing the measured increment width by the predicted increment width (Schöne, 2013), as follows:

$$GI_t = \frac{L_{t+1} - L_t}{L(p)_{t+1} - L(p)_t}$$

Where GI_t is the growth index at t (in years), $L_{t+1} - L_t$ is the measured shell increment at t, and $L(p)_{t+1} - L(p)_t$ is the predicted shell increment length at the same time t. Individual time-series of GI were then standardized as follows (Schöne, 2013):

$$SGI_t = \frac{GI_t - \mu}{\sigma}$$

Where μ is the average of all GI values and σ the standard deviation. The standardized GI (SGI) is a dimensionless measure of how growth deviates from the predicted trend. Positive values represent greater than expected growth, whereas negative values represent less than expected growth. The robustness of the SGI chronology was tested. A frequently used assessment of the robustness of composite chronologies is the expressed population signal (EPS) (Wigley et al., 1984), which is given as:

$$EPS = \frac{n * R_{bar}}{\left(n * R_{bar} + (1 - R_{bar})\right)}$$

Where R_{bar} is the average of all correlations between pairs of SGI chronologies and n is the number of specimens used to construct the stacked chronology. EPS > 0.85 indicates that the variance of a single SGI chronology sufficiently expresses the common variance of all SGI series. All these analyses were carried out using COFECHA (Grissino-Mayer, 2001) and the R package dplR (Bunn, 2008).

Environmental datasets

The SGI master chronology was compared with annual climatic indices reflecting climate and ocean dynamics over the North Atlantic Ocean on a decadal or multi-decadal time scale: the Atlantic Meridional Oscillation (AMO) (Schlessinger & Ramankutty, 1994), the North Atlantic Oscillation (NAO) (Hurrell, 1995), and the Sub-Polar Gyre (SPG) index (Hakkinen & Rhines, 2004).

The AMO is an index reflecting sea surface temperature variations in the North Atlantic. The dataset used in this study extends from 1870 to 2010 and is available at http://www.cgd.ucar.edu/cas/catalog/climind/AMO.html.

The NAO is the difference in atmospheric pressure between Acores high pressures and Icelandic low pressures, which drive the westerlies. Several datasets on NAO are available and can differ significantly (even in the last decades) depending on the atmospheric data used (mainly their location) and their treatments. In this study, we used three datasets:

- The DFO (Canada) dataset covers 1895–2017 on a yearly basis and is available at:

http://www.meds-sdmm.dfo-mpo.gc.ca/isdm-gdsi/azmp-pmza/climat/nao-oan-eng.htm

- CRU (University of East Anglia) from 1821 to present, now on a monthly and yearly basis and available at:

https://crudata.uea.ac.uk/cru/data/nao/index.htm

- NCEP reanalysis of NOAA from 1950 to present on a monthly basis, available at:

ftp://ftp.cpc.ncep.noaa.gov/wd52dg/data/indices/nao_index.tim

The SPG time series used in this study came from Berx and Payne (2017) and spans 1992–2016 on a monthly basis; it is available at: https://data.marine.gov.scot/dataset/sub-polar-gyre-index.

To assess the spatial correlation between SGI and North Atlantic hydrology, we used the gridded objective analysis of world ocean temperature and salinity (averaged from the surface to 100 m) of the UK Met Office Hadley centre EN4.2.1 (Good et al., 2013, with bias corrections from Levitus et al., 2009). This dataset has a spatial resolution of 1°, 42 vertical levels, and a

monthly time step, and extends from 1900 to present. We decided to use only the last 66 years (1950–2015) because of the larger uncertainties of environmental measurements during the first half of the 20th century. These data are available at: https://www.metoffice.gov.uk/hadobs/en4/download-en4-2-1.html#l09_analyses.

To test the effect of regional and local environmental conditions on shell growth, the master chronology was also compared to regional environmental datasets (Fig. 1).

Instrumental temperature and salinity measurements were obtained from oceanographic Station 27 (surface to 175 m; 47.55°N, 52.583°W). This historical hydrographic station located 7 km off St. John's Harbour in the Avalon channel provides more than 50 years of *in situ* measurements of surface ocean parameters in monthly sampling resolution. Station 27 data are available from June 1946 onwards. However, because of data gaps in the years 1946–1949 (more than 4 measurements/year missing), only data from 1950 onwards were used in this study.

The SGI data were also compared to LC volume transport along the Tail of Grand Bank (TGB) at several transects from 1992 to 2013 (Han & Li, 2008), which are available at: http://www.meds-sdmm.dfo-mpo.gc.ca/isdm-gdsi/azmp-pmza/climat/labrador/transport-eng.htm.

The long-known Shelf Slope Front (SSF), which lies between cold fresh shelf water and warm slope water at the South (Gatien, 1976), was also used. The latitudinal position of the SSF was digitized from 1973 to present, between -65°W and -50°W at each 1° of longitude from sea surface temperature–based analysis charts of the Bedford institute, available at: http://www.meds-sdmm.dfo-mpo.gc.ca/isdm-gdsi/azmp-pmza/climat/gulf-golfe/slope-plateau-eng.htm.

The DFO ice coverage surface over the Newfoundland shelf (in km^2) from 1963–2016, reported on a monthly basis, is available at: http://www.meds-sdmm.dfo-mpo.gc.ca/isdm-gdsi/azmp-pmza/climat/ice-glace/coverage-couverture-eng.htm.

Finally, to reveal the potential relationships between shell growth and local phytoplankton dynamics, SGI master chronology was compared to monthly satellite chlorophyll *a* measurements (1998–2015). The data were downloaded from the GlobColour website (http://hermes.acri.fr) and are weighted monthly averages of single-sensor products

(SeaWiFS/MERIS/MODIS/VIIRSN merged chlorophyll concentrations) over the area 46.6–47.3°N / 56.0–56.6°W (i.e., waters surrounding the SPM archipelago within ca. 30 km).

Statistics

For comparisons between the master chronology and environmental datasets, the Pearson correlation was used and, in some cases, the Spearman rho correlation. The commonly used *p* value of 0.05 was chosen as the threshold value for significance of the correlations.

Results

Chronology construction

The shell-based growth records of the 32 live-collected *A. islandica* specimens from surface waters (<15 m) of SPM covered the time interval from 1850 to 2015 (Fig. 3). The shortest and longest time series that were used to build the master chronology were 41 and 166 years, respectively. The average length of these 32 time series was 106.94 years (1σ=33.39), and 23 were longer than 100 years. Shells had strongly synchronous detrended growth patterns among individuals, with wide increments between 1915 and 1955 and narrow increments from 1981 to 2015. Correlations between each detrended time series and the average of others were all positive and statistically significant ($p<0.05$), with a mean of 0.537 (series intercorrelation). Average mean sensitivity calculated according to Eq. 2 in Biondi and Qeadan (2008) was 0.270. Since 1889 and until 2015, running EPS values (15-year windows with 8-year overlaps) largely remained above the critical threshold of 0.85 (Wigley et al., 1984) (Fig. 3).

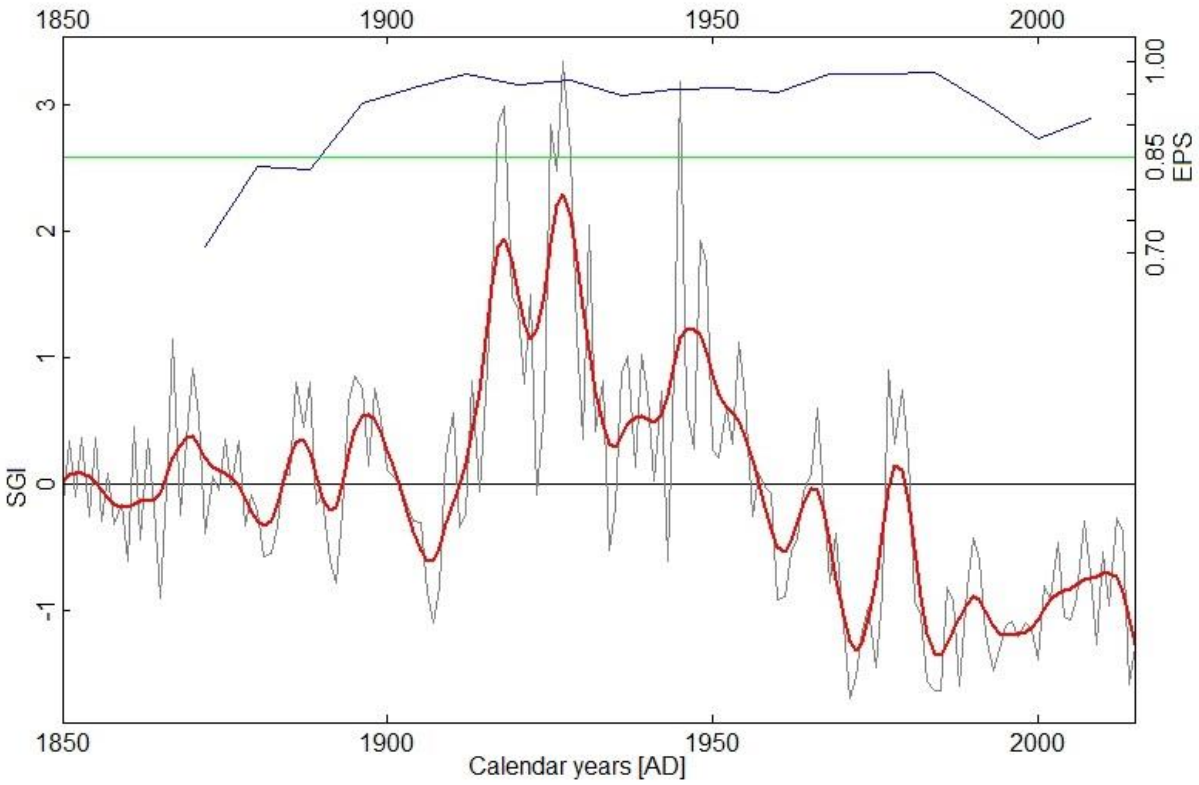

Figure 3: SPM SGI master chronology (grey curve) from A. islandica and its 10-year running mean (red curve). EPS values (blue curve) from the master chronology computed in 15-year running windows with arbitrary EPS threshold value 0.85 (green line) above which the master chronology is statistically robust.

Shell growth variability and environmental data

Correlation with global climatic indices (AMO, NAO, SPG)

The correlation between SGI (10-year running mean) and AMO dataset from the UCAR series (1870–2011) was significant (N=142, r=0.34, p<0.05) and remained constant even with time lags of 1 to 2 years. The same correlation applied to a truncated SGI (10-year running mean) time series (1948–2015) was stronger (N=68, r=0.67, p<0.05). Weak negative correlations were found between SGI master chronology and short NAO time series (1950–2015) from the NCEP (N=66, r=-0.36, p<0.05), UK (N=66, r=-0.28, p<0.05), and DFO (N=66, r=-0.36, p<0.05) datasets. *A. islandica* SGI chronology was negatively correlated (N=24, r=-0.56, p<0.05) with the annual SPG index from Berx and Payne (2017) over the period 1992–2015.

Correlation with spatial datasets

The spatial correlations between A. islandica SGI chronology and monthly near surface (average between surface and 100 m) temperature and salinity, from the UK Met Office Hadley centre EN4.2.1, are represented in Figure 4 for mid-winter (February), mid-spring (May), mid-summer (August), and mid-fall (November). Given the spatial heterogeneities of the environmental observations in the first half of the 20th century, the correlations were calculated only for the last 66 years (1950–2015). The most striking features were the strong positive correlations with temperature, which cover a large area in the NE of Newfoundland and south of Greenland, encompassing the Labrador and Irminger seas (Fig. 4). This area broadly delineates the SPG. Positive correlations between GI and near surface salinities were patchier with less geographical extent and concentrated east of Newfoundland.

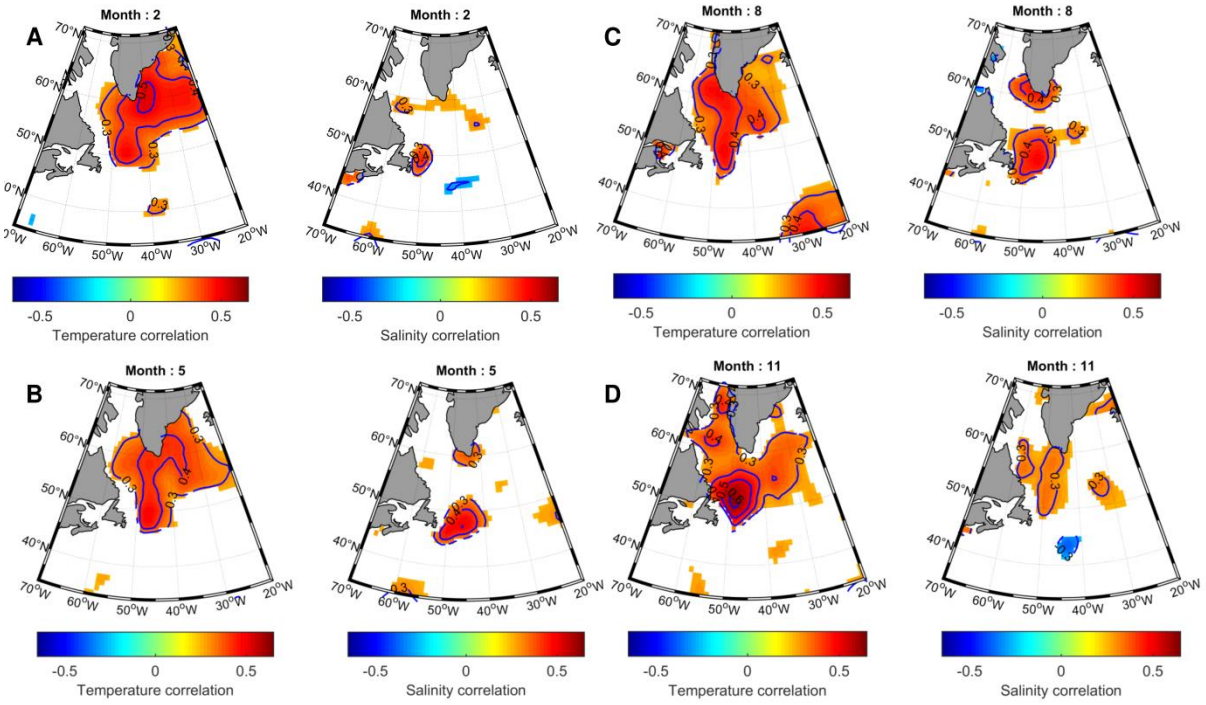

Figure 4: Spatial Pearson correlations between *A. islandica* SGI and detrended monthly near surface (0–100 m) temperature and salinity, from the UK Met Office Hadley centre EN4.2.1, represented for (A) mid-winter (February), (B) mid-spring (May), (C) midsummer (August), and (D) mid-fall (November). Only significant (p<0.05) correlation coefficients above 0.3 are represented.

The average latitudinal position of the SSF is between 42–43°N, and this latitude at each degree of longitude varies with season and year. At each longitude from 50 to 65°W, a time series of the monthly latitude of the SSF (with a minimum of three observations per month) is correlated with SGI. Correlations between growth rate and SSF latitudinal position were always negative and often significant (Fig. 5). Between 60 and 50W, strong negative correlations occurred during the previous fall (October, November, and December) and spring (April, May, and June) to a lesser extent.

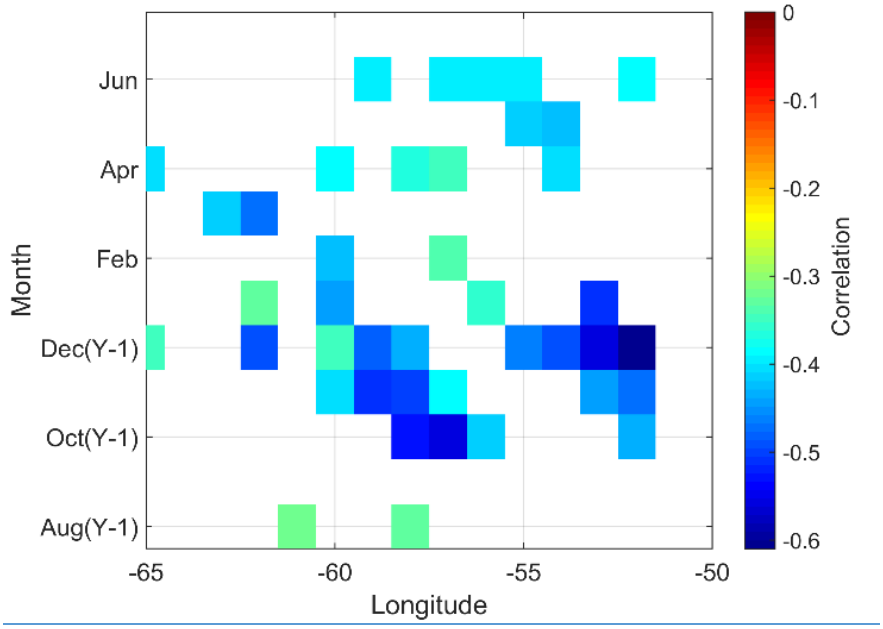

Figure 5: Significant correlations (p<0.05) between growth rate and SSF latitudinal position August (Y-1) and June (Y).

Correlation with regional environmental datasets

The SPG western flank consists of the LC, which includes two branches, a main offshore branch and a smaller inshore one (Matthews, 1914; Smith et al., 1937). Station 27 located in the Avalon channel within the LC inshore branch provides the longest time series in this area. Correlations between SGI chronology and Station 27 (temperature and salinity) time series have been sought at each level monthly from 1950 to 2015 (Fig. 6). Strong positive correlations were observed between shell growth and Station 27 temperature during January and February at all bathymetric levels and almost all year long below 120 m. Correlations with salinity were

weaker but also significant in January and October at almost all bathymetric levels and near the bottom during spring.

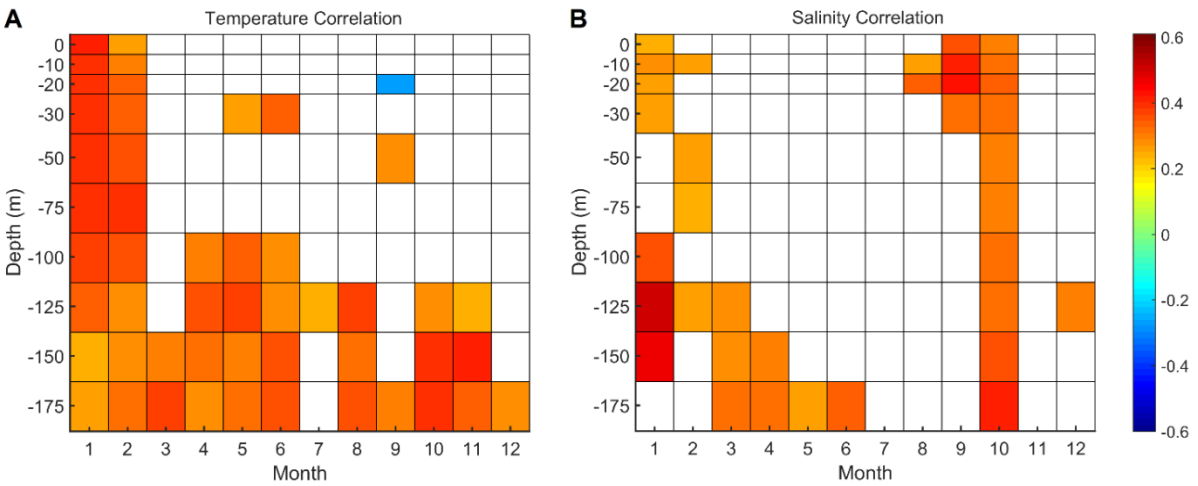

Figure 6: Correlations between GI and Station 27 temperature (A) and salinity (B) time series at each level (in m) for each month (p>0.05 are not displayed).

A key point for LC observation is the TGB where westward transport (Sv) of the offshore LC branch along the slope has been calculated from 1992 to 2013. Strong positive correlations between shell GI and winter transport at TGB were found (N=22, r=0.45, p<0.05) and (N=22, r=0.64, p<0.05) when the series were linearly detrended (Fig. 7).

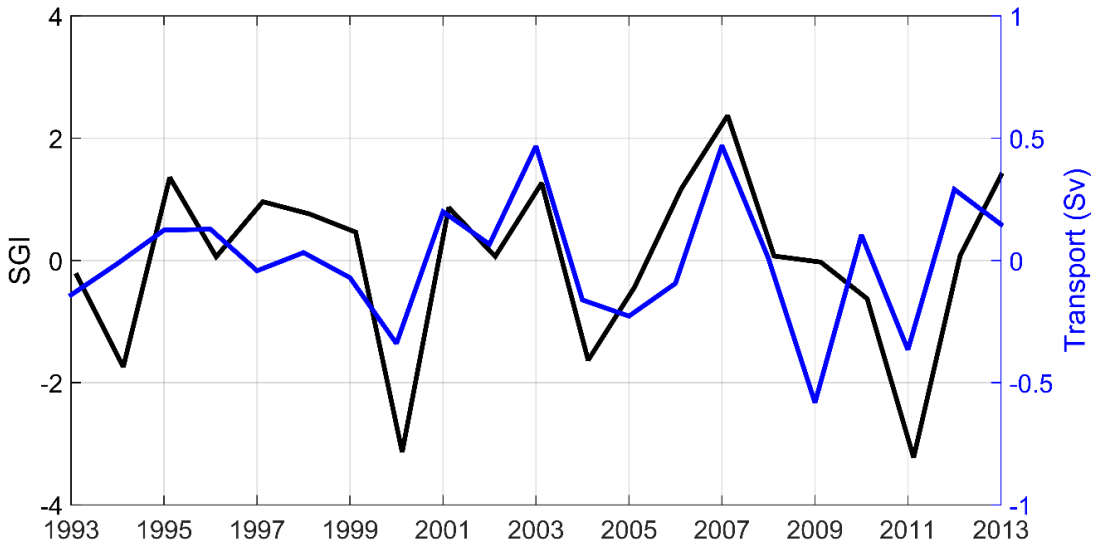

Figure 7: The blue curve represents detrended westward transport in February (in Sv, denoted Tail of GB on Fig. 1). The black curve corresponds to an *A. islandica* detrended growth rate.

Using sea ice cover monthly data over the Newfoundland shelf, a significant negative correlation with the master chronology was found for the last 53 years of observation. The average correlation from January to June is (N=53, r=-0.4, $p<10^{-3}$), with a maximum in February (N=53, r=-0.46, $p<10^{-3}$) and minimum in June (r=-0.34).

Finally, shell growth was positively correlated (N=18, r=0.52, $p<0.05$) with mean local chlorophyll *a* concentration from April to October over the period 1998–2015.

Discussion

Chronology

Synchronous growth determination within a population is key to evaluating if individuals are consistently responding to common external factors (Douglas, 1920; Mette et al., 2016). This study demonstrated that shell growth of contemporaneous individuals of *A. islandica* from SPM shallow waters (<15 m) was highly synchronous based on EPS, the criterion for signal strength. According to Wigley et al. (1984), EPS values >0.85 indicate that the growth signal in a chronology sufficiently represents the whole population signal. In our study, EPS values were >0.85 from 1889 to 2015 (Fig. 3). Moreover, series inter-correlation (0.537) and mean sensitivity (0.270) were fully comparable with those observed in other fish, bivalve, and tree species (e.g., Black et al., 2005; Helama et al., 2007). In addition, the potential application of this chronology for paleo-environmental research is enhanced because the specimens came from the upper few meters of the ocean in an excellent site for capturing changes in North Atlantic climate and oceanography (Pearce et al., 2013). SPM lies in the boundary zone between the North Atlantic subpolar and subtropical gyres, an important site of water mixing (e.g., Sheldon et al., 2016) and one of the most rapidly warming areas on earth (Belkin, 2009). For these reasons, this region seems to be perfect for studying past environmental variations in the uppermost ca. 20 m of the ocean, which directly interacts with the atmosphere and controls weather and climate phenomena (Wanner et al., 2001). To our knowledge, this *A. islandica* growth chronology is the northernmost and shallowest of the Western North Atlantic.

Correlations with environmental parameters

The strength of the common growth signal expressed by *A. islandica* from SPM indicated that our SGI chronology was expressing environmental variability. Several studies have shown that *A. islandica* growth is predominantly governed by temperature and food quantity and quality (Ballesta-Artero et al., 2017; Butler et al., 2010; Marali & Schöne, 2015; Witbaard et al., 1997). They also reveal that local temperature explains less shell growth variability than food supply and quality (see Schöne, 2013, for a review). The *A. islandica* optimal temperature is around 13–15°C. This species is a shallow infaunal filter feeder (Cargnelli et al., 1999) that mainly consumes phytoplankton and organics detritus (Morton, 2011). In terms of food quality, *A. islandica* individuals are described as "real gourmets which feed on the most recent organic matter only" (Erlenkeuser, 1976). The lack of long-term instrumental records of primary production dynamics makes it difficult to relate past shell growth to food supply. Two studies using copepod abundance time series have indirectly demonstrated the importance of food supply for *A. islandica* growth (Wanamaker et al., 2009; Witbaard et al., 2003). Other authors have suggested studying correlations between growth and other environmental variables that are an indirect reflection of phytoplankton production in the surface water (Butler et al., 2013; Schöne, 2013). Therefore, our goal was to identify the environmental drivers that can explain the inter-annual to inter-decadal variations in the *A. islandica* GI over the last 160 years in SPM. Our approach uses environmental datasets sourced from observations as much as possible because climatic indices arising from coupled climate models are rarely successful in accurate reproduction of large spatial scale climatic indexes (Pyrina et al., 2017).

First, we sought correlations of *A. islandica* growth in SPM with AMO and NAO indices. These two large-scale climatic drivers strongly influence marine ecosystem structure (e.g., Carroll et al., 2014) at decadal or multi-decadal time scales. At SPM, the AMO was significantly and positively correlated with SGI, while the NAO negatively related with *A. islandica* growth. These results indicate that part of the growth variability may be explained by low-frequency climate variations. The positive relationship between SGI and AMO, which is the average of near surface temperature over the North Atlantic from America to Europe (Kerr, 2005), seems to indicate that AMO warm phases correspond with *A. islandica* enhanced growth in SPM. However, SGI and NAO showed a negative correlation which indicates that NAO negative phases correspond with enhanced shell growth in SPM. This finding is consistent with Peings

and Magnusdottir's (2014) results for the negative phase of the NAO, showing that it yields more frequent positive AMO. In this region, the positive phase of the NAO (stronger difference in atmospheric pressure) induces stronger northwesterly winds, enhancing deep convection in the Labrador Sea, and sea ice cover over the Newfoundland shelf (Wanner et al., 2001). Positive NAO phases have also been shown to strengthen the LC offshore branch (Han et al., 2010; Han et al., 2014) and the SPG circulation (Rhein et al. 2011) as well as to cool the North Atlantic surface water in turn contributing to a negative AMO index (Visbeck et al., 2013; Wanner et al. 2001) and *A. islandica* negative growth in SPM.

This result seems to be confirmed by positive spatial correlations between *A. islandica* SGI from SPM and temperature within the SPG extent (Fig. 4), suggesting that a warmer SPG correlates with enhanced growth rates of *A. islandica* in SPM. This finding led us to further explore SPG dynamics and its influence on water properties around SPM. The significant negative correlation observed between SPG index and *A. islandica* growth rates in SPM seems to have the same implications as temperature spatial correlations and raises the question of SPG dynamics. The SPG western flank consists of the LC. The LC flows toward the equator and carries cold and less saline water of Arctic origin along the Labrador slope and Grand Banks and extends to the Scotian shelf, finally affecting the whole Middle Atlantic Bight (e.g., Chapman & Beardsley, 1989) (Fig.1). The spatiotemporal structure of the LC along the Labrador coast and over the Grand Banks is complex. On the Newfoundland shelf, it has two branches: a main offshore branch flowing south and feeding the SPG, and a much smaller inshore branch (10 times smaller flow rates) that flows over the Labrador shelf and spreads along the Newfoundland coast over the Grand Banks (e.g., Han et al., 2014; Lazier & Wright, 1993; Matthews, 1914; Petrie & Anderson, 1983; Smith et al., 1937; Wang et al., 2015). In terms of nutrients, the LC transports Arctic water particularly rich in nitrate, phosphate, and especially silicate to subpolar regions (Hàtùn et al., 2017; Torres-Valdes et al., 2013). In the subpolar North Atlantic, silicate is the main limiting nutrient for diatom growth (Allen et al., 2005), which seems to be an important food source for *A. islandica*. For example, Witbaard (1996) linked the period of *A. islandica* low growth rates with a period of low diatom abundance in Fladen Ground. Even if the silicate concentration of the LC offshore branch seems to relate positively to SPG strength (Hàtùn et al., 2017), this pattern is not necessarily present for the LC inner branch, which may influence the SPM region more significantly. Gulf

Stream water and Saint Lawrence Gulf water could also influence SPM hydrodynamics (Petrie & Anderson, 1983).

This possibility led us to investigate the LC inner branch dynamics and its influence on *A. islandica* growth in SPM. On the northern Newfoundland shelf, around 48°30-49°30 N, a sizeable portion of this inner branch strongly bifurcates to the east joining the offshore, shelf break, branch (Wang et al., 2015; Wu et al., 2012). Southward, the inshore branch water transport along the Avalon Peninsula weakens and flows westward along the Newfoundland coast. Over the Grand Banks, between the two main branches, the flow is rather weak, generally flowing southeast-ward and is not fully understood (Brickman et al., 2016; Han et al., 2008; Petrie & Anderson, 1983; Urrego-Blanco & Sheng, 2014). The positive correlations between *A. islandica* SGI and winter temperature and salinity at different bathymetric levels in Station 27 (the oldest, regularly monitored site of the LC inshore branch off eastern Newfoundland, situated southward on the inshore branch bifurcation) seem to confirm that a warmer LC inshore branch during winter associated to a period of higher LC transport (Wang et al., 2015), enhances *A. islandica* growth in SPM. The correlation time lag between Station 27 environmental parameters and *A. islandica* SGI in SPM could be explained by current speed and the distance between Station 27 and SPM. SPM is about 400 km; assuming a mean current speed of 10 cm/s, as shown by (Han et al., 2008; Wang et al., 2015), some part of this water could spread into the SPM region about 2 months later in March or April, at the time of the first spring bloom.

The Grand Bank circulation remains to be addressed. This circulation could affect the SPM region under certain conditions (Peterson et al., 2017; Petrie & Drinkwater, 1993). A part of the offshore branch of LC that follows the continental slope retroflexes to the east, joining the North Atlantic Current (Fig. 1) before reaching the tail end of the Grand Banks (Fratantoni & McCartney, 2009). The remaining LC branch flows westward after the tail of Grand Banks at about 15 to 25 cm/s along the shelf break (Petrie & Anderson, 1983). It then turns northward, toward Cabot Strait and may spread around the SPM region. These observations are corroborated by Urrego-Blanco and Sheng (2014) in a modelling study showing that this northward flow affects the eastern side of the Laurentian channel. This transport at the Grand Bank tail was calculated for 1992 to 2013 and found to correlate positively with *A. islandica* SGI (Fig. 7). This result seems to indicate that *A. islandica* growth in SPM increases with

westward volume transport. This current bringing nutrient rich water from the LC (Hàtùn et al., 2017; Torres-Valdes et al., 2013) toward the SPM region and through the Laurentian Channel (Urrego-Blanco & Sheng, 2014). Offering further evidence of the role of this route is the latitudinal location of the SSF south of the Newfoundland shelf, around 43°N (Fig. 4). In this region, the SSF lies between cold fresh shelf water and warm slope water at the South (Gatien, 1976). The monthly mean position of SSF as a function of longitude south of SPM (between 55–60° W) is around 43°N (about 4° off the SPM region). At a northward speed over the western part of the Grand Banks and in the eastern Laurentian channel of 2 cm/s to 20 cm/s (Greenberg & Petrie, 1988; Urrego-Blanco & Sheng, 2014), the transit time between the front and SPM region will vary from 20 to 200 days. This pattern justifies assessing the correlation between growth rate and SSF position with negative lag of 0 to 1 year (SSF position leads). Correlations between *A. islandica* growth and SSF positions were always negative, meaning that a northward shift of warm slope water leads to decreased *A. islandica* shell growth in SPM.

The positive correlation between shell growth and westward transport and negative correlation between shell growth and northward extension of the SSF finds an explanation in the recent study of Peterson et al. (2017). They showed that "SSF is the surface expression of the southwestward extension of the Labrador Current" and suggest that the more the LC flows west, the more *A. islandica* grows. However, this notion could have led to conflicting correlations with NAO, which is positively correlated with the offshore branch of LC but negatively correlated with shell growth. The findings of Han et al. (2014) clear this inconsistency. They demonstrated that a North–South shift (between Labrador and Nova Scotia shelf breaks) of the LC and a weakening of the offshore LC leads to increased westward transport at the Grand Bank Tail. As a result, the positive and negative phases of NAO lead respectively to increased and decreased offshore LC transport along the northeast Newfoundland shelf break, decreased and increased westward transport of the Grand Bank Tail, northward and southward shifts of the SSF, and finally decreased and increased shell growth (Fig. 8).

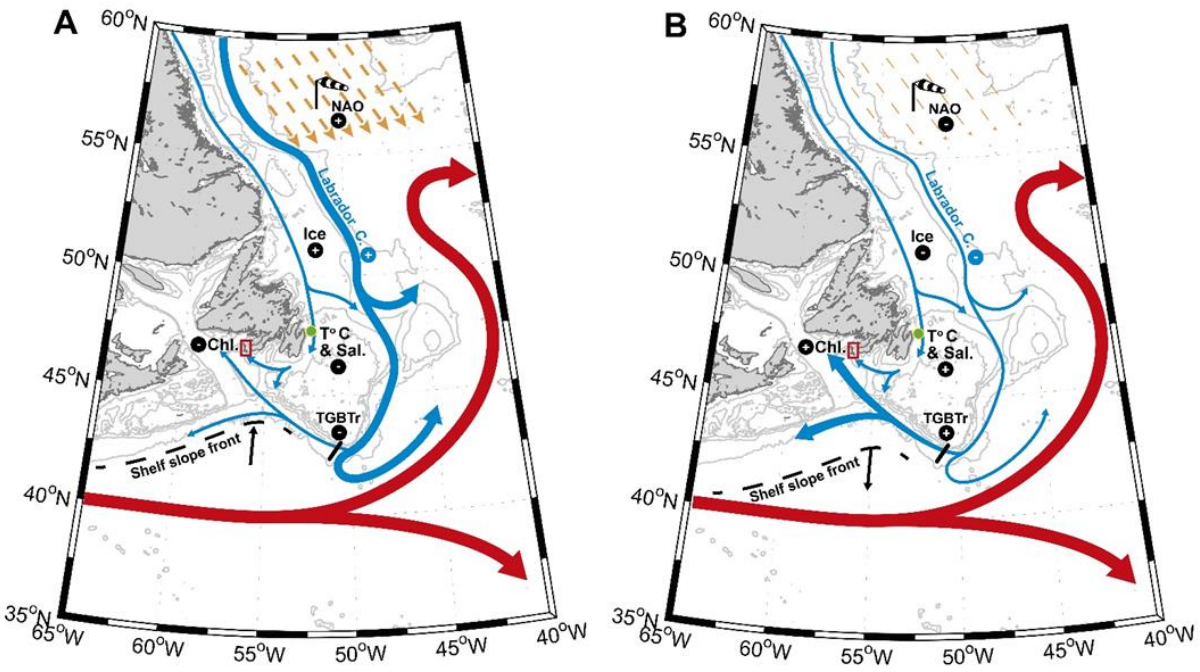

Figure 8: Maps illustrating the environmental scenarios associated with negative (A) and positive (B) growth of *A. islandica* at SPM.

Acknowledgements

First, we thank the LEMAR (UMR 6539) Secretariat team (Anne-Sophie Podeur, Geneviève Cohat, and Yves Larsonneur) for their invaluable assistance during the administrative preparation of the field trip associated with this publication. We also thank the DTAM divers' crew (Yoann Busnot, Luc Thillais, Jean-Marc Derouet) for their invaluable help during *A. islandica* sampling off Miquelon Island. We are sincerely grateful to the Club Nautique Saint-Pierrais for renting their boat and especially to its president, Stephane Salvat, for his incredible availability and kindness. In addition, we express our sincere gratitude to Herlé Goraguer, IFREMER delegate in SPM, for his help with local authorisations and logistics. We thank Eric Dabas for his technical assistance during sclerochronological sample preparation and Sébastien Hervé for conceiving Figures 1 and 8. The authors also thank Pr. J.M. Guarini for the age detrending model conception and Dr. B. Petrie (DFO) and Dr. G. Han (DFO) for their very useful discussion on the regional oceanography. This work was supported by the EC2CO program MATISSE of the CNRS INSU, the Cluster of Excellence LabexMER, and the LIA BeBEST CNRS INEE. This research was carried out as part of the PhD thesis of Pierre Poitevin for the University of Western Brittany with a French Ministry of Higher Education and Research grant.

References

Allen JT, Brown L, Sanders R et al. (2005) Diatom carbon export enhanced by silicate upwelling in the northeast Atlantic. *Nature*, **437**, 728–732.

Ballesta-Artero I, Witbaard R, Carroll ML, Van der Meer J (2017) Environmental factors regulating gaping activity of the bivalve *Arctica islandica* in Northern Norway. *Marine Biology*, **164 (5)**, 116.

Belkin IM (2009) Rapid warming of Large Ecosystems. *Progress in Oceanography*, **81(1–4)**, 207–213.

Berx B, Payne MR (2017) The Sub-Polar Gyre Index - a community dataset for application in fisheries and environment research. *Earth System Science Data*, **9**, 259–266.

Biondi F, Qeadan F (2008) Inequality in paleorecords. *Ecology*, **89(4)**, 1056-1067.

Black BA, Boehlert GW, Yoklavich MM (2005) Using tree-ring crossdating techniques to validate annual growth increments in long-lived fishes. *Canadian Journal of Fisheries and Aquatic Sciences*, **62**, 2277-2284.

Bonitz F, Andersson C; Trofimova T; Hátún H (2018) Links between phytoplankton dynamics and shell growth of *Arctica islandica* on the Faroe Shelf. *Journal of Marine Systems*, **179**, 72-87.

Bunn AG (2008) A dendrochronology program library in R (dplR). *Dendrochronologia*, **26**, 115–124.

Butler PG, Richardson CA, Scourse JD, et al. (2010) Marine climate in the Irish Sea: analysis of a 489-year marine master chronology derived from growth increments in the shell of the clam *Arctica islandica*. *Quaternary Science Reviews*, **29**, 1614–1632.

Butler PG, Wanamaker AD Jr, Scourse JD, Richardson CA, Reynolds DJ (2013) Variability of marine climate on the North Icelandic Shelf in a 1357-year proxy archive based on growth increments in the bivalve *Arctica islandica*. *Palaeogeography, Palaeoclimatology, Palaeoecology,* **373**, 141–151.

Cargnelli LM, Griesbach SJ, Packer DB, Weissberger E (1999) Ocean quahog, *Arctica islandica*, life history and habitat characteristics. NOAA Technical Memorandum NMFS-NE-148. 1–12.

Carroll ML, Ambrose WG Jr, Locke WL, Ryan SK, Johnson BJ (2014) Bivalve growth rate and isotopic variability across the Barents Sea Polar Front. *Journal of Marine Systems*, **130**,167–180.

Chapman DC, Beardsley RC (1989) On the origin of shelf water in the Middle Atlantic Bight. *Journal of Physical Oceanography*, **19**, 384–391.

David P, Delay B, Berthou P, Jarne P (1995) Alternative models for allozyme-associated heterosis in the marine bivalve *Spisula ovalis*. *Genetics*, **139 (4)**, 1719-1726.

Douglas AE (1920) Evidence of climatic effects in the annual rings of trees. *Ecology*, **1**, 24-27.

Dunca E, Mutvei H, Göransson P et al. (2009) Using ocean quahog (*Arctica islandica*) shells to reconstruct palaeoenvironment in Öresund, Kattegat and Skaggerak, Sweden. *International Journal of Earth Sciences*, **98**, 3–17.

Erlenkeuser H (1976). ^{14}C and ^{13}C isotope concentration in modem marine mussels from sedimentary habitats. *Naturwissenschaften*, **63**, 338.

Fratantoni PS, McCartney MS (2009) Freshwater export from the Labrador Current to the North Atlantic Current at the Tail of the Grand Banks of Newfoundland. *Deep-Sea Research I*, **57**, 258–283.

Gatien MG (1976) Study in slope water region south of Halifax. *Journal of the Fisheries Research Board of Canada*, **33**, 2213–2217.

Good SA, Martin MJ, Rayner NA (2013) EN4: Quality controlled ocean temperature and salinity profiles and monthly objective analyses with uncertainty estimates. *Journal of Geophysical Research-Oceans*, **118**, 6704–6716.

Greenberg DA, Petrie BD (1988) The mean barotropic circulation on the Newfoundland shelf and slope. *Journal of Geophysical Research-Oceans*, **93**, 15541-15550.

Grissino-Mayer HD (2001) Evaluating crossdating accuracy: a manual and tutorial for the computer program COFECHA. *Tree-Ring Research*, **57**, 205–221.

Hakkinen S, Rhines P (2004) Decline of subpolar North Atlantic circulation during the 1990s. *Science*, **304**, 555–559.

Halfar J, Hetzinger S, Adey W et al. (2011) Coralline algal growth-increment widths archive North Atlantic climate variability. *Palaeogeography, Palaeoclimatology, Palaeoecology*, **302 (1)**, 71–80.

Han G, Li J (2008) Sea level and geostrophic current features from tandem TOPEX/Poseidon-Jason data in the Newfoundland offshore. *International Journal of Remote Sensing*, **29**, 265–280.

Han G, Lu Z, Wang Z et al. (2008) Seasonal variability of the Labrador Current and shelf circulation off Newfoundland. *Journal of Geophysical Research-Oceans*, **113**, C10013.

Han G, Ohashi K, Chen N et al. (2010) Decline and partial rebound of the Labrador Current 1993–2004: Monitoring ocean currents from altimetric and conductivity-temperature-depth data. *Journal of Geophysical Research-Oceans*, **115**, C12012.

Han G, Chen N, Ma Z (2014) Is there a north-south phase shift in the surface Labrador Current transport on the interannual-to-decadal scale? *Journal of Geophysical Research-Oceans*, **119**, 276–287.

Hátún H, Azetsu-Scott K, Somavilla R et al. (2017) The subpolar gyre regulates silicate concentrations in the North Atlantic. *Scientific Reports*, **7**, 1.

Helama S, Schöne BR, Kirchhefer AJ et al. (2007) Compound response of marine and terrestrial ecosystems to varying climate: pre-anthropogenic perspective from bivalve shell growth increments and tree-rings. *Marine Environmental Research*, **63 (3)**, 185-199.

Hurrell JW (1995) Decadal trends in the North-Atlantic Oscillation - regional temperatures and precipitation. *Science*, **269**, 676–679.

Jones DS (1980) Annual cycle of shell growth increment formation in two continental shelf bivalves and its paleoecologic significance. *Paleobiology*, **6**, 331–340.

Kerr RA (2005) Atlantic climate pacemaker for millennia past, decades hence? *Science*, **309**, 41–43.

Lazier JRN, Wright DG (1993) Annual velocity variations in the Labrador Current. *Journal of Physical Oceanography*, **23**, 659–678.

Levitus S, Antonov JI, Boyer TP et al. (2009) Global ocean heat content 1955-2008 in light of recently revealed instrumentation problems. *Geophysical Research Letters*, **36**, L07608.

Linnaeus C (1767) Systema naturae sive regna tria naturae, secundum classes, ordines, genera, species, cum characteribus, differentiis, synonymis, locis, Tomus 1. Pars 212th ed. Laurentii Salvii, Holmiae 533–1327.

Lutz RA, Rhoads DC (1980) Growth patterns within the molluscan shell: an overview. In: Rhoads DC, Lutz RA (eds) Skeletal growth of aquatic organisms. Plenum Press, New York, pp 203–248.

Marali S, Schöne BR (2015) Oceanographic control on shell growth of *Arctica islandica* (Bivalvia) in surface waters of Northeast Iceland—implications for paleoclimate reconstructions. *Palaeogeography, Palaeoclimatology, Palaeoecology*, **420**, 138-149.

Marchitto TM Jr, Jones GA, Goodfriend GA, Weidman CR (2000) Precise temporal correlation of Holocene mollusk shells using sclerochronology. *Quaternary Research*, **53**, 236–246.

Matthews DJ (1914) Hydrographical Observations in the Labrador Current in 1913. *Journal of the Marine Biological Association of the United Kingdom*, **10 (3)**, 515-517.

Mette MJ, Wanamaker AD Jr, Carroll ML, Ambrose WG Jr, Retelle MJ (2016) Linking large-scale climate variability with *Arctica islandica* shell growth and geochemistry in northern Norway. *Limnology and Oceanography*, **61 (2)**, 748-764.

Morton B (2011) The biology and functional morphology of *Arctica islandica* (Bivalvia: Arcticidae): a gerontophilic living fossil. *Marine Biology Research*, **7**, 540–553.

Nicol D (1951) Recent species of the veneroid pelecypod *Arctica*. *Journal of the Washington Academy of Sciences*, **41**,102–106.

Pearce C, Seidenkrantz M, Kuijpers A et al. (2013) Ocean lead at the termination of the Younger Dryas cold spell. *Nature Communication*, **4**, 1664.

Peings Y, Magnusdottir G (2014) Response of the winter-time northern hemisphere atmospheric circulation to current and projected arctic sea ice decline: A numerical study with CAM5. *Journal of Climate*, **27**, 244–264.

Peterson I, Greenan B, Gilbert D, Hebert D (2017) Variability and wind forcing of ocean temperature and thermal fronts in the Slope Water region of the Northwest Atlantic. *Journal of Geophysical Research Oceans*, **122**, 7325–7343.

Petrie B, Anderson C (1983) Circulation on the Newfoundland Continental Shelf. *Atmosphere-Ocean*, **21 (2)**, 207–226.

Petrie B, Drinkwater K (1993) Temperature and salinity variability on the Scotian Shelf and in the Gulf of Maine 1945-1990. *Journal of Geophysical Research-Oceans and Atmospheres*, **98**, 20079–20089.

Pyrina M, Wagner S, Zorita E (2017) Evaluation of CMIP5 models over the northern North Atlantic in the context of forthcoming paleoclimatic reconstructions. *Climate Dynamics*, **49**, 3673–3691.

Rhein M, Kieke D, Hüttl-Kabus S et al. (2011) Deep water formation, the subpolar gyre, and the meridional overturning circulation in the subpolar North Atlantic. *Deep Sea Research*, **58 (2),** 1819–1832.

Rhoads DC, Lutz RA (1980) Skeletal growth of aquatic organisms. *Plenum Publication Corporation*, New York. 750 p.

Schlessinger M, Ramankutty N (1994) An Oscillation in the Global Climate System of period 65-70 years. *Nature*, **367**, 723–726.

Schöne BR, Fiebig J, Pfeiffer M et al. (2005a) Climate records from a bivalved Methuselah (*Arctica islandica*, Mollusca; Iceland). *Palaeogeography, Palaeoclimatology, Palaeoecology,* **228 (1–2)**, 130–148.

Schöne BR, Dunca E, Fiebig J, Pfeiffer M (2005b) Mutvei's solution: An ideal agent for resolving microgrowth structures of biogenic carbonates. *Palaeogeography, Palaeoclimatology, Palaeoecology*, **228(1–2)**, 149–166.

Schöne BR (2013) *Arctica islandica* (Bivalvia): A unique paleoenvironmental archive of the northern North Atlantic Ocean. *Global and Planetary Change*, **111**, 199–225.

Sheldon CM, Seidenkrantz MS, Pearce C et al. (2016) Holocene oceanographic changes in SW Labrador Sea, off Newfoundland. *The Holocene*, **26 (2)**, 274-289.

Scilab Enterprises (2012). Scilab: Free and Open Source software for numerical computation (OS, Version 6.0.0) [Software]. Available from: http://www.scilab.org

Smith EH, Soule FM, Mosby O (1937) The Marion and General Green expeditions to Davis Strait and Labrador Sea. *Bulletin of the U.S. Coast Guard*, **19**, pp. 259.

Torres-Valdés S, Tsubouchi T, Bacon S et al. (2013) Export of nutrients from the Arctic Ocean. *Journal of Geophysical Research-Oceans*, **118 (4)**, 1625-1644.

Urrego-Blanco J, Sheng J (2014) Study on subtidal circulation and variability in the Gulf of St. Lawrence, Scotian Shelf, and Gulf of Maine using a nested-grid shelf circulation model. *Ocean Dynamics*, **64**, 385–412.

Visbeck M, Chassignet EP, Curry RG et al. (2013) The Ocean's Response to North Atlantic Oscillation Variability. In The North Atlantic Oscillation: Climatic Significance and Environmental Impact, 113-145. American Geophysical Union.

von Bertalanffy L (1938) A quantitative theory of organic growth. *Human Biology*, **10**, 181-213.

Wanamaker AD Jr, Kreutz KJ, Schöne BR et al. (2009) A late Holocene paleo-productivity record in the Western Gulf of Maine, USA, inferred from growth histories of the long-lived ocean quahog (*Arctica islandica*). *International Journal of. Earth Sciences*, **98**, 19–29.

Wanamaker AD Jr, Butler PG, Scourse JD et al. (2012) Surface changes in the North Atlantic meridional overturning circulation during the last millennium, *Nature Communication,* **3**, 899.

Wang Z, Yashayaev I, Greenan B (2015) Seasonality of the inshore Labrador Current over the Newfoundland shelf. *Continental Shelf Research*, **100**, 1–10.

Wanner H, Brönnimann S, Casty C et al. (2001) North Atlantic Oscillation – concepts and studies. *Surveys in Geophysics*, **22**, 321–382.

Wigley TML, Briffa KR, Jones PD (1984) On the average value of correlated time series, with applications in dendroclimatology and hydrometeorology. *Journal of Applied Meteorology and Climatology*, **23**, 201–213.

Witbaard R (1996) Growth variations in *Arctica islandica* L. (Mollusca): a reflection of hydrography-related food supply. *ICES Journal of Marine Science*, **53**, 981–987.

Witbaard R, Duineveld GCA, DeWilde PAWJ (1997) A long-term growth record derived from *Arctica islandica* (Mollusca, Bivalvia) from the Fladen Ground (northern North Sea). *Journal of the Marine Biological Association of the United Kingdom*, **77 (3)**, 801–816.

Witbaard R, Jansma E, Sass Klaassen U (2003) Copepods link quahog growth to climate. *Journal of Sea Research*, **50**, 77–83.

Wu Y, Tang C, Hannah C (2012) The circulation of eastern Canadian seas. *Progress in Oceanography*, **106**, 28–48.

Chapitre 3

Do *Clathromorphum compactum* growth patterns and geochemical composition archive Saint-Pierre & Miquelon environmental variabilities?

Contexte et résumé de l'étude

Ce troisième chapitre utilise des résultats acquis dans le cadre du stage de Master 2 de Valentin Siebert que j'ai dirigé entre janvier et juin 2018. Le choix, d'explorer les possibilités offertes par l'étude sclérochronologique de *Clathromorphum compactum* à Saint-Pierre et Miquelon, a été induit par deux principales raisons. Outre son importante longévité reportée par différentes études, nous avons décidé de travailler sur ce modèle biologique largement représenté à SPM afin de nous affranchir de la tendance ontogénique observée chez *A. islandica* (cf Chapitre 2). De plus, le fait d'étudier la variabilité environnementale passée inscrite dans une espèce d'un autre niveau trophique (ici producteur primaire) doit permettre de valider nos premières observations et d'obtenir une vision plus complète de l'hydroclimat à SPM.

Nous avons alors décidé, d'entamer un travail méthodologique visant à mettre en place un protocole de lecture directe des colonies de *C. compactum* en utilisant, comme pour les coquilles d'*A. islandica*, du bleu de Mutvei. Des stries de croissance ont ainsi pu être mises en évidence. Puis des analyses géochimiques ont été effectuées afin de valider la périodicité annuelle de ces stries. Nous avons ensuite évalué la variabilité, intra-spécimen des informations contenues dans ces structures bio-construites, en étudiant la croissance et la composition en éléments traces de plusieurs portions de différents individus.

Cette étude confirme la possibilité d'étudier la croissance de *C. compactum* en la mesurant de manière directe grâce à une coloration préalable au bleu de Mutvei. Cette méthode, mise au point pendant cette thèse permet maintenant de s'affranchir des mesures géochimiques coûteuses, jusque-là utilisées, pour accéder à cette mesure chez *C. compactum*. Cette avancée doit permettre d'augmenter la profondeur d'échantillonnage des futures études relatives à la croissance de cette espèce et ainsi renforcer la valeur paléoenvironnementale des signaux contenus dans celle-ci.

Finalement, ce troisième chapitre permet de présenter les relations statistiques liant les enregistrements sclérochronologiques de *C. compactum* à SPM et plusieurs variables environnementales mesurées à différentes échelles : globales, régionales et locales. Ce travail confirme les conclusions relatives à l'étude menée précédemment sur *A. islandica*.

Do *Clathromorphum compactum* growth patterns and geochemical composition archive Saint-Pierre & Miquelon environmental variabilities?

Valentin Siebert[1], **Pierre Poitevin**[*1], Laurent Chauvaud[1], Bernd R. Schöne[2], Pascal Lazure[3], Julien Thébault[1]

[1] *Université de Bretagne Occidentale, Laboratoire des Sciences de l'Environnement Marin (UMR6539 UBO/CNRS/IRD/Ifremer), 29280 Plouzané, France*

[2] *Institute of Geosciences, University of Mainz, Johann-Joachim-Becher-Weg 21, 55128 Mainz, Germany*

[3] *Ifremer, Laboratoire d'Océanographie Physique et Spatiale (UMR6523 CNRS/Ifremer/IRD/UBO), 29280 Plouzané, France*

Email addresses:

Valentin Siebert: siebert.valentin@gmail.com

Pierre Poitevin: pierre.poitevin@univ-brest.fr

Julien Thébault: julien.thebault@univ-brest.fr

Bernd R. Schöne: schoeneb@uni-mainz.de

Pascal Lazure: pascal.lazure@ifremer.fr

Laurent Chauvaud: laurent.chauvaud@univ-brest.fr

Corresponding author:

Pierre Poitevin

Université de Bretagne Occidentale

Institut Universitaire Européen de la Mer

Laboratoire des Sciences de l'Environnement Marin (UMR6539 UBO/CNRS/IRD/Ifremer)

F-29280 Plouzané

Tel: +33 2 90 91 55 78

Fax: +33 2 98 49 86 45

Abstract

Records of ocean/atmosphere dynamics over the past centuries are essential to understand processes driving climate variability. This is particularly true for the Northwest Atlantic, a key region with regard to global climate. Over the past decade, rhodoliths have been increasingly used as environmental and climatic archives in the marine realm. Whereas many studies have focused on environmental information recorded in geochemical properties of the coralline algae carbonate structure, e.g., to reconstruct sea surface temperature, less attention has been paid to the use of annual growth increment widths as an environmental proxy. Here, we investigate the possibility to extract climate and environmental information from annual growth patterns of the coralline red algae, *Clathromorphum compactum*, from Saint-Pierre & Miquelon (SPM), an archipelago situated close to the confluence of the warm Gulf Stream and the cold Labrador Current. However, analysis of *C. compactum* growth is challenging due to difficulties in resolving the annual banding pattern. Identification of these growth patterns is usually based on geochemical data of hard structure (e.g., annual variations of structural Mg/Ca allow indirect measurements of increment width). These methods are expensive and therefore prevent from analyzing a large number of specimens that would be representative of the entire population. For this reason, we enhanced the growth line readability by staining polished sections with Mutvei's Solution. Geochemical analyses were also carried out in order to validate the assumption that growth lines observed after staining were formed on an annual basis. Furthermore, growth patterns and trace element composition were investigated on multiple axes of several rhodoliths in order to assess the intra-specimen variability. This study confirms that it is possible to measure annual increment width of Mutvei-stained coralline red algae directly, without using expensive geochemical methods. Moreover, relationships between the *C. compactum* sclerochronological records from SPM and environmental datasets covering different geographical scales confirm the findings related to *A. islandica* growth records.

Keywords:

Sclerochronology, North Atlantic, Climate change, Growth, Environmental proxies, *Clathromorphum compactum*, rhodholith, Saint-Pierre & Miquelon.

Introduction

The Northwest Atlantic Ocean is a key region with respect to climate variability as it represents the starting point of the Atlantic Meridional Overturning Circulation (AMOC) which is an important and active component of the climate system (Rahmstorf, 2003). Southern Newfoundland's coast and the Saint-Pierre & Miquelon (SPM) region lie at the confluence of the main oceanographic currents ruling the North Atlantic Basin. However, despite its importance, the physical flow dynamics of this region is poorly understood (Wu *et al*., 2012). This gap exists mainly because of the lack of long-term environmental records in this area, where they are sparse and spatiotemporally incomplete before the mid-20th century (Halfar *et al*., 2011).

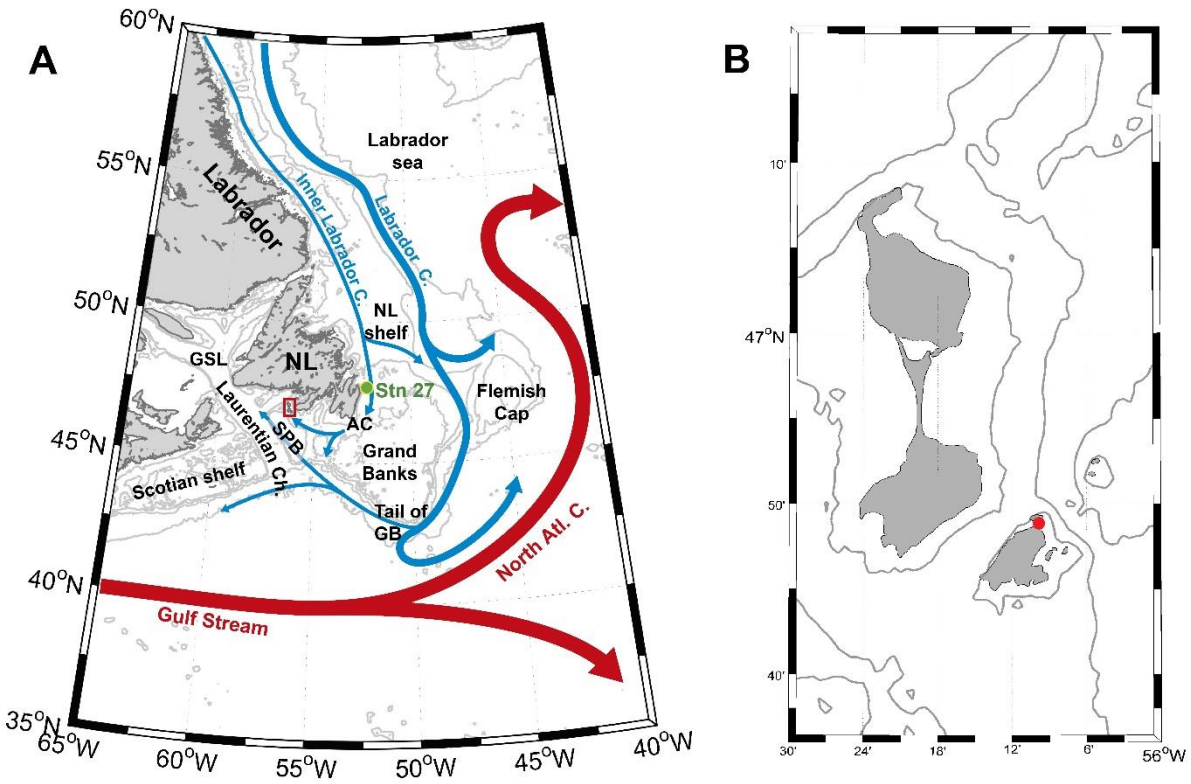

Figure 1: (A) Major features of the regional surface circulation (inspired by Fig.1 in Fratantoni & McCartney, 2009) and main location names. The cold inner and outer LCs are in blue; Gulf Stream and North Atlantic currents are in red. In green is historical hydrographic Station 27 (Stn 27). The main acronyms corresponding to location names are as follows: NL – Newfoundland; SPB – Saint-Pierre Bank; GSL – Gulf of Saint-Lawrence; AC – Avalon Channel; and GB – Grand Banks. (B) Sampling location of *Clathromorphum compactum* (red dot).

In this context of climate change, models are proposed in order to predict climate variations. Nonetheless, these predictions are mostly based on present climate observations on one side and on climate variability over the past centuries on the other side. For this reason, records of past ocean/atmosphere dynamics in recent centuries are essential to understand processes driving climate variability

In the oceanic realm, carbonate hard structures of long-lived marine species hold the potential to extend instrument-derived observations by several decades or centuries. While multi-centennial reconstructions of tropical marine hydrodynamics have been generated since the 1990's (e.g. Dunbar *et al.*, 1994; Saenger *et al.*, 2009), long term records of environmental conditions in higher latitude oceans are relatively scarce and sparse. In the North Atlantic Ocean, geochemical approaches and growth analyses of the bivalve *Arctica islandica* supply the bulk of annual to subannual resolution extra-tropical marine climate data for near-surface water masses (Schöne, 2013 for a review). While growth increment widths of long-lived bivalves have resulted in numerous climate reconstructions (e.g., Wanamaker *et al.*, 2008; Butler *et al.*, 2013), environmental interpretation of growth increment time-series is complex because of growth ontogenetic trend (Goodwin *et al.*, 2009). Raw growth increment time-series must therefore be detrended with mathematical functions (e.g. spline, negative exponential) that can potentially remove low-frequency climate oscillations.

In an attempt to overcome some of these issues, a few studies focused on the use of coralline red algae as archives of environmental and climatic variatibility in oceans (e.g., Kamenos *et al.*, 2008; Williams *et al.*, 2011, Halfar *et al.*, 2011). In the northwest Atlantic Ocean, the species *Clathromorphum compactum* (Kjellman) Foslie 1898 (Rhodophyta; Hapalidiaceae) forms clear annual growth increments which pave the way towards sclerochronological investigations (Moberly, 1968). First, *C. compactum* colonies shows a fairly constant growth rate throughout its lifespan and is not subject to an ontogenetic growth trend (Halfar *et al.*, 2011). Thus, there is no loss of data accuracy in the youngest portions of the algae. Then, its extreme longevity (> 600 years; (Halfar *et al.*, 2013)) allows very long reconstructions. According to previous studies, growth lines are formed during late winter/early spring (Moberly, 1968) due to a cessation in colony development between January and April (Halfar *et al.*, 2008; Halfar *et al.*, 2011) resulting in changes between two morphological structures: (i) small cells with dense calcified walls (growth line) and (ii) large cells with thinner less calcified walls (increment)

(Adey, 1965; Moberly, 1968). Finally, thanks to the wide distribution of *C. compactum* around the Arctic and Sub-Arctic (in North Atlantic and North Pacific Oceans) (Hetzinger *et al.*, 2011; Adey *et al.*, 2013), paleo environmental reconstructions are possible at a large spatial scale. Since 1950, past environmental variability has been investigated using the geochemistry of *Clathromorphum spp.* calcite skeleton (e.g. Chave, 1954; Williams *et al.*, 2018). For example, variations in magnesium concentrations of long-lived coralline algae carbonate structure record ambient seawater temperature over time (Moberly, 1968), while barium content brings information about variations in salinity (Hetzinger *et al.*, 2011, Hetzinger *et al.*, 2013) or river runoffs (Chan *et al.*, 2011). However, most of these geochemical analyses are expensive.

Even if some studies successfully related growth patterns of *C. compactum* with SST fluctuations (e.g., Chave, 1954; Halfar *et al.*, 2008), less attention has been paid to use rhodoliths growth increment widths as a proxy for sea water temperature. The reason for that lies in the difficulty in identifying annual growth lines with optical or scanning electron microscopy (Halfar *et al.*, 2011). In addition, the presence of spherical non-calcified reproduction structures, called conceptacles, can also affect growth line readability. These latest have a global size that can reach the increment width value and are formed during winter season, when rhodolith colonies stop their growth (Moberly, 1968). So far, increment width is mostly measured indirectly through the analysis of annual Mg/Ca ratio cycles in the rhodolith hard parts (Hetzinger *et al.*, 2011). However, the cost of these geochemical tools limits our ability to analyse a large amount of specimens. This financial statement raises the questions of sample size and population representativeness, two crucial aspects of growth dynamics sclerochronological studies. In this context, Sletten *et al.*, 2017 focused on these issues, and try to develop a cheaper tool based on growth lines staining. For instance, Alizarin Red has been used to stain growth patterns of *Phymatolithon calcareum and Lithothamnion sp.* which have naturally more visible growth lines in comparison with *Clathromorphum spp.* (Kamenos *et al.*, 2008; Sletten *et al.*, 2017). Since a decade, another simple technique is frequently used to highlight growth structures in many different taxa (bivalve molluscs, gastropods, barnacles, corals, sclerosponges, fish otoliths, cephalopods and whale's tympanic bulla). This so-called Mutvei's solution combines gentle etching, preservation of water soluble and insoluble components of the organic matrix and differential staining of soluble organics

in a single preparation step (Schöne *et al.*, 2005). Nevertheless, this technique has never been tested on rhodoliths. However, given Mutvei's solution properties, and *C. compactum* morphological structure, this technique may be effective to enhance growth lines visibility.

This study focuses on *C. compactum* colonies from Saint-Pierre and Miquelon. Based on these previous observations, several objectives drove this study. The first one was to perform a population scale growth analysis via direct increment widths measurements using Muvei's solution staining. This included growth patterns reproducibility within individuals (along the greatest number of reading axes) and population growth signal analysis with statistic indicators calculation. The second one focused on *C. compactum* geochemical analyses. Such as growth lines, we verified intra and inter specimens trace elements distribution along multiple LA-ICP-MS transects. Furthermore, trace element signals were compared to growth lines position. Finally, correlations between *C. compactum* data (growth data or geochemical data) from SPM were compared to large and local scales environmental data sets.

Materials & Methods

Sampling

Forty two *C. compactum* specimens were analysed in the present study. All of them were randomly live collected from hard substrate at a depth of 14 m by scuba diving along the north coast of Saint-Pierre island (46°49'03.3"N, 56°09'54.6"W) the 5th of September 2017. As the 42 colonies come from the same location and depth (14m), they all experienced the same environmental conditions. Each colony was measured, weighed and photographed to keep track of their global morphology before starting preparations.

Sample preparation

Three cutting axis were defined on each colony, parallel to the direction of growth (red lines in Figure 2). Colonies were cut along these axes using a low-speed precision saw (Struers, Accutom 50; rotation speed 800 rpm, feed rate 100µm.s^{-1}) equipped with a diamond-coated blade (thickness: 400 µm) continuously cooled by deionized water. The first cutting axis was defined to go through the center of the colony and thick sections (2mm) were then cut on both sides of this central axis. One will be used for the growth measurements (slice n°1 on Figure 2) and the other one for micro-chemical analyses (slice n°3 on Figure 2). The two other

cutting axes were only used for micro-chemical analyses (slices n°2 and n°4 on Figure 2) in order to assess intra-colony variability of trace element distribution. The distance between adjacent cutting axes was variable depending on the size of the colony but never exceeded 6 mm.

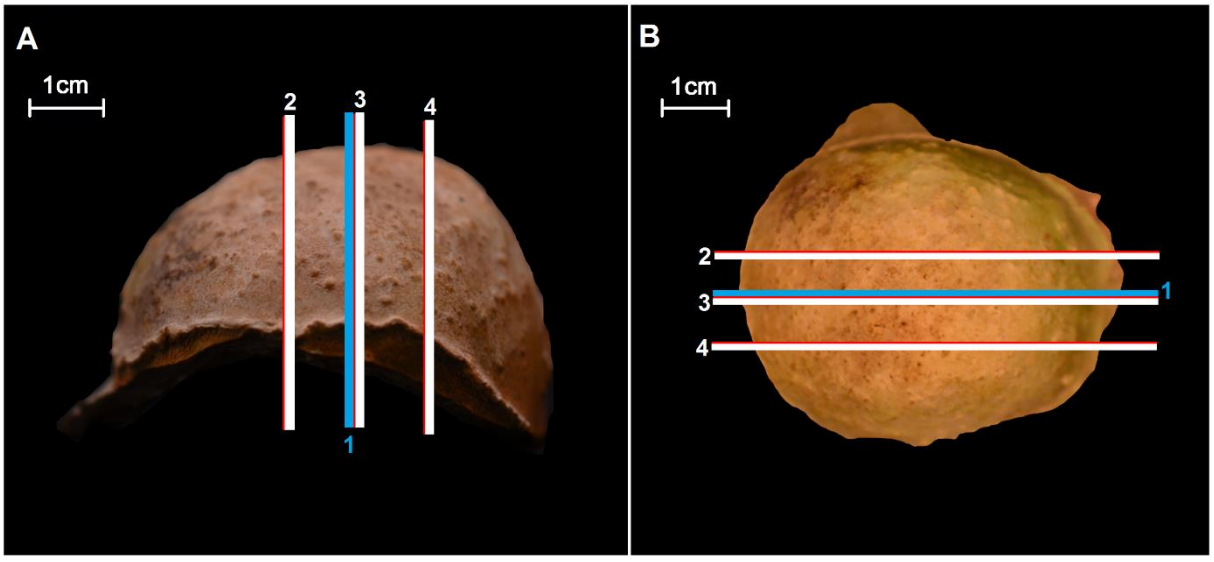

Figure 2: Example of the three cutting axis location performed on each studied rhodoliths (red lines) in a side view (A) and on a top view (B). Thick blue line corresponds to the 2mm thick section stained and used for the growth analyses (n°1). The three other white lines correspond to uncoloured slices intended for geochemical analyses (n° 2, 3, 4). On those photographs, distances between each cutting axis were overstated, in order to enhance figure readability.

These sections were mounted on glass microscope slides and carefully grounded on a rotating polishing table (Struers, TegraPol-35) with a sequence of 1200 and 2400 grit wet-table carborundum paper, followed by polishing with 3-µm and 1-µm diamond liquid (Struers). These cross-sections were ultrasonically cleaned with deionized water between each grinding or polishing step to remove residual abrasive material.

The polished cross-sections (slice n°1 on Figure 2) were then etched in a Mutvei's solution (Schöne et al., 2005) for 45 minutes at 40°C, soaked in a deionized water bath, and left to air dry before imaging. Treatment with Mutvei's solution results in a three-dimensional display of growth patterns and reveals clear annual growth lines (Figure 3).

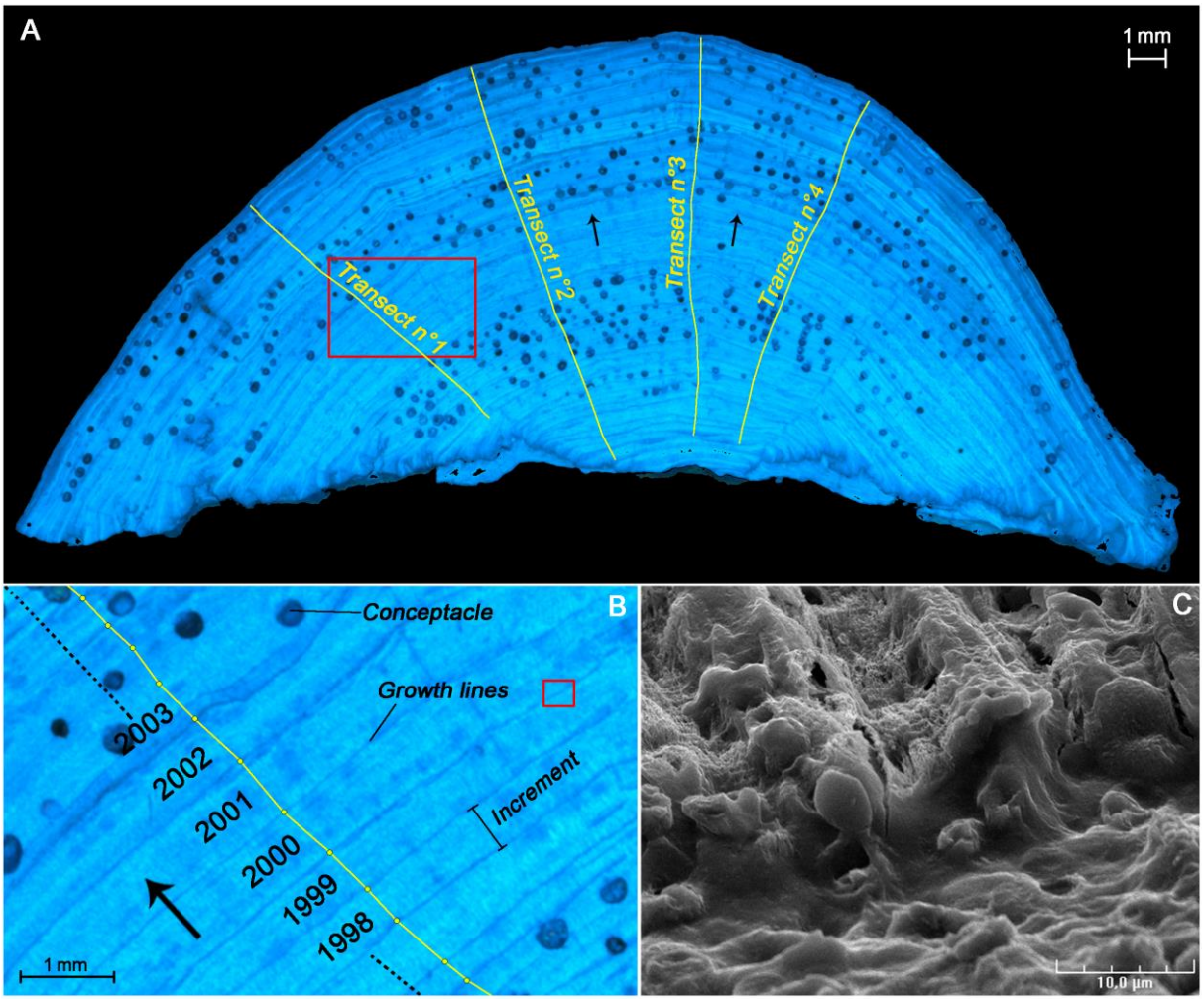

Figure 3: *C. compactum* internal growth patterns after Mutvei's solution. The yellow lines (A) correspond to the trajectory on which annual growth lines (yellow dots) were placed and growth increments measured (B). Black arrows represent the direction of growth (A, B). SEM photograph of one growth line after Mutvei's solution treatment (C).

Growth analyses

Increment width measurements

Stained sections were imaged under reflected light (Zeiss, KL 2500 LCD) using an AxioCam MRc5 installed on a Zeiss Lumar.V12 stereomicroscope equipped with a motorized stage. Photomosaics were constructed using AxioVision 4.9.1 software (Zeiss). The width of all growth increment was measured digitally using the image processing and analysis software ImageJ (NIH Image), from the outer edge of the rhodolith (living portion) to the center (base of the colony, attached to the substrate). In order to assess intra-colony variability, growth rates were measured along several transects (Fig. 3) on slices n°1 (Fig. 2). The number of

transects depended on the global size and morphology of each plant. As all rhodoliths were live-collected, the last visible increment corresponds to the year of their collection (2017).

In order to measure ordinal association between all transects of the same colony, Spearman's rank correlations of increment width measurements were calculated using R software (R Core Team, 2018). If one transect significantly differed from others ($p>0.05$), it was removed from the growth analysis dataset.

Growth population signal analyses and statistic indicators

To see if a common growth signal could be observed between the different *C. compactum* colonies, growth indices (GIs) were calculated for each year and colony by dividing the measured increment width ($L_{t+1} - L_t$) by a predicted increment width ($L(p)_{t+1}$-$L(p)_t$). Given that *C. compactum* is a colonial species, we assumed that there is no ontogenetic decreasing trend in annual growth rate throughout lifetime, and that under constant environmental conditions, the annual predicted increment width ($L(p)_{t+1}$-$L(p)_t$) should be identical from the base to the top of the colony. Therefore, this value was defined individually as the arithmetic mean of the increment width values obtained on the different transects.

$$GI_t = \frac{L_{t+1} - L_t}{L(p)_{t+1} - L(p)_t}$$

Individual time-series of GI were then standardized as follows (Schöne, 2013):

$$SGI_t = \frac{GI_t - \mu}{\sigma}$$

Where μ is the average and σ the standard deviation of all GI values. The standardized GI (SGI) is a dimensionless measure of how growth deviates from the predicted trend. Positive values represent greater than expected growth, whereas negative values represent less than expected growth. The robustness of the SGI chronology was tested.

A frequently used assessment of the robustness of composite chronologies is the expressed population signal (EPS) (Wigley et al., 1984), which is given as:

$$EPS = \frac{n * R_{bar}}{\left(n * R_{bar} + (1 - R_{bar})\right)}$$

Where R_{bar} is the average of all correlations between pairs of SGI chronologies and *n* is the number of specimens used to construct the stacked chronology. EPS > 0.85 indicates that the variance of a single SGI chronology sufficiently expresses the common variance of all SGI series. All these analyses were carried out using COFECHA (Grissino-Mayer, 2001) and the R package dplR (Bunn, 2008).

Trace element analyses

Element-to-calcium ratios were analyzed on cross-sections n°2, n°3 and n°4 using LA-ICP-MS at the Pôle Spectrométrie Océan (European Institute for Marine Studies, Plouzané, France). A Thermo Scientific XSERIES 2 quadrupole inductively coupled plasma mass spectrometer (ICP-MS) coupled to a 193 nm laser ablation system (COMPexPro 102, Coherent Inc.) were used with parameters listed in Table 1.

Table 1: Summary of laser mass spectrometer settings.

Laser energy densities	15 J/cm²
Pulse rate	10 Hz
Spot size	120µm
Scan speed	~ 5µm/s
Gas carrier	Helium (He)
Gas carrier flow	250 mL/min

During acquisition, signal intensities (counts per second = cps) were recorded for ^{25}Mg, ^{43}Ca, ^{55}Mn and ^{137}Ba. The intensity of the isotope of interest was systematically normalized against the ^{43}Ca signal (internal standard) in order to correct for laser beam energy drift, focus

variation at the sample surface, and ICP-MS detection drift. The glass reference material NIST SRM 612 was used as a calibration standard with the values of GeoReM database (Jochum *et al.*, 2005). Finally, the detection limits of elements were: Mg = 9.03 µmol/mol, Mn = 0.61 µmol/mol, Ba = 0.08 µmol/mol.

As the laser moved on the cross-section surface at 5 µm/s and the ICP-MS saved data every 2.28 s, the spatial resolution of these analyses was ca. 11.4 µm.

Three colonies were selected for trace element analyses based on their size and the density and position of conceptacles. Three cross-sections were cut in each of these three colonies (Fig. 2) and three LA-ICP-MS transects were analysed on each cross-section along the direction of growth from the base to the top of the colony (Fig. 4). Before and after each transect, three external standard runs were performed.

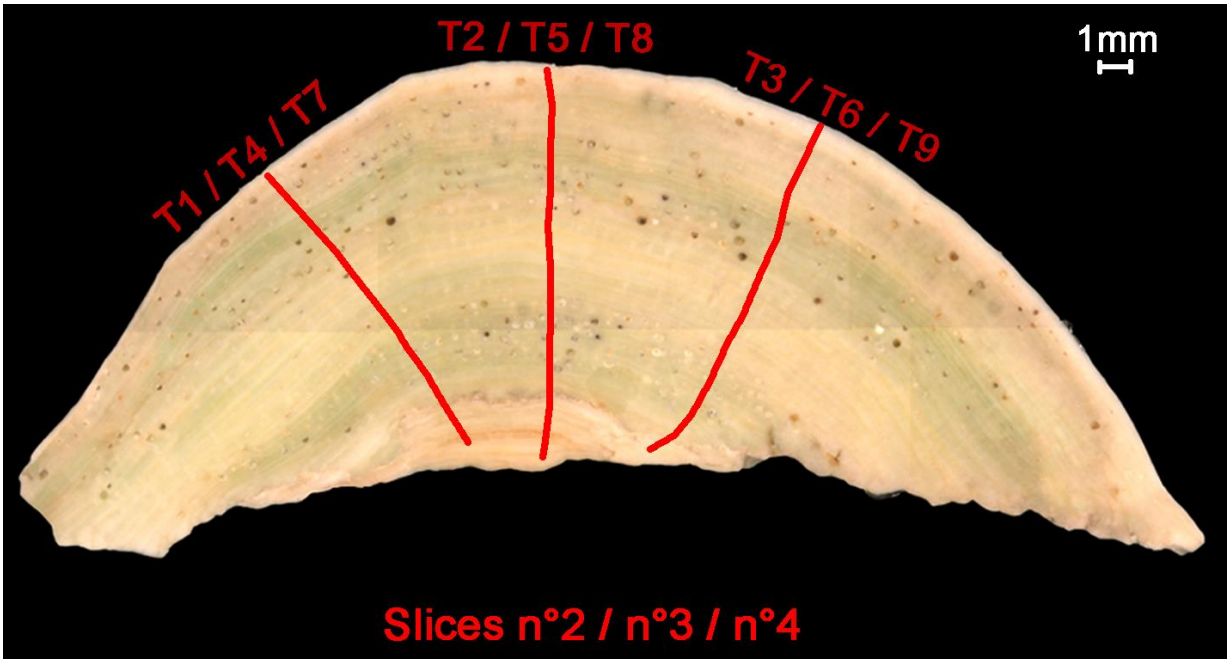

Figure 4: Example of laser transects locations within one slice over the three for one colony. The laser transect position will be approximately the same within the two others cut sections for the specimen.

The results were processed with the R package: ElementR (Sirot *et al.*, 2017). This package automatically calculates concentration ratios for each element, after calculation of the ICP-MS blank level and drift.

Once geochemical analyses were done, each cross-section was stained with Mutvei's solution in order to assign calendar dates to geochemical data. Given that the number of data points per year was different between transects, elemental ratios were mathematically re-sampled using AnalySeries 2.0 (Paillard *et al.*, 1996) in order to allow a better comparison of the data. To this end, intra-annual geochemical measurements were fitted with a cubic spline and the curve re-sampled at 40 regular intervals in order to have exactly 40 data points in each annual increment, in any transect, cross-section, or colony.

Comparison with environmental time-series

The SGI master-chronology was finally compared with different indices reflecting climate and ocean dynamics over the north-west Atlantic Ocean: North Atlantic Oscillation index (NAO) (Hurrell *et al.*, 2001), Arctic Oscillation index (AO) (Thompson & Wallace, 1998), Atlantic Multidecadal Oscillation (AMO) (Knight *et al.*, 2006) and Sub-Polar Gyre index (SPG) (Berx & Payne, 2017). Spearman correlations were used to check for the existence of statistically significant relationships between these annual indices and the SGI master-chronology. Furthermore, large-scale seawater temperature effects on rhodolith growth were assessed from spatial correlation maps using KNMI Climate Explorer (https://climexp.knmi.nl/) and ocean mean temperature data (0-100 meters layer, NOAA-NODC).

As the incorporation of trace elements in the rhodolith skeleton likely results from variations in more specific and local environmental conditions, Mg/Ca ratios will be compared with recorded surface water temperatures from the monitoring Station n°27 (Fig.1) and with NOAA_ERSST_v4 satellite-based SST values extracted from a 200 km² area around Saint-Pierre. Furthermore, a calibration was performed between this last database and Mg/Ca ratio distribution in order to observe whether magnesium is included in the same way through the three studied specimens regarding the SST variations. For this purpose, linear regressions were drawn and the equation slopes obtained for the three specimens were compared using a Student test. Ba/Ca ratio, were compared with recorded surface salinity values from Station 27 (Fig. 1) and with the Labrador Current transport along the Tail of Grand Bank (Fig. 1) at several transects from 1992 to 2013 which are available at: http://www.meds-sdmm.dfo-mpo.gc.ca/isdm-gdsi/azmp-pmza/climat/labrador/transport-eng.htm.

Results

Growth analyses

Mutvei's solution staining

Treatment with Mutvei's solution results in a coloured three-dimensional display of growth patterns and reveals clear annual growth lines (Fig. 3). An alternating pattern of thin dark lines and wide light-colored areas was observed, corresponding respectively to growth lines and increments (Fig. 3B). Beyond this differential staining, Mutvei's solution treatment has another consequence, creating a ditch-like pattern of ca. 10 µm depth where growth lines stand (Fig. 3C).

Intra-specimen variability in growth rate

The number of transect used on slice n°1 (Fig. 2) for increment width measurements differed between colonies, ranging from 2 to 8. Because of conceptacle density or grazing tracks, accurate counting and measurement of annual increments was performed on seven colonies only. Spearman's rank correlation coefficients were calculated between pairs of transects covering the same time period within one colony. Variability in increment widths could exist, but was not observed on all measured specimens (Fig. 5).

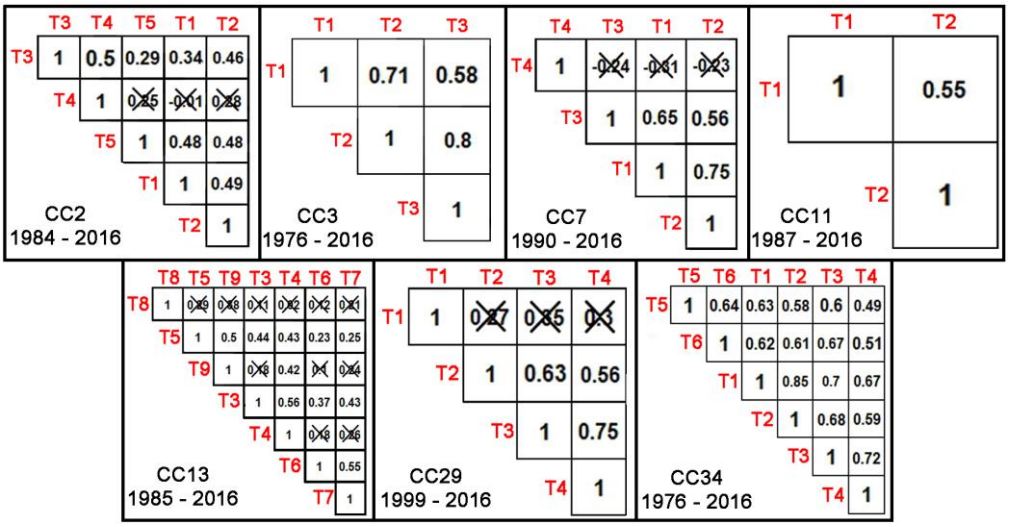

Figure 5: Intra individual variability of annual increment widths over the seven specimens. Values in boxes are Spearman's correlation coefficients, barred ones correspond to a non-significant relationship between pairs of reading transects (*p-value* > 0.05). The indicated dates correspond to the periods when correlations were performed.

In each colony, most increment width time-series obtained from these 2 to 8 transects were significantly correlated to each other. Nevertheless, some transects were significantly different: n°4 in colonies CC2 and CC7, n°4/8/9 in colony CC13, and n°1 in colony CC29 (Fig. 5). These transects were discarded from the dataset.

Population-scale growth signal and chronology construction

Based on the arithmetic mean of annual growth increment widths of all 7 colonies, the average annual growth rate over their lifetime was 260 µm ± 59 µm with a chronology going back to 1970 (Fig. 6A). The inter-series correlation coefficient calculated on the 7 individual SGI chronologies was 0.34. The mean annual SGI values and EPS are shown in Figure 6. The EPS values remained below the critical threshold of 0.85 throughout the entire chronology, showing that the common growth signal expressed by the population was rather weak. The SGI varied considerably over the entire chronology, ranging from a minimum of -1.3 in 1993 to a maximum of 2.2 in 2003. Globally, SGI values seem to be mostly negative between 1970 and 1998 to become positive until 2014 (Fig. 6B).

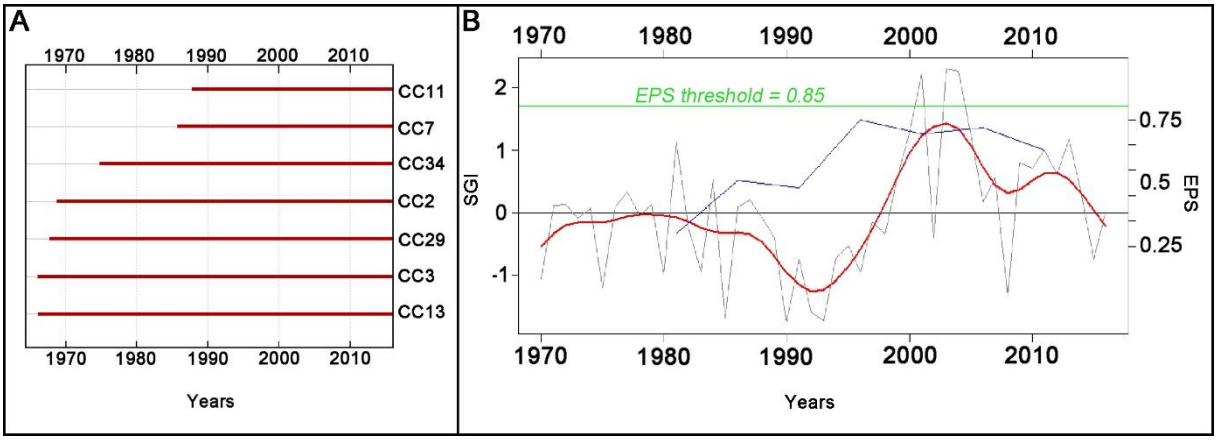

Figure 6: Lifespans of the seven *C. compactum* specimens used for growth analyses. SGI master chronology (grey curve) from *C. compactum* and its 10-year running mean (red curve). EPS values (blue curve) from the master chronology computed in 10-year running windows with the arbitrary EPS threshold value 0.85 (green line).

Environmental comparison

Growth signal presented on Figure 6B was compared to NOAA-NODC 0-100m ocean mean temperature (3-month averages) using KNMI climate explorer. Whatever the season, a

significant positive correlation was highlighted between rhodolith growth dynamics and SST in the North Atlantic basin (Fig. 7), specifically within the subpolar gyre extent.

C. compactum SGI master-chronology was significantly correlated with the annual SPG index (N=25, r=-0.56, p<0.05) and with the AMO index (N=46; r= 0.51, p<0.05). On the other hand, any significant correlations were found between *C. compactum* SGI and the two other atmospheric indices, respectively AO and NAO.

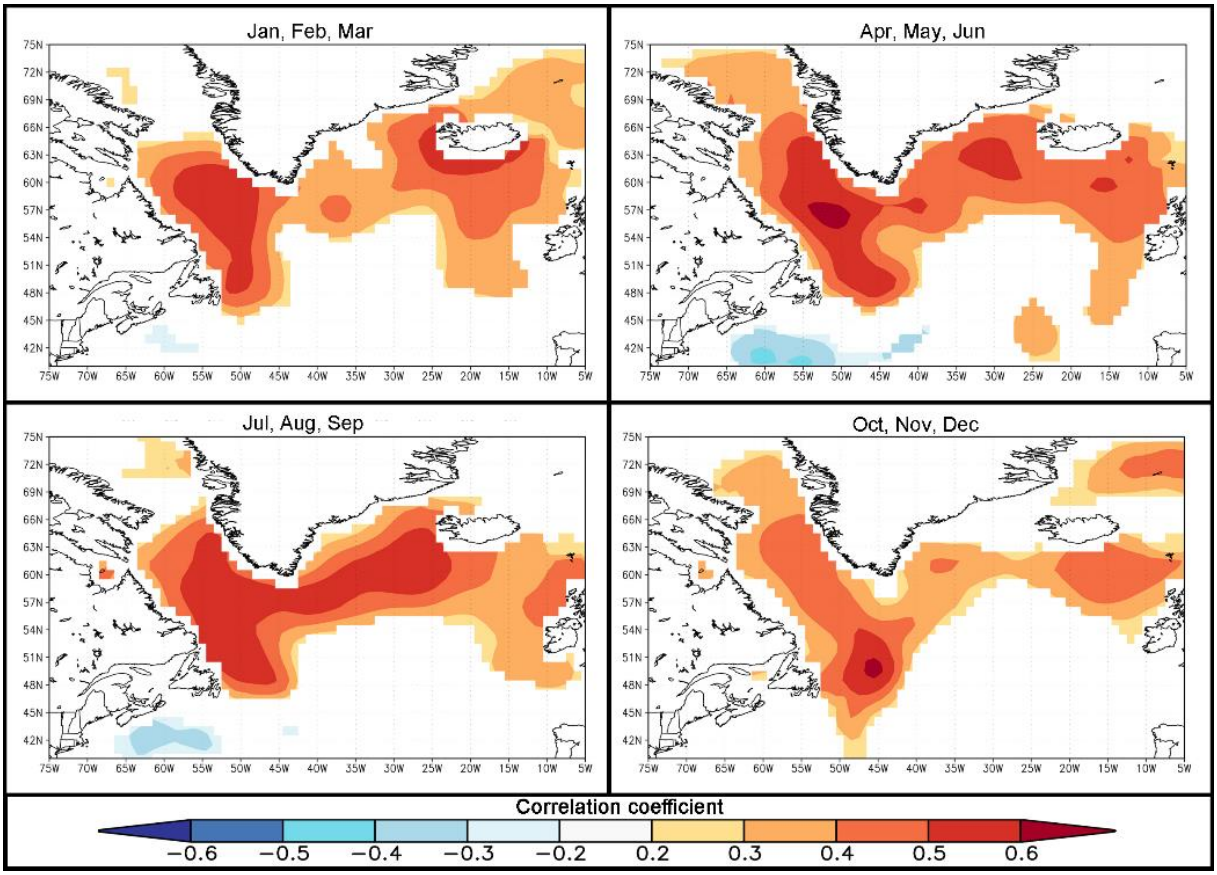

Figure 7: Spatial correlations between *C. compactum* SGI and ocean seasonal mean temperatures between 0-100m (data from the UK Met Office Hadley centre EN4.2.1) using KNMI climate explorer. Only significant (p<0.05) correlation coefficients above 0.3 are displayed.

Trace elements analyses

Trace elements distribution vs growth lines

Once the LA-ICP-MS transects were stained, it was possible to assign calendar dates to geochemical data (Fig. 8A). Figure 8B shows typical element-to-calcium time-series. The overall shape of these profiles, obtained on 1 of the 9 transects ablated in colony CC25, is

representative of the other 26 transects. Mg/Ca ratio variations followed a cyclic annual pattern with maximum values close to the centre of the growth increments and minimum values at or close to the growth lines (Fig. 8B). Ba/Ca ratio also showed a cyclic annual pattern, a bit more noisy and inversely correlated with Mg/Ca variations (r=-0.31, *p<0.05*). Maximum Ba/Ca values usually appeared close to growth lines, while minimum values occurred in the middle of the increments.

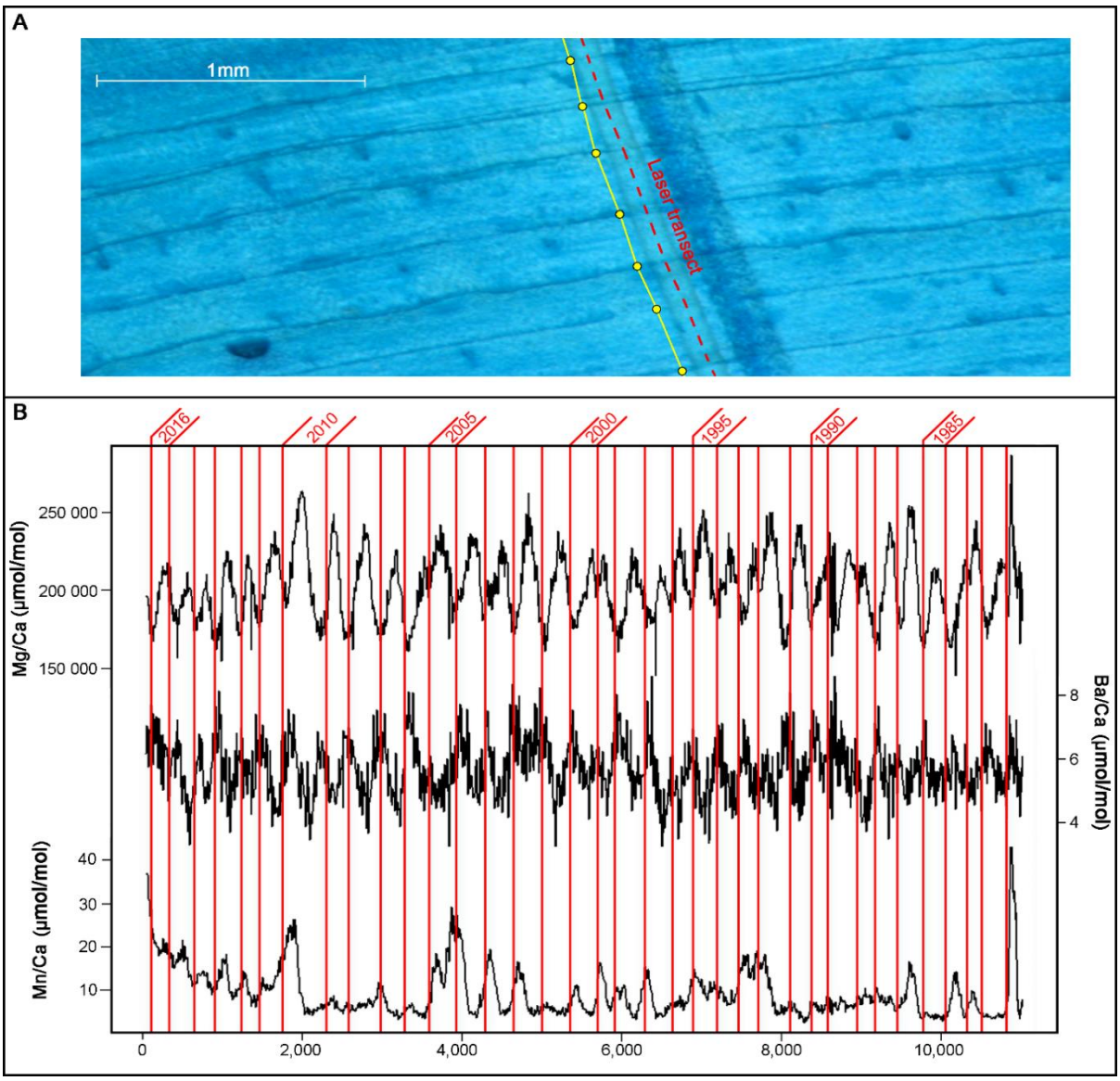

Figure 8: Image of the reading (yellow line and points) process after LA-ICPMS analysis to identify growth lines positions (A). The wider mark on the right of the laser transect correspond to a landmark made in order to identify the desired location of the laser transect before the manipulation. Typical trace elements signal for one LA-ICPMS transect, vertical red lines correspond to growth lines positions.

Mn/Ca pattern was different to Mg/Ca and Ba/Ca ones and without apparent cyclicity. In addition, a trend to higher Mn/Ca values appeared during the last ten years of growth for each colony. The element-to-calcium time-series of the 26 other transects (Fig. 9) could be described in the same way (at least for magnesium and barium) as their overall shapes look like the ones presented on Figure 8.

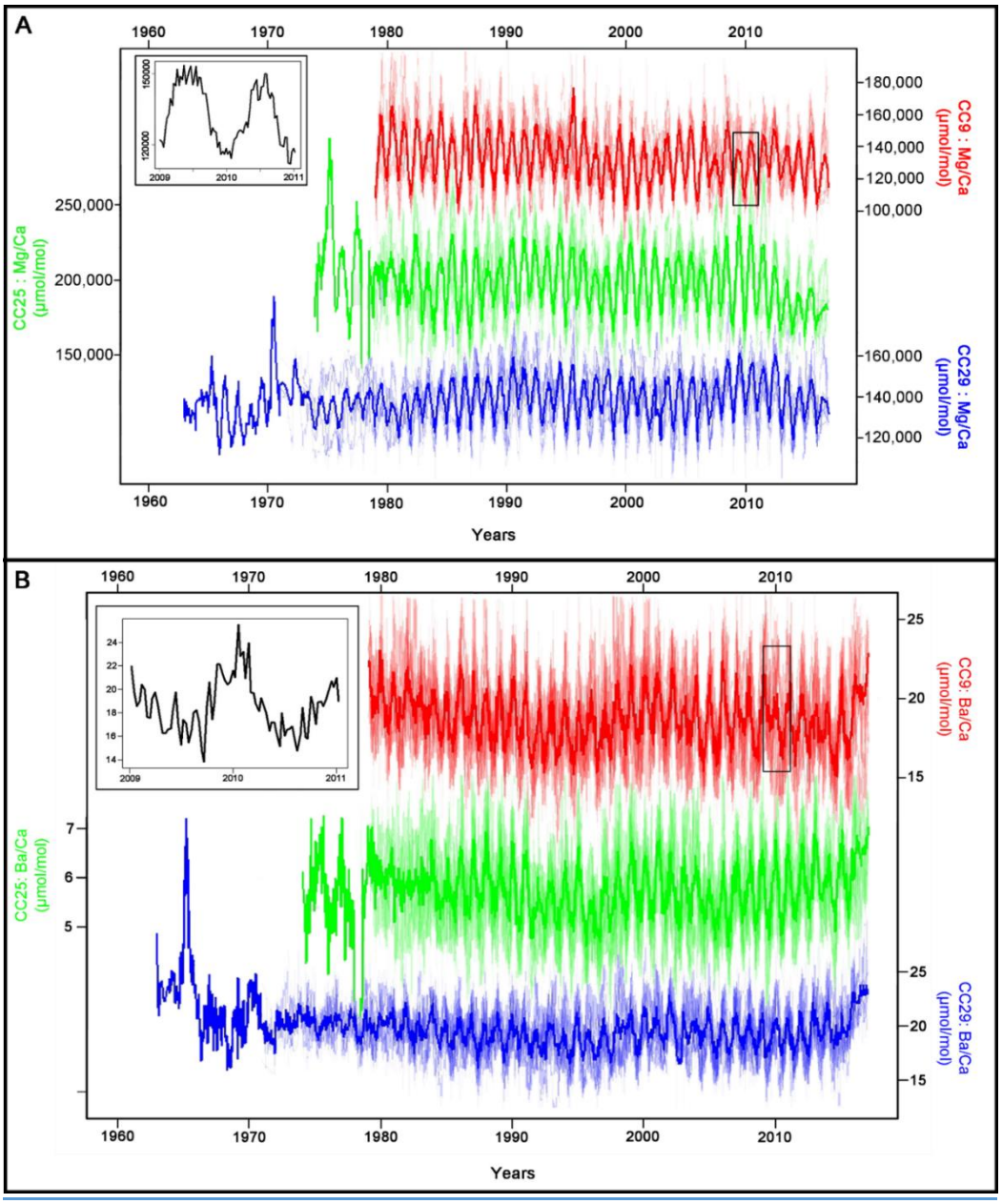

Figure 9: Average values of Mg/Ca (A) and Ba/Ca (B) variations over time for the three studied specimens (bold lines). Light coloured lines represent the nine transects performed on each specimen. Examples of two annual cycles are displayed on the top left for Mg/Ca (A) and Ba/Ca (B).

Intra/inter-specimen trace elements distribution

Years were bounded according to Mg/Ca ratios and re-sampled using AnalySeries software, in order to represent each annual period of growth with the same number of values (40). Spearman's rank correlation coefficients were calculated for each colony and each element in order to compare pairs of transects (Fig. 10). Whatever the colony, Mg/Ca time-series were all significantly correlated, with only one exception (transects n°3 and n°4 on colony CC29). That was also the case for Ba/Ca time-series in which 32 out of 36 pairs of transects were significantly correlated. For Mn/Ca ratios, a stronger variability between transects was observed for CC9 and CC29, but not for CC25 in which all transects were significantly correlated (Fig. 10A).

Given the high intra-colony reproducibility of Mg/Ca and Ba/Ca time-series, average values were calculated for these two elements, for each colony (Fig. 9). Nevertheless, doing the same thing for Mn/Ca values would not be correct because of intra specimen variability, except for CC25 specimen.

CC25 specimen has higher average Mg/Ca values than the two other colonies (CC25: Mg/Ca ~ 200 000 µmol/mol; CC9 and CC29: Mg/Ca ~ 150 000 µmol/mol) (Fig. 9A). Despite this offset, highly significant Spearman's correlations were found between CC9 and CC25 (r=0.78; $p<0.001$), between CC29 and CC25 (r=0.77; $p<0.001$), and between CC9 and CC29 (r=0.79; $p<0.001$) (Fig. 10B).

Regarding Barium, highly significant Spearman's correlations were also observed between Ba/Ca time-series of the three colonies (r=0.67; $p<0.001$ between CC9 and CC25 / r=0.69; $p<0.001$ between CC25 and CC29 / r=0.65; $p<0.001$ between CC9 and CC29) (Fig. 10B).

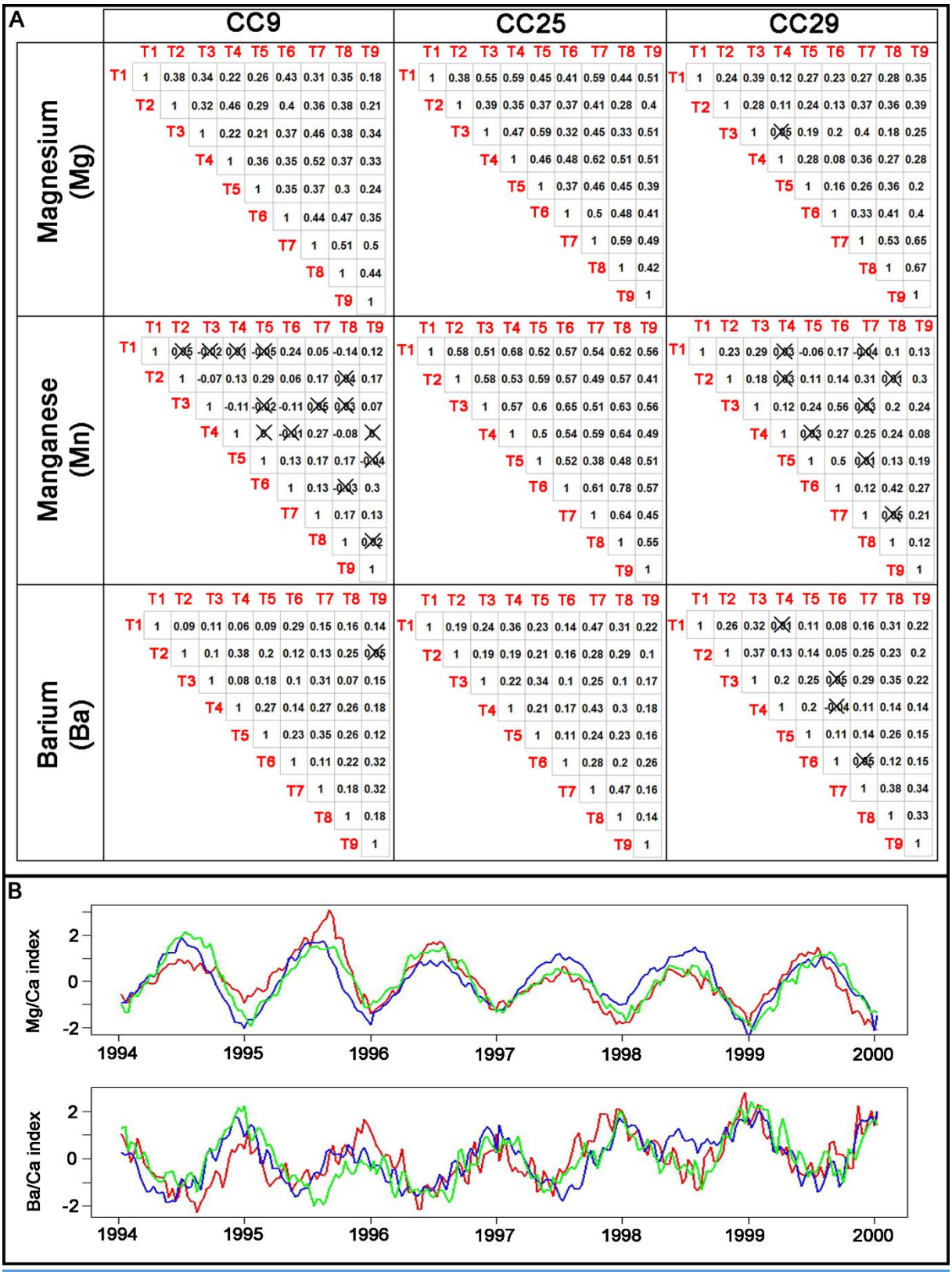

Figure 10: Spearman's correlation coefficients between pairs of transects for each colony and Element/Ca ratios (A). Barred ones correspond to non-significant relationships (*p>0.05*). Mg/Ca and Ba/Ca mean standardized values (red line: CC9 / green line: CC25 / blue line: CC29) representing inter-specimen variability (B).

Intra-specimen variabilities of Mn/Ca time-series were higher than Mg/Ca and Ba/Ca ones. Nevertheless, CC25 presented a low intra-specimen variability compared to CC9 and CC29 (Fig. 10A). Mean values of Mn/Ca were then calculated for this specimen (Fig. 11).

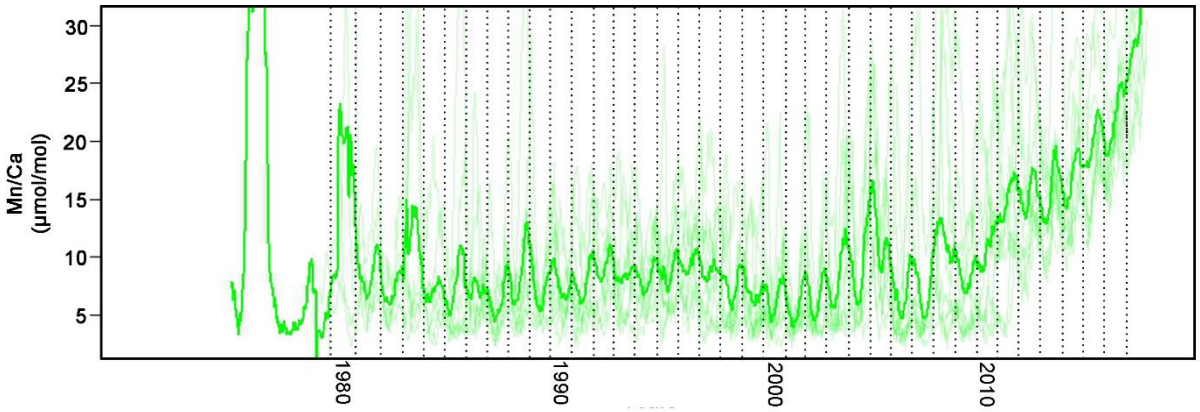

Figure 11: Average Mn/Ca values (bold green line) over time, calculated upon the 9 geochemical transect (light colored green lines) performed on CC25. Year separation (vertical dashed black lines) is based on Mg/Ca annual cycles.

This curve follows a cyclic annual pattern, reaching their annual maxima close to each growth lines (Fig. 11). An overall increase of mean Mn/Ca values started around 2010 (i.e., in the youngest portion of this colony).

Environmental comparisons

Magnesium vs SST

Mg/Ca variations within rhodolith carbonate structures follow local satellite-based SST variations (Fig. 12A). Indeed, a significant linear relationship occurred between Mg/Ca and SST for three colonies (r^2>0.50; *p<0.05*). One calibration equation was then generated for each colony, and their slopes were compared. In the absence of significant differences between these slopes (T=0.55; df=683; *p<0.05* between CC9 and CC25 / T=0.70; df=761; *p<0.05* between CC25 and CC29 / T=0.17; df=778; *p<0.05* between CC9 and CC29), a general temperature equation, representative of the three *C. compactum* specimens, was calibrated (Fig. 12B).

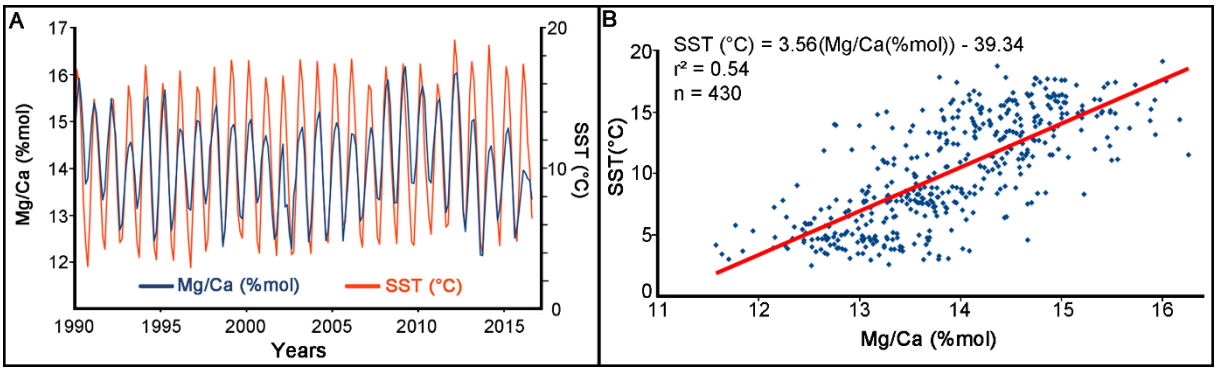

Figure 12: Evolution of Mg/Ca values recorded on rhodoliths and satellite-based SST extracted from a 200 km² area around Saint-Pierre (A) and (B) linear regression between those two parameters for CC29.

Similarly, a significant positive correlation was found between Mg/Ca and SST values measured in Station 27 (r=0.75; *p<0.001*).

Barium vs salinity and Labrador Current transport

Significant positive correlations were found between Ba/Ca values and Tail of Grand Bank Labrador Current transport over the period 1993-2017 (r=0.33; *p<0.05*). Ba/Ca values were also significantly correlated with surface salinities recorded in Station 27 (r=0.31, *p<0.05*).

Discussion

Growth line marking and population growth signal

To our knowledge, this is the first sclerochronological growth study of *C. compactum* based on direct increment width measurements. It is also the first time that *C. compactum* composite growth chronology was statistically evaluated using dendrochronological derived tools (Cook & Kairiukstis, 2013). Therefore, our results would be compared with other studies focused on other biotas.

Mutvei's solution staining

This study demonstrated that Mutvei's solution staining was a good method to reveal annual growth lines on *C. compactum* carbonate structures (with protein colouring and digging effects) (Fig. 3). The main advantages of this technique are: (i) its low cost and (ii) its execution speed compared to micro-chemical analysis and data processing in order to extract growth signals. In addition, Mutvei's solution may also yield important clues to *C. compactum* growth

and biomineralization processes and could lead to new results regarding to micro-chemical analyses. First of all, we showed that growth lines were more strongly stained than growth increments, confirming that *C. compactum* growth was faster in summer (larger less calcified cells) than in winter (smaller more calcified cells) (Moberly, 1968; Halfar *et al.*, 2008). Although it has been proved by Schöne *et al.* (2017), that Mutvei's solution treatment does not affect stable isotopes analysis, it still needs to be demonstrate for trace elements. That is why we decided to apply our staining process on geochemically analysed slices after LA-ICPMS measurements. Nonetheless, some disadvantages still remain. We observed that some portions of few growth lines (considering the entire slice surface) disappear. This could be due to local morphological differences inducing a differential staining, or to micro-grazing tracks altering superficial growth marks. In addition, growth lines were not clearly visible where conceptacles were numerous and dense. This justifies to achieve growth reading along multiple transects and to take the whole slice into account during this measurement process.

Rhodoliths growth signal and statistical indicators

Average vertical growth rates of all specimens were found to be 260 µm per year. This is consistent with *C. compactum* growth rates from the Northwest Atlantic (Adey *et al.*, 2013). Synchronous growth determination within a population is a key to evaluate if individuals are consistently responding to common external factors (Douglas, 1920). That is why the seven specimens' growth signals were compared. On one side, the inter-series correlation of 0.34 is comparable with significant chronologies built using tree rings (Black *et al.* 2010). Though, it is lower than the values usually obtained with several other biotas (e.g. Butler *et al.*, 2013; Wilde & Maxwell, 2018). On the other hand, the EPS values from this study are relatively low and never exceed the threshold of 0.85. This is probably due to the weakness of our sample depth (7 specimens). Indeed, other studies with similar inter-series correlation values usually use more than 20 specimens to complete their growth chronologies (Black *et al.*, 2010). We do not manage to increase our sample depth because of the limited number of colonies collected in SPM in 2017. However, other sclerochronological studies using *Arctica islandica* from SPM (Chapter 2) allowed the construction of a significant *A. islandica* growth master-chronology (with EPS values above 0.85) from ca. 1870 with 32 specimens. This significant growth signal of *A. islandica* was compared to this rhodoliths growth chronology (Fig. 6B). A significant positive relationship was found between *A. islandica* and *C. compactum* growth

patterns in SPM (N=53, r=0.31, p<0.05). This last observation promotes the idea of starting a multiple and diverse environmental proxies approach in SPM. The main advantage of this kind of approach is that each archive records climate variability from its unique "perspective" of habitat, location, life history, or trophic level such that their combination yields a more holistic perspective of the past than any data set could provide on its own (Black *et al.*, 2009). However, we must increase *C. compactum* sample depth before starting this type of study to be sure of encrusting algae population growth response.

Indeed, *C. compactum* specimens were subject to important grazing activities by sea urchins (Steneck, 1986) making most of them unreadable for growth or ageing analyses. Usually, these grazing tracks are easily observable after the first cutting step. However, a slight grazing could reduce the increment size in certain portions of the slice and make some growth lines invisible leading to unreliable growth results. Light conditions could also affect growth rates (Adey, 1970). Light can vary at a very local scale according to sample position and shading provided by macroalgal cover. These external factors affecting rhodoliths growth are not necessarily stable on multidecadal time scale. These inter-specimens local shading signals can be limited by averaging multiple time series from different sites around SPM archipelago. Intra specimens growth variability, mostly related to grazing, can be restricted by multiple growth transect measurements.

Geochemical information within specimen

First of all, we will discuss the way that our chemical analyses were performed. Higher Mg/Ca values for the specimen CC25 are undoubtedly due to machine drift. Indeed, more than 15 days elapsed between CC25 and CC9-CC29 trace elements analyses. Furthermore, the choice of calcium as internal standard does not seem be correct. Regarding to growth lines and increments morphological structures Ca does not seem to be constant in rhodoliths carbonate structure. Thus, express rhodoliths micro chemical results as element to calcium ratios could affect them. But nowadays, there is no alternative solution to fix this issue.

Rhodoliths geochemical information has been used for environmental reconstruction since the middle of 20th century (Chave, 1954). Rhodoliths form high Mg-calcite matrix (Moberly, 1968) where the amount of magnesium is affected by environmental conditions (Halfar *et al*., 2000, Kamenos *et al*., 2008). Warmer temperatures result in a higher incorporation of

magnesium into the skeleton compared to the colder winter temperatures creating alternating bands of high and low magnesium. Nonetheless, to our knowledge any investigations about trace elements distribution within coralline algae specimens have been conducted to date. Authors usually compare at most four LA-ICP-MS transects in order to confirm data repeatability (Halfar *et al.*, 2011; Hetzinger *et al.*, 2013, Hetzinger *et al.*, 2018). However, in order to be considered as environmental proxy, trace elements need to be homogeneously distributed within specimens. Magnesium and barium are homogeneously distributed in our samples. These two elements are included in the same way in *C. compactum* carbonate matrix regardless of colony portion, confirming their environmental proxies' status. In addition, growth lines positions reported from photomosaics and magnesium chemical measurements are consistent. For example, one Mg cycle occur between two observed growth-lines leading to the conclusion of its annual periodicity. However, minimum values of some Mg/Ca cycle does not always correspond to observed growth line, a lag can occur between them. This mismatch can be associated to lines pointing mistakes or to laser digging effects. Nevertheless, it appears that *C. Compactum* growth measurements using Mg/Ca variation is an effective method despite its high financial cost. This study tends to prove that direct growth measurements after Mutvei's solution staining were equally effective and less expensive. All advantages of this new method should allow us to extend *C. compactum* growth readings to more specimens and carry out population growth studies. Regarding Ba/Ca, we also highlighted the annual basis of barium distribution within rhodoliths carbonate matrix in Saint-Pierre & Miquelon.

Furthermore, Mg/Ca values were calibrated with local SST temperature (Fig. 12). The relationship between these two parameters was investigated in other studies (e.g., Chave, 1954; Halfar *et al.*, 2007) using several rhodoliths genus. In comparison to *Clathromorphum nereostatum*, another rhodolith species from North-Pacific (Hetzinger *et al.*, 2009), it seems that magnesium incorporation within *C. compactum* carbonate matrix is more temperature dependent.

To our knowledge, this is the first time that Mn/Ca ratio was measured in *C. compactum*. Stronger intra specimen distribution variability occurs in this alga for Mn/Ca ratio in contrast to Mg/Ca and Ba/Ca (Figure 10A). Nonetheless, this trait does not apply to all measured specimens. For example in CC25 Mn/Ca maximum values are regularly associated to growth

lines (Figure 11) and could be explained by *C. compactum* growth. That is why it might be interesting to perform other manganese measurements from new *C. compactum* specimens to enhance our understanding of its incorporation dynamic. For now, it is not possible to use manganese as an environmental proxy in this species.

In order to calibrate these geochemical tools, it could be interesting to deploy a marine environmental observatory in SPM during a couple of years.

Correlations with environmental parameters

Even if *C. compactum* EPS values never exceed the threshold of 0.85, the good inter-series correlation led us to investigate relationships between *C. compactum* growth and environmental variability.

First, we sought correlations between *C. compactum* growth in SPM and large-scale climatic indices (AMO and NAO). These two drivers strongly influence marine ecosystem structure (e.g., Carroll et al., 2014) at decadal or multi-decadal time scales. At SPM, the AMO was significantly and positively correlated with SGI, while the NAO was not correlated with *C. compactum* growth. These results indicate that part of *C. compactum* growth variability may be explained by near surface temperature over the North Atlantic. This result is consistent with positive spatial correlations between *C. compactum* SGI from SPM and temperature within the Sub Polar Gyre (SPG) extent (Fig. 7). These highlights led us to further explore SPG dynamics and its influence on water properties around SPM. The significant negative correlation observed between SPG index and *C. compactum* growth rates in SPM seems to have the same implications as temperature spatial correlations and raises questions about the SPG dynamics.

The SPG western flank mainly consists of the Labrador Current (LC). The LC flows toward the equator and carries cold and less saline water of Arctic origin along the Labrador slope and Grand Banks and extends to the Scotian shelf, finally affecting the whole Middle Atlantic Bight (e.g., Chapman & Beardsley, 1989) (Fig. 1). The spatiotemporal structure of the LC along the Labrador coast and over the Grand Banks is complex. On the Newfoundland shelf, it has two branches: a main offshore branch flowing south and feeding the SPG, and a much smaller inshore branch (10 times smaller flow rates) that flows over the Labrador shelf and spreads along the Newfoundland coast over the Grand Banks. This possibility led us to investigate the

LC inner branch dynamics and its influence on *C.compactum* in SPM. Station 27 located in the Avalon channel within the LC inshore branch provides the longest SST and SSS time series in this area. Strong positive correlations were found between magnesium and barium concentrations in *C. compactum* calcified structures from SPM and, respectively Station 27 SST and SSS. Hetzinger *et al.*, (2013) found the same significant relationships between *C. compactum* Ba/Ca coming from Eastern Newfoundland coastal waters (also influenced by LC inner branch) and Station 27 salinity.

The Grand Bank circulation remains to be addressed. This circulation could affect the SPM region under certain conditions (Peterson et al., 2017; Petrie & Drinkwater, 1993). A part of the offshore branch of LC that follows the continental slope retroflexes to the east, joining the North Atlantic Current (Fig. 1) before reaching the tail end of the Grand Banks (Fratantoni & McCartney, 2009). The remaining LC branch flows westward after the tail of Grand Banks and turns northward, toward Cabot Strait and may spread around the SPM region (Petrie & Anderson, 1983; Urrego-Blanco & Sheng, 2014). This transport at the tail end of Grand Bank was calculated for 1992 to 2013 and found to correlate positively with SPM *C. compactum* Ba/Ca variations.

Our results point the same direction as those obtained with *A. islandica* (Chapter 2) and tend to confirm the relevance of scientific researches carried out along SPM to study large-scale oceanographic variability and ecosystem dynamics facing global changes.

Acknowledgements

First, we thank the LEMAR (UMR 6539) Secretariat team (Anne-Sophie Podeur, Geneviève Cohat, and Yves Larsonneur) for their invaluable assistance during the administrative preparation of the field trip associated with this work. We also thank the DTAM divers' crew (Yoann Busnot, Luc Thillais, Jean-Marc Derouet) for their invaluable help during *C. compactum* sampling off Saint-Pierre Island. We are sincerely grateful to the Club Nautique Saint-Pierrais for renting their boat and especially to its president, Stephane Salvat, for his incredible availability and kindness. In addition, we express our sincere gratitude to Herlé Goraguer, IFREMER delegate in SPM, for his help with local authorisations and logistics. This work was supported by the EC2CO program MATISSE of the CNRS INSU, the Cluster of Excellence LabexMER, and the LIA BeBEST CNRS INEE. This research was carried out as part of the Ph.D.

thesis of Pierre Poitevin for the University of Western Brittany with a French Ministry of Higher Education and Research grant.

References

Adey W. H. (1965). The genus Clathromorphum (Corallinaceae) in the Gulf of Maine. *Hydrobiologia*, *26*(3–4), 539–573. https://doi.org/10.1007/BF00045545

Adey, W. H. (1970). The effects of light and temperature on growth rates in boreal-subarctic crustose corallines. *Journal of Phycology*, *6*(3), 269-276

Adey, W. H., Halfar, J., & Williams, B. (2013). *The coralline genus Clathromorphum foslie emend. adey: biological, physiological, and ecological factors controlling carbonate production in an arctic-subarctic climate archive*.

Berx B., & Payne M. R. (2017). The Sub-Polar Gyre Index - A community data set for application in fisheries and environment research. *Earth System Science Data*, *9*(1), 259–266. https://doi.org/10.5194/essd-9-259-2017

Black B. A., Shaw D. C., & Stone J. K. (2010). Impacts of Swiss needle cast on overstory Douglas-fir forests of the western Oregon Coast Range. *Forest Ecology and Management*, *259*(8), 1673–1680. https://doi.org/10.1016/j.foreco.2010.01.047

Black B. A, Copenheaver C. A., Frank D. C., Stuckey M. J., & Kormanyos R. E. (2009) Multi-proxy reconstructions of northeastern Pacific sea surface temperature data from trees and Pacific geoduck. *Palaeogeography, Palaeoclimatology, Palaeoecology*, *278*, 40–47. https://doi.org/10.1016/j.palaeo.2009.04.010

Bunn A. G. (2008). A dendrochronology program library in R (dplR). *Dendrochronologia*, *26*, 115–124. https://doi.org/10.1016/j.dendro.2008.01.002

Butler P. G., Wanamaker A. D., Scourse J. D., Richardson C. A., & Reynolds D. J. (2013). Variability of marine climate on the North Icelandic Shelf in a 1357-year proxy archive based on growth increments in the bivalve Arctica islandica. *Palaeogeography, Palaeoclimatology, Palaeoecology*, *373*, 141–151. https://doi.org/10.1016/j.palaeo.2012.01.016

Carroll M. L. , Ambrose W. G. Jr., Locke W.L. , Ryan S.K., & Johnson B.J. (2014) Bivalve growth rate and isotopic variability across the Barents Sea Polar Front. *Journal of Marine Systems*, *130*, 167–180.

Chan P., Halfar J., Williams B., Hetzinger S., Steneck R., Zack T., & Jacob D. E. (2011). Freshening of the Alaska Coastal Current recorded by coralline algal Ba/Ca ratios. *Journal of Geophysical Research: Biogeosciences*, *116*(1), 1–8. https://doi.org/10.1029/2010JG001548

Chapman D.C., & Beardsley R.C. (1989) On the origin of shelf water in the Middle Atlantic Bight. *Journal of Physical Oceanography*, *19*, 384–391.

Chave K. E. (1954). Aspects of the Biogeochemistry of Magnesium 1. Calcareous Marine Organisms. *The Journal of Geology*, *62*(3), 266–283. https://doi.org/10.1086/626162

Cook, E. R., & Kairiukstis, L. A. (Eds.). (2013). *Methods of dendrochronology: applications in the environmental sciences*. Springer Science & Business Media.

Douglas AE (1920) Evidence of climatic effects in the annual rings of trees. *Ecology*, *1*, 24-27.

Dunbar B., Wellington M., Colgan W., & Glynn P. W. (1994). Eastern Pacific sea surface temperature since 1600 A.D.: The record of climate variability in Galápagos corals. *Paleobiology*, *9*(2), 291–315. https://doi.org/10.1029/93PA03501

Fratantoni P. S., & McCartney M.S. (2009) Freshwater export from the Labrador Current to the North Atlantic Current at the Tail of the Grand Banks of Newfoundland. *Deep-Sea Research I, 57*, 258–283.

Goodwin D. H., Schöne B. R., & Dettman D. L. (2009). Resolution and Fidelity of Oxygen Isotopes as Paleotemperature Proxies in Bivalve Mollusk Shells: Models and Observations. *Palaios*, *18*(2), 110–125.

Grissino-Mayer H. D. (2001). Evaluating Crossdating Accuracy : A Manual and Tutorial for the Computer Program COFECHA. *Tree-Ring Research*, *57 (2)*, 205–221.

Halfar J., Adey W. H., Kronz A., Hetzinger S., Edinger E., & Fitzhugh W. W. (2013). Arctic sea-ice decline archived by multicentury annual-resolution record from crustose coralline algal proxy. *Proceedings of the National Academy of Sciences*, *110*(49), 19737–19741. https://doi.org/10.1073/pnas.1313775110

Halfar J., Hetzinger S., Adey W., Zack T., Gamboa G., Kunz B., Williams B., & Jacob D. E. (2011). Coralline algal growth-increment widths archive North Atlantic climate variability. *Palaeogeography, Palaeoclimatology, Palaeoecology*, *302*(1), 71–80. https://doi.org/10.1016/j.palaeo.2010.04.009

Halfar J., Steneck R. S., Joachimski M., Kronz A., & Wanamaker A. D. (2008). Coralline red algae as high-resolution climate recorders. *Geology*, *36*(6), 463–466. https://doi.org/10.1130/G24635A.1

Halfar J., Steneck R., Schöne B., Moore G. W. K., Joachimski M., Kronz A., … Estes J. (2007). Coralline alga reveals first marine record of subarctic North Pacific climate change. *Geophysical Research Letters*, *34*(7), 1–5. https://doi.org/10.1029/2006GL028811

Hetzinger S., Halfar J., Kronz A., Simon K., Adey W. H., & Steneck R. S. (2018). Reproducibility of Clathromorphum compactum coralline algal Mg/Ca ratios and comparison to high-resolution sea surface temperature data. *Geochimica et Cosmochimica Acta*, *220*, 96–109. https://doi.org/10.1016/j.gca.2017.09.044

Hetzinger S., Halfar J., Kronz A., Steneck R. S., Adey W. H., Lebednik P. A., & Schöne B. R. (2009). High-Resolution Mg/Ca Ratios in a Coralline Red Alga As a Proxy for Bering Sea Temperature Variations From 1902 To 1967. *Palaios*, *24*(6), 406–412. https://doi.org/10.2110/palo.2008.p08-116r

Hetzinger S., Halfar J., Zack T., Gamboa G., Jacob D. E., Kunz B. E., … Steneck R. S. (2011). High-resolution analysis of trace elements in crustose coralline algae from the North Atlantic and North Pacific by laser ablation ICP-MS. *Palaeogeography, Palaeoclimatology, Palaeoecology*, *302*, 81–94. https://doi.org/10.1016/j.palaeo.2010.06.004

Hetzinger S., Halfar J., Zack T., Mecking J. V., Kunz B. E., Jacob D. E., & Adey W. H. (2013). Coralline algal Barium as indicator for 20th century northwestern North Atlantic surface ocean freshwater variability. *Scientific Reports*, *3*, 1–8. https://doi.org/10.1038/srep01761

Hurrell J. W., Kushnir Y., & Visbeck M. H. (2001). The North Atlantic Oscillation. *Science*, *291*(5504), 603–5. https://doi.org/10.1126/science.1058761

Jochum K.P., Nohl U., Herwig K., Lammel E., Stoll B., Hofmann A.W. (2005). GeoReM: A new geochemical database for reference materials and isotopic standards. Geostandards and Geoanalytical Research 29(3): 333-338

Kamenos N. A., Cusack M., & Moore P. G. (2008). Coralline algae are global palaeothermometers with bi-weekly resolution. *Geochimica et Cosmochimica Acta*, *72*(3), 771–779. https://doi.org/10.1016/j.gca.2007.11.019

Knight J. R., Folland C. K., & Scaife A. A. (2006). Climate impacts of the Atlantic multidecadal oscillation. *Geophysical Research Letters*, *33*(17), 2–5. https://doi.org/10.1029/2006GL026242

Moberly Jr. R. (1968). Composition of magnesian calcites of algae and pelecypods by electron microproe analysis. *Sedimentology*, *11*, 61–82.

Paillard D., Labeyrie L., & Yiou P. (1996). AnalySeries 1.0: a Macintosh software for the analysis of geophysical time-series. *Eos*, *77*, 379.

Peterson I., Greenan B., Gilbert D., Hebert D. (2017) Variability and wind forcing of ocean temperature and thermal fronts in the Slope Water region of the Northwest Atlantic. *Journal of Geophysical Research Oceans*, *122*, 7325–7343.

Petrie B., & Anderson C. (1983) Circulation on the Newfoundland Continental Shelf. *Atmosphere-Ocean*, *21 (2),* 207–226.

Petrie B, & Drinkwater K (1993) Temperature and salinity variability on the Scotian Shelf and in the Gulf of Maine 1945-1990. *Journal of Geophysical Research-Oceans and Atmospheres*, *98*, 20079–20089.

Rahmstorf S. (2003). The current climate. *Nature*, *421*(6924), 699. https://doi.org/10.1038/421699a

Saenger C., Cohen A. L., Oppo D. W., Halley R. B., & Carilli J. E. (2009). Surface-temperature trends and variability in the low-latitude North Atlantic since 1552. *Nature Geoscience*, *2*(7), 492–495. https://doi.org/10.1038/ngeo552

Schöne B. R. (2013). Arctica islandica (Bivalvia): A unique paleoenvironmental archive of the northern North Atlantic Ocean. *Global and Planetary Change*, *111*, 199–225. https://doi.org/10.1016/j.gloplacha.2013.09.013

Schöne B. R., Dunca E., Fiebig J., & Pfeiffer M. (2005). Mutvei's solution: An ideal agent for resolving microgrowth structures of biogenic carbonates. *Palaeogeography, Palaeoclimatology, Palaeoecology*, *228*(1–2), 149–166. https://doi.org/10.1016/j.palaeo.2005.03.054

Schöne B. R., Schmitt K., & Maus M. (2017). Effects of sample pretreatment and external contamination on bivalve shell and Carrara marble δ18O and δ13C signatures. *Palaeogeography, Palaeoclimatology, Palaeoecology*, *484*, 22–32. https://doi.org/10.1016/j.palaeo.2016.10.026

Sirot C., Ferraton F., Panfili J., Childs A. R., Guilhaumon F., & Darnaude A. M. (2017). Elementr: An R package for reducing elemental data from LA-ICPMS analysis of biological calcified structures. *Methods in Ecology and Evolution*, *8*(12), 1659–1667. https://doi.org/10.1111/2041-210X.12822

Sletten H. R., Andrus C. F. T., Guzmán H. M., & Halfar J. (2017). Re-evaluation of using rhodolith growth patterns for paleoenvironmental reconstruction: An example from the Gulf of Panama. *Palaeogeography, Palaeoclimatology, Palaeoecology*, *465*, 264–277. https://doi.org/10.1016/j.palaeo.2016.10.038

Steneck R. S. (1986). The Ecology of Coralline Algal Crusts : Convergent Patterns and Adaptative Strategies. *Annual Review of Ecology and Systematics*, *17*, 273–303.

Thompson D. W. J., & Wallace J. M. (1998). The Arctic Oscillation signature in the wintertime geopotential height and temperatuer field. *Geophysical Research Letters*, *25*(9), 1297–1300.

Urrego-Blanco J., & Sheng J. (2014) Study on subtidal circulation and variability in the Gulf of St. Lawrence, Scotian Shelf, and Gulf of Maine using a nested-grid shelf circulation model. *Ocean Dynamics*, *64*, 385–412.

Wanamaker A. D., Kreutz K. J., Schöne. B. R., Pettigrew N., Borns H. W., Introne D. S., … Feindel S. (2008). Coupled North Atlantic slope water forcing on gulf of Maine temperatures over the past millennium. *Climate Dynamics*, *31*, 183–194. https://doi.org/10.1007/s00382-007-0344-8

Wilde E. M., & Maxwell J. T. (2018). Comparing climate-growth responses of urban and non-urban forests using L. tulipifera tree-rings in southern Indiana, USA. *Urban Forestry and Urban Greening*, *31*, 103–108. https://doi.org/10.1016/j.ufug.2018.01.003

Williams B., Halfar J., Steneck R. S., Wortmann U. G., Hetzinger S., Adey W. H., … Joachimski M. (2011). Twentieth century δ13C variability in surface water dissolved inorganic carbon recorded by coralline algae in the northern North Pacific Ocean and the Bering Sea. *Biogeosciences*, *8*(1), 165–174. https://doi.org/10.5194/bg-8-165-2011

Williams S., Halfar J., Zack T., Hetzinger S., Blicher M., & Juul-Pedersen T. (2018). Comparison of climate signals obtained from encrusting and free-living rhodolith coralline algae. *Chemical Geology*, *476*, 418–428. https://doi.org/10.1016/j.chemgeo.2017.11.038

Wu Y., Tang C., & Hannah C. (2012). The circulation of eastern Canadian seas. *Progress in Oceanography*, *106*, 28–48.

Chapitre 4

A new ultra-high resolution method developed to track trace elements variations in *Placopecten magellanicus* associated to large diurnal bottom temperature oscillations

Contexte et résumé de l'étude

Rappelons ici que l'une de caractéristiques majeures de SPM est la présence, en période estivale (stratifiée), d'une oscillation diurne de la thermocline. L'objectif principal de ce quatrième chapitre est de déterminer si *Placopecten magellanicus* peut être considéré comme une archive environnementale enregistrant, dans sa coquille, les variations de son environnement direct à haute fréquence (25,82 h). Le choix de cette espèce a été basé sur deux principaux critères : (i) sa présence sur notre site d'étude le long d'un gradient bathymétrique allant de 5 m à 80 m, (ii) son fort taux de croissance (plusieurs centimètres) notamment pendant l'été lorsque l'amplitude de ces oscillations thermiques quotidiennes est la plus importante.

Les compositions en éléments traces (Ba, Mg, U) de deux fragments de *P. magellanicus,* issus de deux sites présentant des conditions thermiques haute-fréquences contrastées en période stratifiée, ont alors été comparées. Pour ce faire, nous avons développé une nouvelle méthode d'analyses LA-ICPMS à ultra haute résolution, permettant de quantifier la composition en éléments traces des coquilles de *P. magellanicus* avec une résolution spatiale de 10 µm. Afin de limiter les effets liés à l'ontogénie lors de la comparaison des signatures élémentaires des deux coquilles sélectionnées, nous avons choisi d'analyser, la même année calendaire (2015) correspondant à la troisième année de croissance des individus prélevés.

Des signaux communs ont alors été observés entre la composition en baryum des deux coquilles analysées. De plus, en comparant ces signaux avec la dynamique de la concentration en chlorophylle *a* autour de l'archipel la même année. Nous pouvons suggérer l'existence d'un lien entre la dynamique de la biomasse phytoplanctonique à SPM et l'incorporation de baryum dans les coquilles de *P. magellanicus*. En revanche, les signatures Mg/Ca contrastées au sein des deux coquilles ainsi que leurs ressemblances avec les profils thermiques de ces deux profondeurs, suggèrent l'existence d'un lien entre l'incorporation de cet élément dans la coquille de *P. magellanicus* et la température.

Concernant l'uranium mesuré dans ces deux coquilles, les signatures élémentaires sont également contrastées entre les deux sites. À 10 m, aucune tendance ne semble caractériser les séries de mesures effectuées. Cependant, à 30 m, les variations de la concentration en uranium mesurées dans la coquille semblent synchrones (cohérentes) avec les variations de la concentration en magnésium. Cette observation suggère que l'incorporation de l'uranium au sein de la coquille de 30 m est également liée aux oscillations thermiques hautes fréquences. En revanche, pour ce qui est du site de 10 m, la disponibilité de l'uranium dans l'environnement pourrait être affectée par d'autres paramètres environnementaux.

En termes d'interprétation des données, ces résultats confirment également un réel besoin d'informations complémentaires sur : (i) la dynamique de la croissance et la physiologie de *P. magellanicus*, (ii) l'enregistrement récurent à haute fréquence de plusieurs variables environnementales le long d'un gradient bathymétrique.

A new ultra-high resolution method developed to track trace elements variations in *Placopecten magellanicus* associated to large diurnal bottom temperature oscillations

Pierre Poitevin[*1], Laurent Chauvaud[1], Christophe Pécheyran[2], Pascal Lazure[3], Aurélie Jolivet[4], Julien Thébault[1]

[1] *Université de Bretagne Occidentale, Laboratoire des Sciences de l'Environnement Marin (UMR6539 UBO/CNRS/IRD/Ifremer), 29280 Plouzané, France*

[2] *Université de Pau et des Pays de l'Adour, Institut des sciences analytiques et de physico-chimie pour l'environnement et les matériaux (UMR5254 CNRS/UPPA), 64053, Pau, France*

[3] *Ifremer, Laboratoire d'Océanographie Physique et Spatiale (UMR6523 CNRS/Ifremer/IRD/UBO), 29280 Plouzané, France*

[4] *TBM environnement/Somme, 115 rue Claude Chappe, Technopole Brest-Iroise, 29280 Plouzané, France*

Email addresses:

Pierre Poitevin: pierre.poitevin@univ-brest.fr

Laurent Chauvaud: laurent.chauvaud@univ-brest.fr

Christophe Pécheyran: christophe.pecheyran@univ-pau.fr

Pascal Lazure: pascal.lazure@ifremer.fr

Aurélie Jolivet: a.jolivet@tbm-environnement.com

Julien Thébault: julien.thebault@univ-brest.fr

Corresponding author:

Pierre Poitevin

Université de Bretagne Occidentale

Institut Universitaire Européen de la Mer

Laboratoire des Sciences de l'Environnement Marin (UMR6539 UBO/CNRS/IRD/Ifremer)

F-29280 Plouzané

Tel: +33 2 90 91 55 78

Fax: +33 2 98 49 86 45

Abstract

Saint-Pierre & Miquelon (SPM) is a small archipelago where instrumental measures based on water column velocity and temperature profiles compiled comprehensive evidence for strong near-diurnal (25.82 h) current and bottom temperature oscillations (up to 11.5°C) which is possibly the largest ever observed — at any frequency — on a stratified mid-latitude continental shelf. The main objective of our study was to identify if *P. magellanicus* can record on its shell these high frequency environmental variations. To this end, we have tried to identify proxies for water temperature and food availability through development of a new ultra-high resolution LA-ICPMS analyses method capable of resolving shell surface elemental composition with a 10 µm resolution. This method was applied on two shell fragments, both representing the third year of growth and 2015 annual growth period, respectively coming from two environmentally contrasted sites, more (30 m depth) or less (10 m depth) affected by high frequency thermal oscillations. Our results strongly suggest a relationship between phytoplankton biomass and barium incorporation into *P. magellanicus* shells at both sites. Even if *P. magellanicus* might present a physiological control of magnesium incorporation, the shape of the two Mg/Ca profiles seems to illustrate that temperature also exerts a control on magnesium incorporation in *P. magellanicus* shells from SPM. While U/Ca and Mg/Ca profiles show a strong positive correlation for 30 m site shell, suggesting that uranium incorporation in *P. magellanicus* shell is at least partially temperature dependent. The absence of such correlation for 10 m site shell suggests differences in uranium environmental availability or in *P. magellanicus* biomineralization between these two sites. The resolution of this new analytical method raises questions about such data interpretation related to *P. magellanicus* growth dynamics and physiology or individual scale based environmental measurements.

Keywords:

Ultra-high resolution LA-ICPMS; *Placopecten magellanicus*; shell chemistry; trace elements; environmental change; bivalve; environmental proxies; North Atlantic; Saint-Pierre and Miquelon; Coastal Trapped Wave.

Introduction

Saint-Pierre & Miquelon (SPM) is a small archipelago at the confluence of major oceanic currents marking the boundary between the North Atlantic Ocean subtropical and subpolar gyres. However, SPM archipelago hydrodynamics is poorly known and its physic observations (sensor deployments) only began very recently. In this context, instrumental measurements based on water column velocity and temperature profiles compiled comprehensive evidence for strong near-diurnal (25.82 h) current and bottom temperature oscillations (up to 11.5°C) from July to October between 10 and 80m depth. This feature is possibly the largest ever observed — at any frequency — on a stratified mid-latitude continental shelf (Lazure *et al*., 2018). The extremely variable physical nature of this sub-tidal environment associated with temperate and subarctic assemblages (habitats) represents a true ecological paradox, making of this site a relevant place to study benthic organism responses to chronic thermal variations.

Biogenic carbonate with recognizable periodic growth bands, such as bivalve molluscs, can incorporate minor and trace elements into their shells in amounts depending on their concentrations in the environment and on the physical and biological properties of the surrounding seawater. However, bivalve shell biomineralization is a complex process, subject to strong physiological and kinetic effects related to metabolism, growth rates, ontogenetic age, shell mineralogy, crystal fabrics and organic matrix (e.g. Carré *et al.*, 2006; Freitas *et al.*, 2008; Freitas *et al.*, 2009; Freitas *et al.*, 2016; Klein *et al*., 1996; Lazareth *et al.*, 2013; Lorens & Bender, 1977; Schöne *et al*., 2013; Shirai *et al.*, 2014). Owing to their wide geographic distribution, economic importance, rapid growth rates, and the presence of annual growth lines on their shell, pectinid bivalves (aka. scallops) offer good opportunities for documenting past environmental conditions (Chauvaud *et al.*, 1998). The occurrence of a clearly visible annual banding pattern on the upper valve of the Atlantic sea scallop, *Placopecten magellanicus* (Chute *et al.,* 2012), and the presence of this species in SPM over a wide bathymetric gradient (5 to 80m), make this species a good candidate to track high-frequency past environmental changes - reflected as variations in the shell geochemical properties – at extremely high temporal resolution.

Spatially-resolved geochemical analysis of biogenic carbonates deposited between two accurately dated growth lines can be performed with a wide set of methods, such as laser

ablation inductively coupled mass spectrometry (LA-ICPMS), secondary ion mass spectrometry ((nano)SIMS) or electron micro probe analyzer (EMPA). Because of its potential for rapid and accurate high-resolution *in situ* trace element analysis at relatively low cost and minimal sample preparation requirements, LA-ICPMS has become a routine analytical tool in a wide area of research applications (Warter & Müller, 2017).

As bivalve growth rates have often been related to environmental variables such as food availability or water temperature (Ballesta-Artero *et al.*, 2017; Butler *et al.*, 2010; Marali & Schöne, 2015; Witbaard *et al.*, 1997) and because of the importance of these two parameters to track environmental and ecological changes, we then understand the interest to track and calibrate elemental proxy records of these two variables. For example, some authors proposed that magnesium to calcium ratios (Mg/Ca) can be used to record water temperature (Ullmann *et al.,* 2013, Bougeois *et al.,* 2014), while there are many reports of strong vital effects in bivalve shells for this element (Lorrain *et al.,* 2005, Wanamaker *et al.*, 2008, Surge & Lohmann, 2008). Uranium to calcium ratio (U/Ca) has also been suggested as a proxy for temperature in shallow water corals (Min *et al.,* 1995; Shen & Dunbar, 1995) and in planktonic foraminiferal carbonates (Yu *et al.*, 2008). Some authors also found a pH effect on U/Ca ratios in both inorganic aragonite and calcite (Kitano & Oomori, 1971; Chung & Swart, 1990). Indeed, U/Ca ratios in calcium carbonate are negatively correlated with pH and [CO_3^{2-}] because in aqueous solutions the carbonate ion complexes with the uranyl ion (UO_2^{2+}) at higher pH (Langmuir, 1978), therefore less uranium is available to be incorporated in shell carbonate. However U/Ca ratio on mollusc shells has rarely been studied (Gilikin & Dehairs, 2012). Barium to calcium ratios (Ba/Ca) profiles in bivalve shells are typically characterized by a flat background signal interrupted by sharp peaks. Many authors suggested synchronization between these peaks and phytoplankton blooms (e.g. Elliot *et al*., 2009; Lazareth *et al*., 2003; Stecher *et al*., 1996; Thébault *et al*., 2009; Vander Putten *et al.*, 2000). Building on the work of Stecher & Kogut (1999), Thébault *et al*. (2009) proposed two main hypotheses to explain the peaks: (1) ingestion of barite originating from assemblages of recently dead diatoms or (2) adsorption of barium onto iron oxyhydroxides associated with diatoms frustules. Background level of Ba/Ca ratios in bivalve shells has also been suggested to be linked with salinity (Gillikin *et al.*, 2006, 2008).

The main objective of our study was to identify whether the calcitic shell of *P. magellanicus* can record the high frequency (25.8 h) environmental variations observed in Saint-Pierre & Miquelon. To this end, we developed a new ultra-high resolution LA-ICPMS analytical method in order to investigate skeletal trace element concentrations with a 10-µm resolution.

Materials & Methods

Sample collection

Two live *P. magellanicus* were collected in September 2016 from Saint-Pierre Bay (Saint-Pierre & Miquelon – NW Atlantic) respectively at 10 m and 30 m depth (Fig. 1). Both individuals were in their fourth year of growth. The deepest location consisted in a homogeneous substrate, made of compacted and stable fine sand. At the shallowest one, the substrate was more heterogeneous and consisted of a mixture of gravels, pebbles and rocks with a seaweed cover. Soft tissues were removed immediately after collection. Both shells were carefully cleaned with freshwater to remove adherent sediment and biological tissues before sample preparation

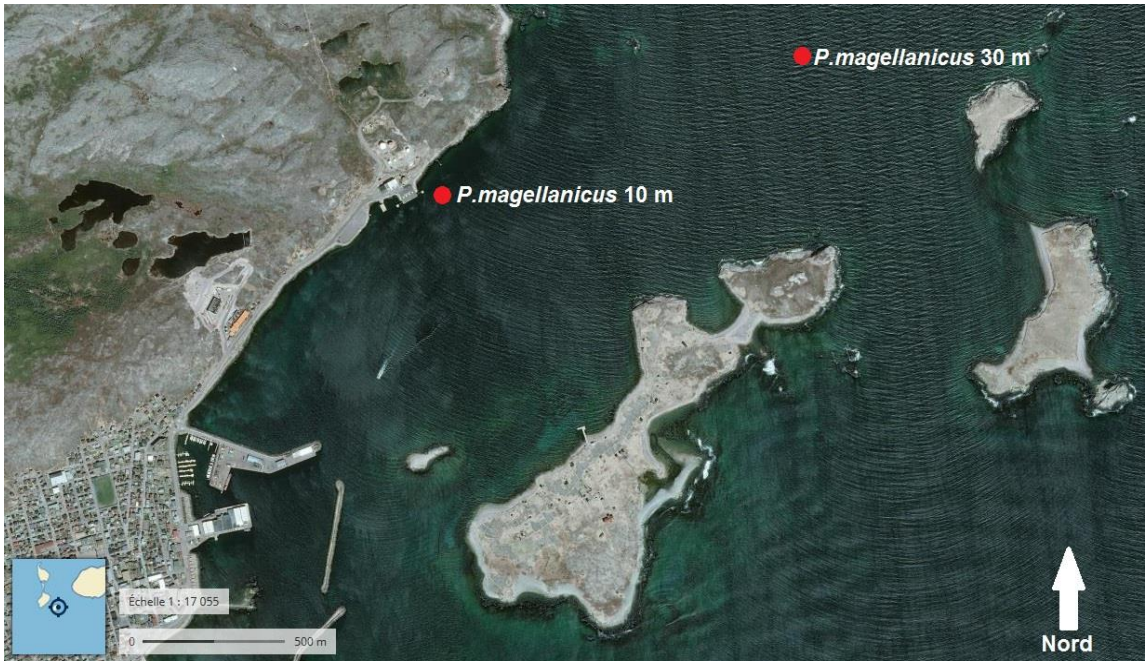

Figure 1: Satellite image of *P. magellanicus* sampling locations (red dots) in Saint-Pierre Bay.

Environmental monitoring

Annual thermal profiles at 10 m and 30 m discussed later were derived from Lazure *et al.,* (2018) study. To refine our vision of thermal variations on the two collection sites (Fig. 1), three multi-parameter probes measuring temperature and pressure every 5 minutes were deployed at 8 m, 12 m and 30 m depth, between 28/08/2017 and 15/09/2017. The 2015 monthly satellite chlorophyll *a* measurements were downloaded from the GlobColour website (http://hermes.acri.fr) and are weighted monthly averages of single-sensor products (SeaWiFS/MERIS/MODIS/VIIRSN merged chlorophyll concentrations) over the area 46.6–47.3°N / 56.0–56.6°W (i.e., waters surrounding the SPM archipelago within ca. 30 km).

Sample preparation

All micro-chemical analyses were performed on *P. magellanicus* upper valves. Indeed, the lower valves might have been contaminated as a result of a prolonged contact with the sediment. For each individual, a fragment of shell of *ca.* 3.5 cm x 1 cm was cut with a diamond saw, including the axis of maximal growth (Fig. 2).

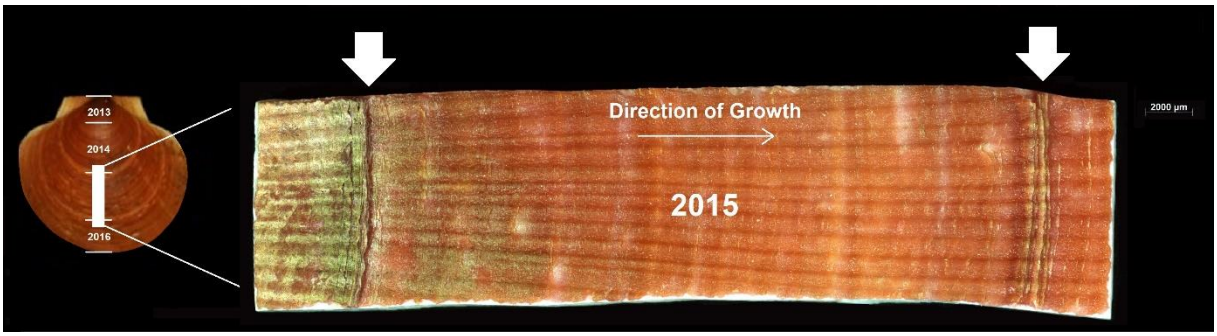

Figure 2: Example of one *P. magellanicus* fragment used for LA-ICPMS analyses. White arrows indicate annual shell growth lines positions defining 2015 increment.

All ultra-high resolution LA-ICPMS analyses were performed one these two shell portions. These fragments represent, for each individual, the third year of growth corresponding to 2015 annual growth periods. The outer shell layer was ultrasonically cleaned with deionized water in order to remove organic matter and sediment particles. In addition, before LA-ICPMS analyses, the outer shell layer of each sample was chemically cleaned with a 15 seconds acetic acid (10 %) bath, soaked in deionized water during 10 seconds, and left to air dry in LA-ICPMS clean room.

Ultra-high resolution fs-LA-ICPMS analysis

Each ICPMS measurement point represents an ablation transect with a 1-mm long arcuate trajectory, parallel to the ventral margin, made by fast round trips of a 10 µm laser spot (Fig. 3). Each transects were bonded in order to analyse the whole "2015 annual period of growth" for the two individuals. The area, covered by a 1000*10 µm transect is equivalent to the area covered by a 110 µm diameter round spot. A UV high-repetition-rate femtosecond laser ablation (fs-LA) system (Nexeya SA, Canejan, France) was employed (Pulse duration: 360fs; wavelength: 257 nm).

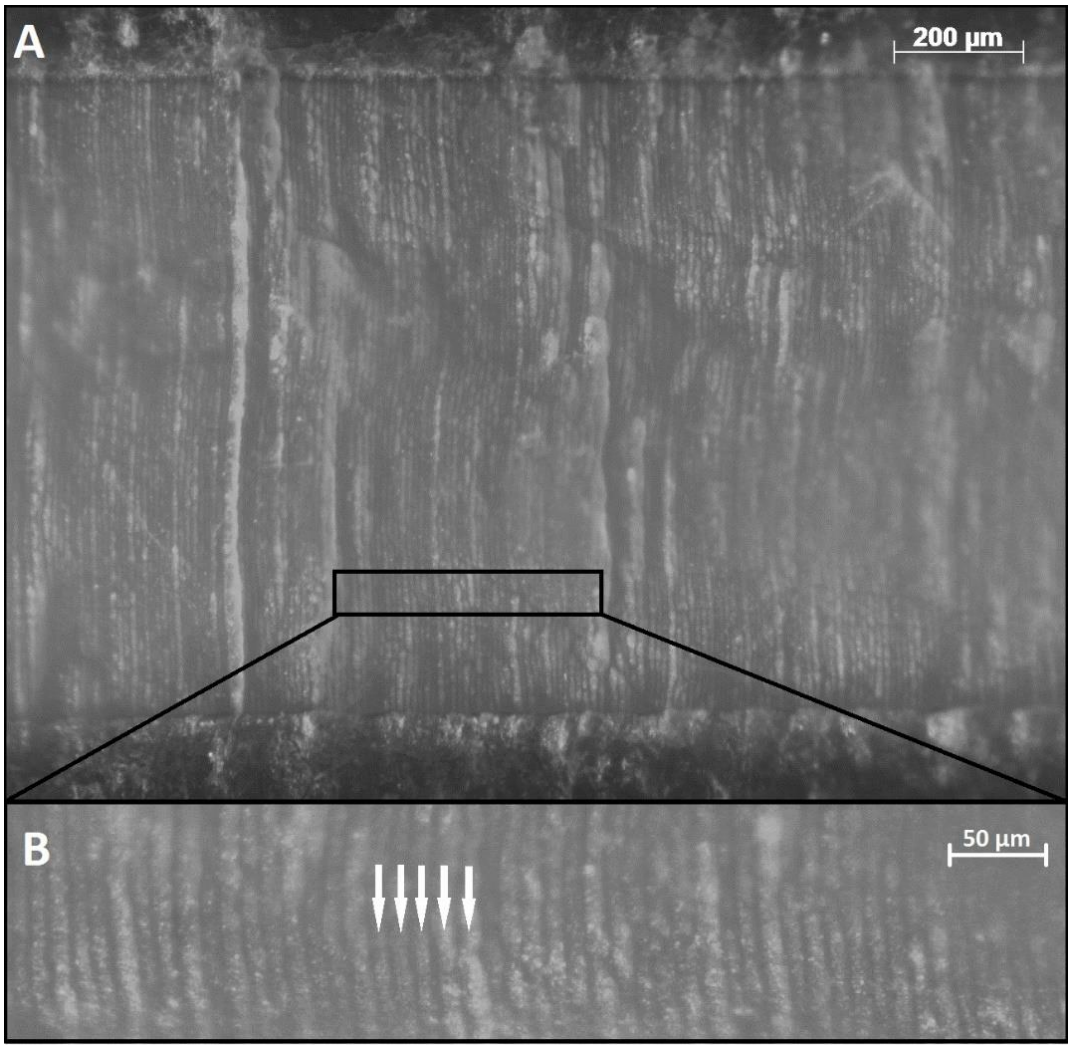

Figure 3: Post ablation picture of a 1.5 mm *P. magellanicus* section showing ca. 150 femtosecond laser ablation transects (A). Zoom on a small fraction of them, with five white arrows pointing one ablation transect (B).

Outer shell layers were analysed for Mg/Ca, Ba/Ca and U/Ca ratios on a High Resolution (Thermo Scientific, USA) inductively coupled plasma quadrupole mass spectrometer (HR-ICP-MS). A helium gas stream carried ablated material to the HR-ICP-MS (carrier gas flow rate 0.68 $L.min^{-1}$). Elemental ratios were quantified by monitoring ^{43}Ca, ^{24}Mg, ^{138}Ba and ^{238}U. Calcium was used as an internal standard to improve the reliability of the concentration measurement (Campana, 1999). Elements were standardized to calcium based on the stoichiometry of calcium carbonate (388 000 $\mu gCa.g^{-1}$ outer shell layer) (Brown & Severin, 2009): Mg/Ca ($\mu g.g^{-1}$), Ba/Ca ($\mu g.g^{-1}$) and U/Ca ($\mu g.g^{-1}$). Quantification of trace elements in shells was achieved by external calibration using both carbonate pellets (Barats *et al*., 2007) and 2 NIST glass standards (610, 612) to ensure the best accuracy. The calibration was done with each standard three times before and after each session with the laser to account for drifting during the day. The limits of detection ($\mu g.g^{-1}$ in shells) achieved in this study were as follows: ^{24}Mg, 0.08, ^{138}Ba, 0.01 and ^{238}U, 0.002. They were based on a 3σ criterion, where σ is the standard deviation of the mean blank count for each isotope. All the elemental concentrations in the outer shell layer were above the detection limits.

Results

Environmental parameters:

Around 10 m depth, the temperature varied from 2 °C in May to a maximum of 16 °C in early September and then decreased to 8 °C in November. At this depth seawater temperature presents a classic seasonal cycle (Lazure *et al.*, 2018) with cold water intrusions (Fig. 4). During the first two weeks of September at 8 m and 12 m in Saint-Pierre Bay, temperature showed high-frequency variations with cold water incursions leading to 4°C (8m) to 6°C (12m) amplitudes (Fig. 4). Along these two weeks, temperatures were 70% of the time above 12 °C (Fig. 4).

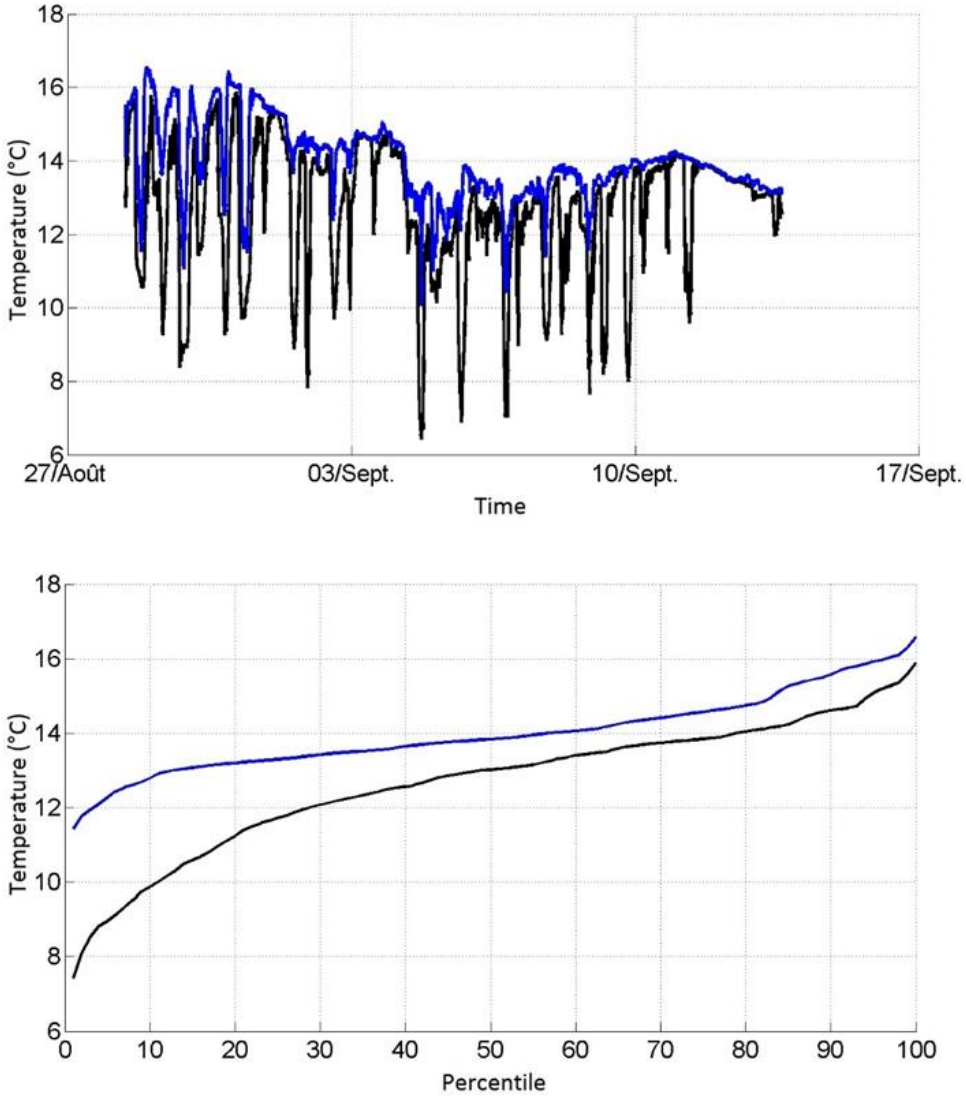

Figure 4: First two weeks of September 2017 time series of seawater temperatures at 8 m and 12m depth (blue and black respectively) (top graphic). Percentile distribution of these temperatures at 8 m and 12m depth (blue and black respectively).

At 30 m depth, the temperature annual profile was radically different. Seawater temperature baseline is mainly cold over the year, showing low seasonal amplitudes (Lazure *et al.*, 2018). However, during the stratified period temperatures showed high-frequency variations whose amplitude increased with sea-surface temperature. During the first two weeks of September (Fig. 5), oscillations were the largest in term of amplitude, reaching nearly 10°C. Temperatures were 80% of the time below 8 °C (Fig. 5).

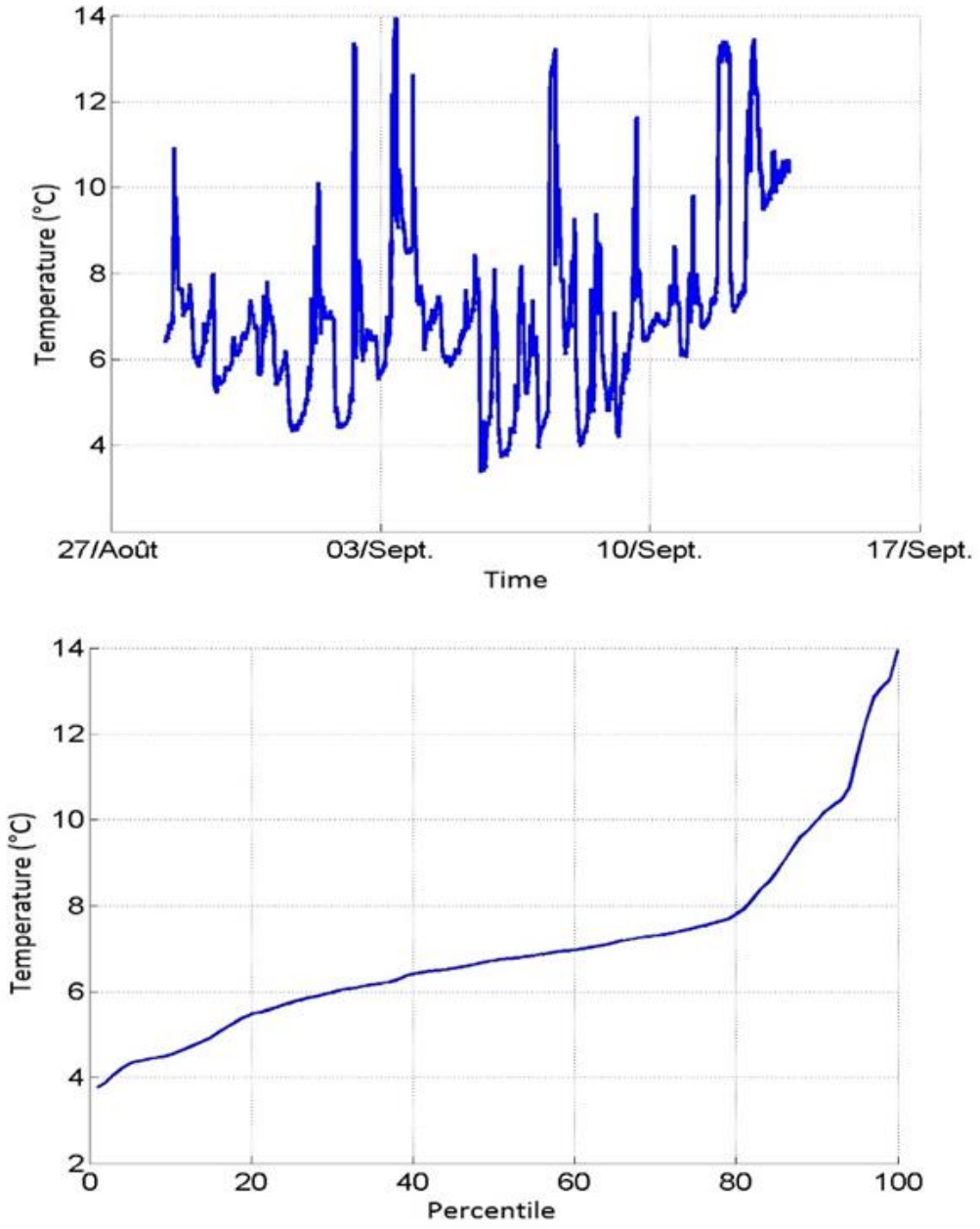

Figure 5: First two weeks of September 2017 time series of seawater temperatures at 30m depth (top graphic). Percentile distribution of these temperatures during these two weeks.

Monthly mean satellite chlorophyll *a* concentrations ranged from 0.46 to 1.22 $mg.m^{-3}$ (Fig. 6). The annual time-series exhibited a background level around 0.7 $mg.m^{-3}$, with one major peak in April - May 2015.

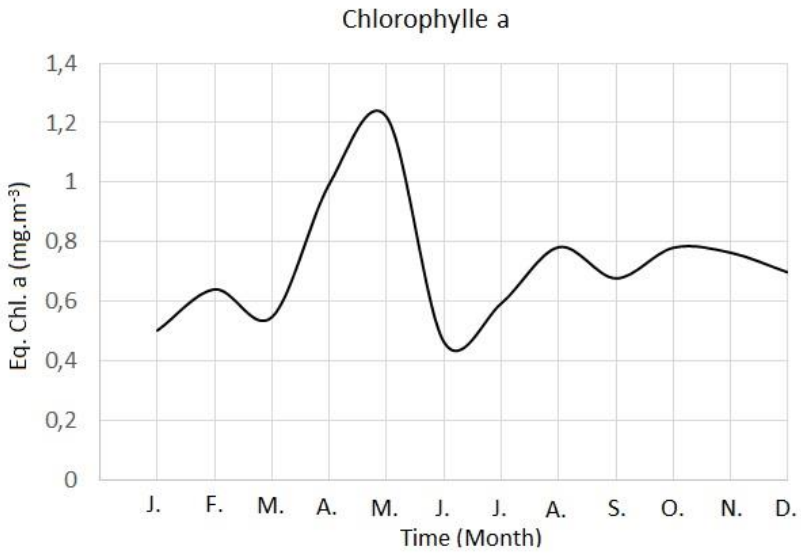

Figure 6: Monthly satellite equivalent chlorophyll a ($mg.m^{-3}$) measurements over 2015.

Ba/Ca ratio profiles in the shell carbonates

Outer shell layer Ba/Ca ratios ranged from 0.61 to 15.71 $\mu g.g^{-1}$ at 10 m and from 0.43 to 12.54 $\mu g.g^{-1}$ at 30 m (Fig. 7).

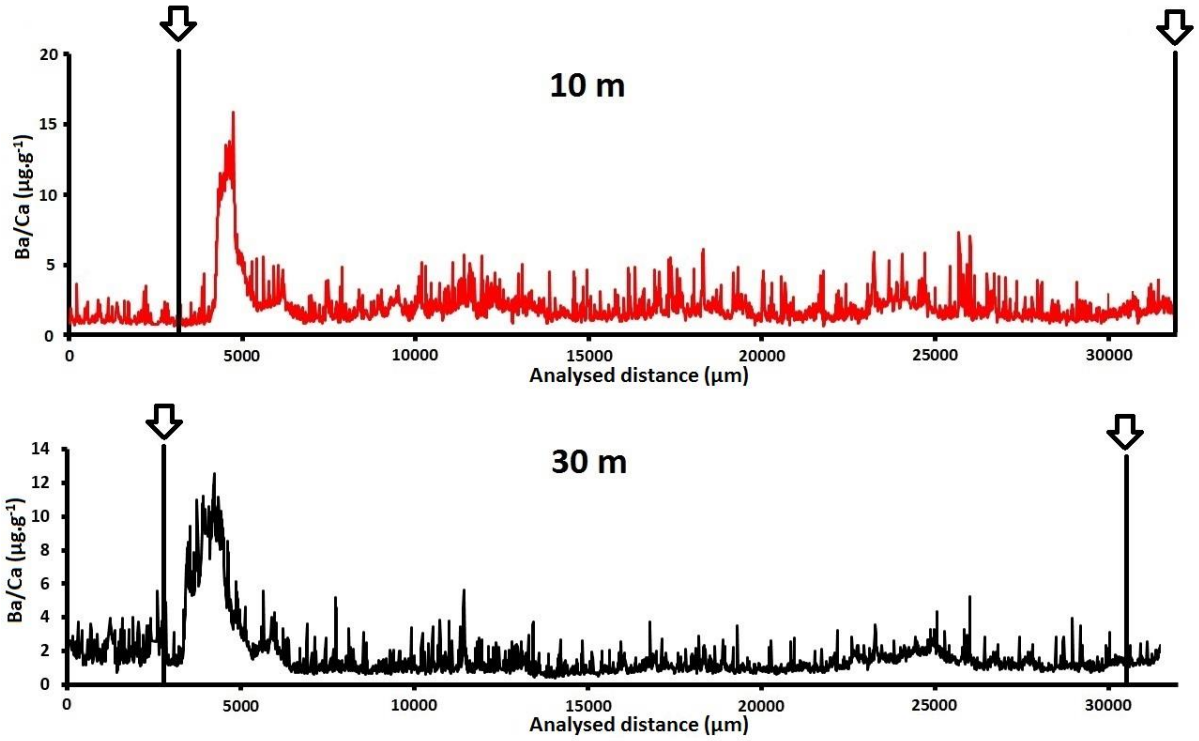

Figure 7: Ba/Ca ($\mu g.g^{-1}$) series at 10 m (red curve) and 30 m (black curve). Vertical lines placed under the arrows indicate the position of winter shell growth lines.

Both series have the same profile with one major peak occurring respectively 370 µm and 830 µm after the "winter 2014/2015" growth line. The main Ba/Ca peak covers 1370 µm and 2220 µm of shell at 10 and 30m, respectively. A secondary smaller Ba/Ca peak occurred immediately after the first one, covering respectively 1230 and 1160 µm at 10 and 30 m. Ba/Ca baseline was the similar for the two time series (ca. 1.5 $\mu g.g^{-1}$).

Mg/Ca ratio profiles

Outer shell layer Mg/Ca ratios ranged from 232 to 1408 $\mu g.g^{-1}$ at 10 m and from 233 to 1495 $\mu g.g^{-1}$ at 30 m (Fig. 8). At 10 m, Mg/Ca profile followed a sinusoidal pattern with stronger high-frequency variations between 15 000 and 25 000 µm (decreasing phase, Figure 8).

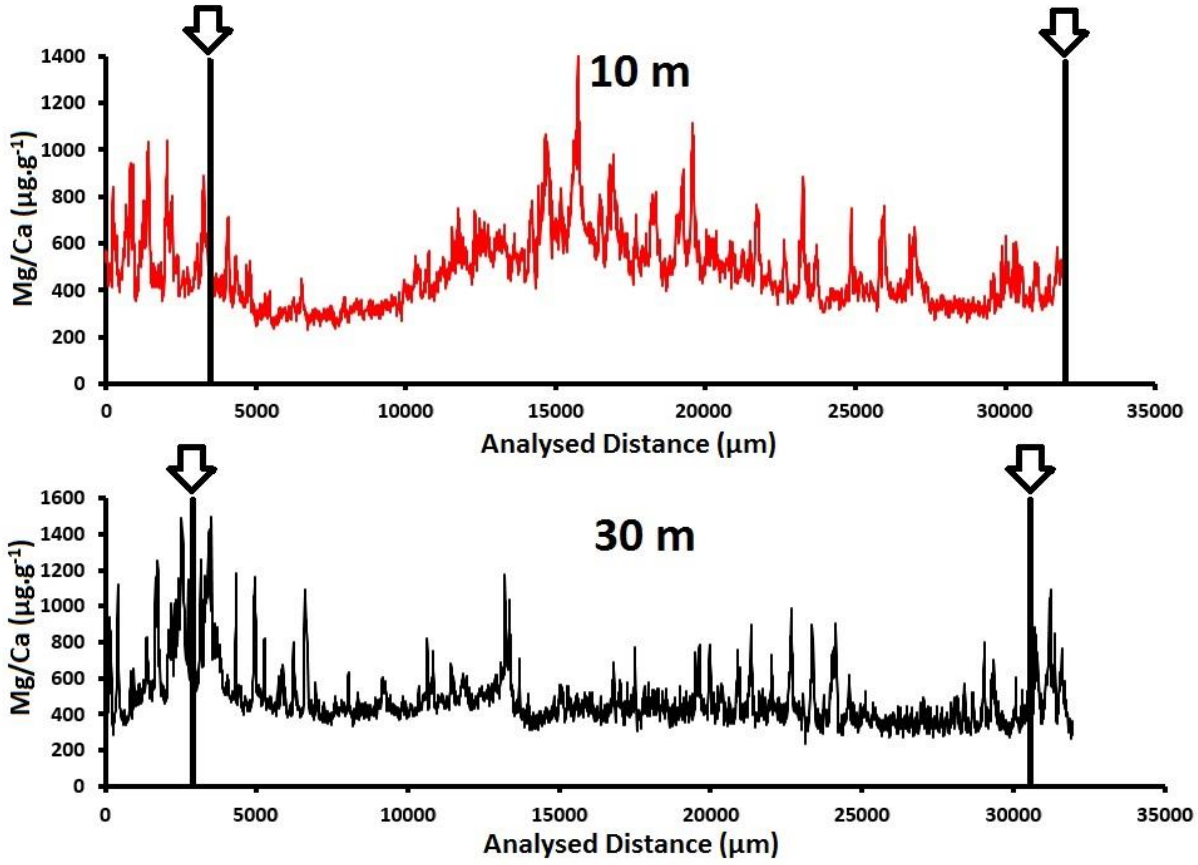

Figure 8 : Mg/Ca ($\mu g.g^{-1}$) series at 10 m (red curve) and 30 m (black curve). Vertical lines placed under the arrows indicate the position of shell growth lines.

However, at 30 m depth, Mg/Ca profile was radically different with a globally flat profile between the two growth lines and high frequency variations mainly between 15000 and 25000 µm.

U/Ca ratio profiles

Outer shell layer U/Ca ratios ranged from 0.003 to 0.16 µg.g^{-1} at 10 m and from 0.004 to 0.36 µg.g^{-1} at 30 m (Fig. 9). At 10 m, U/Ca time series had a relatively flat pattern with high-frequency variations all along the profile. However, at 30 m depth, U/Ca profile was close to Mg/Ca one. This prompted us to represent them on the same graph.

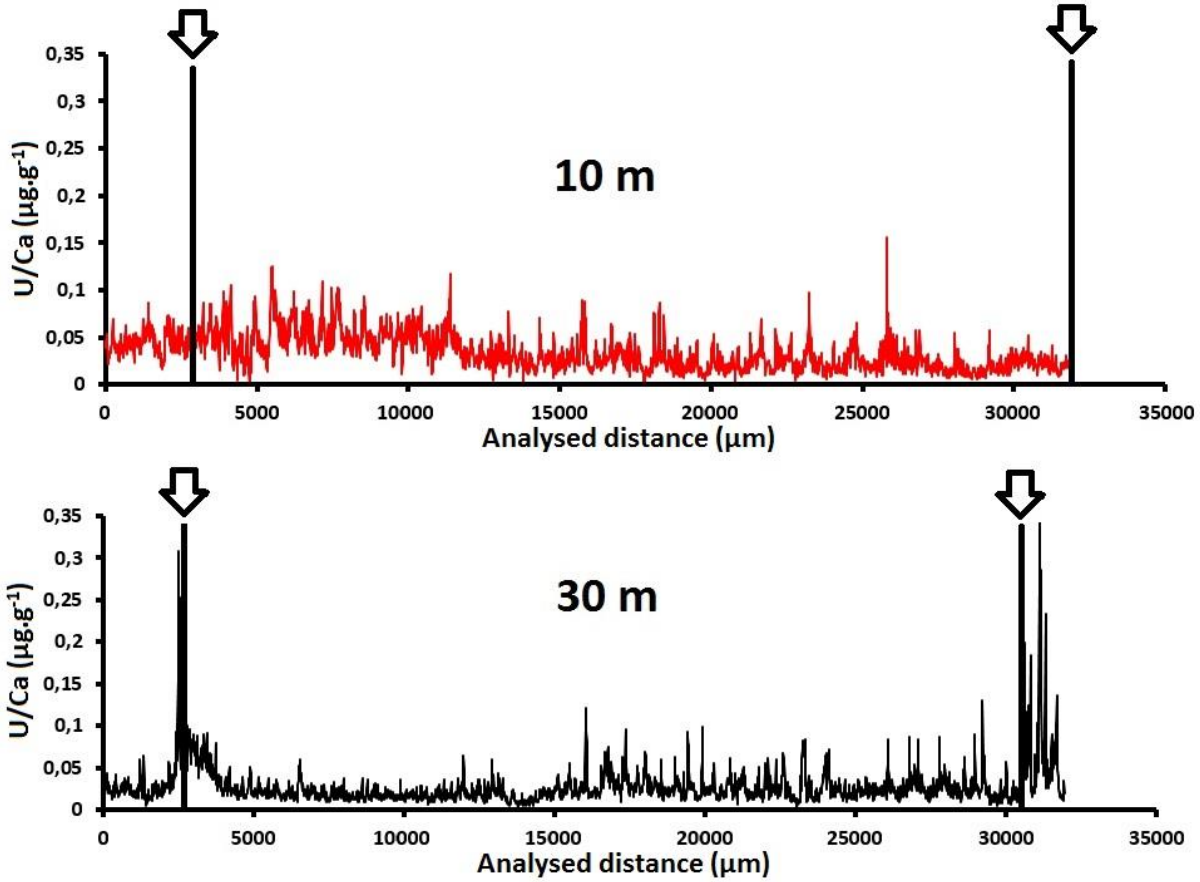

Figure 9: U/Ca (µg.g^{-1}) series at 10 m (red curve) and 30 m (black curve). Vertical lines placed under the arrows indicate the position of shell growth lines.

U/Ca and Mg/Ca comparison at 30m depth:

At 30 m depth, U/Ca and Mg/Ca profiles presented a strong positive correlation (N = 3135, r = 0.62, $p < 0.001$) (Fig. 10). A closer examination of this relationship on a shorter time window (i.e. three high frequency cycles, between 22400 µm and 24250 µm) revealed an even stronger correlation (N=186, r=0.77, p<0.001).

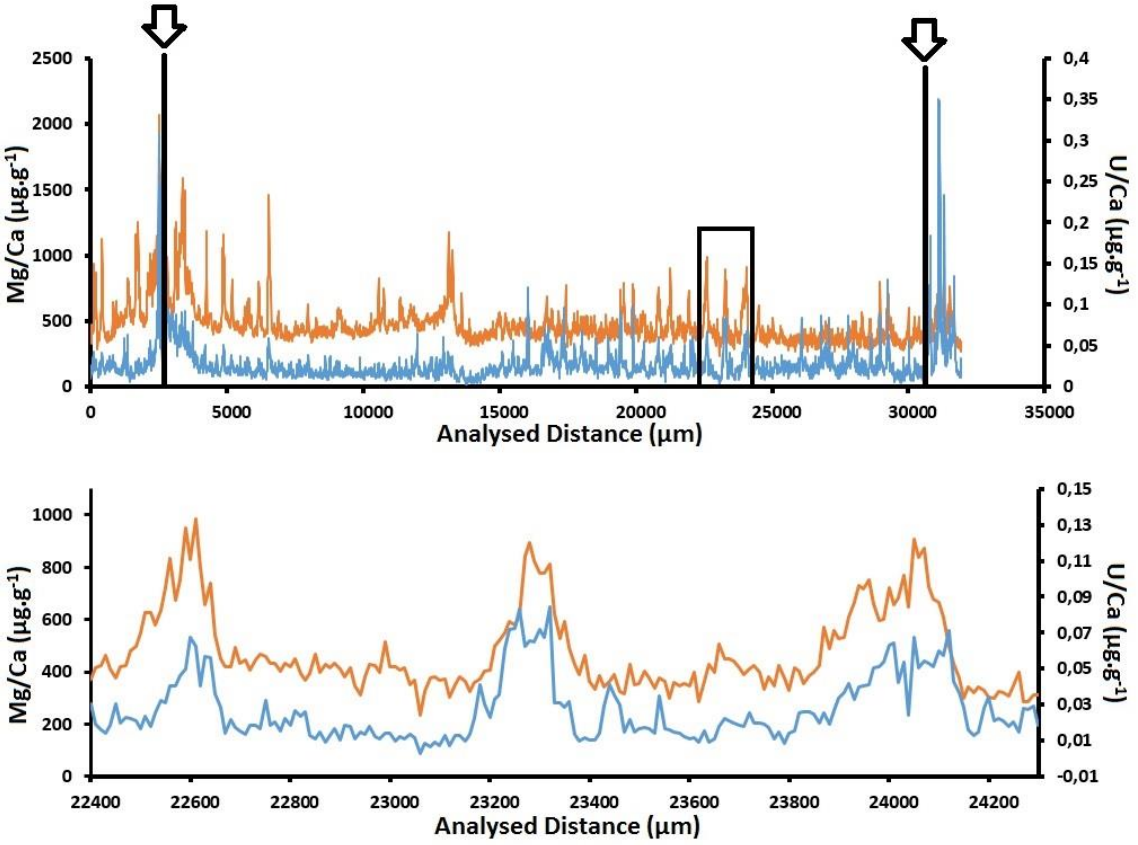

Figure 10: U/Ca (µg.g^{-1}) (blue curve) and Mg/Ca (µg.g^{-1}) (orange curve) series at 30 m. Vertical lines placed under the arrows indicate the position of shell growth lines. The graph bellow represents a close-up on three peaks (black box upper graph).

Discussion

This paper presents the first chemical analyzes performed on *P. magellanicus* shells. Given to the temporal resolution (25.82 h) of the environmental phenomena we wanted to track, it was necessary to develop a new analytical method. Our novel approach using ultra-high resolution fs-LA-ICPMS enables trace element analyses in bivalve shells with a 10-µm resolution. This study gave us first insights about *P. magellanicus* ability to record high-frequency environmental variations within is shell.

Barium

The high degree of similarity between the two Ba/Ca profiles suggests that the occurrence of Ba/Ca peaks was controlled by one or multiple common environmental factors. The pattern of these two Ba/Ca profiles is similar to those observed in cross sections of other bivalve

species (e.g., Gillikin *et al*., 2008; Stecher *et al*. 1996; Vander Putten *et al*., 2000). This confirms the hypothesis which suggests that the choice of analyzing the shell surface or the outer shell layer in cross sections do not have significant influence on Ba/Ca records in shells. In this section, we will discuss several hypotheses to explain temporal variability of Ba/Ca in *P. magellanicus* shell. Background levels of Ba:Ca time-series in bivalve shells have been suggested to record salinity variations (e.g. Gillikin *et al.*, 2006). There is generally a linear inverse relationship between seawater salinity and dissolved barium concentrations (Coffey *et al.*, 1997; Gillikin *et al.,* 2006). However, variability in seawater dissolved barium concentrations as a source for the Ba/Ca peaks in *P. magellanicus* from Saint-Pierre & Miquelon is highly unlikely. Indeed, Saint-Pierre & Miquelon islands, due to their offshore status, are not subject to major riverine inputs and associated variations in salinity (Poitevin *et al.,* 2018). Salinity usually ranges from 31.3 to 32.2 PSU (see Fig.4 in Poitevin *et al.,* 2018) without a clear seasonal trend and, therefore, cannot explain Ba/Ca peaks measured in the shells. Many authors suggested a close relationship between these Ba/Ca peaks and phytoplankton blooms (e.g. Elliot *et al*., 2009; Lazareth *et al*., 2003; Stecher *et al*., 1996; Thébault *et al*., 2009; Vander Putten *et al.*, 2000). In our study, the high similarity of chlorophyll *a* concentration (Fig. 6) and Ba/Ca (Fig. 7) profiles strongly suggest a relationship between phytoplankton biomass and barium incorporation into *P. magellanicus* shells. Indeed, the occurrence of this bloom, in May 2015, seems to be consistent with the starting of *P. magellanicus* annual growth from other Canadian regions (Chute *et al*. 2012; Kleinman *et al*., 1996). Elevated levels of suspended barite ($BaSO_4$), have been suggested to be linked with oceanic diatoms primary productivity (Dehairs *et al*., 1991). Most of the barium released by diatoms after a bloom is labile and only a minor fraction eventually forms barite crystals (Ganeshram *et al.*, 2003). Therefore, if labile barium, either in phytoplankton or released into the dissolved phase, was the cause of the Ba/Ca peaks, these peaks should form near the end of the bloom or very shortly thereafter (Gillikin *et al.*, 2008). Considering the absence of daily growth lines in *P. magellanicus*, we cannot conclude about chlorophyll *a* and Ba/Ca peaks timing. Finally, the two Ba/Ca profiles exhibited a double peak, with a first large amplitude one and a smaller second peak. This observation has also been made in *P. maximus* Ba/Ca profiles (Gillikin *et al.*, 2008). One explanation for this double peak proposed in this study is based on Ganeshram e*t al.* (2003). They found that barite formation can take several weeks to reach its maximum after the beginning of phytoplankton decay. Barite may be formed at

the sediment surface and be ingested by *P. magellanicus* several weeks after the phytoplankton bloom ends.

These observations on Ba:Ca incorporation in *P. magellanicus* shell from Saint-Pierre & Miquelon suggest a real need for complementary information related to local *P. magellanicus* growth dynamics and physiology. It would also be crucial to get insights about the nature and the quantity of benthic and pelagic primary production over the year and along a bathymetric gradient.

Magnesium

In bivalve shells, the relationship between seawater temperature and Mg/Ca ratio is still subject to controversy. Some authors proposed that Mg/Ca ratios can be used to record water temperature (e.g., Bougeois *et al.,* 2014; Lazareth *et al*., 2003; Mouchi *et al.,* 2013; Surge & Lohmann, 2008; Ullmann *et al.,* 2013), while there are many reports of strong vital effects in bivalve shells for this element (e.g., Elliot *et al.,* 2009; Lorrain *et al.,* 2005, Wanamaker *et al.*, 2008,). In this study, we can hardly discuss the importance of vital effects on trace elements incorporation into *P. magellanicus* shell. Indeed, our analyses were only carried out on one year of growth (ontogenetic and calendar) and one individual per site. The only thing we can say about physiological control of Mg incorporation in *P. magellanicus* shell is based on Mg/Ca level. In this study, the mean Mg/Ca ratio (~500 $\mu g.g^{-1}$ corresponding to ~2$mmol.mol^{-1}$) of the calcitic outer shell layer of *P. magellanicus* corresponds to a low value compared to other calcitic shells of mollusks (Lazareth *et al.*, 2007 and references therein). Given the absence of sclerochemical studies about trace element incorporation in *P. magellanicus* shells, we can only try to explain these low Mg concentrations relying on studies based on other calcitic bivalves with low Mg/Ca concentrations. Lorens and Bender (1977) suggested that *Mytilus edulis* biologically regulates the amount of Mg entering the extra pallial fluid to produce low-Mg calcite. Perhaps a similar process occurs in *P. magellanicus* suggesting a physiological control of Mg incorporation that could obscure Mg/Ca signal and seawater temperature relationship. This confirms the need for additional investigations on biomineralization, e.g. through experiments in controlled environments, in order to better understand trace elements incorporation in *P. magellanicus* shell. However, the shape of the two Mg/Ca profiles tends to highlight kind of a temperature control on magnesium incorporation in our shells. At 10 m, the sinusoidal pattern of Mg/Ca ratio may reflect the seasonal seawater temperature

annual cycle at 10 m depth. While at 30 m, the Mg/Ca profile presents a relatively flat baseline with high-frequency variations that could mirror the seawater seasonal temperature trend, namely showing low seasonal amplitudes with high-frequency variations (Lazure *et al.,* 2018). Other studies also point to the non-systematic relationship between Mg/Ca ratio and SST. From a one year study of *M. edulis* growth, Vander Putten *et al.* (2000) observed a positive correlation between Mg/Ca and SST only during spring. Small-scale variations in Mg concentrations in *M. edulis* calcite have also been shown to derive from Mg being concentrated along the margins of calcite prisms (Rosenberg *et al.*, 2001). Indeed, the absence of intra-annual growth lines on the *P. magellanicus* shell is problematic to convert distances into time. That is why; enhancing our knowledge on *P. magellanicus* growth dynamics along this bathymetric gradient in Saint-Pierre & Miquelon would help us to decipher physiological and environmental effects on trace element incorporation in *P. magellanicus* shell calcite. In addition, the lack of high frequency environmental data limits our ability to fully interpret our results and confirms the interest to set up a high frequency observatory along this bathymetric gradient.

Uranium

In our study, U/Ca and Mg/Ca profiles show a strong positive correlation in shells collected at 30 m. However, this is not the case for the shallowest shell for which no significant correlation could be found. These results suggest that (i) environmental uranium availability for *P. magellanicus* are not the same between the two sites and/or (ii) that physiological differences between *P. magellanicus* from 10 m and 30 m sites could lead to differential incorporation of uranium in shells.

Since (i) we do not have information about *P. magellanicus* physiological differences between these two depths, and (ii) only one study previously investigated U/Ca ratio as a potential paleo environmental proxy in bivalve shells (Gilikin & Dehairs, 2012), it seems difficult to draw conclusions about the kind of processes influencing uranium incorporation in *P. magellanicus* shells.

To our knowledge, U/Ca ratio as a paleo environmental proxy has only been studied once in mollusc shell. In this study, Gilikin and Dehairs (2012) tried to investigate U/Ca in *Saxidomus gigantea* shell as a potential acidification proxy. The authors conclude that U/Ca may not

reflect environmental variability and could not be considered as a paleo-pH proxy (Gilikin & Dehairs, 2012). Considering our study purpose and resolution, it seems difficult to conclude about U/Ca as a potential acidification proxy in *P. magellanicus* shell, especially as we do not have pH measurements on our study sites. Uranium-to-calcium ratios have also been suggested as a proxy for temperature in shallow water corals (e.g., Min *et al.*, 1995; Shen & Dunbar, 1995) and in planktonic foraminiferal carbonates (e.g., Yu *et al.*, 2008). In our study, the positive correlation between U/Ca and Mg/Ca profiles in the shell collected at 30 m would support this hypothesis. However, this correlation does not hold anymore at 10 m, suggesting that variations in uranium bioavailability differ between our two sites. Indeed, microorganisms have the ability to adsorb radionuclides/metals through extracellular binding involving physical adsorption, ion exchange, complexation and precipitation (Acharya *et al.*, 2009). They also sequester the metal ions by passive/active transport to the interior of the cell, followed by its accumulation. Microbial cells have been shown to reduce, oxidize, adsorb, accumulate and precipitate uranium (Fredrickson *et al.,* 1999; Macaskie *et al.,* 2000). That's why differences in microbial communities between the two sites, related to the nature of the habitat or to depth, could lead to changes in environmental uranium availability and finally to shell U/Ca ratios.

Conclusion

From an analytical point of view, it would be interesting to continue this study by applying this new analytical technique to more individuals. This would allow us to discuss about inter-individual variability within those two sites. Moreover, combining this approach with nano-SIMS $\delta^{18}O$ measurements (temperature proxy) would help us to get insights about the temperature control of Mg and U incorporation in shells.

In term of data interpretation, these results also confirm a real need for complementary information. Some of them should be related to *P. magellanicus* growth dynamics and physiology. Others must concern multiple high frequency environmental data continuously recorded at an individual scale within those two sites.

Acknowledgements

First, we thank the LEMAR (UMR 6539) Secretariat team (Anne-Sophie Podeur, Geneviève Cohat, and Yves Larsonneur) for their invaluable assistance during the administrative preparation of the analytical trip associated with this work in Pau. We also thank Gaëlle Barbotin for her help during fs-LA-ICPMS measurements in Pau. This work was supported by the EC2CO program MATISSE of the CNRS INSU, the Cluster of Excellence LabexMER, and the LIA BeBEST CNRS INEE. This research was carried out as part of the Ph.D. thesis of Pierre Poitevin for the University of Western Brittany with a French Ministry of Higher Education and Research grant.

References

Acharya C, Joseph D, Apte SK (2009) Uranium sequestration by a marine cyanobacterium *Synechococcus elongatus* strain BDU/75042. *Bioressource Technology*, **100**, 2176-2181.

Ballesta-Artero I, Witbaard R, Carroll ML, Van der Meer J (2017) Environmental factors regulating gaping activity of the bivalve *Arctica islandica* in Northern Norway. *Marine Biology*, **164 (5)**, 116.

Barats A, Amouroux D, Pecheyran C, Chauvaud L, Donard OFX (2007) High-Frequency Archives of Manganese Inputs To Coastal Waters (Bay of Seine, France) Resolved by the LA ICPMS Analysis of Calcitic Growth Layers along Scallop Shells (*Pecten maximus*). *Environmental Science & Technology*, **42 (1**), 86-92.

Bougeois L, de Rafélis M, Reichart GJ, de Nooijer LJ, Nicollin F, Dupont-Nivet G (2014) A high resolution study of trace elements and stable isotopes in oyster shells to estimate Central Asian Middle Eocene seasonality. *Chemical Geology*, **363**, 200-212.

Brown RJ, Severin KP (2009) Otolith chemistry analyses indicate that water Sr:Ca is the primary factor influencing otolith Sr:Ca for freshwater and diadromous fish but not for marine fish. *Canadian Journal of Fisheries and Aquatic Sciences*, **66 (10)**, 1790-1808.

Butler PG, Richardson CA, Scourse JD, et al. (2010) Marine climate in the Irish Sea: analysis of a 489-year marine master chronology derived from growth increments in the shell of the clam *Arctica islandica*. *Quaternary Science Reviews*, **29**, 1614–1632.

Campana SE (1999) Chemistry and composition of fish otoliths: pathways, mechanisms and applications. *Marine Ecology-Progress Series*, **188**, 263-297.

Carre M, Bentaleb I, Bruguier O, Ordinola E, Barrett NT, Fontugne M (2006) Calcification rate influence on trace element concentrations in aragonitic bivalve shells: Evidences and mechanisms. *Geochimica et Cosmochimica Acta*, **70**, 4906-4920.

Chauvaud L, Thouzeau G, Paulet YM (1998) Effects of environmental factors on the daily growth rate, *Journal of Experimental Marine Biology and Ecology*, **227**, 83–111.

Chung GS, Swart PK (1990) The concentration of uranium in freshwater vadose and phreatic cements in a Holocene ooid cay; a method of identifying ancient water tables. *Journal of Sedimentary Research*, **60**, 735-746.

Chute AS, Wainright SC, Hart DR (2012) Timing of shell ring formation and patterns of shell growth in the sea scallop *Placopecten magellanicus* based on stable oxygen isotopes. *Journal of Shellfish Research*, **31**, 649- 662.

Coffey M, Dehairs F, Collette O, Luther G, Church T, Jickells T (1997) The behaviour of dissolved barium in estuaries. *Estuarine, Coastal and Shelf Science*, **45**, 113-121.

Dehairs F, Stroobants N., Goeyens L (1991) Suspended barite as a tracer of biological activity in the Southern Ocean. *Marine Chemistry*, **35**, 399–410.

Elliot M, Welsh K, Chilcott C, McCulloch M, Chappell J, Ayling B (2009) Profiles of trace elements and stable isotopes derived from giant long-lived *Tridacna gigas* bivalves: Potential applications in paleoclimate studies. *Palaeogeography Palaeoclimatology Palaeoecology*, **280**, 132-142.

Fredrickson JK, Kostandarithes HM, Li SW, Plymale AE, Daly MJ (1999) Reduction of Fe(III), Cr(VI), U(VI) and Te(VII) by *Deinococcus radiodurans* R1. *Applied Environmental Microbiology*, **66**, 2006–2011.

Freitas PS, Clarke LJ, Kennedy H, Richardson CA (2008) Inter- and intra-specimen variability masks reliable temperature control on shell Mg/Ca ratios in laboratory- and field-cultured *Mytilus edulis* and *Pecten maximus* (bivalvia). *Biogeosciences*, **5**, 1245-1258.

Freitas PS, Clarke LJ, Kennedy H, Richardson CA (2009). Ion microprobe assessment of the heterogeneity of Mg/Ca, Sr/Ca and Mn/Ca ratios in *Pecten maximus* and *Mytilus edulis* (bivalvia) shell calcite precipitated at constant temperature. *Biogeosciences*, **6**, 1209-1227.

Freitas PS, Clarke LJ, Kennedy H, Richardson CA (2016) Manganese in the shell of the bivalve *Mytilus edulis*: Seawater Mn or physiological control? *Geochimica et Cosmochimica Acta*, **194**, 266-278.

Ganeshram RS, Francois R, Commeau J, Brown-Leger SL (2003) An experimental investigation of barite formation in seawater. *Geochimica et Cosmochimica Acta*, **67**, 2599-2605

Gillikin D, Dehairs F, Lorrain A, Steenmans D, Baeyens W, Andre L (2006) Barium uptake into the shells of the common mussel (*Mytilus edulis*) and the potential for estuarine paleo-chemistry reconstruction. *Geochimica et Cosmochimica Acta*, **70**, 395-407.

Gillikin D, Lorrain A, Paulet YM, Andre L, Dehairs F (2008) Synchronous barium peaks in high-resolution profiles of calcite and aragonite marine bivalve shells. *Geo-Marine Letters*, **28**, 351-358.

Gillikin D, Dehairs F (2012) Uranium in aragonitic marine bivalve shells, *Palaeogeography, Palaeoclimatology, Palaeoecology*, **373**, doi: 10.1016/j.palaeo.2012.02.028.

Kitano Y, Oomori T (1971) The coprecipitation of uranium with calcium carbonate. *Journal of the Oceanographic Society of. Japan*, **27**, 34–42.

Klein R, Lohmann K, Thayer C (1996) Sr/Ca and C-13/C-12 ratios in skeletal calcite of *Mytilus trossulus*: Covariation with metabolic rate, salinity, and carbon isotopic composition of seawater. *Geochimica et Cosmochimica Acta*, **60**, 4207-4221.

Kleinman S, Hatcher B, Scheibling R (1996) Growth and content of energy reserves in juvenile sea scallops, *Placopecten magellanicus*, as a function of swimming frequency and water temperature in the laboratory. *Marine Biology*, **124**, 629-635.

Langmuir D (1978) Uranium mineral-solution equilibria. *Geochimica et Cosmochimica Acta*, **42**, 547–569.

Lazareth CE, Vander Putten E, André L, Dehairs F (2003) High-resolution trace element profiles in shells of the mangrove bivalve *Isognomon ephippium*: a record of environmental spatio-temporal variations? *Estuarine, Coastal and Shelf Science*, **57**, 1103–1114.

Lazareth CE, Guzman N, Poitrasson F, Candaudap F, Ortlieb L (2007) Nyctemeral variations of magnesium intake in the calcitic layer of a Chilean mollusk shell (*Concholepas concholepas*, Gastropoda), *Geochimica et Cosmochimica Acta*, **71**, 5369-5383.

Lazareth CE, Le Cornec F, Candaudap F, Freydier R (2013) Trace element heterogeneity along isochronous growth layers in bivalve shell: Consequences for environmental reconstruction. *Palaeogeography, Palaeoclimatology, Palaeoecology*, **373**, 39-49.

Lazure P., Le Cann B., Bezaud M. (2018) Large diurnal bottom temperature oscillations around the Saint Pierre and Miquelon archipelago. *Scientific Reports*, **8**, Article number: 13882.

Lorens R, Bender M (1977) Physiological Exclusion of Magnesium from *Mytilus edulis* Calcite. *Nature*, **269**, 793-794.

Lorrain A, Gillikin D, Paulet YM, Chauvaud L, Le Mercier A, Navez J, André L (2005) Strong kinetic effects on Sr/Ca ratios in the calcitic bivalve *Pecten maximus*. *Geology*, **33 (12)**, 965-968.

Macaskie LE, Bonthrone KM, Yong P, Goddard D (2000) Enzymatically-mediated bioprecipitation of uranium by a *Citrobacter sp.*: a concerted role for extracellular lipopolysaccharides and associated phosphatase in biomineral formation. *Microbiology*, **146**, 1855–1867.

Marali S, Schöne BR (2015) Oceanographic control on shell growth of *Arctica islandica* (Bivalvia) in surface waters of Northeast Iceland—implications for paleoclimate reconstructions. *Palaeogeography, Palaeoclimatology, Palaeoecology*, **420**, 138-149.

Min GR, Edwards RL, Taylor FW, Recy J, Gallup CD, Beck JW (1995) Annual cycles of U/Ca in coral skeletons and U/Ca thermometry. *Geochimica et Cosmochimica Acta*, **59**, 2025-2042.

Mouchi V, de Rafélis M, Lartaud F, Fialin M, Verrecchia E (2013) Chemical labelling of oyster shells used for time-calibrated high-resolution Mg/Ca ratios: a tool for estimation of past seasonal temperature variations. *Palaeogeography. Palaeoclimatology. Palaeoecology*, **373**, 66–74.

Poitevin P, Thébault J, Schöne BR, Jolivet A, Lazure P, Chauvaud L (2018) Ligament, hinge, and shell cross-sections of the Atlantic surfclam (*Spisula solidissima*): Promising marine environmental archives in NE North America. *Plos One*, **13(6)**, e0199212.

Rosenberg GD, Hughes WW, Parker DL, Ray BD (2001) The geometry of bivalve shell chemistry and mantle metabolism, *American Malacological Bulletin*, **16**, 251–261.

Schöne BR, Radermacher P, Zhang Z, Jacob DE (2013) Crystal fabrics and element impurities (Sr/Ca, Mg/Ca, and Ba/Ca) in shells of *Arctica islandica*-Implications for paleoclimate reconstructions. *Palaeogeography, Palaeoclimatology, Palaeoecology*, **373**, 50-59.

Shen GT, Dunbar RB (1995) Environmental controls on uranium in reef corals. *Geochimica et Cosmochimica Acta*, **59**, 2009-2024

Shirai K, Schöne BR, Miyaji T, Radarmacher P, Krause RA Jr., Tanabe K (2014) Assessment of the mechanism of elemental incorporation into bivalve shells (*Arctica islandica*) based on elemental distribution at the microstructural scale. *Geochimica et Cosmochimica Acta*, **126**, 307-320.

Stecher HA, Krantz DE, Lord CJ, Luther GW, Bock KW (1996) Profiles of strontium and barium in *Mercenaria mercenaria* and *Spisula solidissima* shells. *Geochimica et Cosmochimica Acta*, **60 (18)**, 3445-3456.

Stecher HA, Kogut MB (1999) Rapid barium removal in the Delaware estuary. *Geochimica et Cosmochimica Acta*, **63**, 1003–1012.

Surge D, Lohmann KC (2008) Evaluating Mg/Ca ratios as a temperature proxy in the estuarine oyster, *Crassostrea virginica*. *Journal of Geophysical Research*, **113**, G02001.

Thebault J, Chauvaud L, L'Helguen S, Clavier J, Barats A, Jacquet S, Pecheyran C, Amouroux D, 2009. Barium and molybdenum records in bivalve shells: Geochemical proxies for phytoplankton dynamics in coastal environments? *Limnology and Oceanography*, **54**, 1002-1014.

Ullmann CV, Böhm F, Rickaby REM, Wiechert U, Korte C (2013). The Giant Pacific Oyster (*Crassostrea gigas*) as a modern analog for fossil ostreoids: isotopic (Ca, O, C) and elemental (Mg/Ca, Sr/Ca, Mn/Ca) proxies. *Geochemistry, Geophysics, Geosystems*, **14**, 4109–4120.

Vander Putten, E, Dehairs F, Keppens E, Baeyens W (2000) High resolution distribution of trace elements in the calcite shell layer of modern *Mytilus edulis*: Environmental and biological controls. *Geochimica et Cosmochimica Acta*, **64**, 997-1011.

Wanamaker AD, Kreutz KJ, Wilson T, Borns HW, Introne DS, Feindel S (2008) Experimentally determined Mg/Ca and Sr/Ca ratios in juvenile bivalve calcite for *Mytilus edulis*: implications for paleotemperature reconstructions. *Geo-Marine Letters*, **28**, 359-368.

Warter V, Müller W (2017) Daily growth and tidal rhythms in Miocene and modern giant clams revealed via ultra-high resolution LA-ICPMS analysis - A novel methodological approach towards improved sclerochemistry. *Palaeogeography, Palaeoclimatology, Palaeoecology*, **465**, 362-375.

Witbaard R, Duineveld GCA, DeWilde PAWJ (1997) A long-term growth record derived from *Arctica islandica* (Mollusca, Bivalvia) from the Fladen Ground (northern North Sea). *Journal of the Marine Biological Association of the United Kingdom*, **77 (3)**, 801–816.

Yu J, Elderfield H, Jin Z, Booth L (2008) A strong temperature effect on U/Ca in planktonic foraminiferal carbonates. *Geochimica et Cosmochimica Acta*, **72**, 4988–5000.

Discussion Générale

Discussion générale :

Ce travail de thèse est construit sur un socle de connaissances démontrant les spécificités hydrodynamiques de l'archipel de SPM à différentes échelles spatiales et temporelles. L'objectif central de ce travail était alors d'en quantifier l'influence sur différents organismes pour en reconstruire leurs variabilités passées. Pour ce faire, nous avons utilisé plusieurs outils sclérochronologiques appliqués à différentes archives biogéniques. Le choix des modèles biologiques a été motivé à la fois par la résolution temporelle des informations environnementales passées que nous cherchions à obtenir ainsi que par l'emprise biogéographique du modèle biologique candidat. Pour ce faire, nous avons développé une approche pluridisciplinaire spécifique à chacune de ces échelles. La première était centrée sur l'étude des variations de croissance d'espèces longévives tels que *A. islandica* et *C. compactum*, et sur les informations environnementales passées enregistrées au sein des pièces calcifiées de celles-ci. Une réflexion intégrant des problématiques d'océanographie physique, de modélisation mathématique et d'autoécologie associées à des variations environnementales ont alors été engagées. La seconde partie concernait l'étude biogéochimique haute résolution des coquilles de *P. magellanicus* pour en identifier la capacité à enregistrer des informations environnementales à une échelle sub-journalière. Ce travail, a lui aussi nécessité une réflexion associant : mesures environnementales *in situ* à hautes résolutions, réponses éthologiques et biologiques ainsi que du développement de méthode d'ablation laser ultra-haute résolution associée à des techniques d'analyses biogéochimiques (Notons que notre tentative de comparaison de méthodes analytiques en chimie élémentaire à échouer lors de l'arrêt du nano SIM de Pau).

Cette démarche pluridisciplinaire a permis d'apporter de nombreux éléments de réponses relatifs à la variabilité des conditions environnementales passées de l'archipel de Saint-Pierre et Miquelon et du bassin Nord Atlantique aux différentes échelles de temps considérées (de l'heure au siècle). Elle a également soulevé différentes questions propres à la sclérochronologie et à son intégration au sein d'autres champs disciplinaires.

Suivi des variations environnementales à grande échelle

Cette partie traite principalement des variations de croissance d'*A. islandica,* de *S. solidissima* et de *C. compactum* à SPM (Chapitres 1, 2 et 3). Nous avons décidé d'échantillonner ces trois

espèces subtidales à une profondeur inférieure ou égale à 15m pour nous situer au plus proche de l'interface océan atmosphère et tenter de nous affranchir le plus possible des oscillations thermiques quotidiennes observées en période estivale autour de l'archipel. Retenir ces trois espèces pour étudier la variabilité interannuelle d'une réponse biologique (croissance annuelle) à des forçages hydroclimatiques comportait plusieurs avantages. En effet, la croissance est un processus biologique fondamental, alimenté par une multitude de facteurs intrinsèque (intra-individuel) et extrinsèque (environnementaux) qui sous-tendent des problématiques individuelles, populationnelles et écosystémiques.

Synthèse des principaux résultats :

Les travaux réalisés sur *A. islandica* et *C. compactum* ont mis en relation des réponses biologiques avec plusieurs variables environnementales mesurées à différentes échelles : globales, régionales et locales. Des corrélations significatives entre ces mesures de croissances et des indices climatiques globaux tels que l'AMO, la NAO et l'indice SPG ont alors été identifiées. D'un point de vue spatial, de fortes corrélations positives entre ces chronologies de croissance et les températures de surface (0-100m) au sein du Gyre Sub-Polaire (SPG) ont également été trouvées. Au vu de ces résultats globaux, nous avons alors cherché des explications locales pouvant lier les réponses biologiques de ces organismes à ces variables très générales. La difficulté identifiée ici est liée à l'absence totale d'observations récurrentes de plusieurs paramètres physiques et biologique dans les eaux côtières de SPM. Toutefois, des corrélations ont pu être mises en évidence entre les informations enregistrées au sein des structures carbonatées de ces deux organismes avec : (i) la température et la salinité (Station 27) de la branche côtière du courant du Labrador, (ii) la couverture de glace de mer le long des côtes Terre-Neuviennes, (iii) le transport vers l'Ouest du courant du Labrador offshore au sud des Grands Bancs ainsi qu'avec (iv) la dynamique du Shelf Slope Front au sud de l'archipel. De façon non exhaustive, ces principaux résultats nous ont finalement permis d'identifier clairement des masses d'eau influençant l'hydrodynamisme de SPM. D'un point de vue écosystémique, nous disposons maintenant d'une description plus fine des conditions hydroclimatiques associées aux variations de croissance d'*A. islandica* et de *C. compactum* à SPM sur une période passée relativement longue (166 ans). Pour finir, cette première approche nous a permis d'évaluer la pertinence du choix de ce site pour étudier des variations hydroclimatiques et écosystémiques sur de longues périodes et à l'échelle globale. Ce dernier

constat a participé à l'obtention pour SPM, très récemment, du label de Site d'Étude en Écologie Globale (SEEG) attribué par l'Institut Écologie et Environnement du CNRS (INEE).

Nous pouvons également mettre en perspective ces résultats en les comparants avec les variations de croissance de *S. solidissima* (Chapitre 1) à SPM. Il convient de rappeler que cette étude avait comme objectif, dans le cadre de ce travail doctoral, de m'approprier des méthodes sclérochronologiques. De plus, compte tenu de la longévité bien moins importante de *S. solidissima* par rapport aux deux espèces citées précédemment. Nous avions choisi de ne pas faire d'interprétations éco-environnementales des chronologies de SGI de *S. solidissima* à SPM. Il semble à présent intéressant de comparer les chronologies d'indices de croissance de cette espèce et d'*A. islandica*. Une forte corrélation positive ($N = 17$, $r = 0.81$, $p < 0.05$) a ainsi été mise en évidence entre ces deux séries de mesures entre 1998 et 2014, période commune pendant laquelle ces deux chronologies de croissance étaient statistiquement robustes (EPS > 0.85). Ce résultat complémentaire, renforce donc l'interprétation faite précédemment en y apportant une vision issue d'un modèle biologique de même niveau trophique qu'*A. islandica*, partageant le même type d'habitat et dont les sites de prélèvement sont éloignés de seulement quelques centaines de mètres. Ce constat renforce donc les considérations établies précédemment entre la variabilité des conditions environnementales à Saint-Pierre et Miquelon et la croissance d'*A. islandica* en y apportant une vision indépendante issue de mesures de croissances coquillières faites extemporanément sur une autre espèce de bivalve.

Réflexions associées à l'étude sclérochronologique de la croissance des bivalves :

Ce travail a également permis d'entamer différentes réflexions associées à l'étude de la croissance des bivalves.

La première réflexion est relative à la trajectoire de croissance des mollusques bivalves et à leur forme. Il est largement acquis au sein de la communauté scientifique que les mesures d'incréments de croissance sont faites sur des coupes perpendiculaires à une valve et suivant l'axe de croissance maximale de l'espèce étudiée. Or, comme l'a démontré D'Arcy Thompson dans son livre « On Growth and Form » en 1917 la trajectoire de croissance des bivalves est curviligne. Ainsi, il serait intéressant de travailler sur un modèle de forme, spécifique à chaque

espèce, permettant d'ajuster les mesures faites individuellement le long d'une coupe « droite ». L'importance de ce biais peut cependant être discutée à travers nos travaux menés sur différentes parties de la coquille (ligament, chondrophore et couche externe) de *S. solidissima.* Ces trois archives, issues des mêmes individus, étant affectées différemment par ces contraintes de forme, présentent pourtant des indices de croissances standardisées relativement proches. Cependant, une quantification précise de ce biais, entreprise au sein du groupe BeBEST, semble nécessaire pour aboutir à une interprétation environnementale plus robuste de ce type de donnée.

La remarque suivante concerne l'extraction des signaux environnementaux à partir des mesures brutes d'incréments de croissance faites sur l'exosquelette des bivalves. La déconvolution des signaux hydroclimatiques, au sein d'une série de données incluant le développement d'un organisme, impose de retirer la tendance ontogénique de ces séries en y appliquant un modèle de croissance. Cette phase appelée « detrending » s'appuie encore aujourd'hui sur des méthodes développées à des fins dendrochronologiques. Or, comme nous l'avons indiqué précédemment, la dynamique de croissance d'un arbre ou d'un bivalve ne sont évidemment pas identiques y compris d'un point de vue géométrique. Actuellement, cette tendance liée à la biologie de l'animal est majoritairement retirée grâce à l'utilisation de modèles mathématiques purement théoriques comme des splines cubiques (e.g., Schöne *et al*., 2003). L'utilisation de ce type d'ajustement nous pousse à nous interroger sur la nature des informations retirées de nos mesures brutes d'incréments de croissance. Concrètement, retire-t-on des informations environnementales à basses et moyennes fréquences en plus de celles liées à l'ontogénie de l'animal ? Quelques études (e.g., Royer *et al.*, 2013) essaient de répondre à ces questions en utilisant des modèles de « detrending » ayant un fondement biologique, comme les équations de von Bertalanffy (von Bertalanffy, 1938). Dans le cas d'*A. islandica*, la présente étude a montré que l'utilisation de ce type d'équation n'est pas satisfaisante. En effet, nos séries de mesures d'incréments de croissance couvrent régulièrement des périodes supérieures à 100 ans et le nombre de variables associées aux équations de von Bertalanffy n'est jamais supérieur à 4, ce qui est insuffisant pour modéliser correctement une trajectoire de croissance contenant autant de points. Le choix a donc été fait de développer un modèle de croissance dynamique reposant sur l'équation générale de

von Bertalanffy dérivée à plusieurs reprises et permettant de ne plus être limité par le nombre de variable d'ajustement de celle-ci (Chapitre 2).

Perspectives

Cette partie propose un inventaire non exhaustif de travaux déjà entamés, ou non, pouvant compléter les études déjà exposées précédemment.

Les travaux réalisés dans ces 3 chapitres mériteraient d'être compilés et éventuellement amendés par un volet dendrochronologique qui renforcerait le lien entre océan et atmosphère. Cela semble réalisable, grâce à la présence sur l'archipel de la seule forêt boréale française (Fig. 1) qui abrite différentes espèces d'arbres longévives et dont l'intérêt dendrochronologique n'est plus à démontrer. C'est notamment le cas de *Picea glauca*, *Picea mariana* et *Abies balsamea* (e.g., Drake *et al.*, 2010 ; Krause, 1997 ; McGuire *et al*., 2008 ; Szeic & MacDonald, 1996 ; Tardif *et al*., 2008).

Figure 1 : Photographie illustrant la présence d'une forêt boréale à Saint-Pierre et Miquelon (**©Benjamin Deroche, Saint-Pierre-et-Miquelon, Août 2017).**

L'intérêt principal de ce genre d'étude intégrant différents types d'archives (terrestres et marines) dans un site particulier est d'obtenir une vision plus complète et précise de la variabilité environnementale passée de celui-ci. En effet, chacune de ces espèces enregistre des conditions environnementales passées qui lui sont propres (atmosphère, océan) et qui dépendent de son niveau taxonomique, trophique et des caractéristiques du site dans lequel elle a été prélevée (Black *et al.*, 2009). La combinaison de toutes ces informations issues de plusieurs types d'archives devrait permettre d'avoir une vision plus holistique de la variabilité environnementale passée à SPM et à terme, d'offrir la possibilité d'en prédire l'évolution.

Des travaux concernant le lien entre ces observations à grande échelle et les oscillations thermiques liées à l'onde côtière de marée piégée autour de SPM ont déjà été initiés et mériteraient d'être poursuivis. En effet, une étude de croissance similaire à celle présentée dans le second chapitre de cette thèse a été réalisée sur des *A. islandica* collectés à 24m. Les chronologies des indices de croissance standardisés des individus collectés dans ces deux sites ne sont pas exactement identiques (Fig. 2).

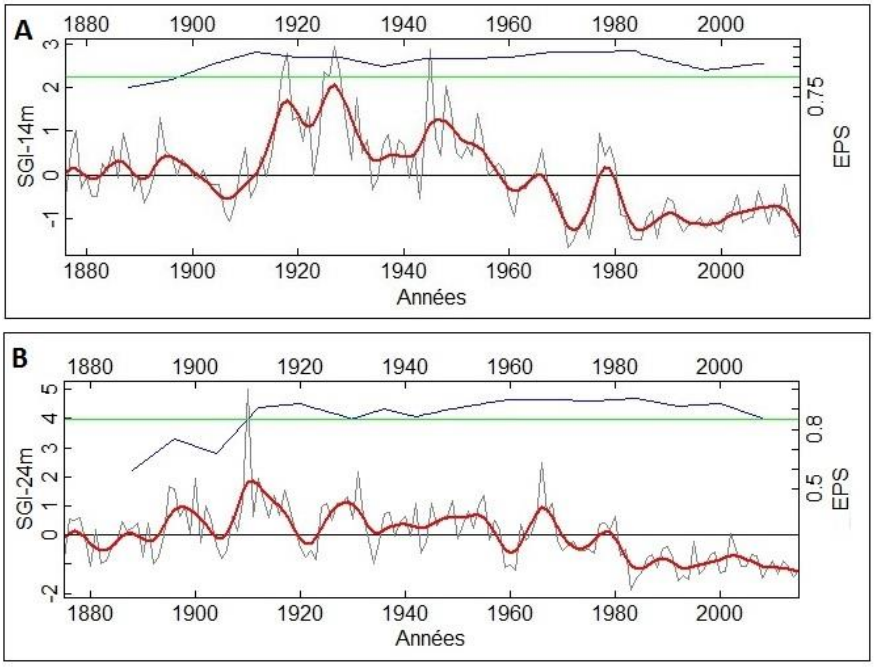

Figure 2 : Chronologie des indices de croissance standardisées (SGI) à 14 m (A) et 24m (B) d'*A. islandica* à SPM. La courbe bleue représente l'indicateur statistique (EPS) et la ligne verte le seuil de 0.85 au-dessus duquel le signal de croissance exprimé peut être considéré comme commun inter-individuellement.

Or, lorsque l'on réalise une analyse spectrale du signal de croissance d'*A. islandica* obtenu à 24m un pic significatif ayant une fréquence comprise entre 17.5 et 20 ans ressort clairement. Cette observation, suggère une possible influence relative aux changements d'inclinaison de l'orbite lunaire à l'équateur qui varie entre 18.3° et 28.6° sur une période de 18,6 ans appelée "cycle nodal" (Lisitzin, 1974 ; Ray, 2007).

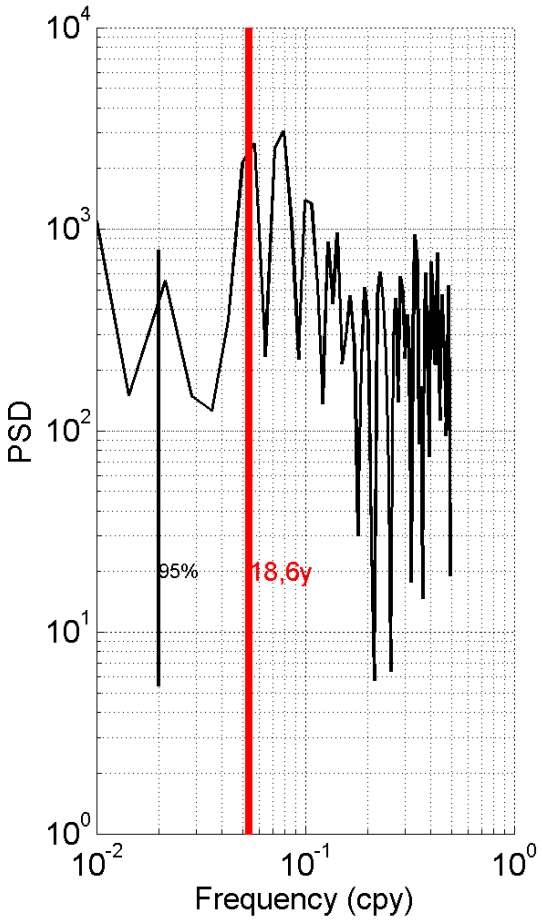

Figure 3 : Analyse spectrale des croissances standardisées à 24m en cycle par an (cpy).

De la même manière que les cycles vives eaux-mortes eaux modulent les courants maximum et le mélange vertical de la colonne d'eau, le cycle nodal serait également susceptible de faire varier ce mélange avec une période de 18,6 ans. L'une des particularités de ce cycle est sa capacité à moduler les ondes diurnes d'environ 15% (O1 (± 19%) et K1 (± 11%)) alors que sa modulation des ondes semi diurnes est de l'ordre de 3% (Ray, 2007). Cependant, la mise en évidence de ce cycle requiert de longues séries temporelles de mesure *in situ* qui sont rarement disponibles. C'est pourquoi, de nombreuses publications suggérant l'évidence de ce

cycle ont été remises en cause (Ray, 2007). Néanmoins, quelques séries temporelles existent telles que les mesures journalières de la température de la mer au pied des phares des côtes de la Colombie Britannique (Sud-Ouest du Canada) depuis les années 1920. Dans cette région proche de l'Oregon, les courants diurnes sont forts et traduisent la présence d'ondes côtières piégées (CTW) de même nature qu'à SPM. Loder & Garrett (1978) ont ainsi apporté la première preuve de l'existence de ce cycle qui se manifeste par des températures plus froides quand les courants sont maximaux à cause du mélange plus important sur la colonne d'eau.

Ce constat nous a alors poussés à nous interroger sur l'impact de ce cycle nodal sur la production primaire des sites soumis aux oscillations thermiques diurnes à hautes fréquences autours de SPM. L'analyse spectrale des valeurs d'incréments de croissance standardisés d'*A. islandica* à 24m, nous montre effectivement un pic correspondant à cette période de 18,6 ans. Le mécanisme sous-jacent pourrait être lié à un accroissement du mélange qui favoriserait directement (transfert) ou indirectement (pompage de nutriments) la production primaire et la croissance de ces bivalves. Ces premières analyses prometteuses méritent d'être affinées mais il pourrait s'agir de la première mise en évidence d'un cycle à 18,6 ans imprimé dans un organisme marin.

Suivi des variations environnementales à l'échelle sub-horaire

Cette partie traite principalement des variations microchimiques enregistrées dans la coquille de *Placopecten magellanicus* à SPM (Chapitre 4). Nous avons décidé de prélever cette espèce à 10 m et 30 m de profondeur afin d'en comparer la composition en éléments traces au sein de deux sites plus ou moins affectés par les oscillations thermiques quotidiennes observées en période estivale autour de cet archipel. La décision faite d'étudier la composition en élément traces de *P. magellanicus* repose sur plusieurs raisons. Certaines sont d'ordre biologique et concernent sa présence à SPM le long d'un gradient bathymétrique allant de 5 m à 80 m ainsi que son fort taux de croissance (plusieurs centimètres) notamment lorsque l'amplitude des oscillations thermiques quotidiennes est la plus importante. L'autre est analytique et concerne le coût financier relativement faible des analyses La-ICPMS. Cette étude nous a alors permis d'obtenir une première vision relative aux informations contenues dans la coquille de cette espèce au sein de deux sites présentant des conditions environnementales contrastées, avant d'effectuer d'autres analyses plus coûteuse.

Synthèse des principaux résultats

L'objectif principal de ce travail était de déterminer si *P. magellanicus* pouvait enregistrer dans sa coquille les variations environnementales à haute fréquence (25,8 h) observées à SPM. Pour ce faire, nous avons développé une nouvelle méthode d'analyses LA-ICPMS à ultra haute résolution, permettant de quantifier la composition en éléments traces des coquilles de *P. magellanicus* avec un pas d'échantillonnage de 10 µm. Cette méthode a été appliquée à deux fragments de coquille provenant de deux sites plus (30 m de profondeur) ou moins (10 m de profondeur) affectés par les oscillations thermiques haute fréquence (25,8h). Afin de limiter les effets liés à l'ontogénie sur la composition élémentaire des coquilles sélectionnées, les deux fragments comparés représentaient la même année calendaire (2015) correspondant à la troisième année de croissance des individus prélevés.

Des signaux communs ont alors été observés concernant la composition en baryum des deux coquilles. De plus, la similarité existante entre la dynamique de la concentration en chlorophylle *a* autour de l'archipel pendant l'année 2015 et la « signature » des profils de baryum dosés dans les coquilles suggère l'existence d'un lien entre la biomasse phytoplanctonique et l'incorporation de baryum dans les coquilles de *P. magellanicus*.

En revanche, les signatures Mg/Ca contrastées observées au sein des deux coquilles suggèrent l'existence d'un lien entre l'incorporation de cet élément dans la coquille de *P. magellanicus* et la température. En effet, à 10 m, le caractère sinusoïdal du signal de magnésium mesuré dans la coquille, semble cohérent avec la signature thermique observée à cette profondeur autour de SPM. De même, à 30 m, la concentration en magnésium dans la coquille suit une ligne de base relativement plate avec des variations haute-fréquences qui semblent suivre la signature thermique observée à la même profondeur.

Concernant l'uranium mesuré dans ces deux coquilles, les signatures élémentaires sont également contrastées entre les deux sites. À 10 m, aucune tendance ne semble ressortir des mesures effectuées. Cependant, à 30 m, les mesures d'uranium faites dans la coquille semblent cohérentes avec les variations de la concentration en magnésium. Cette observation suggère que l'incorporation de l'uranium au sein de la coquille de 30 m est également liée aux oscillations thermiques hautes fréquences. En revanche, pour ce qui est du site de 10 m, la disponibilité de l'uranium dans l'environnement semble affectée par d'autres paramètres.

Réflexions associées à cette étude sclérochronologique haute fréquence

Ce travail a permis d'entamer différentes réflexions autour : (i) de la méthode mise en place pour mesurer les variations sclérochimiques au sein de de la coquille de *Placopecten magellanicus* à SPM ; (ii) et de l'interprétation des résultats obtenus.

D'un point de vue analytique, il serait intéressant de poursuivre ce travail en appliquant cette technique analytique à davantage d'individus. Cela nous permettrait de discuter de la variabilité interindividuelle au sein de ces deux sites et donc de valider nos hypothèses, voire de travailler sur l'hétérogénéité spatiale des signaux enregistrés dans les valves de ces mollusques. De plus, combiner cette approche avec des mesures nano-SIMS de $\delta^{18}O$ pourrait nous aider à interpréter la dépendance thermique de l'incorporation du magnésium et de l'uranium au sein de la coquille de *P. magellanicus*. Cette approche avait, bien entendu, été programmée lors de ce travail de thèse, la contingence en a voulu autrement.

En termes d'interprétation des données, ces résultats confirment également un réel besoin d'informations complémentaires. Certaines d'entre elles sont liées à la dynamique de la croissance et à la physiologie de *P. magellanicus*. D'autres concernent l'enregistrement récurrent à haute fréquence de différentes données environnementales à une échelle individuelle au sein de ces deux sites. Ces travaux ont également ouvert une réflexion écosystémique descriptive (e.g., assemblages faunistiques) et fonctionnelle (e.g., trophique), relative aux spécificités environnementales mises en avant par ces travaux de doctorat.

Perspectives

Comme pour la partie précédente, les paragraphes suivants vont proposer un inventaire non exhaustif de travaux déjà entamés, ou non, pouvant compléter les études à haute-fréquence déjà exposées précédemment.

Un premier travail, visant à mesurer le plus finement possible les variations environnementales associées à ces oscillations thermiques journalières (25.8 h), a déjà été initié en 2017. Au cours de celui-ci, nous souhaitions quantifier, à l'échelle de quelques mètres carrés, l'influence de ces oscillations thermiques récurrentes sur différents paramètres environnementaux. Nous avons alors installé des instruments mesurant à haute fréquence : la température, la conductivité de l'eau de mer, la concentration en oxygène, mais également la taille et le déplacement des particules, le courant à différentes échelles et la concentration

en chlorophylle *a*. Ce travail était couplé à des observations haute-fréquences (25 Hz) des mouvements valvaires de *P. magellanicus* par accélérométrie (Fig. 4).

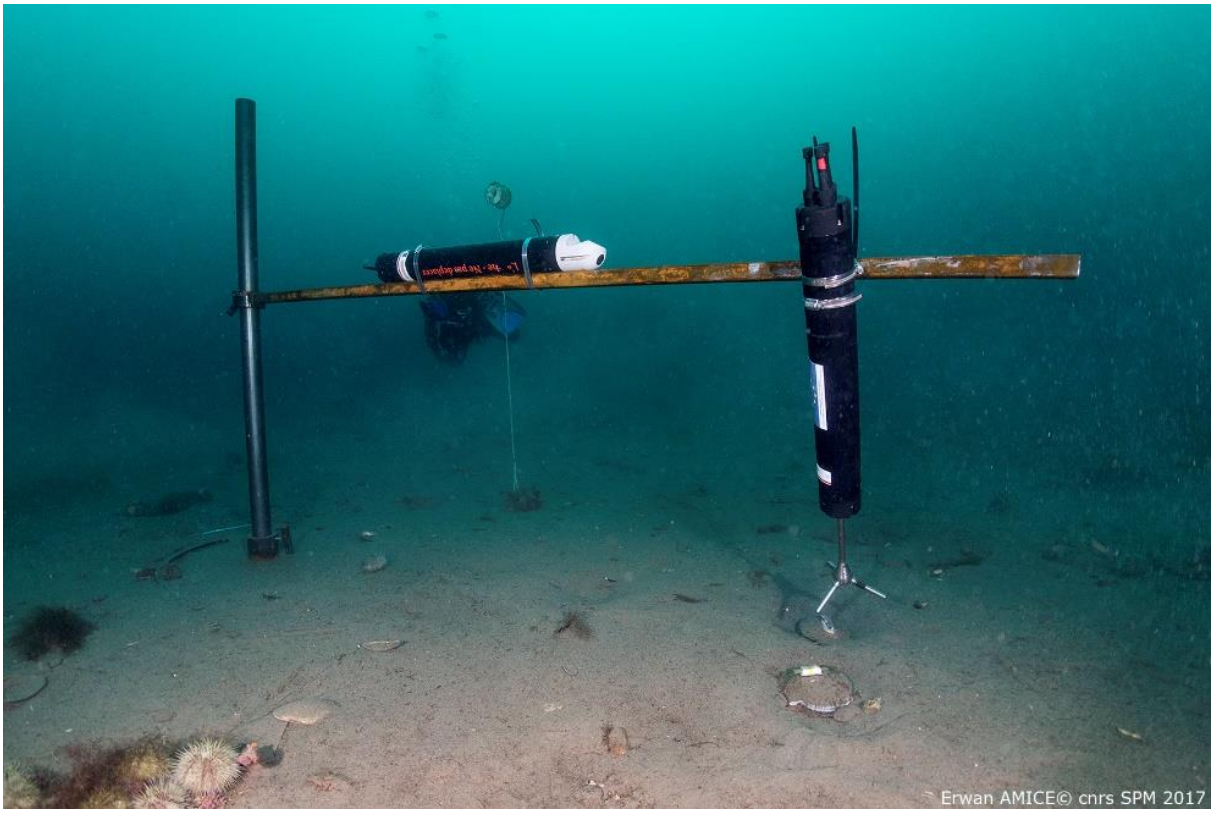

Figure 4 : Photo *in situ* d'un ADCP et d'un ADV placés au-dessus d'un *P. magellanicus* équipé d'un accéléromètre (Source : E. Amice/CNRS).

Le choix a été fait de mesurer l'activité valvaire de ce bivalve, par accélérométrie, car cette variable constitue l'un des premiers niveaux de réponse d'un organisme. Celle-ci intègre également un grand nombre d'informations, tout en restant non intrusive et non invasive. Les premiers résultats montrent qu'il n'y a pas de corrélation significative entre les mouvements valvaires des individus instrumentés en 2017 et les variations thermiques mesurées simultanément à 30 m (Fig. 5). Ces résultats nous amènent à nous interroger sur la pertinence de l'outil « accéléromètre » pour mesurer l'activité valvaire de *P. magellanicus*. Ces résultats posent également des questions relatives à l'adaptation et à l'adaptabilité des organismes ectothermes sub-tidaux de SPM soumis à ces contraintes thermiques quotidiennes.

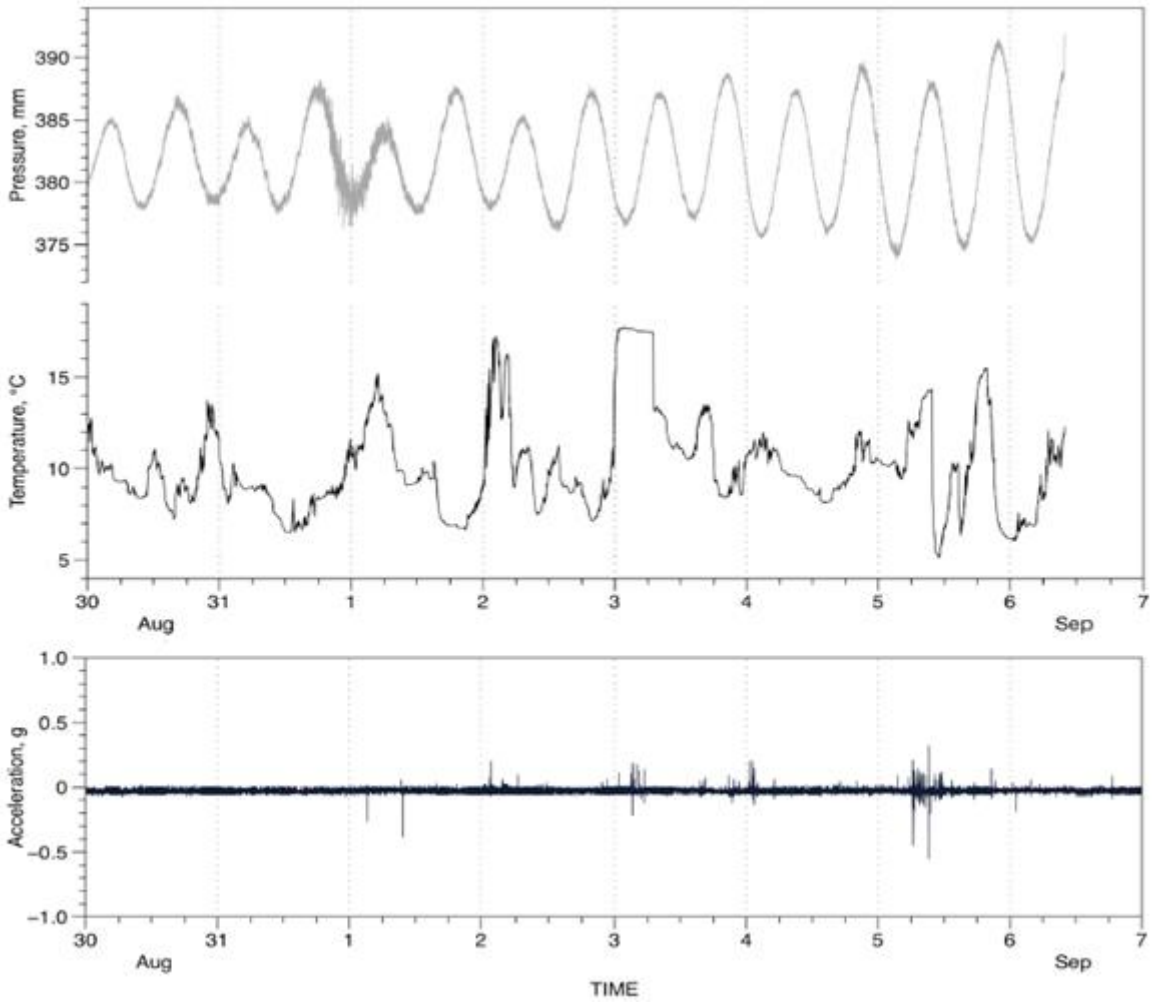

Figure 5 : Mesures de la température et de la pression à 30m, du 30 août au 7 septembre 2017 en rade de Saint-Pierre. Le dernier graphique représente la somme des 3 vecteurs d'accélération mesurés sur un *P. magellanicus* équipé d'un accéléromètre pendant la même période et sur le même site.

Dans ce contexte, la forte abondance individuelle, associée à l'absence de réponses valvaires de *P. magellanicus* à ces oscillations thermiques répétées, de même que la présence d'une espèce longévive telle qu'*A. islandica* dans un milieu aussi variable, sont assez paradoxales. En effet, dans le reste de son aire de répartition, la stabilité de l'environnement et un faible taux de production d'espèces réactives de l'oxygène ont été avancées comme des raisons expliquant la longévité de cette espèce (Ungvari *et al.,* 2011). Ainsi, il est probable que les populations peuplant cette zone thermiquement ultra-variable mettent en œuvre des mécanismes originaux leur permettant de supporter ces conditions. Par exemple, chez *P. magellanicus*, la synthèse d'HSP (« heat shock proteins »), suite à une augmentation de température en laboratoire (10°C à 20°C), n'est mesurée qu'au bout de 24h (Brun *et al.*, 2008).

Cette réponse semble inadaptée dans le cas de stress thermiques aigus et répétés à haute fréquence. Il est donc possible que des mécanismes différents des réponses « classiques » soient mis en place suite à un choc thermique d'une ampleur égale à ceux survenant à SPM.

Dans le cadre de cette étude, des prélèvements ont déjà été effectués et des analyses sont actuellement en cours (collaboration Labex Mer de l'IUEM) pour étudier les mécanismes adaptatifs et/ou d'acclimatation, potentiellement originaux mis en œuvre par *A. islandica* et *P. magellanicus* pour perdurer dans cet environnement unique. Ces prélèvements ont été effectués sur des animaux subissant ou non des oscillations thermiques. Concernant les individus prélevés dans des sites thermiquement ultra variables, un échantillonnage a été réalisé avant et après l'oscillation. Pour ce faire, nous avons au cours de ce travail doctoral, développé une méthode associant, en plongée, dissection et fixation RNA Later (Fig. 6). Nous attendons les résultats propres à la transcriptomique, protéomique et lipidomique.

Figure 6 : Photo d'une fixation au RNA Later suite à des dissections sous-marines d'*A. islandica* à 25m (Source : E. Amice/CNRS).

Les premières informations dont nous disposons concernent la génétique des individus. Pour ce faire, des marqueurs neutres (SNPs) d'*A. islandica* (2189 SNPs) et *P. magellanicus* (3924 SNPs), prélevés à des profondeurs plus (24 m et 30 m) ou moins (8 m ,12 m et 14 m) affectées

par les oscillations thermiques haute fréquences (25,8 h), ont été comparés. 30 individus de *P. magellanicus* ont respectivement été prélevés à chacune des trois profondeurs suivantes : 8 m, 12 m, et 30 m. Il convient de rappeler que chacun de ces points d'échantillonnages sont distant de moins d'1 km entre eux. De même, 30 individus d'*A. islandica* ont respectivement été prélevés à 14 m et 24m au sein de deux sites distants d'environ 5 km. L'indice F_{ST} mesurant le degré de différenciation entre des populations a alors été calculé pour chacune des espèces. Concernant *A. islandica,* la différenciation génétique était significative (F_{ST} = 0.003, p < 0.001) entre les individus provenant des deux profondeurs. En ce qui concerne *P.magellanicus*, les F_{ST} estimés ne sont significativement différents que pour les individus issus du site de 30m (F_{ST} = [0.002-0.003], p < 0.001). Les résultats de l'analyse multivariée (Jombart *et al.*, 2010) faite, sur chaque espèce, pour comparer la structure génétique des différents groupes d'individus entre eux (Fig. 7) semblent nous inviter à la même conclusion.

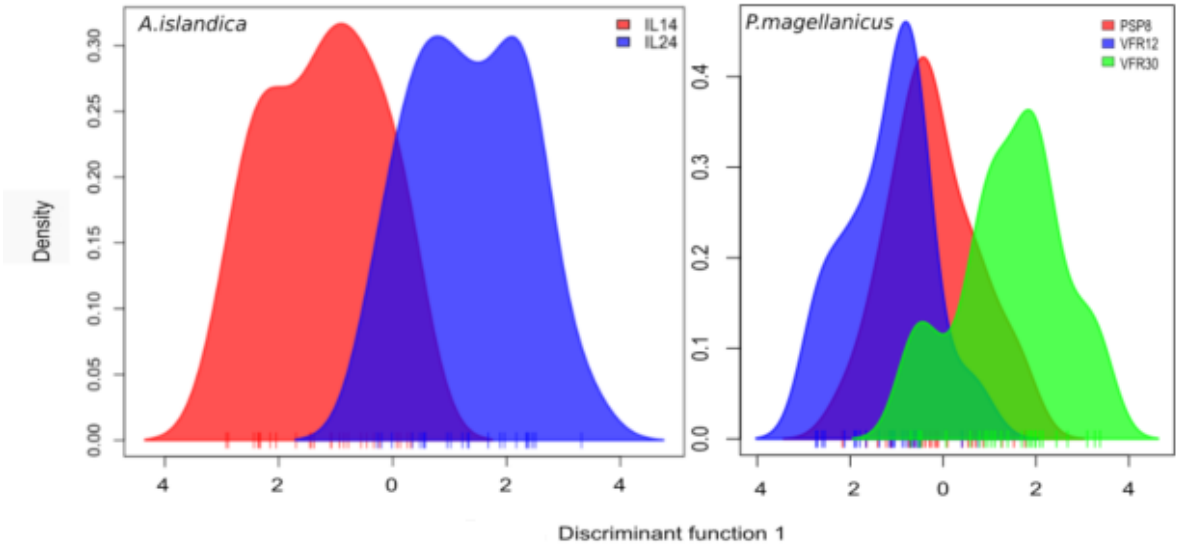

Figure 7 : Graphiques de densité du premier axe de la DACP (Jombart *et al.*, 2010) montrant pour, *A. islandica* et *P. magellanicus*, la séparation entre les échantillons issus d'individus soumis (IL24 et VFR30) ou non (PSP8, VFR12 et IL14) à des oscillations thermiques quotidiennes (25.8 h).

Ces résultats semblent refléter une pression de sélection contrastée, et indiquer une structuration génétique de ces deux espèces de bivalves le long d'un gradient bathymétrique à SPM. Cette observation, faite à une échelle spatiale incroyablement faible (< 1 km pour *P. magellanicus* ; < 5 km pour *A. islandica*), semble inédite. De plus, ces premiers résultats

nous permettent d'avoir une première vision, sur deux espèces aux cycles vitaux contrastés, du rôle évolutif des mécanismes de résistance à ces ondes thermiques chroniques. Ce premier travail pose alors une multitude de question. À savoir, quels sont les processus moléculaires, au niveau du transcriptome et du protéome, mis en jeu face à ces changements thermiques ? La composition lipidique des membranes cellulaires joue-t-elle un rôle dans la réponse des organismes à ces variations de température ? Si oui, quels sont les composés impliqués ? Les réponses observées aux différentes échelles d'organisation (transcriptomique, protéomique et lipidomique) ont-elles une valeur adaptative ?

Autant d'interrogations qui confirment l'intérêt d'une approche intégrative multi-échelle relative à l'auto-écologie des organismes ectothermes sub-tidaux le long d'un gradient bathymétrique à SPM.

Références

Black BA, Copenheaver CA, Frank DC, Stuckey MJ, Kormanyos RE (2009) Multi-proxy reconstructions of northeastern Pacific sea surface temperature data from trees and Pacific geoduck. *Palaeogeography, Palaeoclimatology, Palaeoecology*, **278**, 40–47.

Brun NT, Bricelj VM, MacRae TH, Ross NW (2008) Heat shock protein responses in thermally stressed bay scallops, *Argopecten irradians*, and sea scallops, *Placopecten magellanicus*. *Journal of Experimental Marine Biology and Ecology*, **358**, 151–162.

Drake DC, Naiman RJ, Helfield JM (2002) Reconstructing Salmon Abundance in Rivers: An Initial Dendrochronological Evaluation. *Ecology*, **11**, 2971-2977.

Jombart T, Devillard S, Balloux, F (2010) Discriminant analysis of principal components: a new method for the analysis of genetically structured populations. *BMC Genetics*, **11**, 94.

Krause C (1997) The use of dendrochronological material from buildings to get information about past spruce budworm outbreaks. *Canadian Journal of Forest Research*,**27** , 69–75.

Lisitzin E (1974) Sea Level Changes, *Elsevier*, New York.

Loder JW, Garrett C (1978) The 18.6-year cycle of sea surface temperature in shallow seas due to variations in tidal mixing. *Journal of Geophysical Research*, **83**, 1967–1970.

McGuire AD, Ruess RW, Lloyd A, Yarie J, Clein, JS, Juday GP (2010) Vulnerability of white spruce tree growth in interior Alaska in response to climate vatiability: dendrochronological, demographic, and experimental perspectives. *Canadian Journal of Forest Research*, **40**, 1197-1209.

Ray RD (2007) Decadal Climate Variability: Is there a tidal connexion? *Journal of Climate*, **20**, 3542-3560.

Szeicz JM, MacDonald GM (1996) A 930-year ring-width chronology from moisture sensitive white spruce (*Picea glauca* Moench) in Northwestern Canada. *The Holocene*, **6**, 345–351.

Tardif JC, Conciatori S, Leavitt SW (2008) Tree rings, $\delta^{13}C$ and climate in *Picea glauca* growing near Churchill, subarctic Manitoba, Canada. *Chemical Geology*, **252**, 88-101.

Ungvari Z, Ridgway I, Philipp EE, Campbell CM, McQuary P, Chow T, Coelho M, Didier ES, Gelino S, Holmbeck MA, Kim I, Levy E, Sosnowska D, Sonntag WE, Austad SN, Csiszar A (2011) Extreme longevity is associated with increased resistance to oxidative stress in Arctica islandica, the longest-living non-colonial animal. *The Journals of Gerontology Series A: Biological Sciences and Medical Sciences*, **66**, 741–75

UNIVERSITE SCIENCES BRETAGNE DE LA MER LOIRE ET DU LITTORAL

UBO Université de Bretagne Occidentale

Titre : Sclérochronologie à Saint-Pierre et Miquelon : De l'échelle sub-horaire aux reconstructions multi-décennales

Mots clés : Sclérochronologie, Changement climatique, Atlantique Nord, Proxies environnementaux, Océanographie, Saint-Pierre et Miquelon

Résumé : Les écosystèmes côtiers sont exposés aux changements climatiques entraînant des modifications de leur structure et de leur fonctionnement. Cependant, nous disposons de peu d'information sur la variabilité de leurs propriétés environnementales avant 1950. Les parties dures des organismes marins ont le potentiel d'étendre les observations instrumentales, à différentes échelles spatiales et temporelles, afin d'améliorer notre compréhension des processus environnementaux passés

Cette thèse de doctorat a pour cadre Saint-Pierre & Miquelon (SPM), un petit archipel situé à la confluence de grands courants océaniques marquant la frontière entre les gyres subtropicaux et subpolaires de l'Atlantique Nord. Outre sa position clé à l'échelle mondiale comme indicateur de l'évolution du climat, des spécificités locales induisent une dynamique très particulière conduisant, lors de la période stratifiée, à la génération des plus importantes oscillations thermiques quotidiennes jamais observées.

Ce travail est basé sur l'analyse des structures calcifiées d'organismes marins locaux, afin de mieux comprendre la variabilité environnementale passée à ces deux échelles. Les relations observées entre les enregistrements sclérochronologiques issus des différents modèles biologiques étudiés dans cette thèse et plusieurs types de données environnementales, nous ont permis de mettre en avant la position privilégiée de SPM pour étudier la variabilité océanographique, les réponses biologiques de différentes espèces benthiques et la dynamique des écosystèmes côtiers, à différentes échelles de temps (de la marée aux 165 dernières années) et d'espace (de celle de l'archipel à celle de l'Atlantique Nord).

Title: Sclerochronological approaches in Saint-Pierre & Miquelon: from sub-hourly to multidecadal environmental reconstructions

Keywords: Sclerochronology, Climate change, North Atlantic, environmental proxies, Oceanography, Saint Pierre and Miquelon

Abstract: Coastal ecosystems are exposed to global climate change leading to modifications of their structure and functioning. However, little is known about their environmental variability before 1950. The hard parts of long-lived marine biota hold the potential to extend instrumentally derived observations, at different temporal and spatial resolutions, in order to enhance our understanding of past environmental processes.

This PhD dissertation takes place on Saint-Pierre & Miquelon (SPM), a small archipelago at the confluence of major oceanic currents marking the boundary between the North Atlantic Ocean subtropical and subpolar gyres. In addition to its global key position, a local phenomenon, leads, during the stratified period, to the largest (up to 12°C amplitude) daily (25.8 h) temperature oscillations ever observed-at any frequency-on a stratified mid latitude continental shelf. This work is based on calcified structures of local marine organism analyses, to gain insights about past environmental variability at these two scales. The relationships observed between the sclerochronological records from these different marine biota and several environmental dataset, allowed us to highlight the relevant position of SPM for studying multiple scale oceanographic variability, biological responses of different benthic species and the dynamics of coastal ecosystems, at different time scales (from the tide to the last 165 years) and space scales (from SPM archipelago to North Atlantic Ocean).